VOLUME I

Hydrogeological Assessment of the Northern Regions of Ghana

Agence canadienne de développement international

Canadian International Development Agency

Water Resources Commission

FINAL TECHNICAL REPORT

Hydrogeological Assessment Project of the Northern Regions of Ghana (HAP)

CIDA Ref: 7038883

CEA Ref: 604138

INRS Ref: R1325

ISBN Ref: 978-2-89146-708-7

December 2011

SNC•LAVALIN International

INRS Université d'avant-garde

SUMMARY

A thorough understanding of regional hydrogeology is the necessary basis for sustainable development of groundwater resources. This is particularly true for semi-arid areas such as northern Ghana where groundwater is currently the most feasible option and the main source for water supply in rural communities, while becoming increasingly so for urban areas. The construction of reliable wells satisfying community needs is however problematic in some areas where information is non-existent or not readily accessible and certain aspects of regional hydrogeology require further investigation. In this context, this study aims to improve groundwater resource management and development in northern Ghana through the inventory, collection and synthesis of existing hydrogeological information, as well as by targeted field work intended to complement this information. The work described in this report was carried out as part of the Hydrogeological Assessment Project (HAP) of the Northern Regions of Ghana supported by the Canadian International Development Agency.

The study area covers approximately 97 704 km^2 and roughly consists of the nothern half of Ghana, which is located between Togo to the east, Ivory Coast to the west and Burkina Faso to the north. It includes the three northern regions of Ghana: Upper West, Upper East and Northern regions. With a large part of the country below 300 m of elevation, Ghana is generally considered as lowland. The climate in northern Ghana is characterized by high annual temperatures (~ 28°C) and a relatively short (~ June to Oct.) but intense rainy season with an average annual rainfall around 990 mm. Vegetation, which is mainly controlled by climate, grades from moist tropical forest in the south-west of the study area to Sudan savannah in the north. The Volta River has the largest watershed in Ghana and its tributaries drain the entire study area. The simplified geology of northern Ghana can be summarized in two main geological contexts: Precambrian basement rocks (PCB) (41 % of the total study area) and Palaeozoic rocks from the Voltaian sedimentary basin (VSB) (59 %). These contexts also serve as a basis for the delineation of the main hydrogeological contexts. In both contexts, most consolidated rocks are overlain by a weathered layer (regolith) that is generally less than 30 m thick but that can be as thick as 140 m in the Wa district in the extreme northwest part of the study area.

The inventory and collection of existing hydrogeological information that were carried out in northern Ghana notably allowed relevant publications and reports to be registered, electronically preserved and disseminated among stakeholders of the water sector. The main Geographical Information System (GIS) layers were obtained from various organizations within Ghana and from additional public sources. Hydrogeological data from 6 major stakeholder electronic databases were collected, validated and consolidated in one database to serve as a basis for future hydrogeological projects in northern Ghana. Targeted field work notably involved drilling and construction of 27 new monitoring wells that supplemented the existing Water Resources Commission monitoring well network. These wells were submitted to pumping tests and geophysical borehole logging. Groundwater level as well as groundwater quality monitoring of these wells was initiated in October 2007 and is still ongoing. Additional specific field work included rainfall, soil porewater and shallow groundwater sampling which allowed the evaluation of groundwater recharge through the chloride mass balance (CMB) method. As part of a regional geochemical characterization aimed at improving knowledge of groundwater dynamics and groundwater quality issues, groundwater from more than 100 monitoring and existing boreholes in northern Ghana was also sampled and analysed.

The synthesis and analyses of the collected data and information allowed a better definition of the two main hydrogeological contexts, the VSB and the PCB. In the latter, the lower part of the saprolite is defined as a leaky aquifer but mainly acts as a reservoir of groundwater feeding the underlying permeable fractures, which provide most of the yield. The lower part of the saprolite can also provide significant amounts of water when weathering has enhanced hydraulic conductivity. In the VSB, the main aquifer is generally located in fractured rock as the regolith is often thinner and may not store significant amounts of water. This is supported by typical borehole characteristics, regional hydrostratigraphic cross sections and interpolated regolith

thickness that were derived from the consolidated database. Variations in surface topography and regolith thickness observed on cross sections indicate the potential for localized and isolated aquifers. General statistics on key hydrogeological parameters were summarized for both hydrogeological contexts. Potential drilling success rates were also estimated using data from existing reports. Representative drilling success rates, which vary by region, range from 32 % (Tolon Kumbugu) to 82 % (Bawku East) and are on average lower for the VSB than for the PCB.

Hydrogeochemical characterization showed that groundwaters of the PCB display mixed-cations (Ca+Na+Mg) and bicarbonate (HCO_3)-dominated water types. Their level of mineralization is generally moderate, indicating rock matrix-groundwater interactions of moderate extent and proportional residence and travel time in the geological formations. In contrast, groundwaters of the VSB are generally sodic (Na-dominated) in nature. HCO_3 is also the most commonly found ion, although some groundwaters exhibit a rather Cl-dominated water type. Such water types are indicative of more advanced evolution stages and longer residence and travel time for groundwater in the VSB formations, which is supported by the longer 14C apparent ages of these more evolved water types. Heavier mineralization of groundwater occurs in phase with higher total dissolved solids contents. Comparison of groundwater geochemical data with guidelines of the World Health Organization (WHO) for drinking water shows that groundwater in the Northern Regions of Ghana is generally of good quality. In the VSB, certain groundwater quality issues arise in wells located in the geological formations of the Oti-Pendjari group, in which WHO guidelines exceedances are often recorded for arsenic, fluoride, lead, chloride and nitrates. High fluoride concentration are also observed in intrusive rocks and metamorphized Precambrian basement formations, notably in the Bongo-Bolgatanga area. Groundwater in the Obosum group may display mediocre quality with regard to iron, lead and chloride. While groundwater quality is primarily controlled by the geology and mineralogy of formations through which it flows, pumping equipments or metal casings utilized for well installation may however be responsible for elevated iron and manganese recorded at certain wells. Additionally, nitrates and nitrites contamination, which is stricly point-specific in the project area, could originate from human and agricultural activities taking place at the surface.

Groundwater recharge was initially evaluated using two methods, the soil moisture balance (SMB), based on climate data, and the unsaturated zone chloride mass balance (CMB), based on analyses of porewater extracted from soil samples collected under HAP. Estimated recharge rates for these methods range from 1.8 to 15.9 % (19-205 mm) of average annual rainfall for the SMB and 1.1 to 7.8 % (12-80 mm) of average annual rainfall for the unsaturated zone CMB. Since previous work suggests that localized recharge represents a major portion of the overall recharge, the saturated zone CMB was also implemented to better assess the overall recharge processes and magnitude. Resulting recharge estimates derived from shallow groundwater samples collected in hand-dug wells range from 0.5 to 36.5 % (5-389 mm) of average annual rainfall. Estimated groundwater production would represent a relatively small proportion of the estimated recharge, between 0.1 % and 1.3 % of average annual recharge from SMB estimates. Groundwater could thus provide a greater supply of potable water in northern Ghana, either for rural communities or small towns.

Although current groundwater production in Ghana is considered to have a minor effect on the regional water balance, efforts should be maintained and increased towards ensuring the sustainable management of groundwater resources since an increase in groundwater production is thought to be imminent. While this project has provided a basis for such an approach by synthesizing available hydrogeological data and consolidating existing databases, additional work is still required to improve knowledge and understanding of northern Ghana hydrogeology. As new hydrological and hydrogeological data becomes available and the GIS-based database instituted within the Water Resources Commission (WRC) is updated, some of the analyses carried out in this project should be revisited to confirm or refute observations reported here. For reliable and continuous datasets, groundwater level data could also be used to evaluate groundwater recharge and improve understanding recharge/discharge processes.

Continued groundwater quality monitoring will also provide a valuable dataset required for adequate groundwater resource development and management in the North of Ghana.

The present final HAP technical report could be thought as the first of regular reports on the state of groundwater resources in the north of Ghana. In order to maintain the WRC hydrogeological database and continuously enhance the knowledge and understanding of groundwater resources, it is necessary to regularly report on the state of the resources (on a 5-year basis). Such reports should include the following sections: 1) an inventory of data and reports integrated in the WRC hydrogeological database, 2) an analysis of the acquired groundwater monitoring data and interpretation of temporal trends in terms of groundwater availability, 3) an update of the estimation of groundwater use and of the population access to a reliable water source, including groundwater, and 4) the identification of arising issues and concerns related to groundwater resources, and recommendation of the relevant key studies that could takle these issues. Such a report could also document the state of surface water resources, so as to form a basis for the informed management of all water resources and could also eventually cover the whole of Ghana, rather than only its northern part.

TABLE OF CONTENTS

TABLES

FIGURES

APPENDICES

LIST OF ACRONYMS AND ABBREVIATIONS

CGIAR	Consultative Group for International Agriculture Research
CIAT	International Centre for Tropical Agriculture
CIDA	Canadian International Development Agency
CMB	Chloride mass balance
CSI	Consortium for Spatial Information
CSIR	Council for Scientific and Industrial Research (Ghana)
CWSA	Community Water and Sanitation Agency (Ghana)
DANIDA	Danish International Development Agency
DEM	Digital Elevation Model
FAO	Food and Agriculture Organization of the United Nations
GDRC	Global Runoff Data Centre
GEF	Global Environment Facility
GGS	Ghana Geological Survey Department
GIS	Geographical Information System
GLOWA	Globalen Wasserkreislauf (Global Change in the Hydrological Cycle)
GoG	Government of Ghana
HAP	Hydrogeological Assessment Project of the northern regions of Ghana
HSD	Hydrological Service Department (Ghana)
IUSS	International Union of Soil Science
IWMI	International Water Management Institute
MSD	Ghana Meteorological Services Department
NASA	National Aeronautics and Space Administration (USA)
NDPC	National Development Planning Commission (Ghana)
NGO	Non-governmental organization
PCB	Precambrian basement
pET	Potential evapotranspiration
PSA	Particle size analysis
SD	Standard deviation
SMB	Soil moisture balance
SRI	Ghana Soil Research Institute
SRTM	Shuttle Radar Topographic Mission (NASA)
SWERA	Solar and Wind Energy Resource Assessment
UNEP	United Nations Environment Programme
UNICEF	United Nations International Children's Fund
USDA	United States Department of Agriculture
VSB	Voltaian sedimentary basin
WHO	World Health Organization
WRC	Water Resources Commission (Ghana)
WRI	Water Research Institute (Ghana)
WSSPS2	Water and Sanitation Sector Program Support (second phase)
WTB	Water table fluctuation
WVI	World Vision International

1. INTRODUCTION

1.1 Background

Following a competitive process, the SNC-Lavalin Inc. and Institut National de la Recherche Scientifique – Centre Eau, Terre, Environnement (INRS-ETE) Joint Venture was selected as Canadian Executing Agency (CEA) for the Hydrogeological Assessment Project (HAP) in the northern regions of Ghana. Implemented in conjunction with the Water Resource Commission (WRC) of Ghana, the key project stakeholder, the HAP was originally a 30 month project which has been extended until March 2011.

The HAP contributed to the collection and analysis of scientific data on groundwater with the long term objective of improving groundwater resource management and development in the northern regions of Ghana, and thus played a role towards achieving the WATSAN targets set within the Ghana Poverty Reduction Strategy through "…and enhanced knowledge base and understanding of the hydrogeological conditions in the north of Ghana".[1]

1.2 Project Goal and Objectives

The Project Goal is to "*improve groundwater resource management and development in the north of Ghana*". The Project Purpose is to "*improve the knowledge base and understanding of the hydrogeological setting in the north of Ghana*", and to "*contribute to the capacity development primarily of the personnel of the Water Resource Commission (WRC) and its partner institutions in technical and institutional aspects of groundwater planning and development*".

As such, the targeted Project outcomes are:

- Increased access, by Ghanaian water resources institutions and other relevant agencies, to accurate groundwater resource information for the north of Ghana;
- Enhanced technical and institutional capacity of Ghanaian water resource institutions in the collaborative management of groundwater resources, integrating the use of gender analytical tools for analyzing planning data.

1.3 Methodology and Report Structure

This present report is the final technical report documenting the work and analyses carried out during the HAP. It covers the period from January 2006 to March 2011 and has been prepared in collaboration with the HAP WRC counterpart and the CEA Team members. This final report presents work carried out for the following activities:

- Inventory and review of available data (sections 3 & 4)
- Complementary field work (section 4)
- Hydrogeological synthesis (section 5)

An overview of the role of groundwater in water supply in Ghana is also presented in section 2 to describe the context into which this project was initiated. The data inventory and review, which were crucial to the subsequent activities, required a significant amount of time and resources to be dedicated to finding and gathering available information. This activity notably allowed the collection of key hydrogeological project reports and databases scattered in various organisations involved in the groundwater sector of northern Ghana, such as the private sector, donor agencies, NGOs and government institutions. Concurrently, scientific papers, theses and technical reports dealing directly or indirectly with the hydrogeology of northern Ghana were also collected. These documents were subsequently reviewed and catalogued into a digital library in order to preserve and facilitate their distribution to relevant stakeholders in Ghana. As

[1] Memorandum of Understanding between the Government of Canada and Ghana for the Hydrogeological Assessment Project (April 2005)

for available databases, their content was validated and then consolidated into one unique database for a more efficient use.

Complementary field work was also carried out in order to fill specific data gaps identified prior to or at the beginning of the project through a consensus-building approach. This notably included construction of monitoring wells to supplement the existing monitoring network, borehole geophysical surveys and pumping tests for the new monitoring wells, groundwater sampling campaigns for new and existing wells and specific field work related to groundwater recharge evaluation.

Subsequent to these activities, a hydrogeological synthesis was prepared using the information and data collected. During the analyses and review of these data, emphasis was placed on regional hydrogeology in order to support groundwater resources development and management for the northern regions. In addition to a summary of hydrogeological contexts and typical hydraulic characteristics of aquifers, the preparation of this synthesis comprises a regional water balance, groundwater recharge evaluation and groundwater geochemical characterization.

This report is accompanied by an atlas containing maps that summarize available information, interpreted data and main results of the HAP. The maps are grouped under the following themes: physiography, hydrology, geology, and hydrogeology. For convenience, simplified versions of some of these maps are also presented in this report.

2. GROUNDWATER AS WATER SUPPLY IN GHANA

This chapter presents an overview of the role and importance of groundwater as a source of potable water in northern Ghana. A short summary of the socio-economical context and the population and settlement patterns in the northern regions is first presented as complementary information. Subsequently, data on water supply coverage is presented, followed by a sub-section on the role and growing importance of groundwater as water supply in Ghana.

2.1 Social and economic activities of northern Ghana

It is evident that during the pre-independence era, education suffered as a priority of human development. This educational disparity served to preserve the status of the north as labour reserve for the mines and the plantations in the south. The only effective opportunity for economic advancement during the first half of the 20th century for the people of the north was migration south or subsistence agriculture.

As northern Ghana is part of the guinea zone, it is characterized by less favorable conditions for agriculture than in the south. Not only does rainfall decreases the further north one travels in Ghana, but the rain is also concentrated in shorter periods with characteristic torrential rains. As a result of the higher run-off induced by this rainfall pattern and of soils poor in organic matter, crop production can only take place in one, often erratic, season. Yet, despite these more difficult conditions, many more households in northern Ghana are dependent on agriculture than in southern Ghana (72 % versus 44 %).

The land-locked nature of northern Ghana, linked to the Coast by a single road passing through the Kumasi metropolis, severely limits alternative economic opportunities. Only a small percentage of the workforce is made up of professionals, administrative or clerical staff, while a more significant proportion is into sales, services, and transport and production. The highest proportion of the workforce in the rural setting (~ 88%) is in agriculture while in the urban and municipalities, the majority of the workforce (~ 55%) is engaged in sales, services, and transport and production. In both the rural and urban settings, the proportion of males in agriculture and related activities in the north of Ghana is higher than that of females.

2.2 Population and settlement patterns

Northern Ghana constitutes about a third of the country’s land mass and accommodates about 20% of the population. The area is characterized by dispersed settlement. The pattern derives basically from a system of fixed cultivation, which is rare in tropical areas. The layout of a house reflects family structure; similarly, patterns of land holdings reflect stages in community evolution. Originally circular, home-farms are divided by inheritance into radial strips, diminishing in size over the generations. Settlement dispersal commences with domestic fission within agnatic lineages. Society is strongly patriarchal, and ancestor-worship has a powerful influence. Study of lineage affiliation indicates a spread of settlement from ancestral core areas, usually in defensible hilly areas. Because of high per capita cost of provision of services, there is a need to concentrate settlement, if any degree of modern development is to be achieved. Lack of a major cash crop to finance local development is one obstacle, but greater still are the social difficulties confronting any attempt to re-cast the settlement pattern.

2.3 Water supply coverage

Water supply coverage in Ghana would be around 64 % of the total population according to data from the World Health Organization and UNICEF (2000) (Figure 2-1). From the same report, it is stated that 87 % of the urban population (~ 6.7 M inhabitants) and 49 % (~ 6.1 M inhabitants) of the rural population had access to safe[2] and adequate water supply in 2000.

Figure 2-1 – Water supply coverage in Africa (data from WHO-UNICEF, 2000)

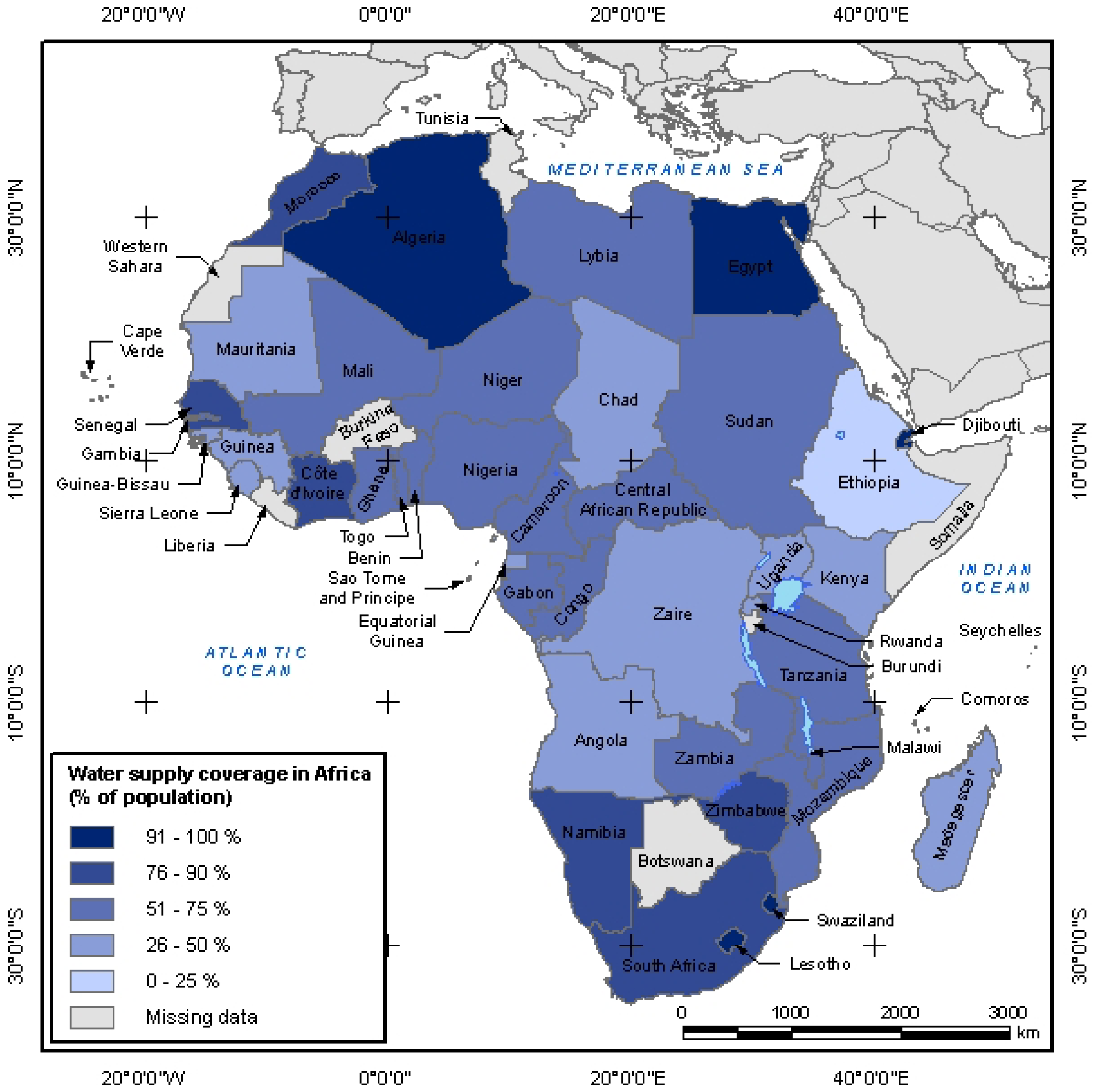

[2] Definition of safe access: 1) CWSA: All-year-round potable water supply of 20 L per capita per day for point sources and 45 L per day for small towns (piped schemes); facility should be within 500m walking distance from farthest house in community and should serve 300 persons per borehole/standpipe and 150 persons for hand dug wells; 2) WHO-UNICEF: Availability of at least 20 L per person per day from an "improved" source within 1km of user's dwelling (N.B.: see WHO-UNICEF, 2000 for "improved" source definition).

There are, however, inconsistencies concerning water supply coverage data in Ghana (Table 2-1). For instance, data from the World Resources Institute (2003) indicate that percentages of households that had access to safe water in 2000 were respectively of 91 and 62 % in urban and rural areas. While not always in agreement, available data clearly indicates that mean water supply coverage has been steadily increasing in both rural and urban areas for the last few years, but that water supply coverage is consistently lower in rural areas (Figure 2-2).

Figure 2-2 – Data trend on access to safe water supply for urban & rural areas of Ghana

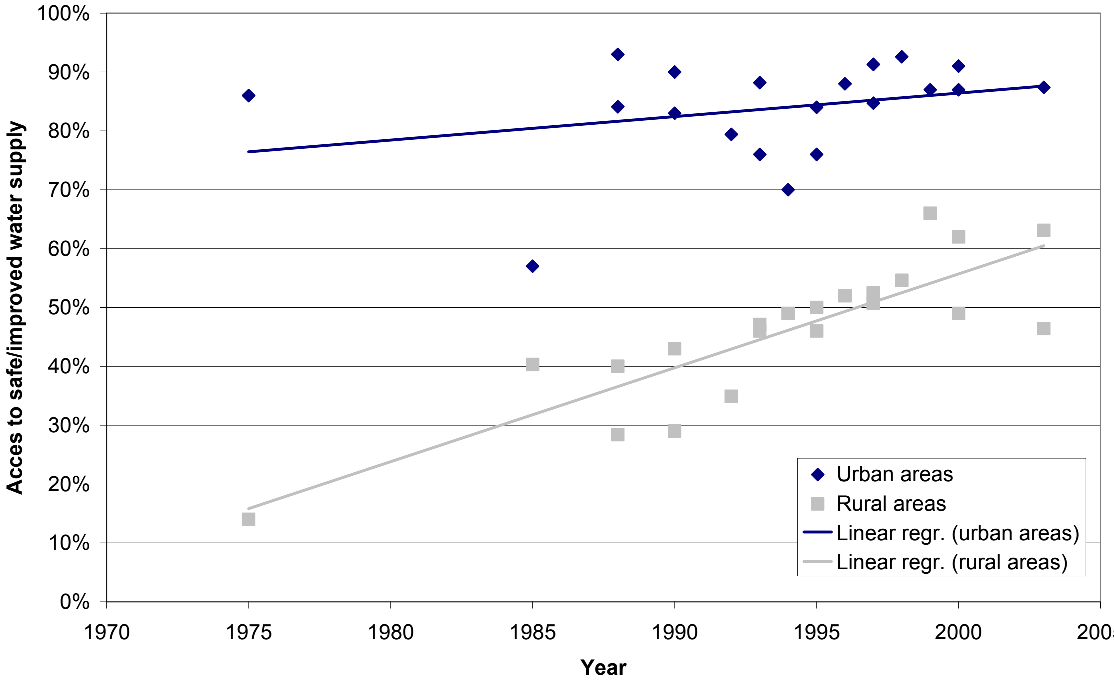

Table 2-1 – Safe water supply coverage data for urban & rural areas in Ghana

Year	Access to safe water supply (% of population)			References
	Overall	Urban	Rural	
1975	-	86 %	14 %	International Monetary Fund, 2000
1985	-	57 %	40 %	International Monetary Fund, 2000
1988	-	84 %	28 %	World Health Organisation and UNICEF, 2004
	-	93 %	40 %	African Development Bank, 2004
1990	-	83 %	43 %	World Health Organisation and UNICEF, 2000
	-	90 %	29 %	Food and Agriculture Organization, 1995
1992	51 %	79 %	35 %	Centre for Policy Analysis, 2002
1993	-	76 %	46 %	African Development Bank, 2004
	-	88 %	47 %	World Health Organisation and UNICEF, 2004
1994	-	70 %	49 %	African Development Bank, 2004
1995	-	76 %	46 %	International Monetary Fund, 2000
	-	84 %	50 %	World Health Organisation and UNICEF, 2004
1996	-	88 %	52 %	African Development Bank, 2004
1997	67 %	91 %	53 %	Centre for Policy Analysis, 2002
	62 %	85 %	51 %	International Monetary Fund, 2005
1998	-	93 %	55 %	World Health Organisation and UNICEF, 2004
1999	-	87 %	66 %	African Development Bank, 2004
2000	-	91 %	62 %	World Resources Institute, 2003
	-	87 %	49 %	World Health Organisation and UNICEF, 2000
2003	74 %	87 %	63 %	International Monetary Fund, 2005
	-	-	46 %	National Development Planning Commission,2004

2.4 Role and importance of groundwater

Groundwater plays a vital role as the source of water for supply schemes throughout Ghana since it is well suited to meet the dispersed demand inherent in settlement patterns of rural populations. Generally of good quality (microbiological and chemical), groundwater can usually be available relatively close to demand and its development as rural water supply is cheaper when compared to surface water supply schemes. Furthermore, deep groundwater sources generally have a slow response to changes in rainfall, making it generally less vulnerable to drought than surface water bodies such as lakes and rivers.

Traditionally, various sources have been used for domestic water supply in Ghana, including streams, rivers, lakes, ponds, dug-outs, impoundment reservoirs, springs, rain harvesting and hand-dug wells (Dapaah-Siakwan and Gyau-Boakye, 2000). Some problems are however associated with those sources, such as contamination of surface water (bacteriological or chemical), insufficient quantity of water from rain harvesting or from hand-dug wells in dry season.

Considering problems associated with alternate sources of water and the fact that groundwater is often considered one of the most economical and feasible sources of potable water supply, groundwater resources are being increasingly utilized in Ghana in order to meet the rising water supply needs. In fact, following the 1969-1970 Water Resources Sector Studies commissioned by the Government of Ghana, it became official policy to use groundwater for water supply in rural communities with less than 2 000 inhabitants (Gyau-Boakye and Dapaah-Siakwan, 1999). Following recommendations from the same source, rural communities with 2 000-5 000 inhabitants were to be supplied with piped systems using surface water or groundwater.

Although it is difficult to state the exact percentage of the national population depending on groundwater resources from available information, data from the 1998-1999 Ghana Living Standards Survey (GLSS) indicates that at least 33.9 % of the overall population relies directly on hand-dug wells and boreholes (i.e. drilled wells) fitted with handpumps (see Table 2-2) (NDPC, 2003). The total number of wells in Ghana would exceed 60 000, with approximately 15 000 boreholes and 45 000 hand-dug wells (Agyekum, 2004). The percentage of population depending on groundwater resources is however probably higher since the origin of water (i.e. surface water or groundwater) is usually not specified for piped systems and natural sources (e.g. springs, surface water or well fields …). Other water-supply related data derived from research in the Ghanaian portion of the Volta River Basin reveals that 37.6 % of the population living in the Basin (estimated to 6.91 M) was dependant on groundwater in 2001 (all sources included – piped systems, boreholes, hand-dug wells) (Martin and van de Giesen, 2005). While the latter percentage may not be representative of the whole country, it can give, with the 1998-1999 GLSS value, a general idea of the range to be expected.

Table 2-2 – Source of drinking water in Ghana (NDPC, 2003)

Source of drinking water	Ghana	Urban (> 5000 persons)	Rural (< 5000 persons)
Pipe-borne	41.6 %	80.3 %	18.8 %
Borehole / well	33.9 %	10.8 %	47.2 %
Natural sources	24.6 %	8.8 %	33.9 %

Moreover, rural communities account for an increasingly larger fraction of the overall population dependant on groundwater. According to Gyau-Boakye (2001), approximately 52 % of the rural population relied on groundwater resources (all sources included) for water supply in 1998 as compared to a proportion of 41 % estimated in 1984. While groundwater is particularly important in rural areas, its role is also crucial in some urban areas of Ghana such as the Upper East and Upper West Regions, where more than 80 % of the urban population is served by groundwater-fed piped systems (Martin and van de Giesen, 2005).

As for any type of water supply, some difficulties arise from the development of groundwater resources in Ghana. Because of low population density and poor economic base, point sources such as hand-dug wells and boreholes fitted with handpumps are mainly utilized in groundwater development. As mentioned earlier, low drilling success[3] rate (below 50 %) and high variability of well yields are frequent in some regions due to various factors such as lacking or unavailable information on hydrogeological framework or simply because of the nature and complexity of the geological and hydrogeological environments. Overexploitation of aquifers has also been reported in some regions as a result of excessive reliance on groundwater resources, poor design criteria and inadequate abstraction rate (Gyau-Boakye, 2001). Although chemical and bacteriological quality of groundwater in Ghana is generally acceptable, localized problems, from natural or anthropogenic origin, have been identified. The most notable problems include high concentrations of iron (causing aesthetic problems mostly), manganese, and fluoride (causing health problems such as dental and possibly skeletal fluorosis) (Gyau-Boakye, 2001). In addition to these problems, other factors affecting the water supply sector in general include insufficient technical and managerial water sector personnel and inadequate or insufficient regulations of water resources development and management. There has however been recent progress on this front as a comprehensive national water sector policy was published in June 2007 (GoG, 2007) to integrate and harmonize the various activities of key stakeholder institutions. In September 2006, regulations were also approved concerning the mandatory registration of well drillers for groundwater development (WRC, 2006).

[3] The success rate generally refers to the number of successful boreholes divided by the total number of boreholes drilled; the definition of a successful borehole is variable but handpump yield (i.e. ~ 13 L/min) is often considered as the minimum yield for success (Dapaah-Siakwan and Gyau-Boakye, 2000).

3. DESCRIPTION OF THE STUDY AREA

This section presents the main characteristics of the study area and is aimed at complementing the hydrogeological synthesis presented in section 5. Data and information used to prepare this section were collected concurrently to existing hydrogeological data and were usually readily available (see section 4.1).

Ghana is located on the south central coast of West Africa between latitudes 4°44'N and 11°11'N and longitudes 3°15'W and 1°12'E. The study area roughly consists of the upper half of the country and is located between latitudes 7°58'N and 11°11'N and longitudes 2°57'W and 0°34'E (Figure 3-1). It comprises the three northern regions of Ghana, namely the Upper East Region, Upper West Region and Northern Region, which respectively account for 9 %, 19 % and 72 % of the total study area (97 704 km^2). The northern regions are bordered by Côte d'Ivoire to the west, Burkina Faso to the north, Togo to the east and the Volta and Brong-Ahafo regions of Ghana to the south.

Figure 3-1 – Location map of study area (northern Ghana)

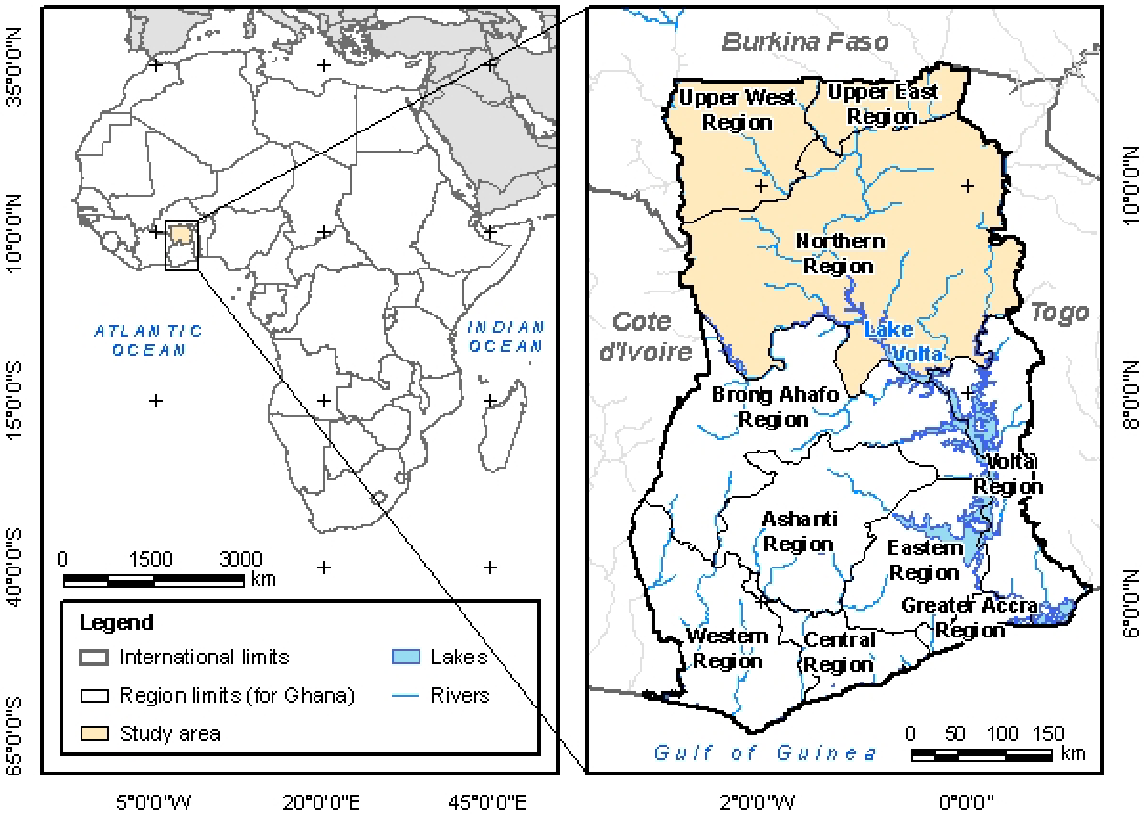

As of 2000, the respective population of the Upper East, Upper West and Northern regions was 920 089, 576 583 and 1 820 806, with 73 % to 84 % being rural (Ofei, 2003). Rural communities are scattered throughout the study area except for a few zones such as protected areas or floodplains where agriculture is not possible or not viable. The urban population is mostly concentrated in the regional capitals, respectively Bolgatanga, Wa and Tamale. Table 3-1 lists the official districts in these regions as of 2011 (http://ghanadistricts.com) and the corresponding old districts that existed at the beginning of the project. As some of the official districts were recently created, official district limits were not yet available in electronic format so that corresponding old district limits were used for analysis purposes.

The northern regions are relatively underdeveloped in comparison to the other regions of Ghana, with about 75 % of the active population engaging in food crop farming. As of 1999, poverty by income measure was highest in the three regions of northern Ghana (84 % in Upper

West, 88 % in Upper East and 69 % in Northern) with food crop farmers having the highest incidence of poverty (NDPC, 2003). Environmental and social indicators for northern Ghana are below national average notably for education, health, nutrition and access to potable water (CIDA, 1999). While efforts have been made to transfer power and responsibilities from central to local government in order to improve conditions, progress has been slow and the positive impact of economic growth and development at national scale is not as significant in the north as it is in the south.

Table 3-1 – District names for the northern regions of Ghana

	Official district names (2011)		Corresponding district names (2005)	
Region	**District name**	**District ID**	**District name**	**District ID**
Northern	Bole	06-01	Bole	06-01
	Bunkpurugu-Yunyoo	06-02	East Mamprusi	06-03
	Central Gonja	06-03	West Gonja	06-10
	Chereponi	06-04	Saboba Chereponi	06-06
	East Gonja	06-05	East Gonja	06-02
	East Mamprusi	06-06	East Mamprusi	06-03
	Gushiegu	06-07	Gushiegu Karaga	06-04
	Karaga	06-08	Gushiegu Karaga	06-04
	Kpandai	06-09	East Gonja	06-02
	Nanumba North	06-10	Nanumba	06-05
	Nanumba South	06-11	Nanumba	06-05
	Saboba	06-12	Saboba Chereponi	06-06
	Savelugu Nanton	06-13	Savelugu Nanton	06-07
	Tamale Metropolitan	06-14	Tamale	06-08
	Sawla-Tuna-Kalba	06-15	Bole	06-01
	Tolon Kumbungu	06-16	Tolon Kumbungu	06-09
	West Gonja	06-17	West Gonja	06-10
	West Mamprusi	06-18	West Mamprusi	06-11
	Yendi	06-19	Yendi	06-12
	Zabzugu Tatale	06-20	Zabzugu Tatale	06-13
Upper East	Bawku Municipal	07-01	Bawku East	07-01
	Bawku West	07-02	Bawku West	07-02
	Bolgatanga Municipal	07-03	Bolgatanga	07-03
	Bongo	07-04	Bongo	07-04
	Builsa	07-05	Builsa	07-05
	Garu-Tempane	07-06	Bawku East	07-01
	Kassena Nankana West	07-07	Kassena Nankana	07-06
	Kassena Nankana	07-08	Kassena Nankana	07-06
	Talensi-Nabdam	07-09	Bolgatanga	07-03
Upper West	Jirapa	08-01	Jirapa Lambussie	08-01
	Lambussie Karni	08-02	Jirapa Lambussie	08-01
	Lawra	08-03	Lawra	08-02
	Nadowli	08-04	Nadowli	08-03
	Sissala East	08-05	Sissala	08-04
	Sissala West	08-06	Sissala	08-04
	Wa Municipal	08-07	Wa	08-05
	Wa East	08-08	Wa	08-05
	Wa West	08-09	Wa	08-05

3.1 Physiography

Three broad physiographic regions can be distinguished in northern Ghana: 1) savannah high plains covering all of Upper East and Upper West regions and the western part of the Northern Region, 2) Voltaian sedimentary basin (VSB) covering most of the remainder of the Northern Region and 3) scarps bordering the VSB, also found within the Northern Region. The whole country is generally classified as lowland, with less than 10 % of the country above 300 m elevation. In the study area, the highest areas are located around Gambaga and Damongo scarps while the lowest areas are found in the middle of the VSB (Figure 3-2). Hills can rise as much as 300 m above plains and valleys (Gill, 1969) and inselbergs can mostly be found in the northwest part of the study area.

Figure 3-2 – Topography of northern Ghana (data from CIAT, 2004)

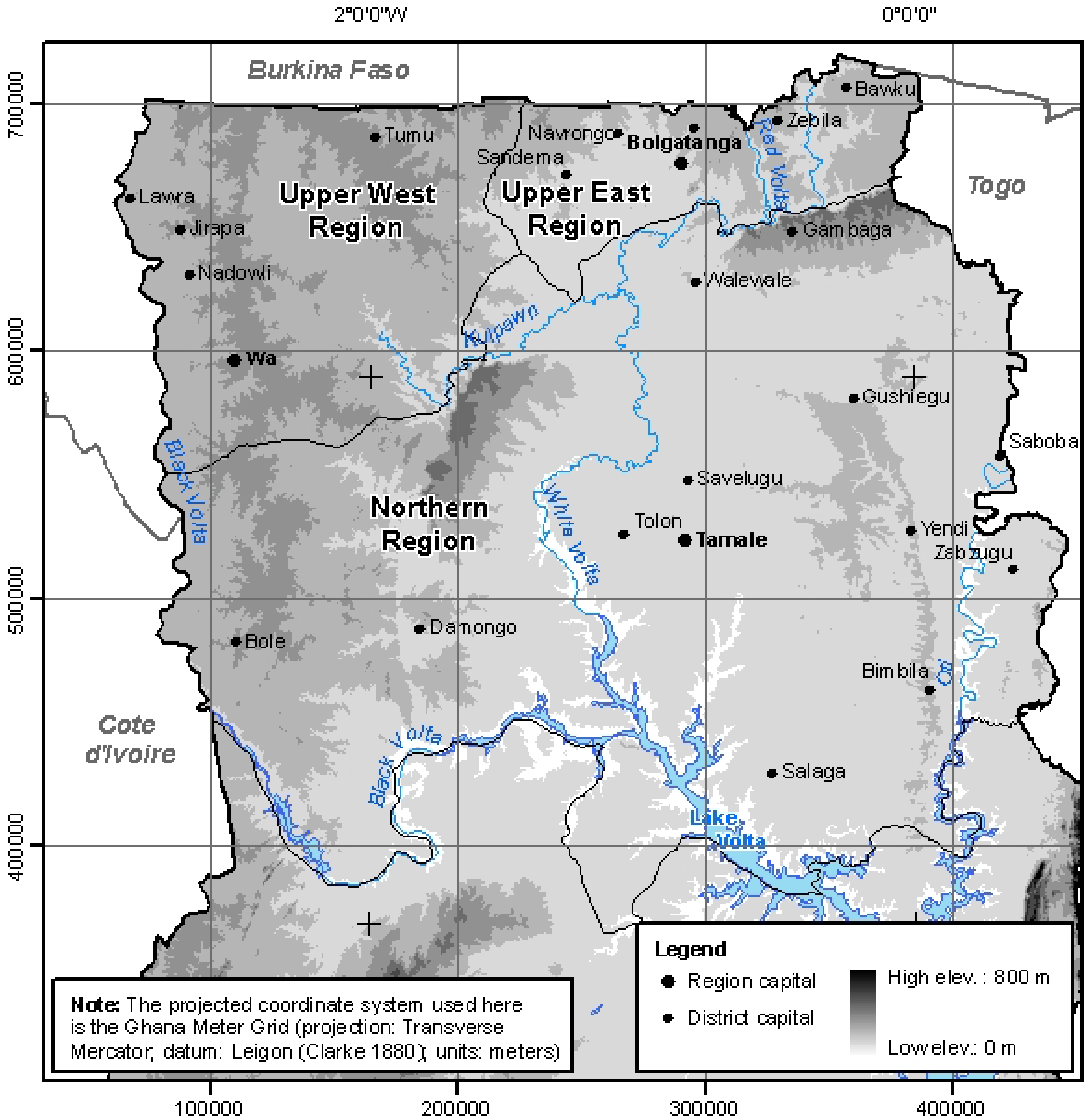

3.2 Vegetation

From south to north, vegetation grades from equatorial rain forest in the extreme southwest of the country, through a transition zone to a belt of moist semi-deciduous tropical forest. Towards the north, the semi-deciduous tropical forest grades into another transition zone and eventually into the Guinea savannah, where woodland predominates over grassland. The latter zone covers most of northern Ghana (Figure 3-3) except for a small portion in the extreme northeast, where it is gradually replaced by the Sudan savannah, where grassland prevails over woodland (Gill, 1969).

In northern Ghana, three major land uses can be distinguished: cultivated savannah woodland (open and closed) (58 % of total land area), savannah woodland (open and closed) (25 %), grassland with/without scattered trees and shrubs (7 %) (Figure 3-4).

Figure 3-3 – Vegetation in northern Ghana (data from IWMI-GLOWA obtained in 2006)

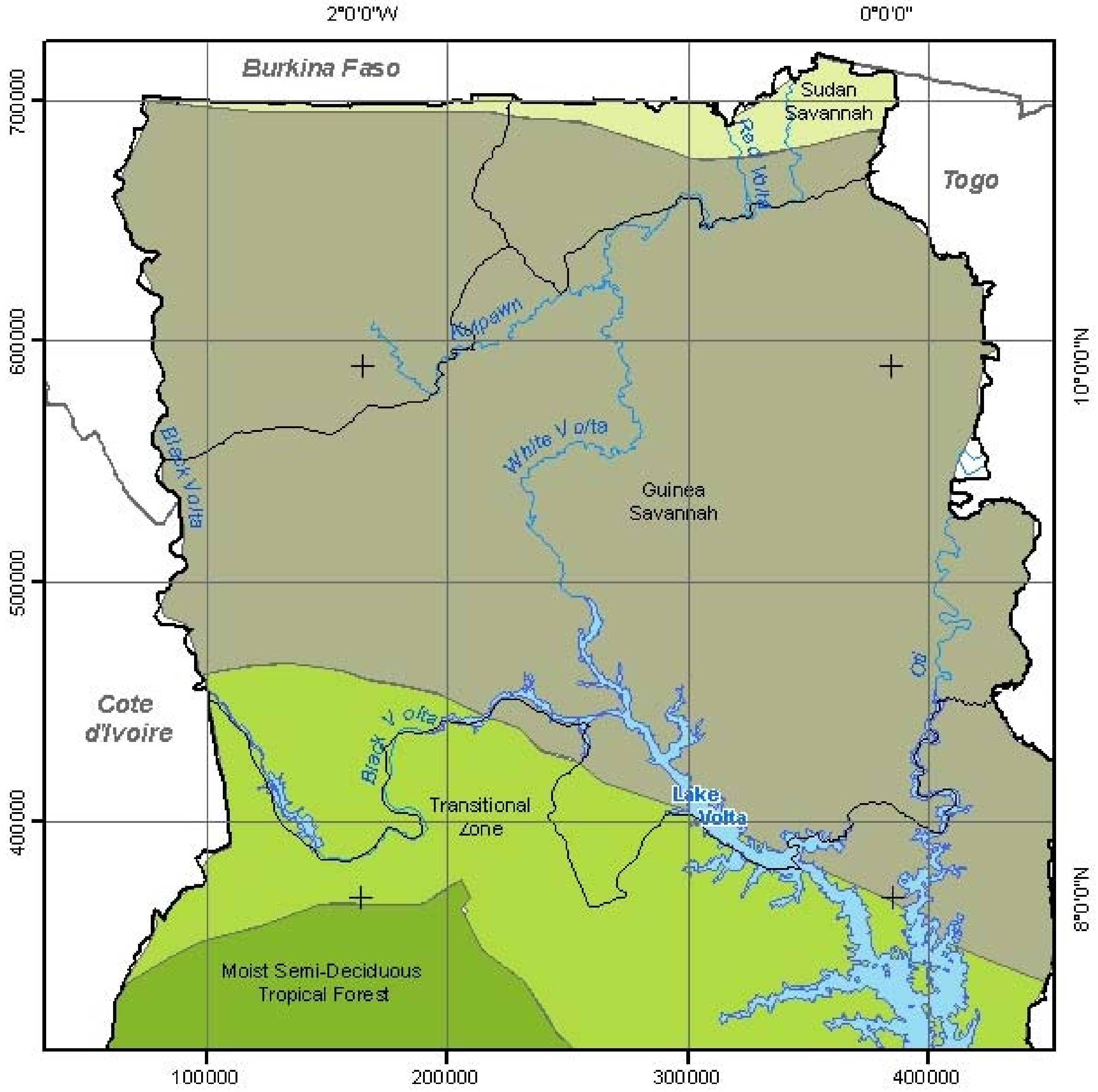

The woodland savannah is characterized by drought-resistant trees such as acacias, mango trees, shea nut trees, neems and baobabs. Land classified as cultivated is usually used for small-scale rain-fed agriculture in the form of compound or bush farming. Compound farms are located near the farmer's homes and crops grown usually include maize, vegetables and tobacco. In bush farms, which are generally located within 10 km of the community, a mixture of cereals/vegetables crops notably including maize, sorghum, millet, rice, yam, cassava and groundnuts are generally cultivated. Irrigated agriculture is also practiced in northern Ghana, though the irrigated land area only occupied about 30 km^2 as of 2000 (Braimoh, 2004). Not all land classified as cultivated is actually farmed as the small scale rain-fed plots are usually scattered among tree vegetation or grassland used for livestock grazing. Other minor land use classes notably include riverine savannah vegetation along major watercourses, grass and herb, and unclassified zones. Rock outcrops have been reported by the Ghana Geological Survey Department (GGS) field personnel but would be generally be scarce within the study area, scarp zones excepted.

Figure 3-4 – Land use in northern Ghana (data from SWERA, 2005)

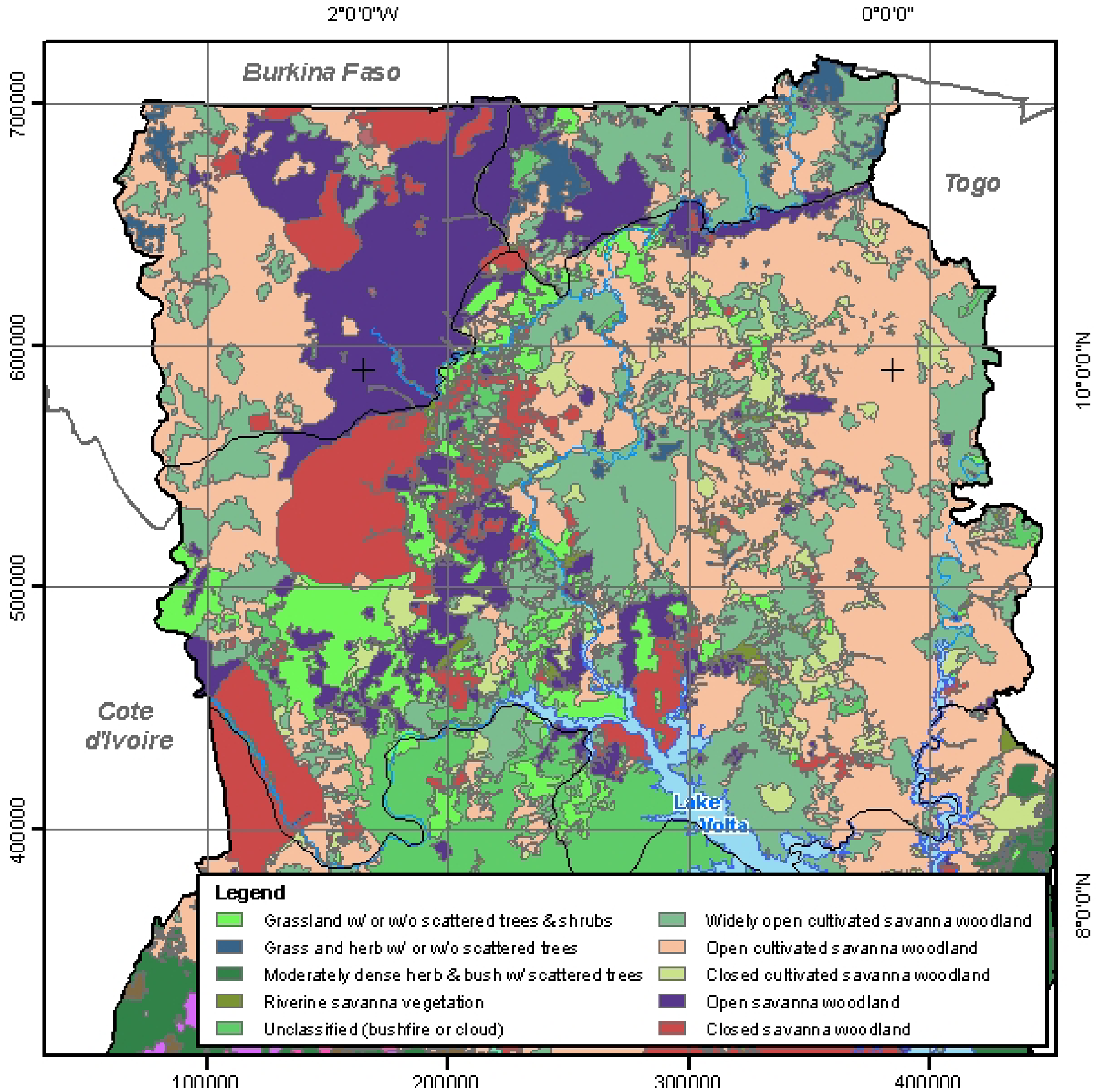

3.3 Climate

In the northern regions, as throughout Ghana, the climate is characterized by high temperatures and a variable amount, duration and seasonal distribution of rainfall. These characteristics are typical of sub-tropical, semi-arid climate zones in West Africa. Rainfall in the north of Ghana generally decreases with increasing latitude and its distribution throughout the year is uneven. Figure 3-5 shows the rainfall pattern based on annual average rainfall for the 1971-2007 period at 140 meteorological stations throughout Ghana (N.B.: 24 of these stations are located in the study area). For the study area, annual rainfall ranges from around 800 mm in the extreme north (Bongo) to 1 250 mm in the south-eastern portion of the Northern Region (Salaga). Monthly climate data were also obtained from the Ghana Meteorological Services Department (MSD) for the 1961-2005 period for six meteorological stations: Bole, Kete-Krachi, Navrongo, Tamale, Yendi, Wa (Figure 3-6). Typically, the northern regions are characterized by a single rainy season from late May to October. The intensity and duration of the rainy season varies with latitude and the extreme north usually experiences a shorter and more intense rainy season than the south. Annual rainfall values are characterized by standard deviations ranging from 15-20 % of rainfall. Work by Friesen *et al.* (2005) in the Volta River basin indicates similar but slightly lower inter-annual variability with a coefficient of variation of 8 %. For most stations, dry periods of the early 1970s and 1980s can be differentiated (Figure 3-7).

Figure 3-5 – Average annual rainfall pattern in northern Ghana (data from MSD, 2008) (N.B.: data from meteorological station with names shown in bold were used to estimate recharge using the soil moisture balance method - see Section 5.3.2)

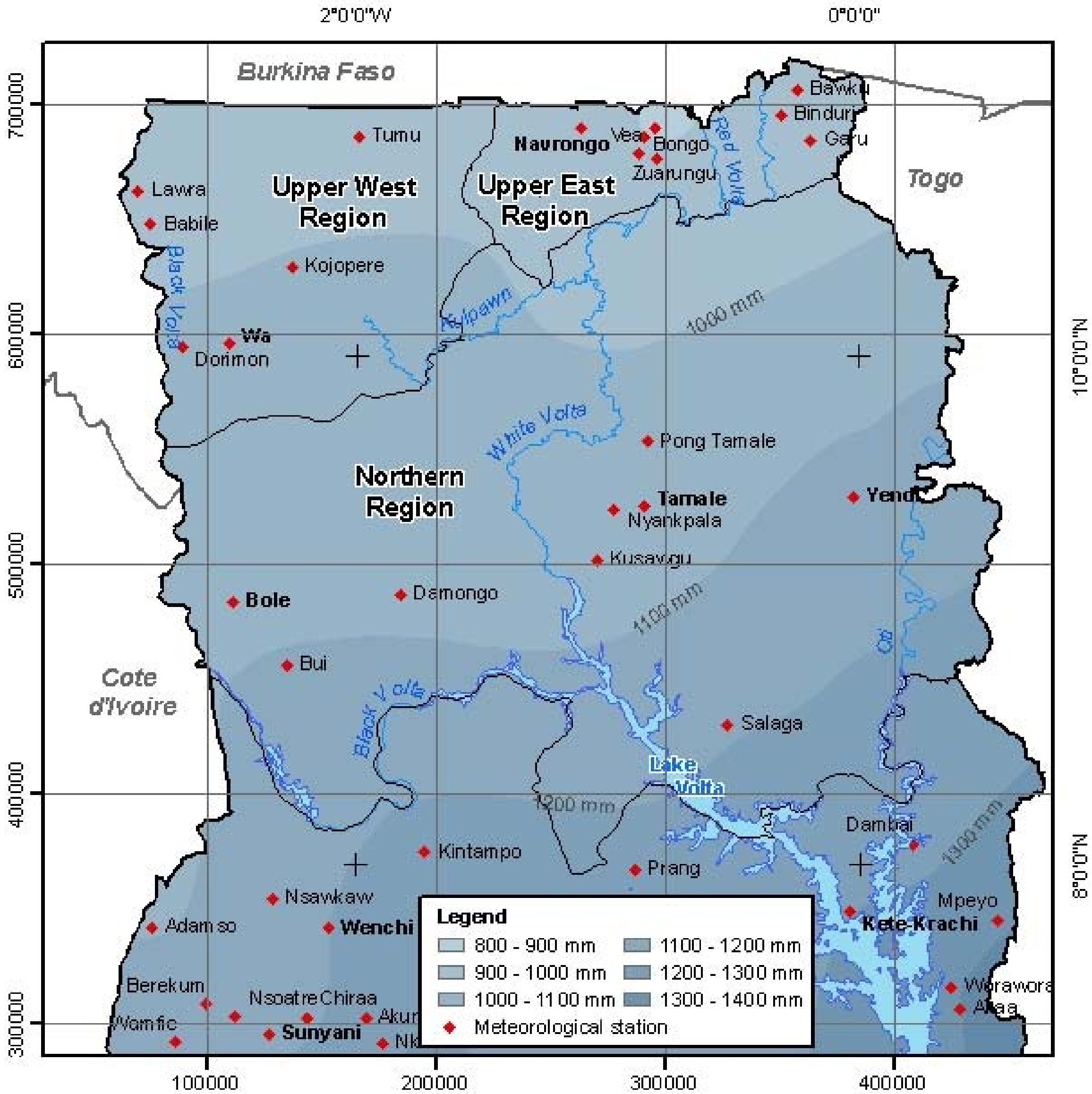

Temperatures in northern Ghana are relatively high with annual averages ranging from 27 °C to 29 °C and annual extremes ranging from about 17 °C to 40 °C. Due to the rather low relief, the major influence on temperature is the distance to the sea. Temperatures are thus cooler in the south than in the north. Based on monthly data from the Ghana Meteorological Services Department (MSD) for the 1961-2005 period, the highest monthly mean temperature generally occurs in March or April. Temperatures usually start to decrease at the onset of the rainy season, around May or June, to reach an annual low in December or January (Figure 3-6).

Potential evapotranspiration (pET) was estimated using the Penman-Monteith method recommended by the FAO as its validity has been demonstrated in humid and dry climates (Allen *et al.*, 1998). For the five meteorological stations located in the northern regions, annual average potential evapotranspiration rates derived from monthly data range from 987 to 1 192 mm per year (Table 3-2 and Figure 3-6).

For comparison purposes, the Thornthwaite method was also applied to monthly data. This method is based on air temperature rather than radiation used by the Penman-Monteith method. Results for both methods are compared in Table 3-3. They show a relatively good correlation (coefficient of determination between 0.69-0.90) but the Thornthwaite method yields much higher values in dry months than the Penman-Monteith method. This discrepancy between methods can be explained by the assumptions made by the Thornthwaite method. As this method is based on air temperature, it considers that the Bowen ratio (sensible heat flux over latent heat flux) remains constant throughout the year. The release of latent heat is however variable in time, being generally smaller in dry months when readily available water is limited. It follows that the Thornthwaite method would tend to overestimate potential values in dry periods experienced in arid and semi-arid regions. A previous study evaluating four evapotranspiration methods in Ghana (Acheampong, 1986) revealed similar observations regarding the Thornthwaite method. Equation parameters and the complete calculation procedure used for each pET estimation method are defined in Appendix A.

Figure 3-6 – Average monthly profiles for selected climate variables in northern Ghana (data from MSD, 2006)

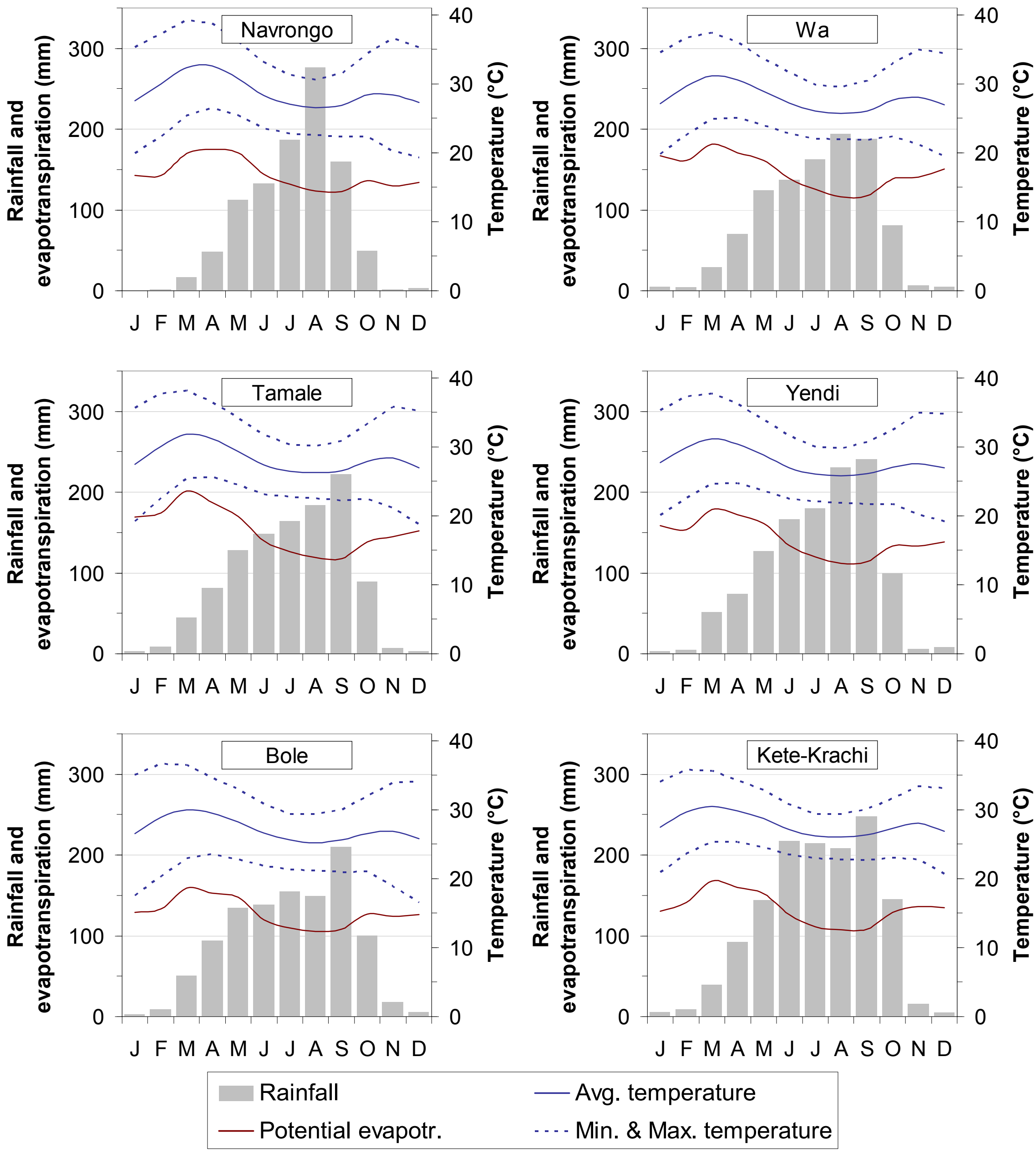

Figure 3-7 – Historical annual rainfall in northern Ghana (data from MSD, 2006)

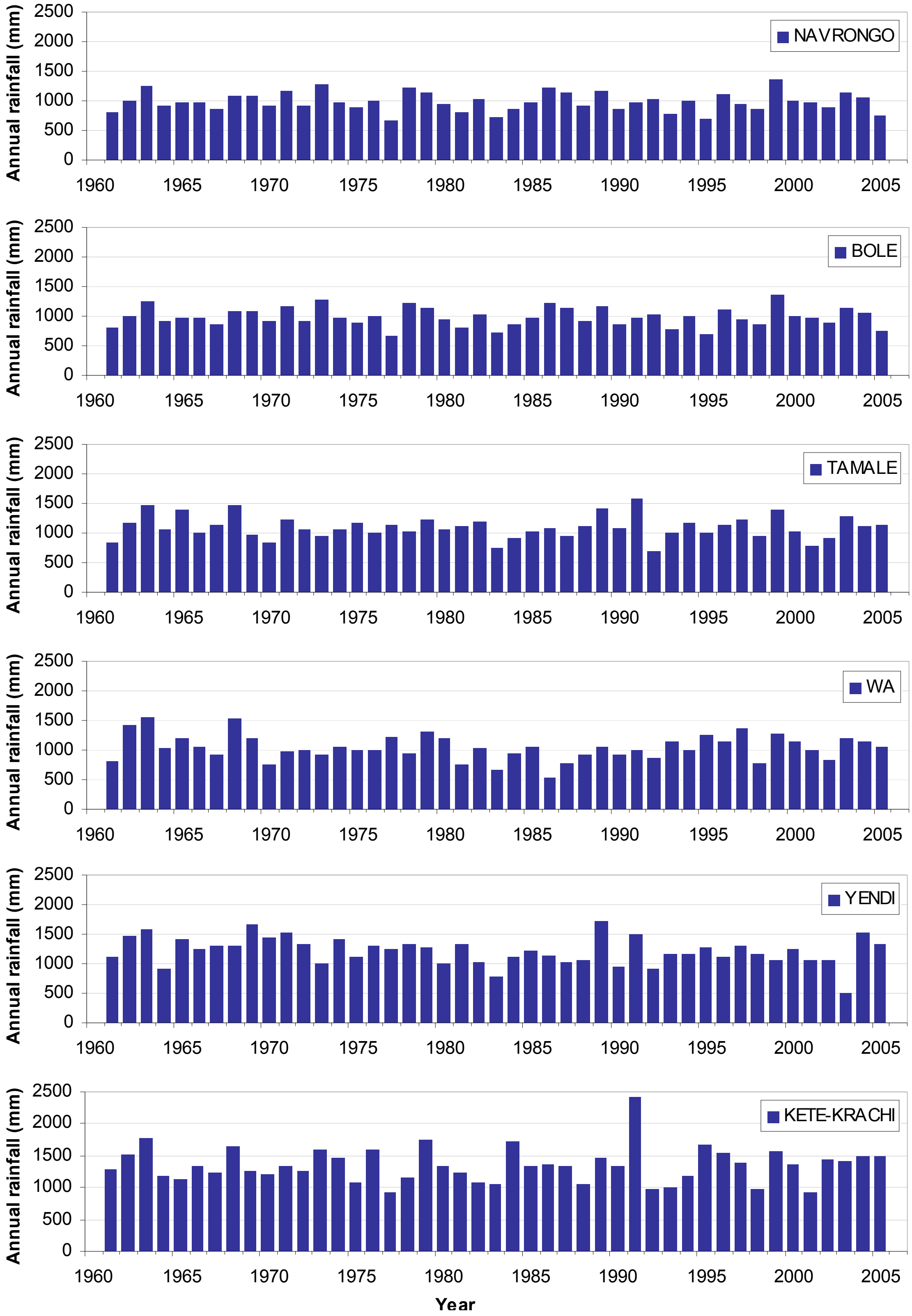

Table 3-2 – Average annual values for selected climate variables in northern Ghana (data from MSD, 2006)

Station	Navrongo	Wa	Tamale	Yendi	Bole	Kete-Krachi
Region	Upper E.	Upper W.	Northern	Northern	Northern	Volta
Rainfall (mm/y)	987	1 007	1 083	1 192	1 069	1 346
Potential evap. (mm/y)	1 723	1 770	1 839	1 710	1 541	1 606
Avg. temp. (°C)	28.9	27.9	28.3	27.9	27.1	27.8
Min. temp. (°C)	19.3	19.5	18.7	19.2	16.6	20.7
Max. temp. (°C)	39.3	37.4	38.2	37.7	36.6	35.8
Min. rel. humidity (%)	40.3	44.0	44.6	46.7	50.1	54.9
Max. rel. humidity (%)	68.8	71.8	75.9	78.0	83.9	88.9
Sun hours (h)	7.8	7.6	7.3	7.2	7.0	7.0
Wind speed (m/s)	0.91	1.25	1.57	1.26	0.84	1.10

Table 3-3 – Comparison of results for potential evapotranspiration (pET) estimation methods (derived from monthly data for the 1961-2005 period)

Station	Navrongo	Wa	Tamale	Yendi	Bole	Kete-Krachi
Region	Upper E.	Upper W.	Northern	Northern	Northern	Volta
pET ± SD (mm/y) (Penman-Monteith)	1 723 ± 145	1 770 ± 123	1 839 ± 127	1 710 ± 235	1 541 ± 98	1 606 ± 78
pET ± SD (mm/y) (Thorthwaite)	2 369 ± 286	2 028 ± 221	2 161 ± 253	2 014 ± 204	1 801 ± 171	1 987 ± 193

3.4 Hydrography

The whole project area is drained by the Volta River system which comprises the Red, Black and White Volta Rivers as well as the Oti River. These rivers, together with their basins (or watersheds) and sub-basins, are shown in Figure 3-8 and were derived from the Digital Elevation Model using the ArcGIS software hydrology functions as the basins initially obtained from the SWERA Geospatial Toolkit contained errors in some areas.

The Volta River has the most extensive basin in Ghana, draining almost three-quarters of the total land area. The river itself is also the longest in the country with a main channel of approximately 1 400 km (Andreini *et al.*, 2000). It flows out to sea near the town of Ada, in southeast Ghana and its vast basin of about 400 000 km^2 extends over five other countries: Côte d'Ivoire, Burkina Faso, Mali, Togo and Benin. Downstream of the confluence of the Black Volta and White Volta Rivers, the river is usually referred to as the Lower Volta River. The high annual variability in the amount of rainfall causes seasonal variations in the flow of many rivers, especially those in the northern regions where many streams and rivers are intermittent. River valleys are generally bordered by alluvial terraces although some rivers are guided by structural features such as escarpments.

The Black Volta which originates from Burkina Faso flows north-eastwards and then turns south and eventually becomes the border, first between Ghana and Burkina Faso and then between Ghana and Côte d'Ivoire. The Red Volta originates in the central part of Burkina Faso, near Ouagadougou, and flows south-eastwards to the border with Ghana. After crossing the border, it joins the White Volta. The White Volta originates in the north of Burkina Faso and also flows south-eastwards to the border with Ghana. Afterwards, it flows west and then more or less south into Lake Volta. In Burkina Faso, the Black, Red and White Volta are respectively known as the Mouhoun, Nazinon and Nakanbe. The Oti River takes its source in Benin and flows north-eastward at first and then sharply turns west and eventually southwest passing through Togo. It serves as border between Ghana and Togo for approximately 100 km before entering Ghana near Chereponi in the Northern Region. While some tributaries of the Volta River in northern Ghana are intermittent during the dry season, overflow often occurs in many streams and rivers during the wet season.

The flow of the Volta River itself is regulated since the construction of the Akosombo dam in the 1960s for hydro-electricity. The mean annual discharge of the river was estimated at 35 billion m^3 before the construction of the dam and at 31 billion m^3 after (Andreini *et al.*, 2000). The reservoir (Lake Volta) created by this dam and the younger Kpong dam (downstream of Akosombo) is one of the largest artificial lakes in the world covering roughly 8 500 km^2 at full capacity. Other dams are also present upstream on the White Volta (e.g. Kulpawn, Sisilli, Tono, Vea) and the Black Volta (e.g. Bui). Gauging stations operated by the Ghana Hydrological service Department (HSD) are located on the main rivers or their main tributaries: Black Volta (Bui, Bamboi stations), White Volta (Daboya, Kpasenkpe, Nabogo, Nawuni, Paga, Pwalugu, Yarugu stations), Red Volta (Nangodi station), Oti (Saboba station), Sisilli (Nakong, Wiase stations), Nasia (Nasia station) and Kulpawn (Yagaba station). The dataset provided by the HSD for these gauging stations covers the period from early 1950's to 2008 but however contains multiple data gaps of variable time length (from days to decades) (Appendix D on USB flash drive). In some cases, it was possible to fill data gaps from another streamflow dataset obtained from Global Runoff Data Centre (GRDC).

Figure 3-8 – Hydrography and majors basins in northern Ghana (derived from DEM)

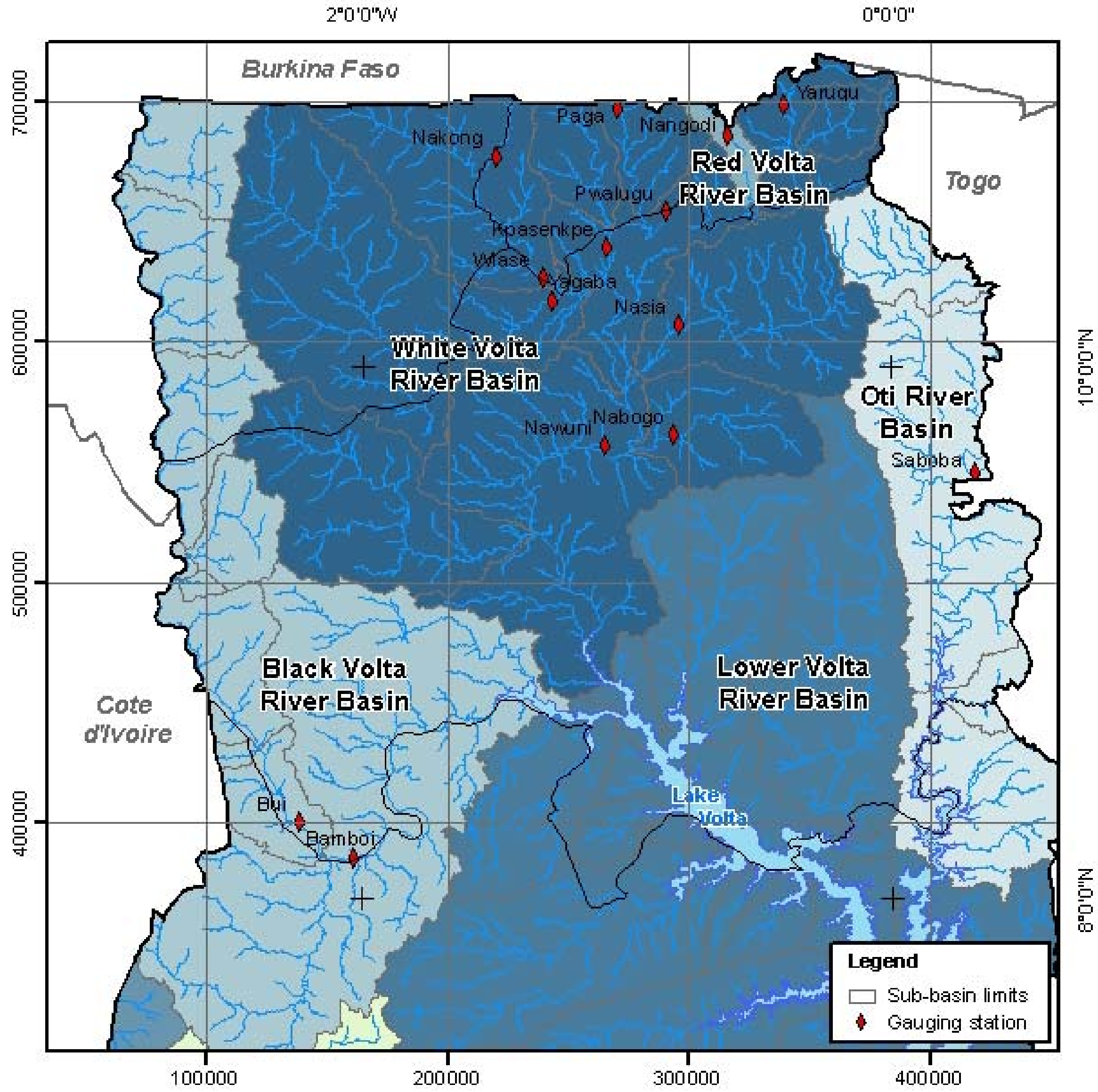

3.5 Soils

In the north of Ghana, weathered products of bedrock generally constitute the parent materials from which the soils are formed. The mineralogy of the parent rock, the degree of weathering and the different hydrological conditions encountered (e.g. along slopes) have a significant influence on the texture of the soils. Over granites and sandstones, soils will tend to develop relatively coarse textures (from coarse sands to loams) while phyllites, shales and mafic rocks will weather into finer material such as silts and fine sands. Soils developed in valley bottoms and floodplains also tend to have finer textures that can vary from sandy loams to clays. In many areas, the alternation between wet and dry conditions can favour the hardening of subsoils[4] through leaching of minerals. The organic matter content of the soils is usually low (< 2 %) as a consequence of high temperatures and annual burning of vegetation.

Figure 3-9 – Soils in northern Ghana (data from SRI obtained in 2006)

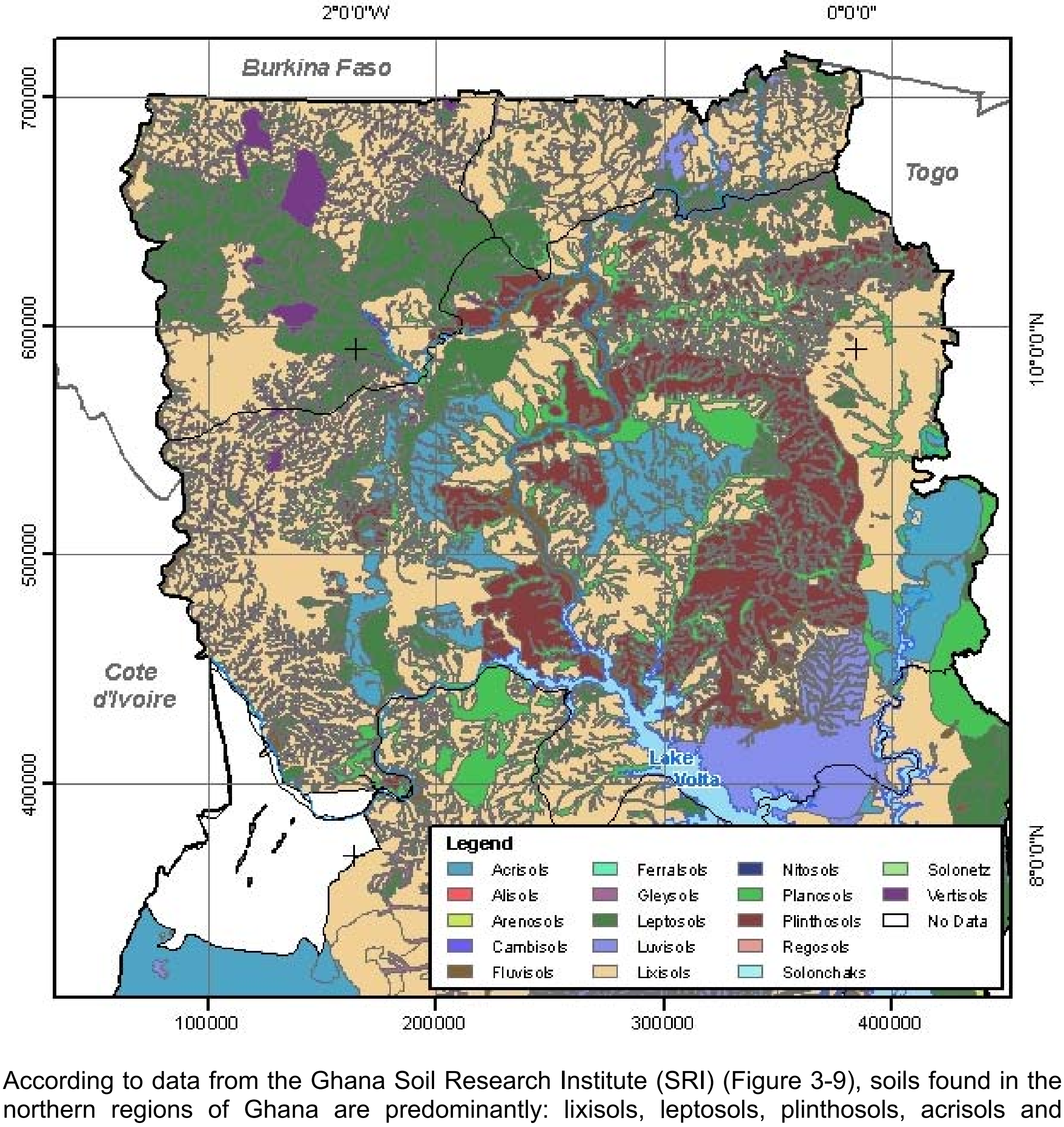

According to data from the Ghana Soil Research Institute (SRI) (Figure 3-9), soils found in the northern regions of Ghana are predominantly: lixisols, leptosols, plinthosols, acrisols and

[4] Soil portion between the layer used for farming (i.e. topsoil) and the depth to which most of the plant roots grow (Adu, 1969).

luvisols. The following soils are also found to a lesser extent: fluvisols (e.g. in floodplains along Red and White Volta rivers), vertisols (e.g. along many streams in Upper West Region and western part of the Northern Region), planosols (e.g. along most streams in the Northern Region), arenosols (e.g. in floodplains along Black Volta River), gleysols (e.g. along minor streams in Upper East Region). A brief description of each major soil type is given below but a more detailed description of all these soils can be found in various publications, notably the World reference base for soil resources (IUSS, 2006) and the SRI publications, available through the Council for Scientific and Industrial Research (CSIR) (www.csir.org.gh). Information on soils in specific areas within the study area can also be found in Agyare (2004), Martin (2006) and Ofosu (2005).

The most common soil type in the study area is the lixisol which can be found in many types of settings in northern Ghana. Its soil texture, generally varying from sandy loam to silty clay, will depend on the underlying parent material but it is generally characterized by higher clay content in the upper part of the profile and coarser material as depth increases (Martin, 2006). Leptosols usually develop as shallow soils upland or mid-slope in gently undulating terrain, scarps or mountainous regions (e.g. over high plains of the Precambrian basement, on the rim of the Voltaian sedimentary basin, along the Akwapim-Togo Range). They generally consist of loamy sand to sandy loam, sometimes gravelly. Plinthosols are often associated with gently sloping areas or in lowlands where waterlogging occurs (e.g. in low-lying areas in the Voltaian sedimentary basin). Upon repeated drying and wetting, hardening can occur as plinthite[5] will change into an indurated layer with hard nodules. Plinthosols usually have sandy clay to sandy silty clay texture. Similarly to lixisols, acrisols can overlie a variety of parent materials but they are mostly found over old land surfaces with gently undulating topography (e.g. along base of scarps). These soils generally have higher clay content in the subsoil than in the topsoil. They mostly consist of sandy loam but silty and clay loams are also found locally. Luvisols generally develop in flat or gently sloping areas (e.g. near Lake Volta, between Salaga and Bimbila) from unconsolidated material and usually have a high silt content.

3.6 Geology

Northern Ghana is located in the eastern portion of the Man Shield, which constitutes the southern portion of the West African Craton (Figure 3-10). For a relatively large portion of the study area, the Precambrian basement rocks of the craton are partially covered by late Proterozoic to early Palaeozoic sedimentary rocks. The latter are part of the Voltaian sedimentary basin which is bounded to the east by the Pan-African Dahomeyide Belt.

According to the 2009 geological map of Ghana (Figure 3-11) (GGS, 2009), rocks of the Precambrian basement underlie about 41 % of northern Ghana. These rocks, have been folded, metamorphosed and intruded by granitoids during and after their emplacement (Leube and Hirdes, 1990). The general structural trend in these rocks is largely influenced by the principal tectonic stress orientation (~ northwest – southeast) (Apambire, 1996) and thus follows an approximate northeast-southwest axis. Fracture patterns may thus develop along that axis (subvertically) but may also develop on the fringe of large intrusions (subvertically, parallel to margins) and in the upper part of bedrock (subhorizontally, from isostatic uplift). In the study area, the Precambrian basement consists mainly of rocks from the Birimian Supergroup and associated granitoid intrusions, although sediments and metamorphosed sediments of the Tarkwaian Group are also present to a smaller extent as a result of the uplift and erosion of Birimian rocks. A small portion of the Buem Structural Unit is also present in the south-eastern corner of the study area. It is part of the Pan-African Dahomeyide mobile belt separating the Man Shield from the Benin-Nigeria Shield. The Buem Structural Unit, representing less than 1 % of the study area, is not thoroughly described here but detailed information can notably be found in Kesse (1985) and Osae *et al.* (2006).

[5] Plinthite is a humus-poor mixture of kaolinitic clay and other weathering products, with quartz and other minor constituents (IUSS, 2006).

The Voltaian sedimentary basin (VSB) consists of a large sedimentary basin that was developed in a gentle synform depression of the West African Craton. It extends northeast across parts of Togo, Benin and Niger and contains a thick succession (up to 700 m) of relatively undeformed Neoproterozoic to Palaeozoic consolidated sedimentary rocks, which lie unconformably on the Precambrian basement (Nathan and Harris, 1970). The rocks are generally flat bedded or gently dipping, except at the margins, notably towards the eastern edge where weak folding has occurred in relation with the Pan-African mobile belt. Fracturing is relatively rare in the interior of the basin but can be observed along escarpments on the southern, western and northern boundaries of the basin (Ofosu, 2005; Nathan and Harris, 1970). Rocks of the VSB underly a large portion of the study area (~ 59 %) and are part of the Voltaian Supergroup, which is subdivided in 3 groups: Obosum, Pendjari-Oti and Kwahu-Morago groups.

Figure 3-10 – Structural geology map of West Africa (Key, 1992)

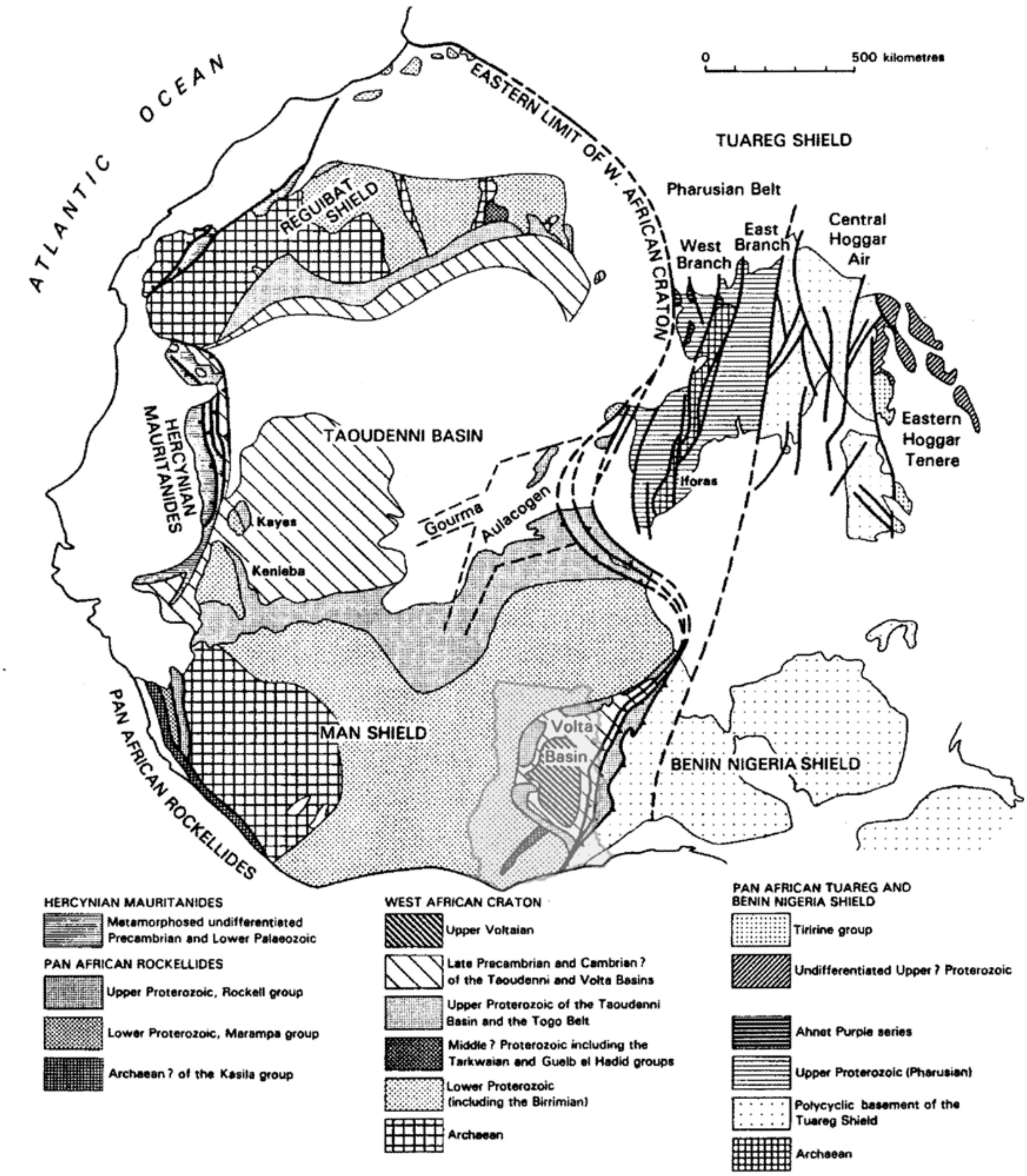

Figure 3-11 – Simplified surficial geology map of northern Ghana (based on 2009 revised GGS geological map)

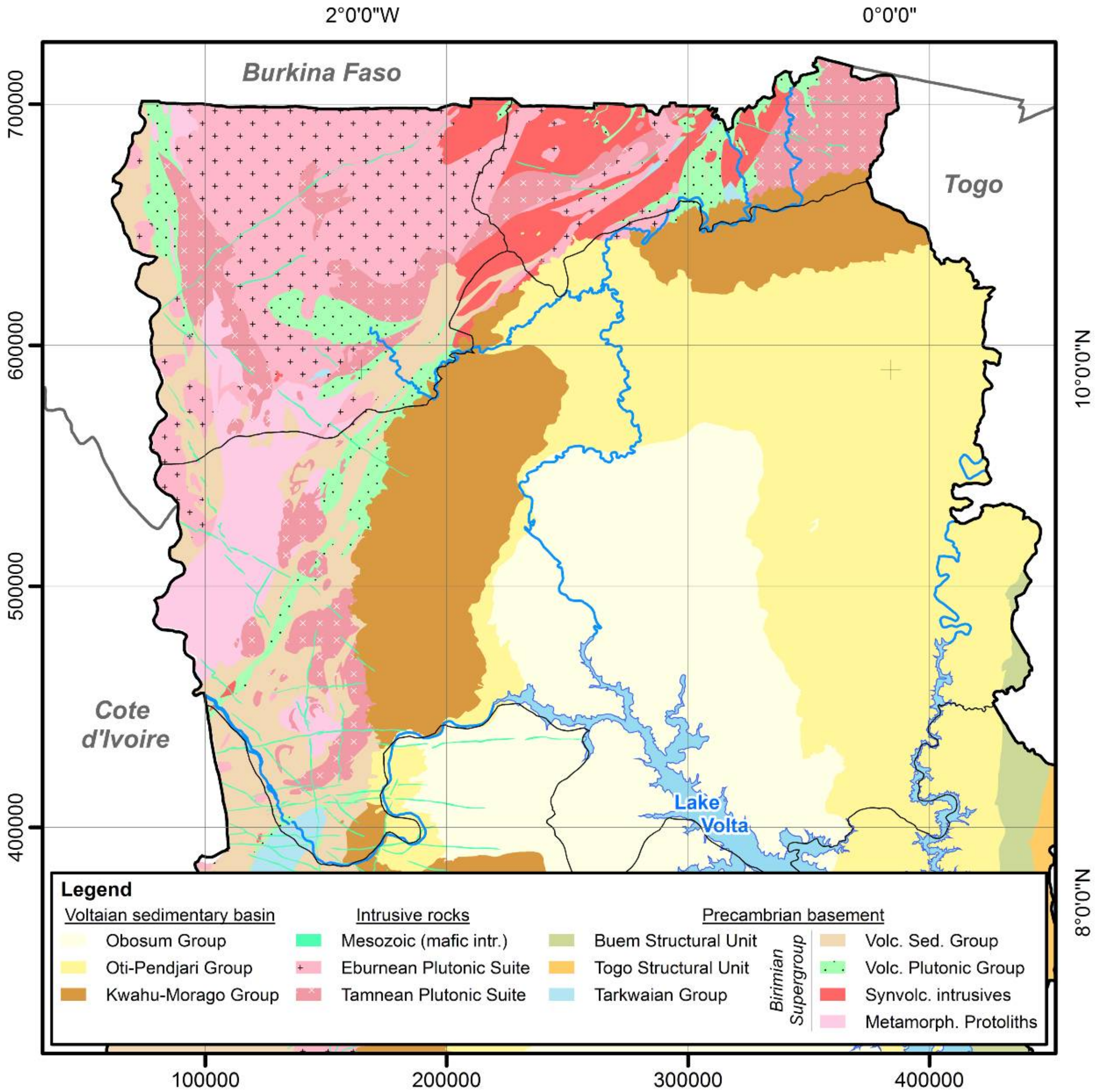

3.6.1 Description of main lithologies

The following section gives a general description of the main lithologies found in the study area based on the geological map provided by the Ghana Geological Survey Department (GGS), which was revised in 2009 by the GGS in collaboration with the BGR. Table 3-4 summarizes the information and presents the extent of each unit in terms of percentage of land area covered. The HAP Final Hydrogeological Atlas provides a more detailed version of the surficial geology map.

3.6.1.1 Precambrian Basement

3.6.1.1.1 Birimian Supergroup

The Birimian Supergroup covers a large portion of the Precambrian basement. It underlies densely populated areas in the south and comprises much of the mineral resources exploited in Ghana (e.g. gold, bauxite …). Rocks of the Birimian Supergroup consists mainly of volcanic and metavolcanic material that form southwest-northeast trending belts between which low grade metamorphosed and folded sediments occur. These rocks are strongly foliated and were intruded by large granitoid masses during the Eburnean event (~ Palaeoproterozoic) (Martin, 2006).

The Volcano-Plutonic Group of the Birimian Supergroup is characterized by volcanic belt environments consisting mainly of low-grade metamorphic basalts intercalated with volcaniclastics and volcanic rocks. Synvolcanic granitoid plutons also intrude most of these belts. The other main group of the Birimian, the Volcano-Sedimentary Group, mainly comprise volcaniclastics, wackes and argillites which were probably derived in large part from adjacent rocks of volcanic belt environments. In some areas, rocks from both groups were also affected by tectonic activity and metamorphism associated to the Eburnean event. Weathering degree of rocks is variable throughout the supergroup, depending largely on the amount of rainfall and on lithology.

Table 3-4 – Description of major lithologies in northern Ghana (based on 2009 revised GGS geological map)

Supergroup	Group	Dominant lithology	Extent of units (% land area)			
			Study area	Upper East	Upper West	Northern
Supracrustal rocks						
Voltaian Supergroup	Obosum	Sandstone, mudstone and conglomerate	19%	0%	0%	26%
	Pendjari-Oti	Sandstone, mudstone, siltstone, and carbonate	28%	2%	0%	39%
	Kwahu-Morago	Sandstone (e.g. Panabako, Poubogou and Tossiegou formations)	13%	6%	<1%	17%
-	Buem Structural Unit	Mafic volcanic rocks, shale, chert and sandstone	<1%	0%	0%	<1%
-	Tarkwaian	Sediments & low-grade metasediments (conglomerate, sandstone and argillite)	<1%	1%	<1%	<1%
Birimian Supergroup	Volcano-Sedimentary	Metasediments (volcaniclastics, wacke, argillite)	5%	<1%	13%	6%
	Volcano-Plutonic	Metavolcanics (basaltic flows, volcaniclastic and subvolcanic rocks)	7%	44%	13%	2%
	Metamorph. Protoliths	Metamorphosed rocks (sericite & biotite schists, granitoid gneiss, amphibolite)	8%	0%	7%	5%
Intrusive rocks						
Mesozoic intrusives		Gabbro, dolerite, norite, serpentinite	<1%	<1%	<1%	<1%
Eburnean Plutonic Suite		Hornblende-biotite granitoids (granite, tonalite, diorite) & K-feldspar-grranitoids	11%	14%	51%	<1%
Tamnean Plutonic Suite		Hornblende-biotite granitoids (tonalite, , granodiorite) & alkali granite, syenite)	8%	32%	15%	3%

3.6.1.1.2 Tarkwaian Group

The Tarkwaian Group consists mainly of metamorphosed sediments derived from the Birimian Supergroup that are intruded by laccoliths. The sediments were deposited in shallow narrow basins and folded along the same axis as those of the Birimian Supergroup that they overlie unconformably. Common rocks of the Tarkwaian Group include sandstone, conglomerate (may be polymictic as well as quartz-pebble) and minor argillite, siltstone and tuff.

3.6.1.1.3 Buem Structural Unit

The Buem Structural Unit is composed of volcanic rocks and of material mostly eroded from the neighbouring Togo Structural Unit (sedimentary rocks and metamorphosed derivatives). The volcanic material, including basaltic flow, sub-volcanic rocks, volcanic agglomerates and volcaniclastics, mainly occurs in the upper part of the formation while sedimentary rocks, such as chert, shale, siltstone and sandstone, mostly form the basal and intermediate part. The Buem Structural Unit is highly folded along a more or less northeast-southwest line, and is located west of the Togo Structural Unit in the eastern part of Ghana (Kesse, 1985). Rocks of this formation would date back to the Neoproterozoic (Osae *et al.*, 2006), i.e. during the pan-African orogenic cycle[6].

3.6.1.1.4 Intrusive rocks

Three major types of intrusive rocks are recognized in northern Ghana:

- Mesozoic intrusives
- Granitoids of the Eburnean Plutonic Suite
- Granitoids of the Tamnean Plutonic Suite

The Mesozoic intrusives represent less than 1% of the study area and consist mainly of mafic dykes. The Eburnean Plutonic Suite which mainly consists of peraluminous granitoids is the most widespread intrusive rock type in northern Ghana covering about 11% of the study area. Associated intrusions are mostly located in Birimian basin sediments but also locally in some Birimian volcano-plutonic belts. This intrusive type also include minor K-rich granitoids (e.g. Bongo Granite in the Upper East Region). Granitoids of the Tamnean Plutonic Suite correspond to smaller and older masses that are prominently developed along a northeast trend, in northwestern and northern Ghana but that may also be traced to other parts of Ghana (GGS, 2009).

3.6.1.2 Voltaian Supergroup

3.6.1.2.1 Obosum Group

The Obosum Group mostly consists of continental sandstone, coarsely grained (even conglomeratic) in some cases, and intercalated with mudstones and siltstones. Formations of this group include: Tamale, Sang, Densubon and Dunkro formations. Deposition of these sediments, which would originate from the Dahomeyide-Pharusian Belt, accompanied the Pan-African orogenic cycle. Sediments were transported by high-energy systems, such as alluvial fans and braided rivers, emanating from the nearby high relief terrain.

3.6.1.2.2 Pendjari-Oti Group

The consolidated sediments of the Pendjari-Oti Group would originate from a glacial event followed by a prolonged marine incursion and subsidence of the basin. They form the most extensive sedimentary sequence in Ghana. It comprises eight formations: Bunya, Chereponi, Bimbila, Tease, Ejura, Afram, Akroso and Kodjari formations. The first two, Bunya and Chereponi formations, consist mainly of medium grained sandstone while the Bimbila Formation consists of mudstone and siltstone intercalated with sandstone. The Tease and Ejura formations both comprise thinly bedded sandstone with the former being locally coarse-grained. The Afram Formation consists of mudstone and siltstone with sporadic limestone beds

[6] This event refers to the formation of mountains at the periphery of the West African Craton during the Neoproteozoic and Palaeozoic, and includes uplift along the Dahomeyide-Pharusian Belt (eastern limit of the West African Craton, east of Ghana) (Guiraud, 1988; Key 1992).

and the Akroso Formation consists of pebbly sandstone with large-pebble conglomerate. Finally, the Kodjari Formation has two members, the Darebe Member consisting of siliceous tuff interbedded with sandstone and the Buipe Member consisting of limestone with basal tillite/conglomerate. Undifferenciated rocks of the Oti-Pendjari Group also included slightly greenish rocks including mudstone, siltstone, sandstone and greywacke (Affaton *et al.*, 1980). The group covers a fairly large surface area, mainly in the Oti River Basin.

3.6.1.2.3 Kwahu-Morago Group

The Kwahu-Morago (Bombouaka) Group would consist of sediments laid down within a passive margin setting at a time the Rodinia Supercontinent was subject to regional subsidence. Sediments were deposited on a peneplaned surface of the Birimian basement by old river systems. Rocks of this group mainly consist of hard sandstone. The Morago Group which is found in the north/north-western part of the VSB includes four formations: Panabako, Damongo, Poubougou and Tossiegou formations. They all consist of sandstone with various textures except for the Poubougou Formation which consists of mudstone and siltstone intercalated with sandstone. The Kwahu sub-Group which is found in the western/south-western part of the VSB comprises six sandstone formations: Anyaboni, Obocha, Abetifi, Mpraeso, Damongo and Yabraso formations. The surface area occupied by this group which consists of bands on the rim the VSB is relatively small in comparison to the other VSB groups and is sparsely inhabited.

3.6.2 Weathered layer

Most of the geological formations in the study area are overlain by a regolith comprising *in situ* chemically weathered material and, to a lesser extent, transported surface material. Weathering processes involved are briefly summarized below. Available information reveals that the thickness of the regolith is generally less than 30 m but can be as thick as 140 m in the Upper West Region (Dapaah-Siakwan and Gyau-Boakye, 2000). In the Bongo and Bolgatanga districts of the Upper East Region, Apambire (1996) reports that the thickness of the regolith developed over Birimian and Tarkwaian rocks ranges from 11.6 m to 33.2 m with an average of 23.3 m, while it ranges from 2.7 m to 37.0 m with an average of 19.5 m over granitoid intrusions. In sedimentary rock terrains, the regolith would be slightly thinner. Additional work by Acheampong (1996) in the southern part of the VSB revealed a regolith of 4 m to 20 m in thickness. The thickness of the residual soil layer, which constitutes the upper part of the regolith, generally ranges from 1 to 3 m but could measure up to 10 m (Smedley, 1996). Outcrop areas are relatively rare except where underlying rocks such as quartz-rich granitoids preferentially resist weathering and develop into inselbergs, in particular in the Upper East Region. Spatial distribution of the regolith thickness is discussed in Section 5.1.3.

3.6.2.1 Overview of weathering processes

Regolith developing over bedrock as a result of chemical weathering usually exhibits a progressive degradation from fresh bedrock to residual soil. The typical zones forming the weathered profile are (from top to bottom) (Chilton and Foster, 1995):

- residual soil (usually sandy-clayey material possibly underlain by indurated layer)
- saprolite (completely to slightly decomposed rock with decreasing clay content with depth)
- saprock (remnants of unweathered bedrock in an altered matrix)
- fresh (variably fractured) bedrock

While the thickness of these zones can vary, their sequence remains the same. The first two zones, i.e. residual soil and saprolite, form the regolith while the saprock is usually considered as a part of bedrock. The weathering front, that is the interface between fresh bedrock and saprock, is generally sharp in coarse-grained massive crystalline rocks and diffuse and gradational in fine-grained rocks. Degree and depth of weathering depend largely but not exclusively on bedrock lithological and structural characteristics (e.g. mineral grain size, mineral solubility, relative proportions of Fe-Mg minerals, intensity of fracturing …), climatic conditions, geomorphological characteristics, age of land surface and aquifer characteristics (e.g. flow, recharge, geochemistry …). While chemical weathering usually occurs without significant changes in volume, removal of dissolved material through groundwater flow reduces overall mass. As a result of this unloading of the bedrock, fractures can open to greater depth, thus allowing groundwater to flow deeper (Jones, 1985). Section 5.1.1 further discusses the typical thicknesses of the regolith zones in the two geological and hydrogeological contexts of northern Ghana, the Precambrian basement and the Voltaian sedimentary basin.

3.6.2.2 Residual soil zone

Residual soils are formed by intensive leaching and bioturbation of the underlying saprolite. They are almost always above the water table and generally comprise surface material (often undissociated from transported material) and other layered features such as laterites.

Under warm climatic conditions, there is little or no humus accumulating in the soil. Consequently, in the absence of humic acid, Al_2O_3 and Fe_2O_3 are relatively insoluble and thus accumulate as hydrates forming laterites, while silica and other major elements (Na, Ca and Mg) are leached down to the water table (Larsson, 1984). Laterites are often fine-grained, concretionary and hardened (sometimes referred to as duricrust) when the geomorphological cycle is advanced (Wright, 1992; Larsson, 1984).

3.6.2.3 Saprolite and saprock zones

The saprolite and saprock zones are formed as a result of *in situ* chemical weathering of bedrock. The upper part of the saprolite zone usually shows deeper weathering than the lower part and the saprock zone, which exhibit a larger proportion of primary minerals and a smaller amount of secondary clay minerals. Degree of weathering, which decreases with depth, can be expressed as ratios of leached versus residual elements (e.g. $SiO_2/Al_2O_3+Fe_2O_3$). Major factors influencing chemical weathering in these zones are summarized below.

Figure 3-12 – Conceptual hydrogeological model of the weathered layer in Africa (Chilton and Foster, 1995)

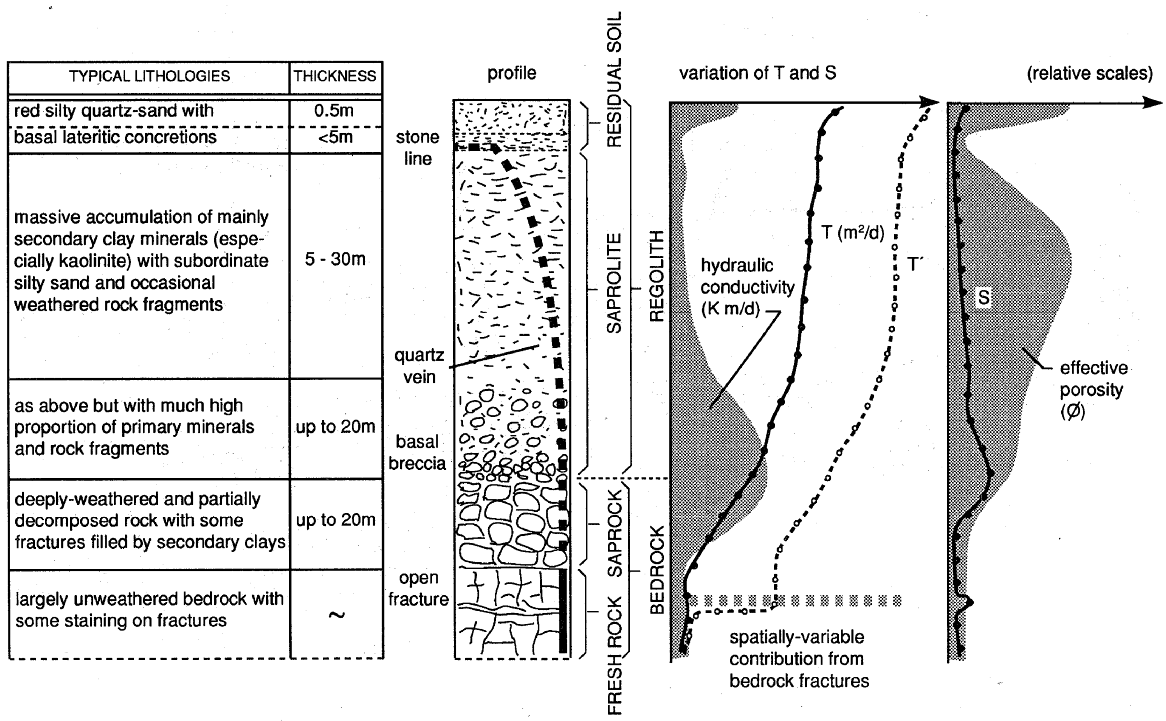

Groundwater flow is one of the principal geomorphological agents in the chemical weathering processes of bedrock through hydrolysis and dissolution (Jones, 1985). In basement rocks, which usually exhibit low primary porosity and hydraulic conductivity, weathering can cause substantial increase in both properties. This is illustrated in Figure 3-12 which shows a conceptual model of the weathered layer for basement rock areas. On the left of the figure, typical lithologies are described and illustrated while the two graphs on the right illustrate relative variations of material characteristics (i.e. transmissivity (T), storage (S), hydraulic conductivity (K) and effective porosity (Φ)) with depth. As these two graphs show (starting from fresh rock), porosity gradually increases while hydraulic conductivity rapidly increases at first as a result of fracturing and then gradually decreases with the formation of secondary clay minerals. At a later stage (i.e. near surface), more aggressive weathering can result in secondary clay minerals dissociation, thus re-increasing hydraulic conductivity (Wright, 1992). The distribution and extent of these zones of enhanced hydraulic conductivity within the regolith determines the presence of aquifers (Jones, 1985).

The physico-chemical environment also affects chemical weathering. Parameters such as redox conditions, pH, dissolved oxygen and partial pressure of carbon dioxide have significant impact on reactions occurring in the unsaturated zone or the saturated zone (Jones, 1985). Hydrolysis reactions involving minerals such as feldspars are common above and close to the water table. However, under saturated conditions (e.g. at saprock depth), weathering processes controlling early stages of matrix alteration are not well understood. According to Acworth (1987), one of the possible mechanisms is oxidation of biotite by mildly acidic water with high oxygen content.

4. DATA COLLECTION AND FIELD WORK

This section presents the methodology and outcome of the data collection and complementary field work carried out during the project. Part of the information gathered from these activities was complementary information used to describe the main characteristics of the study area in section 3, but the major portion was used to prepare the hydrogeological synthesis presented in section 5 and to develop an appreciation of the main data gaps presented in section 6.2.

4.1 Available data and their source

The first step in the data collection process involved the identification, gathering and compilation of hydrogeology-related documentation (hard and/or electronic copies). The documents targeted by this activity were mainly scientific publications (i.e. papers, conference proceedings, theses) and reports from various sources, such as national or regional water authorities, private consultants and drilling companies, donors, research institutions and Non-Governmental Organizations (NGOs). Close to 200 scientific publications were obtained from Internet, university libraries and stakeholders in the water sector of Ghana. The exercise also resulted in the collection of over 350 key reports. Of these, over 80 were electronically preserved (i.e. scanned in PDF format) to ensure their continued availability. Authors and publishers agreed to have the documents freely distributed to facilitate access and dissemination of the information to water sector stakeholders in Ghana. The complete list of scientific publications and reports is available in a digital library provided in Appendix E (USB flash drive). The PDF files of the documents available electronically are also accessible through this digital library.

Concurrently to the collection of documents, electronic data were also obtained from various sources. Electronic databases containing hydrogeology-related information were identified and obtained from the following stakeholders:

- Agence Française de Développement (AFD) (MS Excel file)
- Canadian International Development Agency (CIDA) (MS Excel file)
- European Union (EU) (MS Excel file)
- Global Change in the Hydrological Cycle Project (GLOWA) (MS Access file)
- Water Research Institute (WRI) (Ground Water for Windows (GWW) file)
- World Vision International (WVI) (Ground Water for Windows (GWW) file)

The first three databases, obtained via the Community Water Supply and Sanitation Agency (CWSA), contained only new records[7] from recent projects carried out mainly in the Northern Region. The GLOWA database contained records collected from different sources, notably private drilling companies, regional CWSA offices and the WRI. Although research conducted under the GLOWA project mostly concerns the Volta Basin, this electronic database contained records for all of Ghana. The WRI database was considered the most complete hydrogeological database for the northern regions of Ghana at the time of data collection as it comprised records from many water supply projects carried out in the northern regions. The WVI database contained records created under WVI projects and some records from the WRI database for the Northern Region that were considered as duplicates for the consolidation of collected data. A few records from various smaller water supply projects were also obtained from the CWSA.

Most of the base layers used for the preparation of maps and for GIS spatial analysis (i.e. administrative limits, cities, transportation, land use) were obtained from the Solar and Wind Energy Resource Assessment (SWERA) Geospatial Toolkit (http://swera.unep.net). The hydrography base layer was obtained from the latter in shapefile format and, later in the project, was also obtained in ArcInfo interchange format (i.e. e00 files) from the Ghana Survey Department along with other thematic data (i.e. cultural, forest, hypsographic, hydrographic,

[7] A record of a specified database usually refers to a drilled well (or borehole) with all its associated data

landform, transport and utility features). Other layers were obtained from contacts or websites of the following organizations:

- Climate data: Ghana Meteorological Services Department (MSD) and GLOWA
- Geology: Ghana Geological Survey Department (GGS)
- Soil: Ghana Soil Research Institute (SRI)
- Digital Elevation Model (SRTM data): International Centre for Tropical Agriculture (CIAT) through the Consortium for Spatial Information of the Consultative Group for International Agriculture Research (CGIAR-CSI)

As stated in section 3.3, climate data obtained include annual average rainfall for the 1971-2007 period for 140 stations and monthly climate data (i.e. temperature, rainfall, humidity, wind, sun hours) for the 1961-2005 period for six synoptic stations of northern Ghana. Subsequently, a daily climate dataset covering the 2000-2005 period for eight synoptic stations was also obtained through contacts with the GLOWA project for the preparation of the soil moisture balance. Details of this daily climate dataset are discussed in section 5.3.2. Additional daily (1950-2010) and monthly (1934-2005) climate data were also obtained near the end of the project for non-synoptic meteorological stations although many of them contained multiple data gaps of variable time length (from days to decades).

Daily hydrometric data were also obtained from the Ghana Hydrological Services Department (HSD) for fifteen gauging stations in northern Ghana. The period covered ranges from 1951 to 2008 although the datasets were also characterized by data gaps of variable time length (from days to decades).

4.2 Development of the HAP consolidated database

The content of the electronic databases obtained through the above mentioned stakeholders were validated and consolidated into a unique database to serve for HAP's purposes as well as future hydrogeological projects in northern Ghana. To facilitate the validation and consolidation process, all databases were converted into MDB files (i.e. Microsoft Access Database files). Some manual data transfer was required for databases in the GWW format as some data fields (e.g. lithology) could not be exported automatically in a convenient format. Prior to consolidation, the content of each database was assessed to identify 1) unique records among all available databases, 2) reliable records among these unique records (N.B.: reliability based on location data) and 3) resultant data gaps within the unique and reliable records. The first objective was aimed at eliminating redundant and duplicate information for data consolidation while the second and third were aimed at establishing the need for additional data collection to achieve project objectives.

4.2.1 Overview of data consolidation

The **identification of unique records** was not done the same way for all databases as reference information (e.g. report ID, project ID …) was not always available. The records from the AFD, EU and CIDA databases were all considered unique since they came from recent projects and were unlikely to have been entered in any other database yet (and thus duplicated). Consequently, a thorough verification of record uniqueness was not undertaken for these databases. For the GLOWA and WVI databases, it was generally possible to determine the presence of redundant records through database queries. As most of these records were originally taken from the WRI database, records from the latter were considered unique while redundant records in the GLOWA and WVI databases were identified as duplicates. The complete methodology is outlined in a preliminary database assessment presented in Appendix D (USB flash drive). As described below, results from this report have been updated since.

The **evaluation of record reliability** was carried out only for the data fields containing well coordinates, i.e. longitude and latitude. As original location data (e.g. hard copies of borehole logs) were generally not available, coordinates reliability was evaluated using spatial analysis functions with respect to administrative boundary and community GIS layers. Records identified as unreliable were flagged and kept for future and more thorough verification. It is important to mention that this was a time consuming task and that, therefore, it was not carried out with the same level of detail for all databases. An example of the process followed for the identification of reliable records is given in the preliminary database assessment report provided in Appendix D. While a complete analysis of all databases could have yielded more reliable records, the effort needed to accomplish this was considered disproportionate at the time in regards to the results that would be obtained.

For HAP's purposes, the following data fields were considered to be the minimum data requirements[8] to carry out the necessary hydrogeological analysis: 1) Well state, 2) Well depth, 3) Lithology descriptions, 4) Static groundwater level, 5) Yield and 6) Water quality data (pH, conductivity. Fe, Mn, F). The **identification of data gaps** for these data fields is twofold: 1) identification of gaps in terms of data quantity and 2) identification of data gaps in terms of spatial distribution of data. The former was simply done through statistical analysis. Records containing information for each of these data fields were compiled in order to evaluate the quantity of data available for each data field. The records resulting from this compilation were then plotted for each data field to assess their spatial distribution. This was done with reference to a 15 x 15 km cell grid that was considered the minimum requirement in term of data distribution for HAP purposes (i.e. minimum density of 1 record per 225 km², with 507 cells in northern Ghana) and considered suitable for the study area given the resources available.

4.2.2 Results

4.2.2.1 Initial assessment

Following the analysis of unique and reliable records, statistics were calculated for each database. Table 4-1 summarizes the results of the initial validation and consolidation process for each of the three regions of northern Ghana. It shows that, for the initial assessment, the total number of unique records for the whole study area was 9 851 and that 7 594 of these records were considered reliable (as far as location data is concerned). Of the unique and reliable records, only 71 contained the minimum required data. These statistics also revealed that there were major gaps in the lithology and water quality data fields.

Table 4-1 – Database content following initial consolidation and validation

	All regions		**Upper West**		**Upper East**		**Northern**	
	Records	Cells	Records	Cells	Records	Cells	Records	Cells
Unique records	9 851	-	-	-	-	-	-	-
Unique & reliable records	7 594	392	1 478	80	2 132	51	3 984	274
… with well depth	4 606	365	445	62	452	38	3 709	273
… with lithology	678	99	16	11	316	32	346	56
… with water level	1 758	310	178	52	279	38	1 301	225
… with yield	3 255	325	300	55	1 828	48	1 127	228
… with water quality	529	211	80	34	65	23	384	155
… with all required fields	71	26	0	0	64	23	7	3
	0.9 %	5.1 %	0 %	0 %	0.8 %	4.5 %	0.1 %	0.6 %

Although further validation could have helped increase the number of reliable records, it was considered that the amount of work needed would be disproportionate in regards of the results expected. This was notably explained by the following problems:

- syntax errors in community and district names
- absence of community names in some databases

[8] Minimum data requirements only apply to hydrogeological data found in available databases; other required data for HAP, such as climate data, are not considered in these requirements.

- presence of new communities in some database
- coordinate discrepancies for the same community

The verification of the spatial distribution of the 71 records identified above revealed that only 26 cells contained one or more boreholes (Figure 4-1) with most of them located in the Upper East Region. Considering that 507 cells were considered necessary to cover the entire study area, it was obvious that additional data were needed, both in terms of quantity and in terms of spatial distribution, to carry out any significant data analysis for HAP's purposes.

Figure 4-1 – Spatial distribution of unique & reliable records highlighting those with all required data fields (initial database assessment)

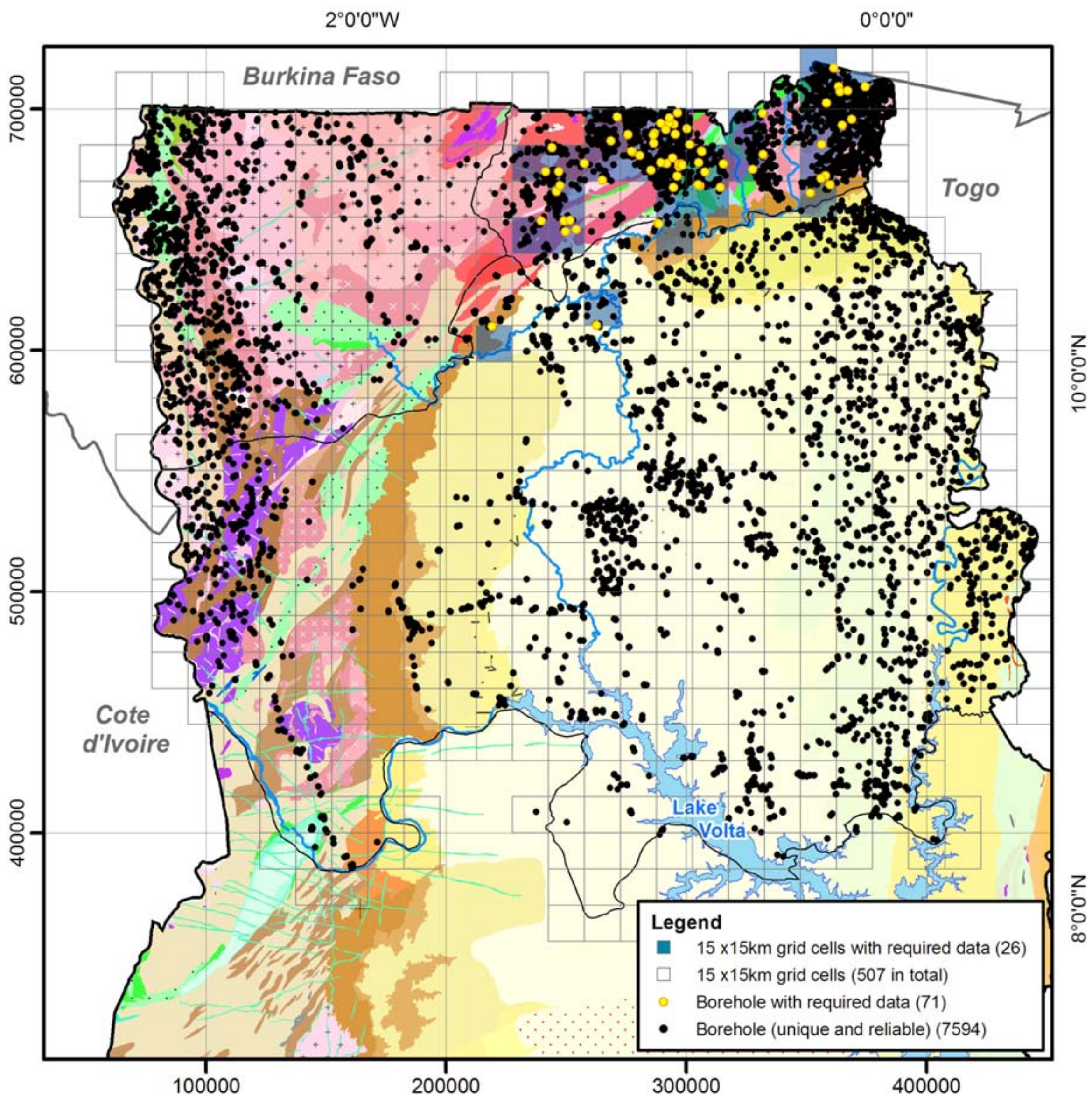

4.2.2.2 Collection and integration of additional data

Given the results of the initial assessment of the databases, additional data were thus collected manually from reports (soft and hard copies) identified earlier in the project. New data consisted mainly of reliable boreholes from water supply project reports that met at least one of the data requirements mentioned earlier. The selection was made mostly on the basis of the following criteria:

- well data location (one well per 15 x 15 km cell)
- well data representative of conditions encountered in the cell

This exercise, which was carried out by WRI staff and detailed in Appendix D (USB flash drive), yielded about 200 new reliable records, 65 of which met all the minimum data requirements.

4.2.2.3 Final consolidated database content

Following the additional data collection, the newly obtained reliable records were appended to the previously consolidated data. In addition to the new records obtained from the reports, new data generated by HAP targeted field work was also added to the consolidated data (N.B.: these are discussed more thoroughly in section 4.3). Thus, the final number of records available , presented in Table 4-2, was 10 139, of which 7 874 were considered unique and reliable records. Of these, 191 had the minimum required data and those were spread out into 125 cells (Figure 4-2).

Table 4-2 – Database content following additional data collection and validation

	All regions		Upper West		Upper East		Northern	
	Records	Cells	Records	Cells	Records	Cells	Records	Cells
Unique records	10 139	-	-	-	-	-	-	-
Unique & reliable records	7 874	408	1 533	82	2 151	46	4 190	280
… with well depth	4 859	384	497	68	465	38	3 897	278
… with lithology	906	256	58	42	327	36	521	178
… with water level	1 998	340	228	61	300	38	1 470	241
… with yield	3 480	342	344	62	1 843	46	1 293	247
… with water quality	676	245	93	37	90	28	493	180
… with all required fields	191	125	7	7	80	28	104	90
	1.9 %	24.7 %	0.1 %	1.4 %	0.8 %	5.5 %	1.0 %	17.8 %

While the validation process and the correction of errors was by no means an exhaustive exercise, the data collected and consolidated under the project were deemed reliable enough to yield sound analysis results. This is notably supported by the fact that the coverage in terms of cells is generally sufficient to provide a meaningful and representative regional distribution of the main hydrogeological properties when the required parameters (well depth, lithology, static groundwater level, yield, water quality) are considered separately. Section 5 describes the hydrogeological synthesis that was based on the analysis of these data and the other information gathered on northern Ghana.

4.2.2.4 Development of a water resources database

While the consolidated hydrogeological data described above were temporarily kept in a flat file (i.e. a single database table termed HAP consolidated database) throughout the consolidation process, all water-related data collected under HAP (i.e. groundwater and surface water data) were eventually integrated into a relational database. This database (termed WRC water resources database) was developed later in the project since it notably required the evaluation of database needs and capabilities at the WRC as well as the evaluation of database models and software that suited those needs. The development of this water resources database is discussed in details in the following report: Water Resources Database Development (SLI-INRS, 2011).

4.3 Field work carried out

Complementary field work was carried out in order to fill data gaps identified earlier in the project but also to address specific needs identified by stakeholders prior to this project. The main field activities carried out by the HAP are summarized in the following sections.

Figure 4-2 – Spatial distribution of unique & reliable records highlighting those with all required data fields (final database content)

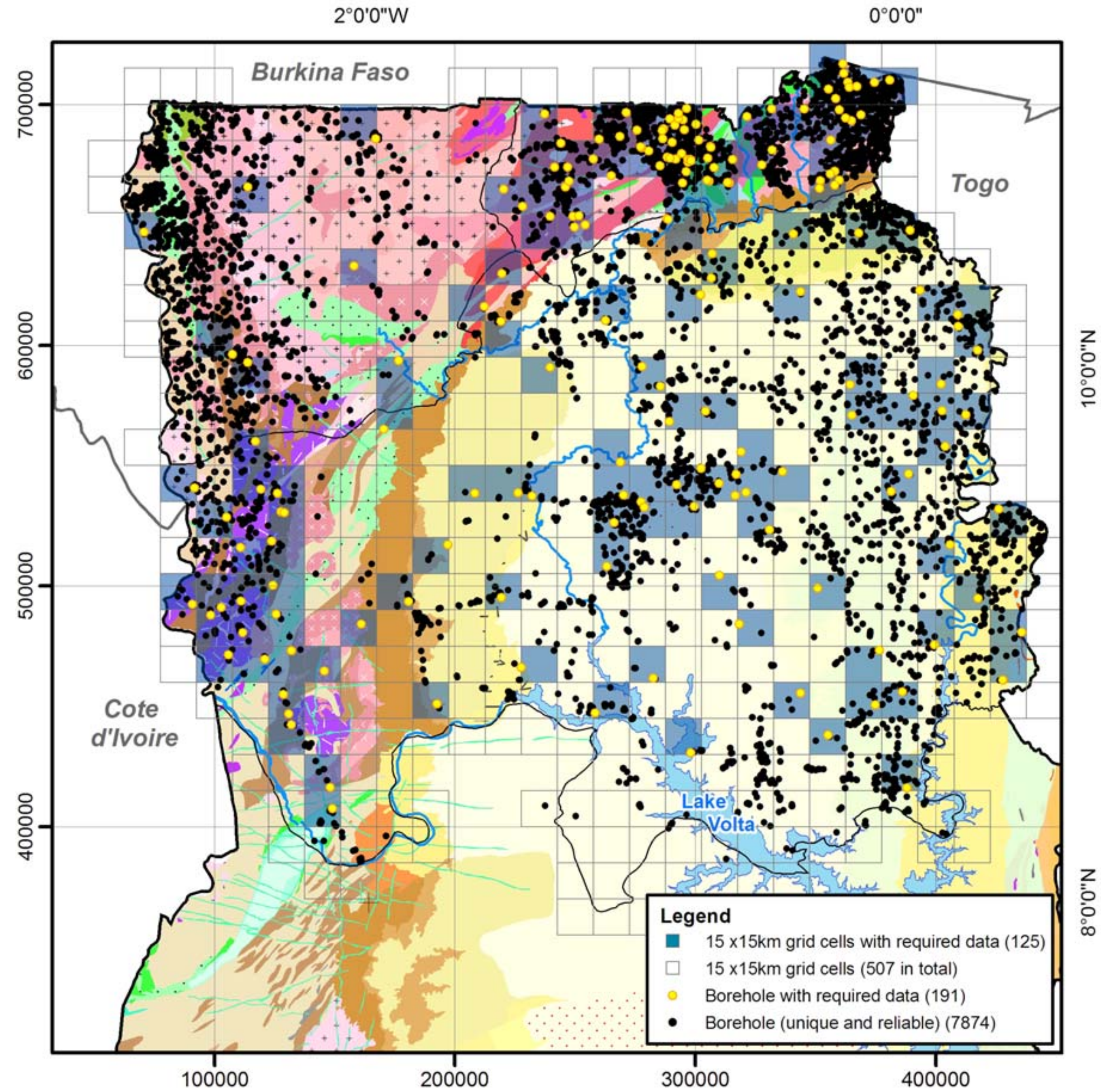

4.3.1 Monitoring wells

As part of HAP, 27 new dedicated monitoring wells were constructed to supplement an existing network of 13 monitoring wells established in the three northern regions by the Water Resources Commission (WRC) through the Water Research Institute (WRI) in 2006 (Figure 4-3 and Table 4-3). The 13 existing monitoring wells were constructed (or acquired through donation) in 2005 during the second phase of the Water and Sanitation Sector Program Support (WSSPS2) funded by the Danish International Development Agency (DANIDA). They are not discussed here but their drilling and construction details can be found in the drilling and borehole construction report prepared by WRI (Appendix D on USB flash drive). Locations of the new HAP monitoring wells were selected through inputs from key stakeholders. Besides improving the spatial coverage of the northern regions of Ghana, new monitoring well locations mainly targeted areas of stratigraphic importance and areas with known groundwater quality problems. Two geophysical techniques, electromagnetic and electrical resistivity profiling, were applied to support the siting of drilling locations. The complete reports on geophysical siting investigations can be found in Appendix D (USB flash drive). The new monitoring wells were drilled in two separate phases: the first 12 boreholes were drilled between early June and late

August 2007 while the remaining 15 boreholes were drilled between October and November 2009. All boreholes were drilled using an air rotary rig. Out of the 12 initial borehole drilling attempts, two boreholes (HAP 05 and HAP 09) had to be abandoned and backfilled, respectively because of a break in the PVC liner and because of an uncontrollable cave-in. These two boreholes were re-drilled but caving reoccurred at the second attempt for HAP 09. It was also noticed later on during the geophysical logging that HAP 03 and HAP 06 were respectively blocked at 32.5 m and 4.6 m, probably as a result of post-well construction caving. These three wells (HAP 03, HAP 06, HAP 09) were thus considered technically negative.

Sampling of drill cuttings was done during drilling at 1 m intervals and at every change in lithology. Open hole design was used where possible in order to allow geophysical logging. Wells penetrating unconsolidated or fractured formations were lined with PVC casing and screens to prevent caving. For all the new wells, concrete aprons were constructed and security fencing was installed. Technically positive wells yielding enough water during airlift tests were submitted to pumping tests and were equipped with dedicated equipment for long-term measurement of water levels. Well logs with construction details can be found in the drilling supervision reports (Appendix D on USB flash drive).

Figure 4-3 – Location of the new and existing monitoring wells

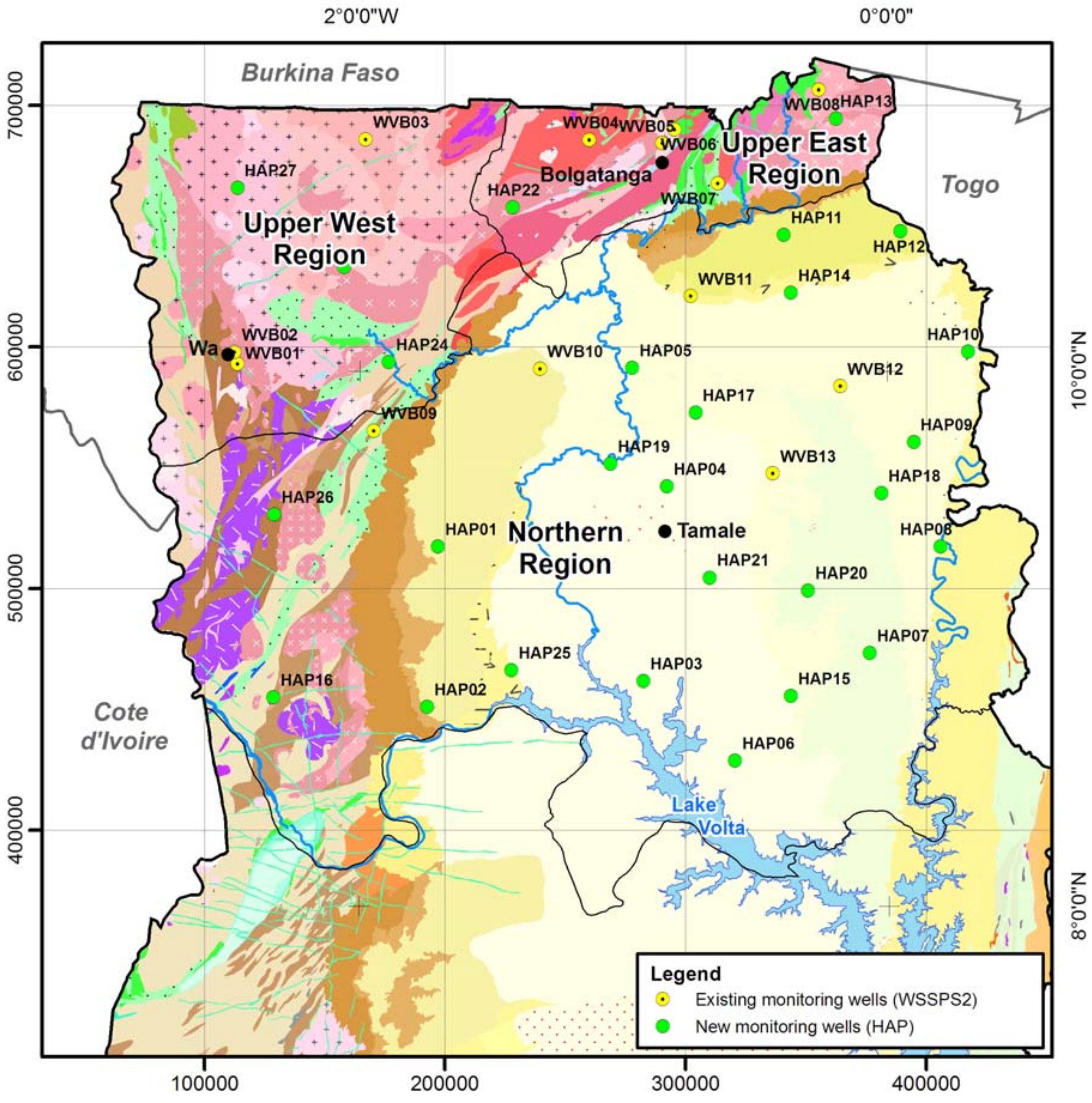

Table 4-3 – Summary information for the new and existing monitoring wells

Well ID (1)	Region (2)	District	Community	Location (degrees) Longitude	Latitude	Drilling date	Depth (m)	Screened intervals (m)	Moni-tered	Remarks
WVB01	UW	Wa Municipal	Wa	-2.463	10.03	05-07-05	104	(open hole)	Yes	-
WVB02	UW	Wa Municipal	Wa	-2.475	10.074	n/a	37.5	n/a	Yes	Donated well
WVB03	UW	Sissala East	Tumu	-1.98	10.872	05-07-08	104	(open hole)	Yes	-
WVB04	UE	Kassena Nankana	Bonia	-1.13	10.872	05-06-19	72	25-30, 41-48, 65-72	Yes	-
WVB05	UE	Bongo	GowrieTingre	-0.853	10.859	05-06-19	90	23-29, 71-77, 83-89	Yes	-
WVB06	UE	Bongo	Bongo-Nayire	-0.807	10.911	99-03	35	n/a	Yes	Donated well
WVB07	UE	Talensi-Nabdam	Datuku	-0.642	10.708	05-06-20	90	(open hole)	Yes	-
WVB08	UE	Bawku Municipal	Bawku	-0.258	11.059	05-06-20	100	(open hole)	Yes	-
WVB09	N	East Gonja	DusieCamp	-1.946	9.781	05-07-06	77	(open hole)	Yes	-
WVB10	N	East Gonja	Yagbum	-1.317	10.014	05-06-22	99	(open hole)	Yes	-
WVB11	N	West Mamprusi	Bugya-Pala	-0.745	10.286	03-04-07	56	(open hole)	Yes	Donated well
WVB12	N	Gushiegu	Tinguli	-0.179	9.948	02-03-15	51	27-36, 45-48	Yes	Donated well
WVB13	N	Gushiegu	Galiwei	-0.435	9.622	05-06-26	99	(open hole)	Yes	-
HAP01	N	West Gonja	Murugu	-1.703	9.348	07-06-25	118	42-109	Yes	-
HAP02	N	West Gonja	Buachepe	-1.742	8.749	07-06-22	158.5	(open hole)	No	Hydraulic. negative
HAP03	N	West Gonja	Chama	-0.926	8.847	07-06-30	151	(open hole)	No	Blocked at 33 m (3)
HAP04	N	Savelugu Nanton	Kanshegu	-0.837	9.574	07-08-04	155	36-48, 60-78, 111-129	Yes	-
HAP05-1	N	West Mamprusi	Janga	-0.972	10.023	07-08-21	166	-	No	Break in PVC liner
HAP05-2	N	West Mamprusi	Janga	-0.967	10.017	07-08-23	166	(open hole)	Yes	-
HAP06	N	East Gonja	Bau	-0.58	8.548	07-07-04	151	(open hole)	No	Blocked at 5 m (3)
HAP07	N	Nanumba	Zabalaya	-0.069	8.951	07-07-07	121	12-21, 62-77, 108-114	Yes	-
HAP08	N	Yendi	Gnani	0.199	9.346	07-07-11	150	53-68, 80-92, 140-149	Yes	-
HAP09-1	N	Saboba Chereponi	Wapuli	0.099	9.739	07-07-13	106	-	No	Cave-in at 22 m
HAP09-2	N	Saboba Chereponi	Wapuli	0.099	9.739	07-07-31	120	(open hole)	No	Blocked at 18 m (3)
HAP10	N	Saboba Chereponi	Tachecku	0.306	10.076	07-07-15	121	9-12, 36-48, 87-100	Yes	-
HAP11	N	East Mamprusi	Nalerigu	-0.392	10.515	07-07-31	155	31-56, 116-140	Yes	-
HAP12	N	East Mamprusi	Nakpeuk	0.05	10.528	07-07-29	166	(open hole)	Yes	-

Notes:
(1) : WVB prefix: existing wells donated or constructed under the WSSPS2 in 2005; HAP prefix: wells constructed under the HAP in 2007
(2) : UW: Upper West Region; UE: Upper East Region; N: Northern Region
(3) : These wells were found to be blocked when the geophysical logging was carried out.

Table 4.3 – Summary information for the new and existing monitoring wells (cont'd)

Well ID (1)	Region (2)	District	Community	Location (degrees)		Drilling date	Depth (m)	Screened intervals (m)	Moni-tered	Remarks
				Longitude	Latitude					
HAP13	UE	Bawku Municipal	Kabingo	-0.1925	10.95	09-10-13	93.81	(open hole)	Yes	-
HAP14	N	East Mamprusi	Tunni	-0.3653	10.298	09-10-15	120	(open hole)	Yes	-
HAP15	N	East Gonja	Lentinkpa	-0.3685	8.78967	09-11-20	151	(open hole)	Yes	-
HAP16	N	Bole	Wakawaka	-2.3232	8.78356	09-10-24	145.9	(open hole)	Yes	-
HAP17	N	Karaga	Tamaligu	-0.7276	9.84989	09-11-11	153	(open hole)	Yes	-
HAP18	N	Yendi Municipal	Sakpiegu	-0.0246	9.54654	09-10-22	80	(open hole)	Yes	-
HAP19	N	Tolon Kumbungu	Nawuni	-1.0494	9.65888	09-11-14	153	(open hole)	Yes	-
HAP20	N	Yendi Municipal	Palari	-0.3032	9.18511	09-11-17	153	(open hole)	Yes	-
HAP21	N	East Gonja	Tantuya	-0.6744	9.23321	09-10-17	140	(open hole)	Yes	-
HAP22	UE	Builsa	Noverinsa	-1.4208	10.619	09-11-06	153	(open hole)	Yes	-
HAP23	UW	Sissala West	Wahabu	-2.0612	10.3933	09-10-29	122	(open hole)	Yes	-
HAP24	UW	Wa East	Yanyounyiri	-1.8899	10.0377	09-10-31	122	(open hole)	Yes	-
HAP25	N	Central Gonja	Kabilpe	-1.4241	8.88775	09-11-12	153	(open hole)	Yes	-
HAP26	N	Sawla-Tuna	Soma	-2.3217	9.46531	09-10-27	128	(open hole)	Yes	-
HAP27	UW	Jirapa	Chepuri	-2.4666	10.6888	09-11-03	153	(open hole)	Yes	-

Notes:
(1) : WVB prefix: existing wells donated or constructed under the WSSPS2 in 2005; HAP prefix: wells constructed under the HAP in 2007
(2) : UW: Upper West Region; UE: Upper East Region; N: Northern Region
(3) : These wells were found to be blocked when the geophysical logging was carried out.

4.3.2 Monitoring well development and pumping tests

The new monitoring wells were developed by surging with compressed air for a period of 3 hours. Technically positive wells for which the airlift yield was higher than 10 L/min were considered successful and were submitted to pumping tests. The latter consisted in a 6-hour constant discharge test, followed by 3-hour recovery test. Groundwater levels were monitored within the monitoring wells themselves as there were no observation wells available nearby.

In all, 23 out of 27 monitoring wells were tested, with discharge rates ranging from 5 to 400 L/min and drawdowns varying between 1.4-45.9 m. The following wells were not tested as they were either technically negative (i.e. blocked or broken) or hydraulically negative (i.e. dry wells or wells with minor yield): HAP 02, HAP 03, HAP 06 and HAP 09. Pumping test data were used to estimate specific capacity and transmissivity (see section 5.2.1).

4.3.3 Geophysical borehole logging

Following the completion of the well installation and pumping tests, geophysical down-hole logging was carried out in the monitoring wells by Water Research Institute personnel. The results of the geophysical logging are not discussed in details here but the complete WRI reports with analyzed geophysical logs can be found in Appendix D (USB flash drive). The geophysical logs were used to validate lithology and well construction details given in the stratigraphic logs and to identify potential inflow zones. Table 4-4 summarizes the geophysical logging carried out in each well.

Table 4-4 – Geophysical logging probes used in new HAP monitoring wells

Well ID	Logging date	Probe used						
		Caliper	TCG (Q=0)	TCG (Q=X)	Flowmeter (Q=0)	Flowmeter (Q=X)	Dual induction	Resistivity
HAP01	2007-10-13		x	x	x	x	x	x
HAP02	2007-08-24	x	x				x	x
HAP03	2007-08-25	x	x					x
HAP04	2007-10-26		x	x	x	x	x	x
HAP05-2	2007-09-03	x	x				x	x
HAP06	2007-08-27	x						
HAP07	2007-08-29		x	x	x	x	x	x
HAP08	2007-10-22		x	x	x	x	x	x
HAP09-2	2007-10-24	x						
HAP10	2007-10-23		x	x	x	x	x	x
HAP11	2007-10-20		x	x	x	x	x	x
HAP12	2007-08-31	x	x					x
HAP13	2009-11-22	x	x	x	x	x		x
HAP14	2009-11-25	x	x	x	x	x		x
HAP15	2009-12-02	x	x	x				x
HAP16	2009-11-14	x	x	x				x
HAP17	2009-12-30	x	x	x	x	x		x
HAP18	2009-11-28	x	x	x	x	x		x
HAP19	2009-12-01	x	x	x				x
HAP20	2009-11-27	x	x	x	x	x		x
HAP21	2009-12-05	x	x	x				x
HAP22	2009-11-20	x	x	x	x	x		x
HAP23	2009-11-19	x	x	x				x
HAP24	2009-11-16	x	x	x				x
HAP25	2009-12-04	x	x	x	x	x		x
HAP26	2009-11-15	x	x	x	x	x		x
HAP27	2009-11-18	x	x	x	x	x		x

Notes: TCG: temperature, conductivity and gamma; Q=0: no pumping; Q=X pumping

Logging was carried out with a Robertson geo-logging system using the following probes: temperature, conductivity, gamma, dual induction, high resolution flowmeter, resistivity and caliper. As for the drilling activities, geophysical logging was carried out in two phases, first between August and October 2007 for monitoring wells HAP01 to HAP12 and, secondly, between November and December 2009 for monitoring wells HAP13 to HAP27. All probes were usually run down each borehole with the following exceptions: 1) for the six fully constructed monitoring wells (i.e. those lined with PVC casing and screens to the bottom), the caliper probe was not used and the dual induction probe was used to take conductivity measurements; 2) for boreholes with low yield, the flowmeter probe was not used. Out of the 27 new monitoring wells, 24 were successfully probed while three of the wells with open-hole construction, HAP 03, HAP 06 and HAP 09, where blocked at different depths, thus preventing lowering of the probes.

4.3.4 Groundwater level and quality monitoring

Monitoring of groundwater level and quality in the new HAP monitoring wells was initiated in October 2007 for HAP01 to HAP12 and in November 2009 for HAP13 to HAP27, following geophysical logging. This activity is aimed at complementing the ongoing monitoring of the existing wells (begun in November 2005) to provide valuable information on the changes in the groundwater quality and groundwater levels on a regional basis.

Transducers (Schlumberger Micro-Diver® and Mini-Diver® dataloggers) were installed in the 24 new monitoring wells considered successful in order to monitor both groundwater pressure (related to groundwater level) (datalogger type DI601 and DI602) and atmospheric pressure (datalogger type DI500) fluctuations in time. Automatic data recording was set to 6-hour intervals for all transducers. Manual groundwater level measurements were taken with a water level meter each time that data were downloaded from the transducers. At the time of writing, groundwater level measurements from the new monitoring wells were available from October 2007 to December 2010 for HAP01 to HAP12 and from November 2009 to December 2010 for HAP13 to HAP27. For the existing monitoring wells, groundwater level measurements were available from November 2005 to December 2010. The measured hydrographs for the existing and new monitoring wells are respectively presented in Figures 4-4 and 4-5 while individual hydrographs are available in Appendix B. It must be pointed out that many transducer failures were reported during the HAP, resulting in several data gaps in the groundwater level dataset, even though efforts were made to minimize these gaps. At the time of writing, the most likely cause for this high failure rate was a manufacturing defect related to the transducer battery assembly, which, according to Schlumberger, was addressed in the most recent replacement transducers provided. The transducers settings and installation details can be found in Table 4-5. Information concerning the installation of transducers in the existing monitoring wells can be found in Appendix D (USB flash drive).

At the time of writing, eight groundwater sampling campaigns had been carried out at the same 24 monitoring wells: Sept. 2007, Dec. 2007, Apr. 2008, Aug. 2008, Nov. 2008, Apr. 2009, Aug. 2010 and Dec. 2010. These sampling campaigns were carried out concurrently to visits for data downloading from the transducers. Prior to sampling, groundwater was pumped for a minimum of one hour. Collected groundwater samples were sent to SGS Laboratory in Tema (Ghana) for the following physico-chemical analyses: pH, conductivity, turbidity, total hardness, total dissolved solids (TDS), calcium (Ca^{2+}), magnesium (Mg^{2+}), sodium (Na^+), potassium (K^+), chloride (Cl^-), nitrate (NO_3^- as N), sulphate (SO_4^{2-}), fluoride (F^-), bicarbonate (HCO_3^-), total phosphate (PO_4^{3-}), ammonia (NH_3 as N), total iron (Fe), total manganese (Mn) and total arsenic (As). For the latter three sampling campaigns (i.e. since Apr. 2009), sampling of the existing monitoring wells (WVB01 to WVB13) was synchronized with that of the monitoring wells drilled under HAP.

Figure 4-4 – Groundwater level fluctuations for the existing monitoring wells

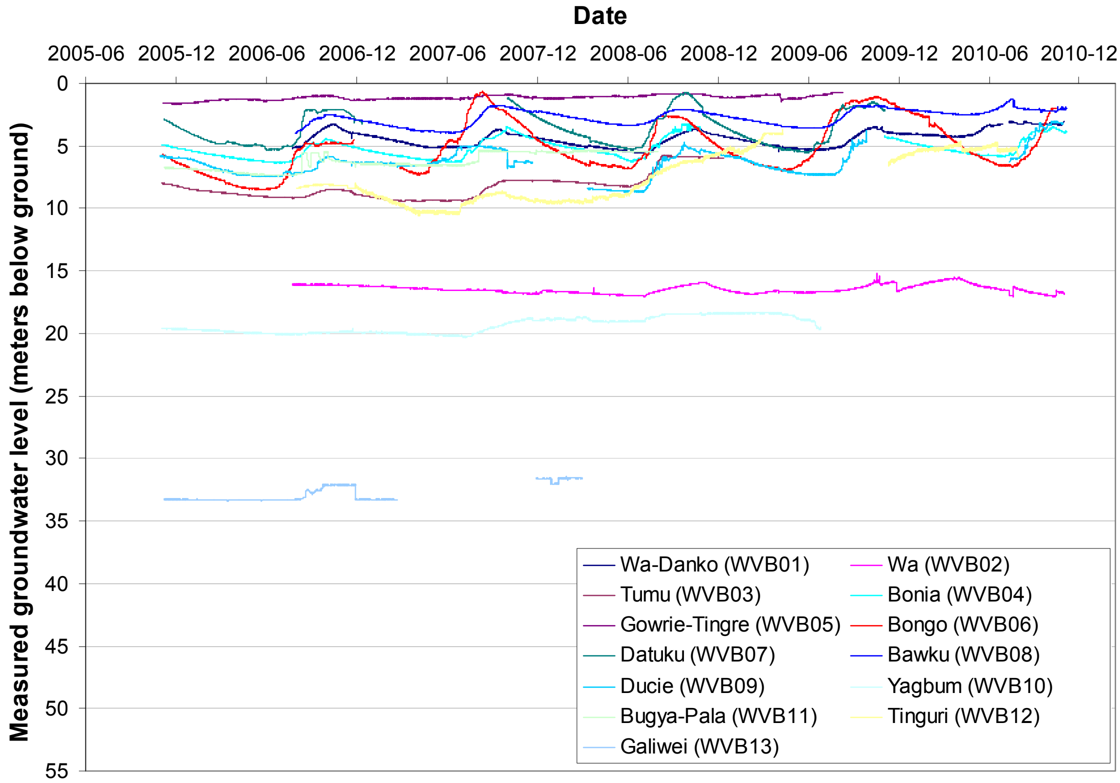

Figure 4-5 – Groundwater level fluctuations for the new monitoring wells

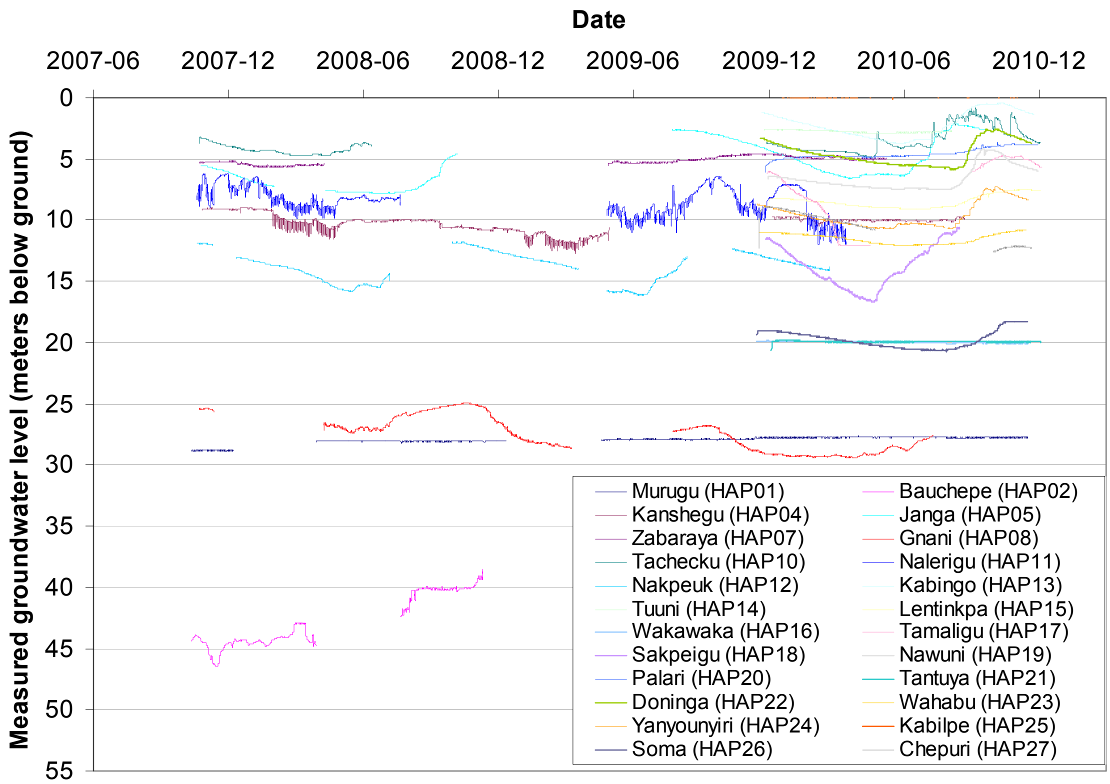

Table 4-5 – Water level transducers setting and installation details

Well ID	Installation date	Static water level (m)	Casing length (m)	Transducer depth (m)	Transducer measuring range (m)	Transducer depth (atm. press.) (m)
HAP01	2007-10-13	29.5	0.56	35	20	10
HAP02	2007-10-13	45.15	0.69	55	20	5
HAP04	2007-10-26	10.18	0.64	18	10	3
HAP05-2	2007-10-25	6.25	0.65	14	10	2
HAP07	2007-10-22	5.95	0.64	12	10	3
HAP08	2007-10-22	25.05	0.57	35	20	5
HAP10	2007-10-23	4.37	0.66	10	10	2
HAP11	2007-10-20	8.64	0.62	14.8	10	3
HAP12	2007-10-20	12.64	0.75	19	20	3
HAP13	2009-11-22	1.8	0.6	8	10	0.8
HAP14	2009-11-25	3.51	0.79	10	10	1
HAP15	2009-12-02	8.99	0.54	16	10	3
HAP16	2009-11-14	20.46	0.58	26	10	5
HAP17	2009-11-30	6.77	0.54	13	10	2
HAP18	2009-11-28	12.05	0.5	18	10	3
HAP19	2009-12-01	7.26	0.76	14	10	2
HAP20	2009-11-27	6.68	0.62	13	10	2
HAP21	2009-12-14	21.15	0.5	28.5	10	5
HAP22	2009-11-20	3.93	0.6	10	10	1.5
HAP23	2009-11-19	11.32	0.29	17	10	3
HAP24	2009-11-20	9.46	0.7	16.5	10	3
HAP25	2009-12-04	-0.15	0.7	8	10	-0.5
HAP26	2009-11-15	19.76	0.39	25	10	5
HAP27	2009-11-18	12.91	0.36	18	10	3

Notes: Static water levels and transducer depths are given in meters below cap.

4.3.5 Groundwater geochemical characterization

Initial review of existing geochemical data for groundwater revealed uncertainties and gaps in the data (e.g. units conversion errors, significant gaps in sample spatial distribution, high variability of the quantity and type of parameters analyzed). Consequently, a regional geochemical characterization of groundwater in northern Ghana was undertaken in order to collect representative data on groundwater geochemical characteristics from existing wells and new monitoring wells. The 90 wells initially targeted for this geochemical characterization (37 monitoring wells and 53 existing wells) were selected according to location criteria (i.e. reliable coordinates, road access, project area spatial coverage, and upgradient/downgradient-wise distribution) and well construction criteria (i.e. well type, construction details, lithology intercepted, anticipated aquifer context). The three sampling campaigns carried out as part of this geochemical characterization are described below and associated data can be found in Appendix D (USB flash drive).

For the first sampling campaign, 107 wells were sampled (Figure 4-6), including 32 monitoring wells and of 75 existing wells (23 hand-dug wells and 52 boreholes), for a total of 116 samples (including 9 duplicate samples for quality control). Because of road flooding, 5 of the targeted monitoring wells and 1 existing well could not be sampled. Also, when the targeted existing wells could not be found in the field, an alternative well (usually the nearest to the targeted location) was selected as replacement. Sampling was carried out by Atomic Energy of Ghana personnel, between August and September 2010, concurrently to the shallow groundwater sample collection (see section 4.3.6.3). Prior to sampling, groundwater was pumped for a minimum of one hour. Collected groundwater samples were sent to the Atomic Energy of Ghana laboratory in Accra and the following parameters were analyzed: pH, redox potential (Eh), dissolved oxygen (DO), turbidity, total hardness, alkalinity, total dissolved solids (TDS), conductivity (EC), calcium (Ca^{2+}), magnesium (Mg^{2+}), sodium (Na^{+}), potassium (K^{+}), chloride (Cl^{-}), nitrite (NO_2^- as N), nitrate (NO_3^- as N), sulphate (SO_4^{2-}), fluoride (F^-), bicarbonate (HCO_3^-), phosphate (PO_4^{3-}), bromide (Br^-), aluminium (Al), copper (Cu), chromium (Cr), cobalt (Co), cadmium (Cd), iron (Fe), manganese (Mn), nickel (Ni), lead (Pb), zinc (Zn) and arsenic (As). In addition, oxygen-18 (^{18}O) and deuterium (^{2}H) stable isotopes were also analysed.

Two additional sampling campaigns were carried out in February 2011 and May 2011 (121 wells sampled in both campaigns). Aside from a few exceptions, the same wells were sampled for these campaigns. The same analyses were also performed with the exception of carbon isotopes (^{14}C and ^{13}C) analyses that were added to the second sampling campaign parameter list.

Figure 4-6 – Location of wells sampled for the groundwater geochemical characterization

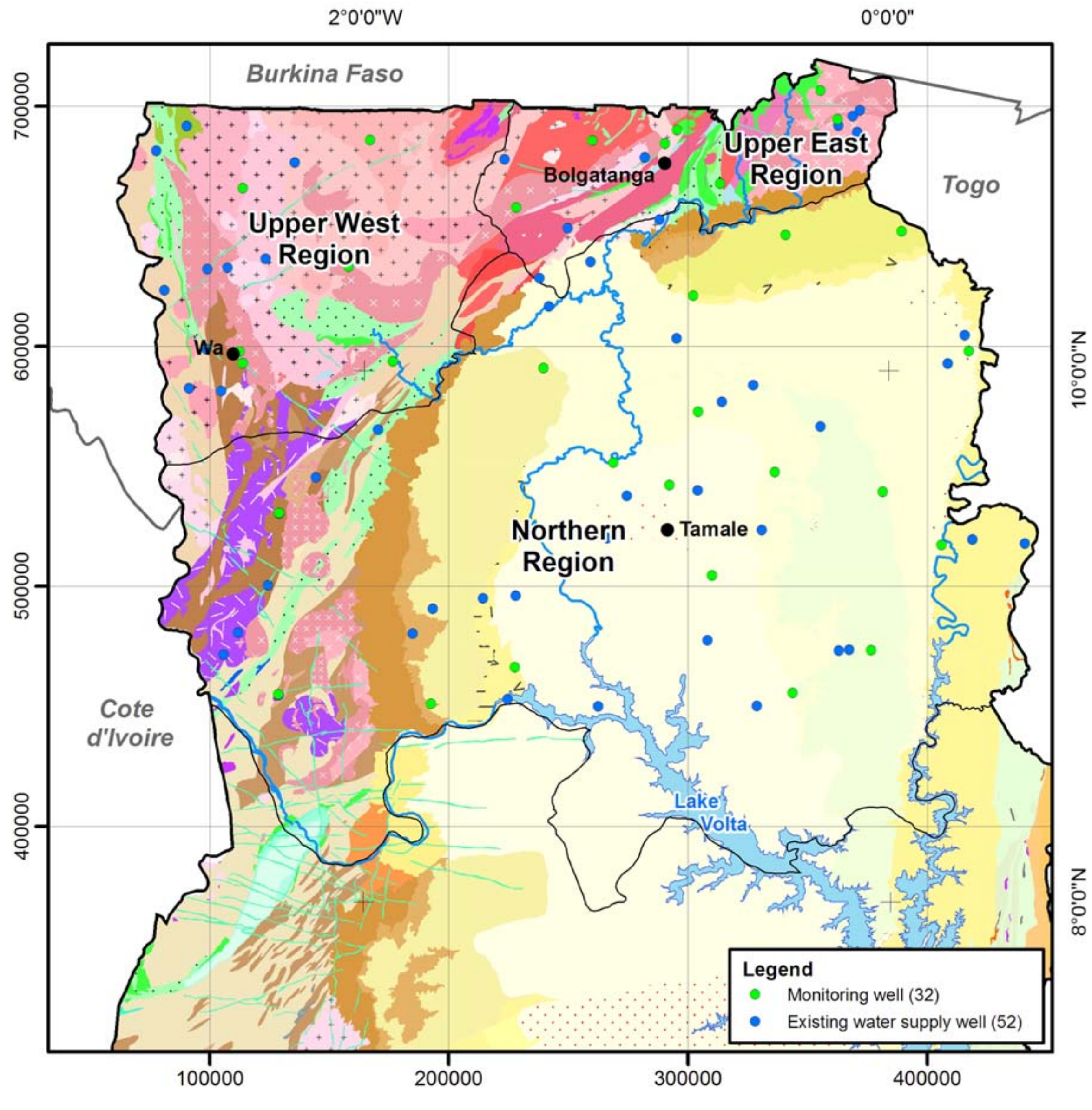

4.3.6 Groundwater recharge evaluation

As part of the evaluation of groundwater recharge, the chloride mass balance method (CMB) was implemented in the northern regions. Methodology and results are presented in section 5.3.3 while related field work is described in the following sections.

4.3.6.1 Rainfall sampling

Atmospheric Cl deposition was estimated from rainfall samples collected at 8 meteorological stations in northern Ghana, namely Navrongo, Wa, Bole, Tamale, Yendi (northern regions), Kete-Krachi (Volta Region), Wenchi and Sunyani (both in Brong-Ahafo Region) (see Figure 3-5). Rainfall events were sampled by MSD personnel directly from rain gauges (bulk sampler type) into sterile containers provided by the laboratory. The sampling was usually done shortly after rainfall events so as to minimize the effect of evaporation. Samples were sealed after collection and kept cool until shipment to the SGS Laboratory in Tema, where they were analyzed for Cl by colorimetry, with a detection limit of 0.1 mg/L. Major rain events were sampled for the 2007-2010 period at all stations, except for the Kete-Krachi station for which samples were only collected in 2007. On average, rain events sampled represented between 47-76 % of the annual average rainfall at stations considered. Nitrate in rainfall was also analyzed for some samples.

4.3.6.2 Soil sampling in the unsaturated zone

A total of 18 unsaturated zone profiles were drilled in the upper part of the weathered layer. The depth and date of sampling for each profile are presented in Table 4-6 while their location is shown in Figure 4-7. To minimize the error associated to Cl flux from run-on/runoff, profiles were carefully sited in the field to avoid locations with steep slopes or depressions and potential groundwater discharge areas. Despite that, soil sampling proved to be difficult as a duricrust was often encountered at shallow depth, which prevented, in some cases, collection of samples below the assumed evapotranspirative zone.

Table 4-6 – Summary information for the unsaturated zone soil sampling for CMB

Profile ID	**Location (dd)**		**Sampling date**	**Profile depth (m)**	**Hydrogeological context**
	Longitude	Latitude			
CMB01	-1.764	9.310	2008-01-30	4.2	Voltaian sed. basin
CMB03	-0.926	8.846	2007-12-15	0.9	Voltaian sed. basin
CMB04	-0.837	9.553	2007-12-13	6.6	Voltaian sed. basin
CMB05	-1.283	10.038	2008-02-07	4.8	Voltaian sed. basin
CMB06	-0.520	8.572	2008-01-29	2.4	Voltaian sed. basin
CMB07	-0.070	8.950	2008-01-17	2.9	Voltaian sed. basin
CMB08	0.199	9.353	2008-01-15	1.7	Voltaian sed. basin
CMB09	-0.270	9.379	2008-01-16	2.6	Voltaian sed. basin
CMB11	-0.181	9.946	2008-01-11	2.3	Voltaian sed. basin
CMB12	0.051	10.528	2008-01-09	3	Voltaian sed. basin
CMB13	-0.751	10.288	2008-01-10	3.9	Voltaian sed. basin
CMB14	-0.292	11.029	2008-02-10	2.7	Precambrian basement
CMB15	-1.077	10.905	2008-02-08	5.7	Precambrian basement
CMB16	-1.980	10.871	2008-02-04	3	Precambrian basement
CMB17	-2.670	10.378	2008-02-02	3.3	Precambrian basement
CMB18	-1.990	10.318	2008-02-03	4.2	Precambrian basement
CMB19	-2.490	9.695	2008-02-01	2.7	Precambrian basement
CMB20	-2.456	8.982	2008-01-31	1.3	Precambrian basement

Soil sampling in the unsaturated zone was carried out during the 2007-2008 dry season, using a truck-mounted hollow stem auger. Samples were collected at 0.3 m intervals until the water table was reached or until refusal. Core samples recovered with a split-spoon sampler were stored in 250 ml Kilner® jars and placed in an ice chest to minimize potential evaporation. All soil samples were sent to the British Geological Survey (BGS) laboratory in Wallingford (UK) for extraction and analysis of porewater. Moisture content was determined upon reception of samples by loss on drying. Extraction was carried out by elutriation for all samples (188 samples, excl. samples damaged during transport) and by centrifugation when moisture content and particle size of samples allowed it (61 samples). For elutriation, 30 ml of deionised water was added to 50 g of soil; resulting supernatant was filtered (0.45 µm) and used for analysis of Cl and NO_3 by ion chromatography (detection limit of 0.1 mg/L). Soil sub-samples (~ 100 g) submitted to centrifugation were usually spun at 14 000 rpm for 35 minutes; accumulated porewater was filtered (0.45 µm) and analyzed for Cl and NO_3 by ion chromatography.

Figure 4-7 – Location of the unsaturated zone soil sampling for CMB

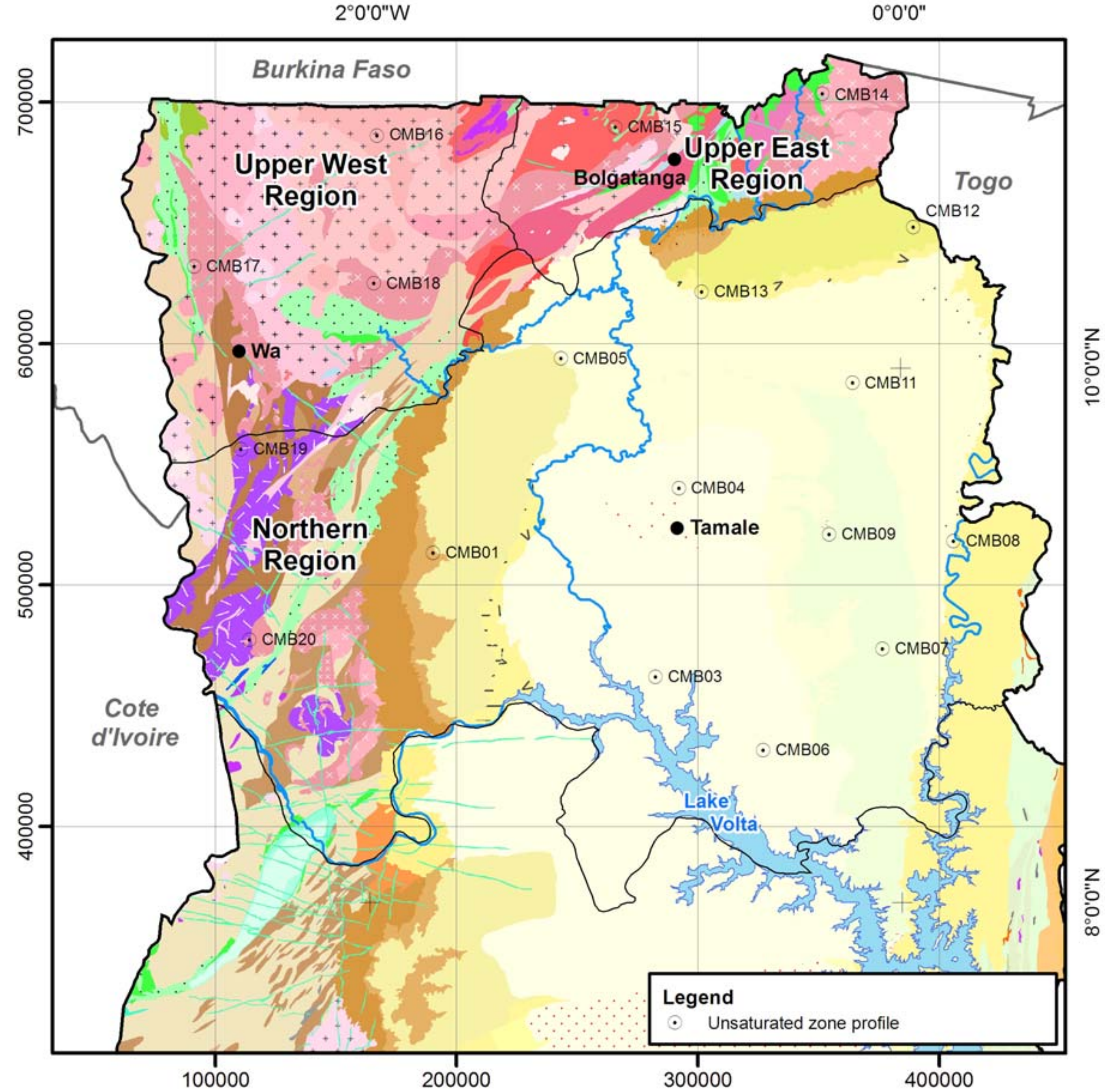

4.3.6.3 *Shallow groundwater sampling*

Shallow groundwater samples were collected at 23 modern hand-dug wells across northern Ghana. This number is much lower than the 90 wells initially targeted to provide adequate spatial coverage for groundwater recharge estimation with the saturated zone CMB method. The main cause of this shortcoming is the plain fact that hand-dug wells proved to be fewer than expected on the planned itinerary for this sampling campaign and the concurrent geochemical sampling campaign (the first one) described in section 4.3.5. As no additional time could be spared to search for hand-dug wells away from the planned itinerary, the objective for the shallow groundwater sampling campaign could not be met. Furthermore, because of field work constraints (e.g. well access) and lack of data records, no information could be collected concerning the well construction (i.e. well depth, construction date, lithology intercepted …).

Table 4-7 summarizes available information concerning these wells while Figure 4-8 shows their location.

Since these wells were usually used for water supply, they were not purged prior to sampling. Samples were collected between August and September 2010. They were sent to the Atomic Energy of Ghana laboratory in Accra and the following parameters were analyzed: pH, redox potential (Eh), dissolved oxygen (DO), turbidity, total hardness total dissolved solids (TDS), conductivity (EC), calcium (Ca^{2+}), magnesium (Mg^{2+}), sodium (Na^{+}), potassium (K^{+}), chloride (Cl^{-}), nitrite (NO_2^{-} as N), nitrate (NO_3^{-} as N), sulphate (SO_4^{2-}), fluoride (F^{-}), bicarbonate (HCO_3^{-}), phosphate (PO_4^{3-}), aluminium (Al), copper (Cu), chromium (Cr), cobalt (Co), cadmium (Cd), iron (Fe), manganese (Mn), nickel (Ni), lead (Pb), zinc (Zn) and arsenic (As).

Figure 4-8 – Location of the shallow groundwater sampling for CMB

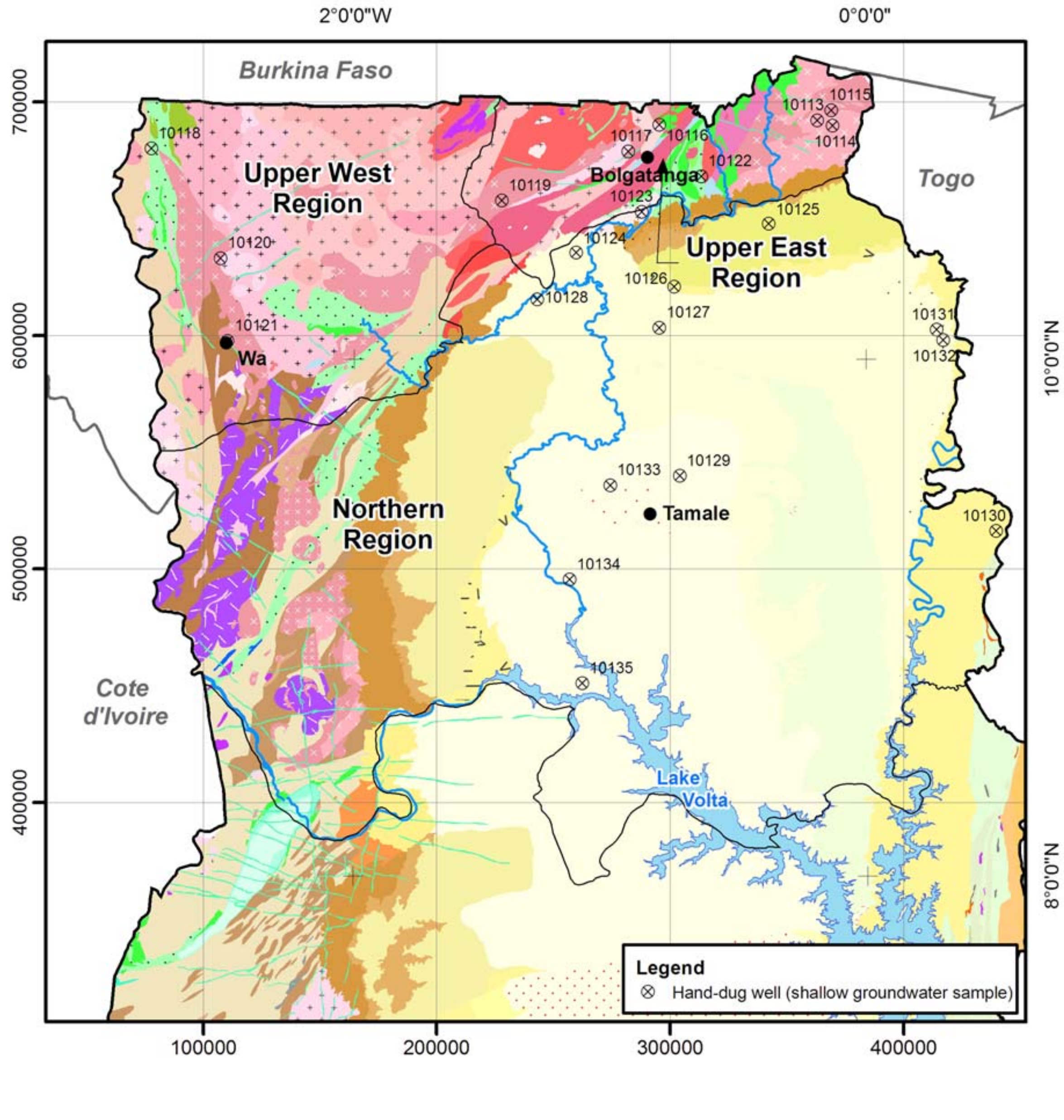

Table 4-7 – Summary information for the hand-dug wells sampled for CMB

Well ID	Location (dd)		Community	Water level (m bgl)	Hydrogeological context
	Longitude	Latitude			
10113	-0.188	10.926	Kuka-Zule	1.50	Precambrian basement
10114	-0.128	10.905	Kugsabilla	1.20	Precambrian basement
10115	-0.133	10.966	Zambala no.1	1.00	Precambrian basement
10116	-0.807	10.911	Bongo-Nayire	1.26	Precambrian basement
10117	-0.928	10.807	Sumbrungu Zorgo	1.20	Precambrian basement
10118	-2.795	10.813	Monyupele	3.30	Precambrian basement
10119	-1.424	10.616	Doringa-Noverinsa	0.80	Precambrian basement
10120	-2.523	10.391	Uwollo	9.12	Precambrian basement
10121	-2.494	10.071	Wa	2.04	Precambrian basement
10122	-0.643	10.710	Dakotu	N/A	Precambrian basement
10123	-0.875	10.574	Arigu	1.00	Precambrian basement
10124	-1.132	10.416	Kunkwa	1.33	Voltaian sed. basin
10125	-0.378	10.527	Nalerigu	0.63	Voltaian sed. basin
10126	-0.749	10.284	Bugya-Pala	1.92	Voltaian sed. basin
10127	-0.807	10.125	Kukobila	0.30	Voltaian sed. basin
10128	-1.284	10.234	Yagaba	1.50	Voltaian sed. basin
10129	-0.728	9.551	Nanton	2.10	Voltaian sed. basin
10130	0.506	9.335	Nakpali	1.50	Voltaian sed. basin
10131	0.277	10.115	Banjani	0.10	Voltaian sed. basin
10132	0.302	10.074	Tacheku	1.65	Voltaian sed. basin
10133	-0.999	9.514	Villi	2.15	Voltaian sed. basin
10134	-1.157	9.149	Yapei	1.87	Voltaian sed. basin
10135	-1.107	8.748	Mpaha	1.00	Voltaian sed. basin

5. REGIONAL HYDROGEOLOGICAL SYNTHESIS

This section presents the hydrogeological synthesis of northern Ghana that could be drawn on the basis of the compilation and review of previous work (section 4.1), the exploitation of data gathered in the consolidated database (section 4.2), and the interpretation of new information obtained from targeted field work (section 4.3).

In the following section 5.1 on hydrogeological setting, general hydrogeological contexts of northern Ghana are first qualitatively described on the basis of previous work (section 5.1.1). This qualitative image of hydrogeological contexts is complemented by the analysis of data compiled in the database, which was used to prepare hydrostratigraphic cross sections (section 5.1.2), define the spatial distribution of regolith thickness in northern Ghana (section 5.1.3) and interpolate groundwater levels in representative basins (section 5.1.4). This analysis provides better insight on the spatial distribution of hydrostratigraphic units and their implications on groundwater flow in northern Ghana.

Analysis of compiled data from the consolidated database and new information obtained from field work also provides a better perspective on the groundwater production potential, which is the focus of section 5.2. Statistics obtained from the database give a quantitative view of well characteristics and aquifer hydraulic properties (section 5.2.1) and of potential drilling success rate (section 5.2.2). Compiled and new data allowed the estimation of groundwater recharge using soil moisture balance and chloride mass balance methods (section 5.3). Following a review of available groundwater quality data compiled in the database, a regional geochemical characterization of groundwater was undertaken to provide representative and reliable data that allowed the preparation of a groundwater quality and geochemistry overview (section 5.4).

This picture of hydrogeological settings, groundwater exploitability and quality in northern Ghana should be helpful for the planning and cost estimation of groundwater supply projects. Based on this hydrogeological synthesis, section 5.5 provides a perspective on the sustainable use of groundwater resources in northern Ghana.

5.1 Hydrogeological setting

5.1.1 Hydrogeological context

In Ghana, the main hydrogeological contexts have been primarily delineated on the basis of geology, which influences groundwater occurrence and availability (Gill, 1969). The two major hydrogeological contexts found in northern Ghana are related to the Voltaian sedimentary basin (VSB) and Precambrian basement (PCB) rocks.

Rocks of the **Precambrian basement (PCB)** usually possess low primary porosities and permeabilities. Groundwater occurrence and flow in this context are therefore mainly controlled by secondary porosity as a result of chemical weathering, faulting and fracturing (from tectonic activity and isostatic uplift). Weathering has a significant impact on the storage capacity of crystalline rocks (Larsson, 1984). However, characteristics of aquifers in such environments are variable, primarily because of the anisotropic nature of fracture networks and the complexity and variable intensity of weathering processes involved in regolith development. The most productive zone in terms of groundwater generally comprises the lower part of the saprolite and the upper part of the fractured bedrock (i.e. saprock), which generally complement each other in terms of permeability and storage. The upper, less permeable, part of the saprolite can act as a confining or semi-confining layer for this productive zone while the lower, usually saturated part of the saprolite is characterized by lower secondary clay content as groundwater flow can remove dissolved minerals, thus creating a zone of enhanced hydraulic conductivity. On average, areas underlain by rocks of the Birimian Supergroup or Tarkwaian Group would exhibit deeper weathering (~ 23 m) than areas underlain by granitoids (~ 15 m), mostly as a result of poorer jointing and fracturing in the latter (Nathan and Harris, 1970). This generally results in a shallower water table and lower borehole yields for the granitoid areas. Within the upper fractured bedrock, aquifers are generally associated with subhorizontal fractures related to isostatic uplift resulting from the removal of overlying material (e.g. erosion or dissolution during weathering) (Wright, 1992). While transmissivity is reported to decrease with depth as fractures close under the increasing overlying weight, the data available suggest that important subvertical fracture or fault zones originating from tectonic activity can be present at great depths (> 150 m) and provide significant amounts of groundwater. Average borehole depth is however less than 80 m in general (Agyekum, 2004). In the Birimian Supergroup, rocks intruded by quartz-veins or pegmatites are also known to yield substantial quantities of groundwater. In some cases, hydraulic connectivity between the lower saprolite and the saprock may vary with weathering intensity and fracture characteristics and lead to separate aquifer systems. When taken separately, the regolith aquifer can exhibit a higher transmissivity than the fractured rock aquifer because of its generally greater saturated thickness. The impervious nature of the upper regolith and/or the presence of an indurated layer at the base of the residual soil zone can also allow the development of a shallow perched aquifer if the upper residual soil zone consists of coarsely textured material. Documentation on the occurrence of shallow aquifers was however not available.

In the **Voltaian sedimentary basin** (VSB), rocks are generally well consolidated and inherently impermeable. Fracturing, faulting and, to a lesser extent, weathering have however increased the permeability of some of these rocks at the local scale (i.e. mostly for harder, older rocks through tectonic activity or low-grade metamorphism). Groundwater mainly occurs and flows in fractured zones, and along bedding planes for some areas, since the primary porosity of these rocks has been destroyed through consolidation and cementation (Sander *et al.*, 1996). The regolith is reported to be unsaturated in many areas and would thus only provide minor amounts of groundwater locally (Acheampong and Hess, 1998). The average thickness of the regolith over the Voltaian sedimentary rocks is approximately 9 m (Nathan and Harris, 1970). Previous investigations in the Nanumba and West Gonja districts revealed average regolith thickness of 6 m and 11.2 m respectively (Bannerman, 1990). The relatively thin regolith in the VSB can be partly explained by the stable clay (in shale) or quartz (in sandstone) composition or by the fine texture or ductile nature of sedimentary rocks found in the Voltaian (e.g. soft unmetamorphosed mudstone) (Larsson, 1984; MacDonald *et al.*, 2005). Deeper weathering may however occur in some areas, such as those underlain by arkose or arkosic sandstone (e.g. in Pendjari-Oti Group) as K-feldspar weathers more easily than quartz and clay minerals. Underlying fracture zones are generally developed in bedrock at depths greater than 20 m below ground surface (Acheampong, 1996) but, on average, required yields for rural supplies are obtained at depths shallower than 100 m. As a result, production potential from deeper fractures has not been investigated thoroughly. Fracture characteristics such as frequency, aperture and connectivity can vary substantially over small distances, making it difficult to locate laterally extensive aquifers. Bannerman (1990) reports that the bulk of productive fracture zones in the West Gonja district of the Northern Region would occur between 13 m and 80 m with an average depth of 27 m. As for the Precambrian basement, the upper part of the regolith can act as a semi-confining layer where it is thick enough. Shallow perched aquifers can also be encountered where coarsely textured surface material overlies a less permeable layer such as ferricrete.

5.1.2 Distribution of hydrostratigraphic units

5.1.2.1 Typical units and statistics

The definition of typical hydrostratigraphic units was largely based on previous work in Ghana (Acheampong, 1996; Asomaning, 1992; Bannerman, 1990; Buckley, 1986; Martin, 2006; Nathan and Harris, 1970) and in similar semi-arid environments in which aquifers are present in deeply weathered Precambrian rocks (Acworth, 1987; Chilton and Foster, 1995; Dewandel *et al.*, 2006; LeGrand, 2004; MacDonald *et al.*, 2005; Taylor and Howard, 2000; Wright, 1992). The information gathered from these sources allowed a qualitative representation of the typical hydrostratigraphy that is valid on a regional scale but that may not be locally representative due to variations in thickness, lateral extent and composition of the regolith. Figure 5-1 illustrates these hydrostratigraphic units and their typical depth range.

Figure 5–1 – Typical hydrostratigraphic units for main hydrogeological contexts

Precambrian basement	
General hydrostratigraphy	**Thickness**
Possible perched aquifer	< 5 m
Leaky semi-confining layer possibly unsaturated locally or during dry season	0-20 m
Leaky aquifer with productive zone in lower part	5-15 m
Leaky fractured aquifer (productive zone mostly associated with sub-horizontal fractures)	15-20 m
Fractured aquifer (variably productive, mostly associated with sub-vertical fractures)	~

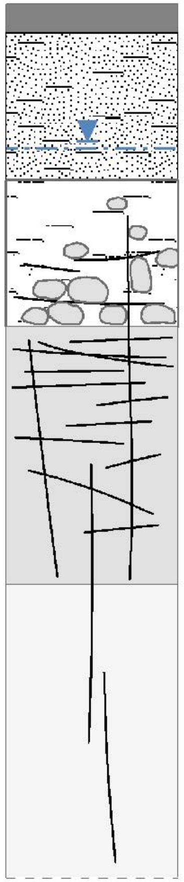

General lithology
Residual soil (see note)
Unconsolidated material with little structure preserved
Highly weathered rock (relatively consolidated with structure mostly preserved)
Fractured/weathered rock (moderately to slightly weathered rock with fracture density decreasing downward)
Fresh rock (largely unweathered and variably fractured)

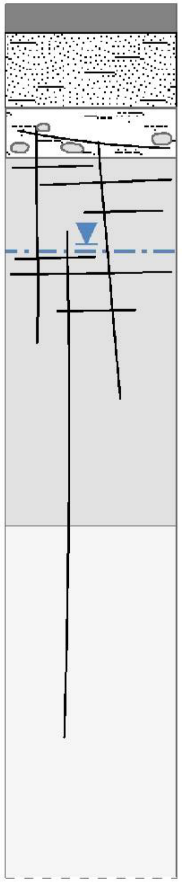

Voltaian sedimentary basin	
Thickness	**General hydrostratigraphy**
< 5 m	Possible perched aquifer
2-15 m	Usually unsaturated zone that can act as a leaky semi-confining layer depending on parent rock and groundwater level
10-80 m	Leaky fractured aquifer (highly variable productive zone depending on lithology, weathering, depth and structure)
~	Fractured aquifer (variably productive, mostly associated with sub-vertical fractures)

Note:
Includes surface material (transported and *in situ* material often undissociated) and indurated layer (e.g. ferricrete) in some places.

In crystalline rocks, intermittent perched aquifers can sometimes be encountered in the shallow residual soil layer if coarsely textured material overlies a less permeable layer. When unsaturated, the field capacity of this layer partly determines the amount of recharge reaching underlying aquifers. Typically, permeability of this layer decreases rapidly towards the underlying saprolite. The main aquifer, as depicted in Figure 5-1, corresponds to the integrated aquifer system discussed in section 5.1.1. The saprolite is defined as a leaky aquifer but it mainly acts as a reservoir of groundwater feeding the underlying permeable fractures. The saprolite is characterized by two distinctive zones, an upper almost completely decomposed zone, and a lower highly weathered zone. The lower, usually more productive zone has an enhanced hydraulic conductivity and retains a much higher proportion of primary minerals than the upper part, which is typically unsaturated with a high proportion of secondary clay. The underlying fractured aquifer may also be divided in two parts for which the shared boundary is not always sharp. The upper part is generally associated with sub-horizontal fractures resulting from surface decompression.

While the upper part of the fractured aquifer usually has a higher fracture density than the lower part, it can also have lower permeability as slight to moderate weathering can result in secondary clay minerals in-filling and sealing fractures. Depending on local conditions, groundwater can leak from the overlying saprolite and recharge this aquifer. The lower part would be more variable laterally as it corresponds to subvertical fractures generated by tectonic forces. The frequency and permeability of such fractures usually decrease with depth. For the integrated aquifer system, the average groundwater level would generally fall in the saprolite layer even though significant water strikes are generally not encountered before saprolite base due to the low permeability of overlying material. This is sometimes misinterpreted as semi-confined conditions (Buckley, 1986).

In the sedimentary rocks of the Voltaian, the main aquifer is generally located in fractured rock as the regolith is often too thin to store significant amounts of water. Consequently, water levels are generally deeper than in the crystalline rock aquifers and fall near or below the base of the regolith. The relatively thin and sandy regolith developed over rocks such as sandstone and siltstone would, on the other hand, facilitate recharge to the underlying fractured aquifer. The thickness and extent of the upper fractured zone is highly variable (Bannerman, 1990). Shallow perched aquifers could also be found locally, where surface material allows, although information on such aquifers is not available.

Subsequently to the qualitative representation of typical hydrostratigraphic units, available data were also used to provide statistics on regolith thickness and its distribution since this unit, along with the fractured bedrock, is commonly targeted for installation of wells. However, it was not possible to provide representative statistics for the fractured bedrock unit as commonly used drilling methods do not generally allow accurate characterization of fractured zones. The regolith unit considered here includes the upper and lower part of the saprolite (N.B.: the residual soil has been left out for statistics calculation in order to consider only *in situ* weathered material). Statistics were computed on unique and reliable boreholes that penetrated the regolith completely and that had lithological descriptions (i.e. 801 boreholes in total). Table 5-1 summarizes the regolith thickness statistics for the main hydrogeological contexts based on geology. Figures 5-2 and 5-3 respectively illustrate the distribution and cumulative distribution of regolith thickness values by hydrogeological context.

Statistics presented here are generally coherent with those presented in previous studies (see section 5.1.1). Some differences are however observed, notably the average regolith thickness over intrusive rocks (~ 28 m) is somewhat higher than that stated in literature (~ 15 m). Most differences observed could perhaps be attributed to the relatively small number of boreholes available to compute statistics over such large areas. While the validation process identified and corrected major errors in the initial consolidated database, errors still present in the electronic data could also cause discrepancies between the statistics presented here and values quoted in the literature.

Table 5-1 – Regolith thickness statistics by hydrogeological context

Hydrogeological contexts		All	Precambrian Basement				Voltaian Supergroup			
		All	All	Birimian & Tarkwaian	Intrusive rocks	Buem	All	Obosum	Pendjari-Oti	Kwahu-Morago
Total boreholes [1]		7874	4195	2019	2159	17	3679	828	2065	786
Boreholes with data on regolith [2]		801	348	174	173	1	453	173	236	44
Distribution of regolith thickness	<10m	218	53	42	11	0	165	71	84	10
	10-20m	197	59	29	30	0	138	50	72	16
	20-30m	216	130	57	73	0	86	21	54	11
	30-40m	114	77	35	42	0	37	17	17	3
	>40m	56	29	11	17	1	27	14	9	4
Total regolith thickness range (m)		0.5-100	1-100	1-57	2-100	-	0.5-83.5	1.8-83.5	0.5-62.5	3 - 72
Probable reg. thickness range (95%) (m) [3]		2-48	2-47.5	1-44.7	6.4-61.3	-	3-49	2.9-51.9	3-45	6 - 48
Mean reg. thickness (m)		20.8	25.2	22.2	28.1	43.4	17.5	17.5	17	20.3
Median reg. thickness (m)		20	25.1	24	26.5	-	14.5	12.2	15	15.2
Standard deviation (m)		13.5	13.3	12.7	13.4	-	12.7	14.5	11	13.9

Notes:
(1) : Only unique boreholes with reliable coordinates were considered
(2) : Only boreholes penetrating entire regolith are considered here (N.B.: regolith includes residual soil and weathered material above bedrock)
(3) : Regolith thickness range for the middle 95% of the distribution

Figure 5-2 – Distribution of regolith thickness by hydrogeological context

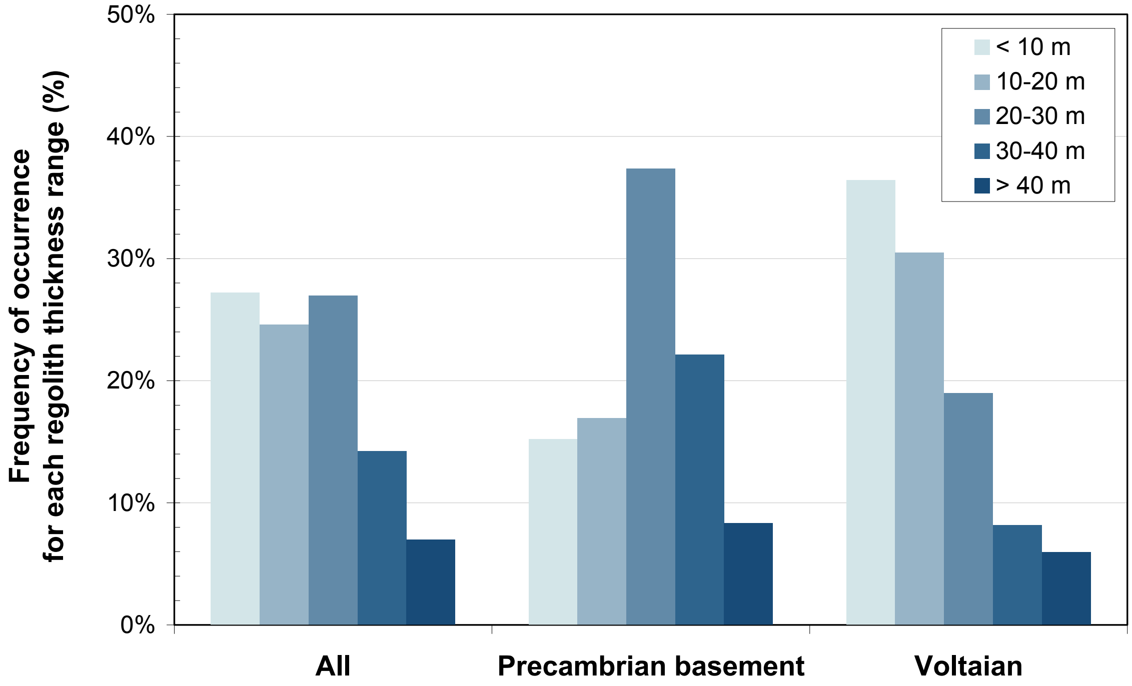

Figure 5-3 – Cumulative distribution of regolith thickness by hydrogeological context

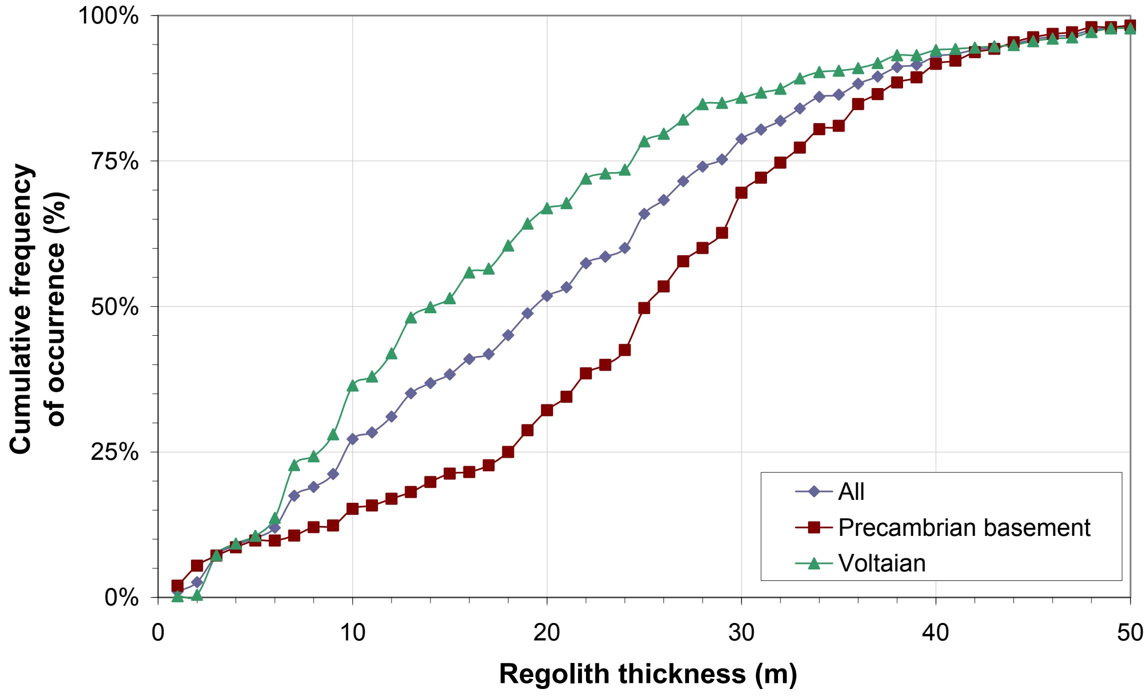

Overall, values presented in Table 5-1 reveal that the regolith is generally thinner over the Voltaian sedimentary basin (~ 17.5 m) than over the Precambrian basement (~ 25.2 m). This is also illustrated in Figure 5-2 showing that most boreholes considered in the VSB are characterized by a regolith thickness lower than 10 m while the bulk of boreholes considered for the Precambrian basement are within the 20-30 m thickness range. The cumulative frequency distribution (Figure 5-3) also reveals that the range within which the bulk of regolith thickness values are located is slightly broader for the Voltaian (~ 7-40 m) than for the Precambrian basement (~ 18-40 m), suggesting a more variable regolith thickness.

5.1.2.2 Hydrostratigraphic cross sections and their implications

Three regional cross sections were prepared to illustrate the thickness and continuity of the regolith in relation with topography. Areas with dense borehole coverage were selected in the two main hydrogeological contexts for the location of the cross sections:

- Navrongo-Bawku cross section (west-east in Precambrian basement) (~ 164 km)
- Wa-Bole cross section (north-south in Precambrian basement) (~ 165 km)
- Savelugu-Gushiegu cross section (west-east in VSB) (~ 171 km)

Five hydrostratigraphic units were considered for the cross sections: residual soil, upper and lower parts of weathered layer, fractured and fresh bedrock. The lower part of weathered layer and the fractured bedrock are considered separately here in order to better illustrate regolith thickness variations. On the basis of lithological descriptions and complementary information (e.g. screened intervals, groundwater levels), these units were assigned to unique and reliable boreholes in the HAP database.

Figure 5-4 shows the locations (or traces) of the cross sections. For each cross section, boreholes with lithological descriptions that were within 5 km of the trace were used and projected onto the trace so that the relative horizontal distances on the cross sections are projected distances. Hydrostratigraphic unit depths and screened interval depths (when available) were plotted on the cross sections with respect to surface topography. Interpolation of the surface of each hydrostratigraphic unit was done using a simple linear interpolation between boreholes. Resulting values were subsequently adjusted with respect to surface topography. As few boreholes provided detailed information on the fractured bedrock, the latter was approximated by a constant 80 m thick layer adjusted with respect to surface topography. This constant thickness was derived from the few available deep boreholes. The resulting cross sections are presented in Appendix D (USB flash drive) and a selected portion of one of the cross sections is shown in Figure 5-5.

Analysis of the cross sections reveals a variable regolith thickness in both hydrogeological contexts, Precambrian basement and Voltaian sedimentary basin (Figure 5-5). However, the regolith appears to be generally thicker in the Precambrian basement when compared with the Voltaian sedimentary basin, especially for the upper part of the weathered zone. This is in agreement with the statistics presented in the previous section. The thickness and continuity of the regolith may have significant implications as areas characterized by thin regolith could represent preferential recharge areas. However, to identify recharge areas adequately, additional information would be required, notably concerning soil texture, vegetation, land use and slope. Other types of data that could also help identify recharge areas would be well hydrographs and hydrogeochemical data. The latter are respectively discussed in section 5.3 and 5.4.

Another observation from the cross sections is that screened intervals, which generally correspond to productive aquifer zones, are generally shallower in the Precambrian basement and located in the lower part of the weathered layer, whereas in the Voltaian they are mostly located in the fractured bedrock. This could imply that the minimum required yield would generally be reached through shallower boreholes in the Precambrian basement than in the Voltaian sedimentary basin. But again, such a comparison should be taken with caution as it notably does not consider the sustainability of the resource.

The variations in surface topography and regolith thickness could also lead to localized and isolated aquifers, especially in the Precambrian basement setting. The prevalence of such discrete aquifers in similar contexts was also mentioned in previous studies (Bannerman and Ayibotele, 1984; Larsson, 1984; Omorinbola, 1984).

Figure 5-4 – Locations of hydrostratigraphic cross sections and selected boreholes

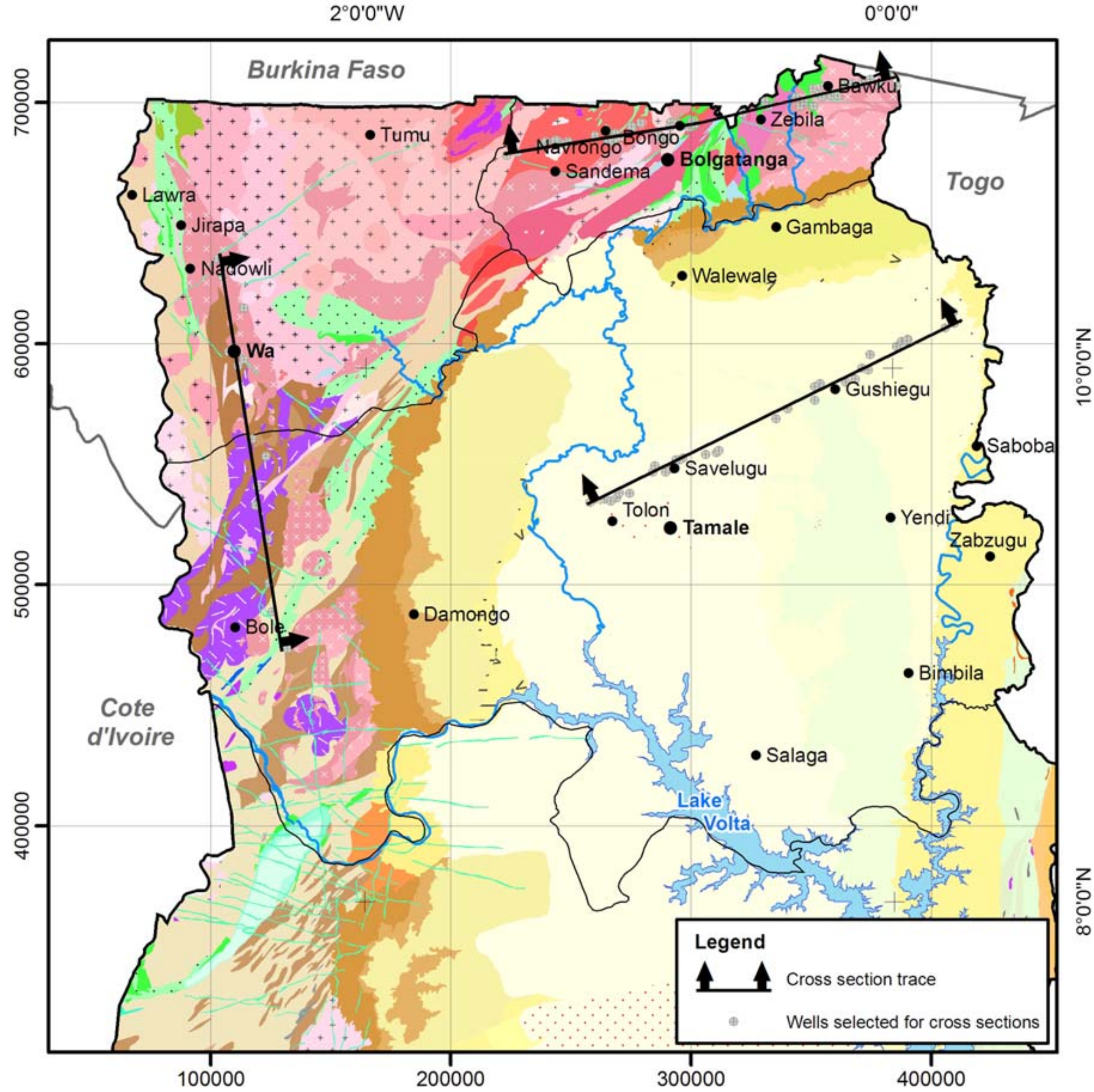

5.1.3 Spatial distribution of regolith thickness

Regolith thickness was interpolated over the study area to complement the cross sections and illustrate potential lateral variations in thickness. The interpolation results are intended to give an idea of general regional trends in regolith thickness variations. Given the variability of regolith thicknesses over short distances, it is however possible that thicknesses encountered locally will differ from regionally interpolated values.

With the exception of a few boreholes that were removed as they represented probable anomalous values, regolith thicknesses were interpolated using the same boreholes that were used to compute statistics in section 5.1.2.1 (i.e. 801 boreholes). The interpolation was carried out separately for each of the two main hydrogeological contexts as thicknesses in these contexts are considered independent. A Matlab program from Marcotte (1991) was used to interpolate values by ordinary kriging on a 5 km grid. The experimental and model variograms used for kriging in both contexts are presented in Figures 5-6 and 5-7 along with the variogram model parameters. Both variogram models have strong nugget effects, reflecting regolith thickness variability over short distances. Only omnidirectional variograms are shown as directional variograms computed (0°, 45°, 90°, 135°) did not reveal significant anisotropy.

Figure 5-5 – Selected portion of the Wa-Bole hydrostratigraphic cross section

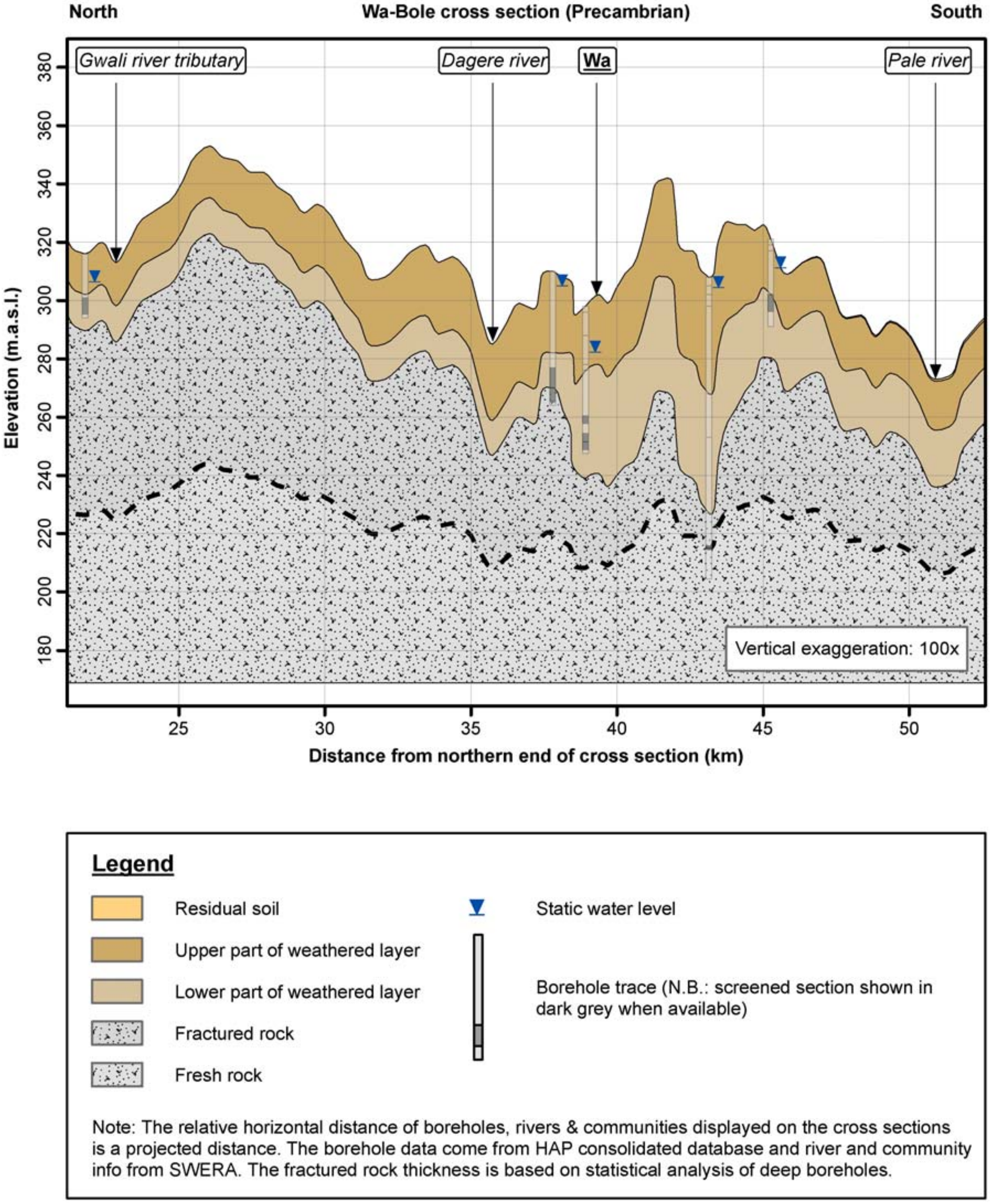

Interpolated values from both contexts were subsequently joined and exported into ArcGIS for graphical representation (Figure 5-8). Two color schemes were used for the figure to emphasize that values for each context were interpolated separately. Boreholes used for the interpolation are also displayed on the figure to highlight areas of poor data density and thus likely to be characterized by higher uncertainty.

As expected from literature, Figure 5-8 reveals a generally thinner regolith over the rocks of the Voltaian sedimentary basin than over the Precambrian basement. Areas where the estimated regolith is thinnest are located around Pigu (northern Savelugu Nanton district) while the highest interpolated regolith thicknesses are found west of Bole. Within the PCB, broad areas are found with generally uniform regolith thickness, whereas in the VSB regolith thickness is quite variable. The regional variations of thickness shown in Figure 5-8 could help to identify potential recharge areas. While this is briefly discussed in section 5.3, additional work would be required in order to verify the relation identified between regolith thickness and recharge. Another aspect that could be further investigated with additional information (e.g. multi-level well to characterize vertical gradient) is flow conditions encountered at regional scale. Areas with thicker regolith would more likely be characterized by confined or semi-confined conditions than areas with thinner regolith. The interpolated regolith thickness could also be used as an indicator of aquifer vulnerability along with other information such as depth to groundwater and location of groundwater recharge areas since commonly used vulnerability assessment methods in temperate climates are not appropriate to assess vulnerability at regional scale in semi-arid and arid climates (Robins *et al.*, 2007). While such an approach at regional scale will not replace the need for local vulnerability assessment, it can suggest potentially vulnerable areas (where regolith is thinner) that could be further investigated.

Figure 5-6 – Experimental and model variograms for kriging of regolith thickness (Precambrian basement)

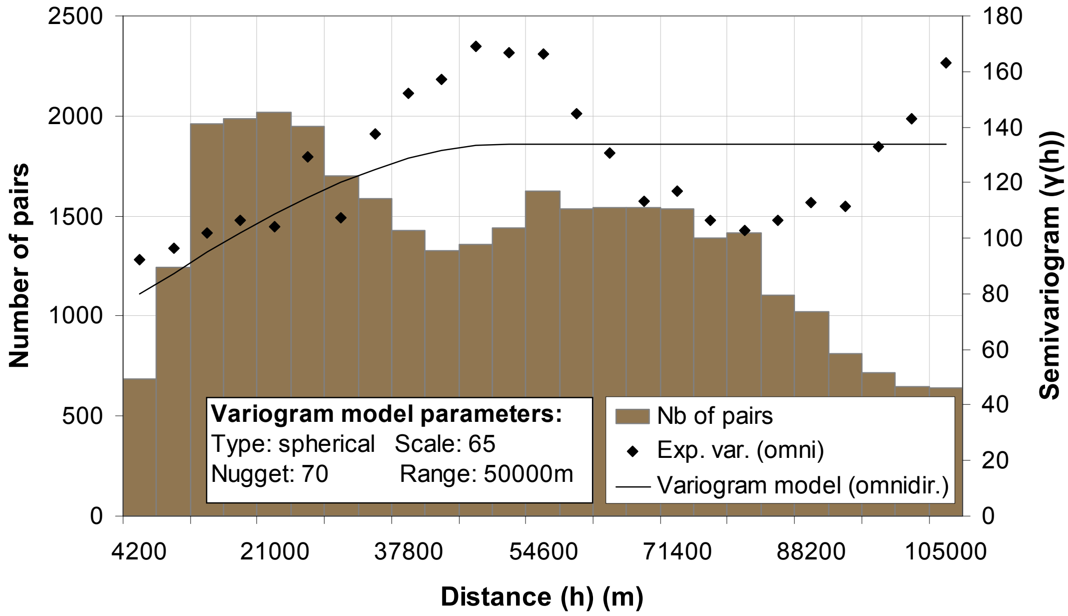

Figure 5-7 – Experimental and model variograms for kriging of regolith thickness (Voltaian sedimentary basin)

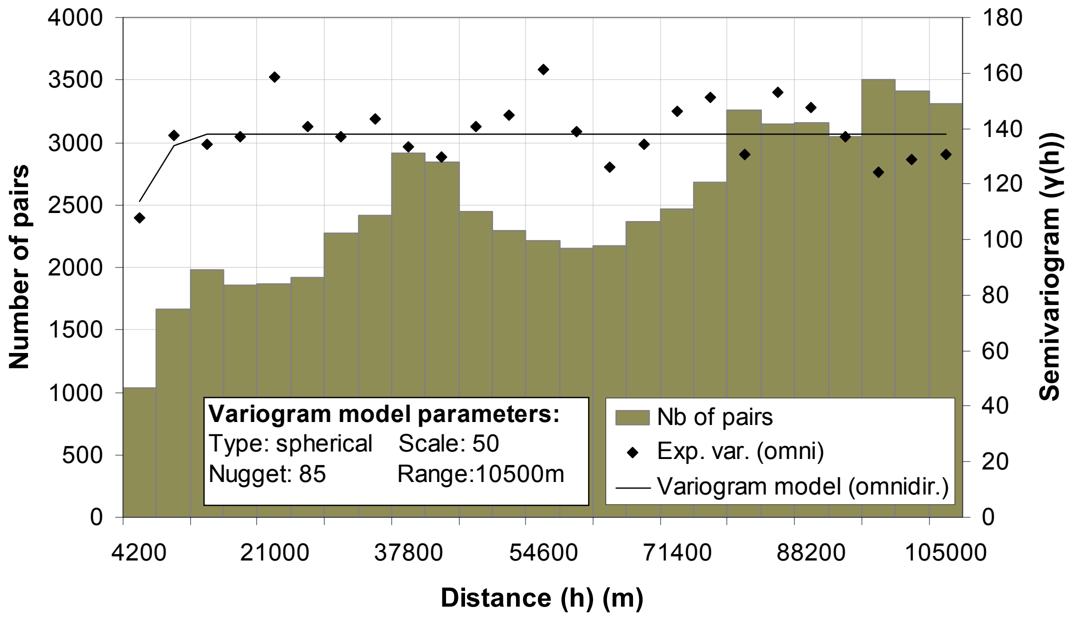

Figure 5-8 – Regolith thickness interpolated separately for the Precambrian basement and Voltaian sedimentary basin (shown by different color schemes)

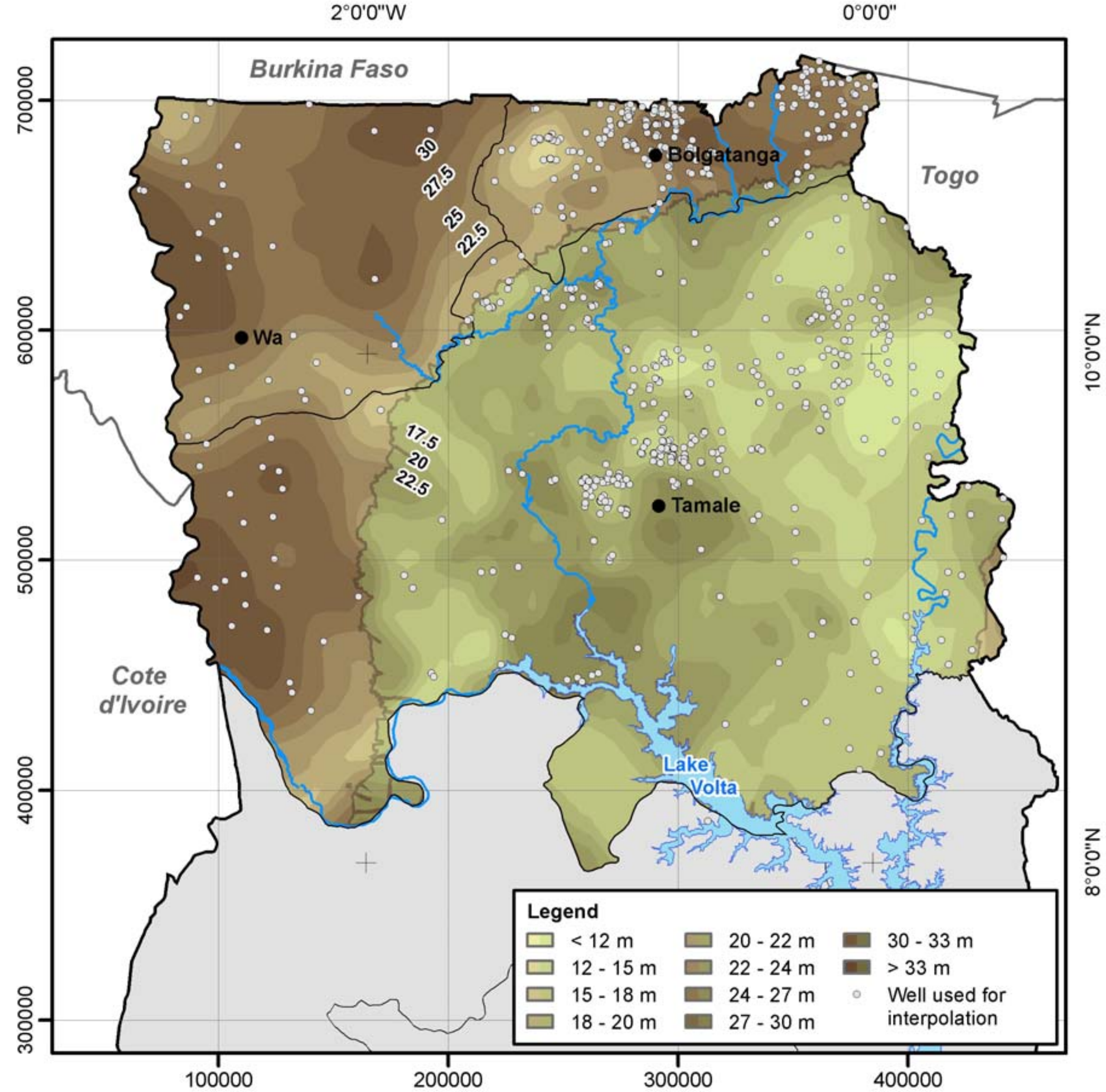

5.1.4 Groundwater levels and flow in representative basins

Available groundwater level data were not sufficient to allow the drawing of a potentiometric map over northern Ghana. However, as a first step towards the assessment of aquifer dynamics in northern Ghana, groundwater level maps were prepared for two representative hydrological basins within which more groundwater level data were available: the Nabogo basin located in the VSB and the Tamne Basin located in the Precambrian basement (Figure 5-9). Selection of these basins was mostly based on the availability of boreholes with groundwater level measurements as well as gauging stations with stream flow data. As groundwater level data were scarce even within the selected basins, three different methods were applied to provide representative groundwater level maps.

5.1.4.1 Methods used to map potentiometric surfaces

Three interpolation methods were used with direct and indirect data to estimate the potentiometric surfaces in the two basins selected: 1) geostatistical method with water levels of rivers, 2) geostatistical method with water levels of rivers and groundwater levels in wells and 3)

GIS method based on topographical and hydrological controls. The use of these methods requires that we assume the existence of a hydraulic link between the main rivers and the integrated aquifer system intercepted by most wells. While this may not be representative of conditions everywhere in the basins and throughout the year, groundwater flow is likely to mimic surface flow relatively closely at the regional scale considered.

Figure 5-9 – Location of representative basins selected for groundwater level mapping

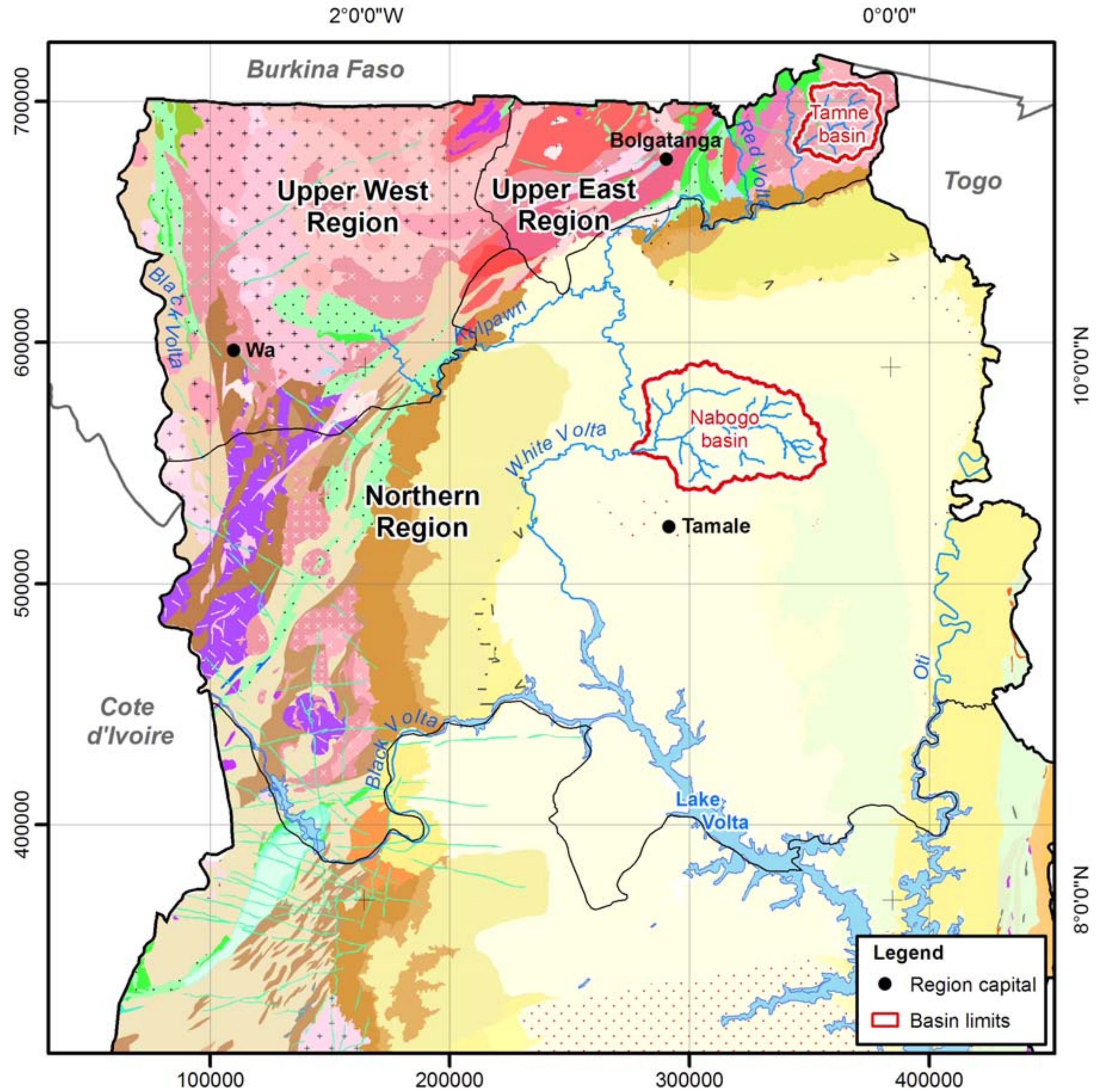

The first two methods use ordinary kriging to interpolate groundwater levels. They respectively use water levels of rivers, assumed to be equivalent to groundwater elevation along rivers at the scale considered, and groundwater levels of available wells in addition to water levels of rivers. For the calculations, rivers elevations were converted to point data in ArcGIS. Ordinary kriging was carried out in Matlab (Marcotte, 1991) on a 1 km grid and results were exported in ArcGIS for contouring.

The third method is largely based on a method proposed by Salama *et al*. (1996), which estimates depth to groundwater with respect to terrain morphology (i.e. slope, elevation) and hydrological characteristics of the basins (i.e. proximity to rivers, drainage density, hydraulic link between surface water and groundwater). Hydrogeological characteristics of the basins were also considered qualitatively as spatial distribution of hydrogeological parameters such as hydraulic conductivity and porosity were not available for the basins. The elevation and slope classes as well as the main rivers considered in the calculations are presented in the following sections for each basin. Groundwater levels were estimated for each slope/elevation classes using the following empirical relation in ArcGIS using raster overlay (layers of 90 x 90 m cells):

$$Z_w = Z - AS\ln\left(1000\tan S\right) \quad [5.1]$$

where Z_w is the estimated groundwater elevation (meters above sea level or m asl), Z is the topographic surface elevation (m asl), S is the slope (degrees) and A is an elevation scaler (m/deg) given by:

$$A = B\left(\frac{Z - Z_{\min}}{Z_{\max} - Z_{\min}}\right) \quad [5.2]$$

where B represents a hydrogeological factor estimated for each slope/elevation classes. The value of B decreases from steep sloped areas (~ 25 m/deg) to flat areas (~ 0.25 m/deg). The influence of rivers was taken into account by reducing B for each cell falling within 90 m of main rivers (N.B.: a 0.25 to 0.75 reduction factor was used depending on slope/elevation class considered). Although Salama *et al.* (1996) demonstrated that this method can be used with good results using only indirect data, available groundwater level data were used to optimize the hydrogeological factor B. The latter was estimated at well locations where groundwater levels were available. Resulting values were used to assign representative values of B to each slope/elevation classes.

5.1.4.2 Results for the selected representative basins

The **Nabogo River** basin is a sub-basin of the White Volta River basin and is located approximately 40 km north of Tamale, between latitudes 9°32'N and 10°01'N and longitudes 0°59'W and 0°15'W. It drains an area of about 2 900 km^2 and includes many small streams, most of which join with the Nabogo River upstream of the Nabogo gauging station, located near the town of Nabogo. Elevation within the basin ranges from 106 to 269 m above sea level, with an average of 152 m. The basin overlies a part of the Voltaian sedimentary basin where the most common rocks intercepted by the available wells consists of shale, mudstone and sandstone.

The **Tamne River** basin is a sub-basin of the White Volta River basin and is located just south of Bawku, between latitudes 10°46'N and 11°04'N and longitudes 0°22'W and 0°02'W. The basin covers an area of about 848 km^2. While there is no official gauging station inside the basin, the Tamne River joins the White Volta River approximately 20 km downstream of the Yarugu gauging station. Two other gauging stations, Nangodi and Pwalugu respectively located on Red Volta River and the White Volta River (downstream of Tamne), allowed the calculation of the annual average streamflow. Elevation within the basin ranges from 169 to 348 m above sea level, with an average of 219 m. The basin overlies a part of the Precambrian basement where the most common rocks intercepted by the available wells are part of the Tamnean Plutonic Suite.

Table 5-2 summarizes general statistics and information for both basins. Climate data were taken from the climate dataset described in section 3.3 and from the soil moisture balance presented in section 5.3.2. Streamflow data were taken from the HSD and Global Runoff Data Centre datasets; periods covered for each station are 1951-95 for Pwalugu, 1958-90 for Nangodi, 1966-90 for Yarugu and 1962-2004 for Nabogo. The average values only consider years with less than 30 days of data missing.

Elevation, slope, river and groundwater level data used to estimate the potentiometric surfaces were taken or derived from the digital elevation model of Ghana (CIAT, 2004) and the HAP consolidated database (section 4.2). As stated in Table 5-2, the Nabogo and Tamne basins respectively contain 108 and 40 wells with reliable coordinates, lithological descriptions, yield and groundwater level data.

Table 5-2 – General information and statistics for the selected representative basins

		Nabogo River basin	Tamne River basin
Basin characteristics	Location (approx. extent)	-0.98° to -0.25°	-0.37° to -0.04°
		9.53° to 10.02°	10.77° to 11.07°
	Basin area	2 901 km²	848 km²
	Avg. elevation	152 m	219 m
	Elevation range	106 - 269 m	169 - 348 m
	Avg. slope	0.87°	1.04°
	Slope range	0° - 10.7°	0° - 21.0°
	Dominant lithology	Shale, mudstone,sandstone	Tamnean Granitoids
		Pendjari-Oti Gr. (Voltaian)	Intrusive rocks
Available wells inside basin	Number of wells (1)	108	40
	Avg. well depth	44.0 m	37.2 m
	Well depth range	24 - 99 m	22.6 - 55 m
	Avg. depth to groundwater	9.1 m	6.1 m
	Depth to groundwater range	2.1 - 32.5 m	0.6 - 12.7 m
	Avg. well yield	102.6 L/min	46.7 L/min
	Well yield range	7 - 720 L/min	2 - 127 L/min
	Avg. specific capacity	102.6 L/min•m	7.1 L/min•m
	Specific capacity range	0.3 - 720 L/min•m	1 - 27 L/min•m
	Avg. regolith thickness	16.5 m	27.4 m
	Regolith thickness range	2.7 - 40 m	7.8 - 37 m
	Avg. screen depth (midpoint)	31.8 m	29.0 m
	Screen depth range (midpoint)	2.0 - 68 m	19 - 50 m
	Avg. screen length	11.3 m	11.7 m
Nearest meteorological station	Station name	Tamale	Navrongo
	Location & elevation (approx.)	-0.85°, 9.5° (173 m)	-1.1°, 10.9° (201 m)
	Avg. annual rainfall	1 040 mm	963 mm
	Annual rainfall range	791 – 1 269 mm	750 – 1 138 mm
	Avg. annual pot. evapotr.	1 944 mm	1 968 mm
	Annual pot. evapotr. range	1 900 – 1 986 mm	1 879 – 2 087 mm
	Avg. annual actual evapotr.	862 mm	758 mm
	Annual actual evapotr. range	694 - 987 mm	657 - 867 mm
	Avg. annual runoff	130 mm	120 mm
	Annual runoff range	99 - 159 mm	94 - 142 mm
	Avg. annual recharge	48 mm	84 mm
	Annual recharge range	0 - 123 mm	0 - 162 mm
Gauging station	Station name	Nabogo	Pwalugu
	Location & elevation (approx.)	-0.82°, 9.74° (110 m)	-0.85°, 10.58° (123 m)
	Area upstream of station	2 093 km²	4 785 km²
	Avg. annual streamflow	10.8 m³/s	122.5 m³/s
	Station name	-	Nangodi
	Location & elevation (approx.)	-	-0.62°, 10.87° (184 m)
	Avg. annual streamflow	-	23.3 m³/s
	Station name	-	Yarugu
	Location & elevation (approx.)	-	-0.4°, 10.98° (170 m)
	Avg. annual streamflow	-	69.0 m³/s
	Avg. ann. streamflow (Tamne) (2)	-	5.4 m³/s

Notes:
(1) : Only wells with reliable coordinates & data on lithology, gw level or yield are considered
(2) : Avg. annual streamflow for Tamne basin was roughly estimated from streamflow difference of downstream (Pwalugu) and upstream stations (Nangodi & Yarugu).

For the **first interpolation method**, water levels of main rivers were used for the estimation of groundwater levels. The experimental and model variograms used for kriging are respectively presented in Figures 5-10 and 5-11 for both basins. Directional variograms were prepared for both basins at 0°, 45°, 90° and 135° but a linear omnidirectional variogram model was used as no significant anisotropy was present.

Figure 5-10 – Experimental and model variograms for kriging of groundwater levels with river data (Nabogo basin)

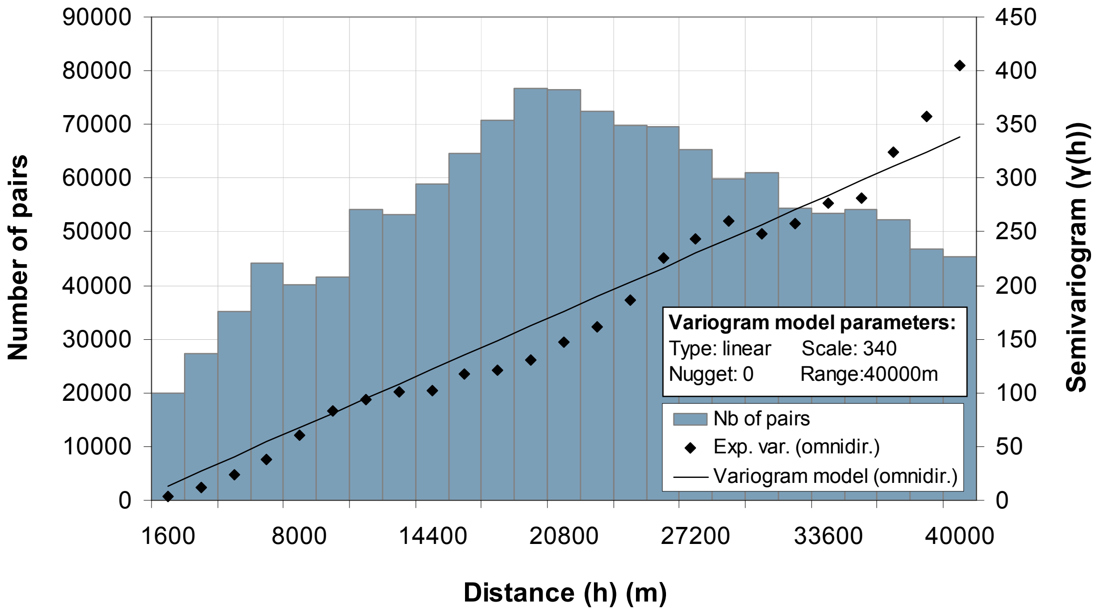

Figure 5-11 – Experimental and model variograms for kriging of groundwater levels with river data (Tamne basin)

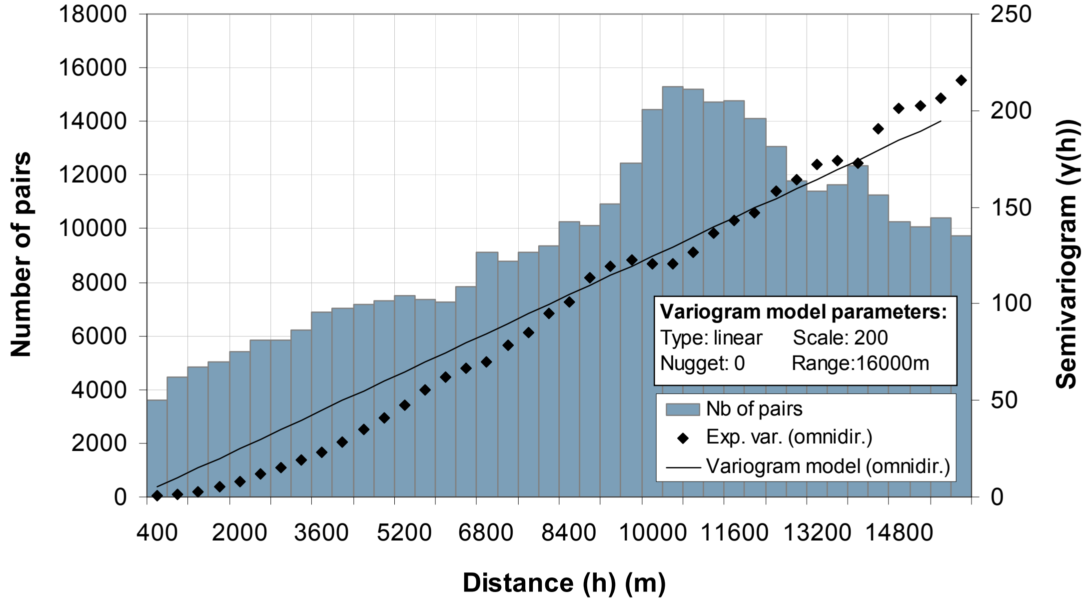

For the **second interpolation method**, a similar approach was followed. Kriging was applied to groundwater level data in addition to water levels of rivers. The experimental and model variograms are respectively illustrated in Figures 5-12 and 5-13 for both basins. As for the first method, directional variograms were prepared but did not show significant differences from the omnidirectional linear variogram model used for kriging.

Figure 5-12 – Experimental and model variograms for kriging of groundwater levels with well and river water levels (Nabogo basin)

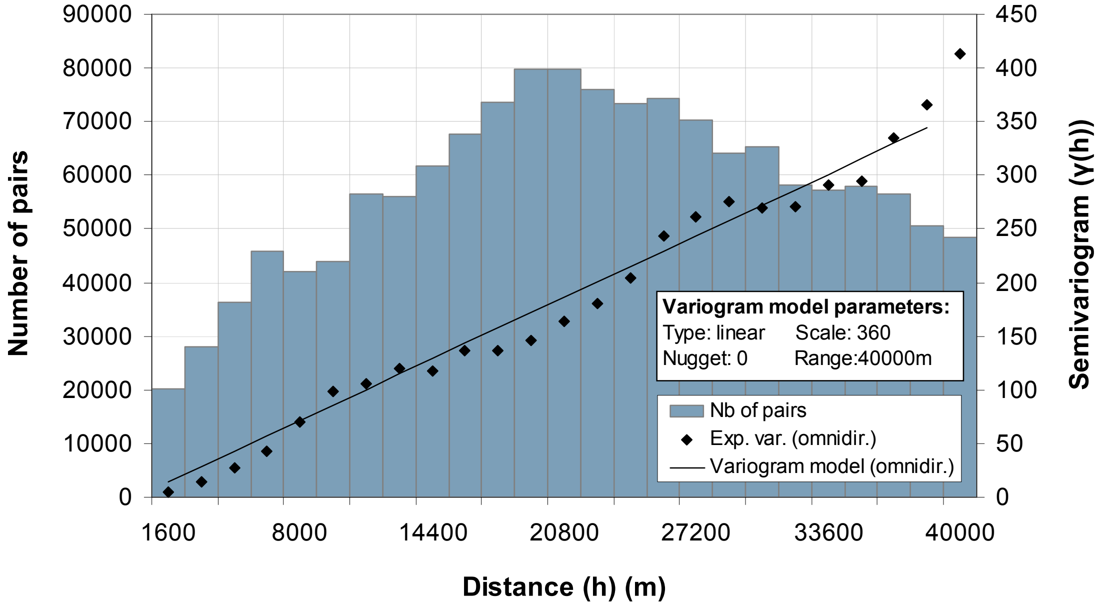

Figure 5-13 – Experimental and model variograms for kriging of groundwater levels with well and river water levels (Tamne basin)

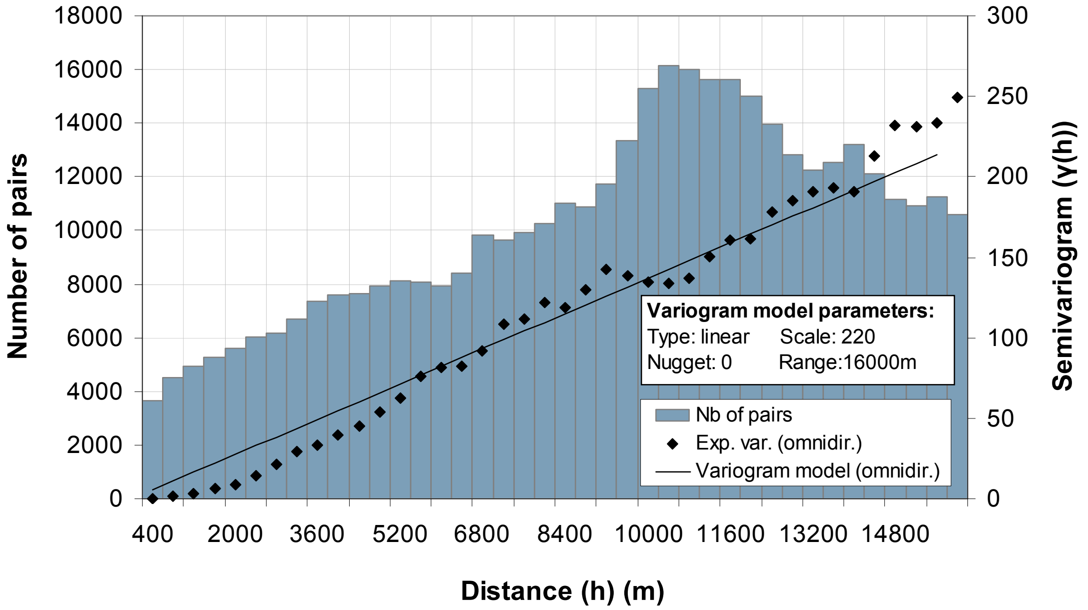

The elevation and slope classes used with the **third estimation method** are respectively presented in Figures 5-14 and 5-15 for the Nabogo and Tamne basins. These, in conjunction with the proximity to rivers and the groundwater levels for available wells, were used to estimate and optimize B factors for each elevation/slope classes.

The surface elevation within the basins and the potentiometric surfaces estimated with all three methods are presented in Figures 5-16 and 5-17 for the Nabogo and Tamne basins respectively. For the second and third method, the wells used for calculations are also shown on the figures along with their respective measured groundwater levels.

Figure 5-14 – Elevation and slope classes used for the Nabogo basin

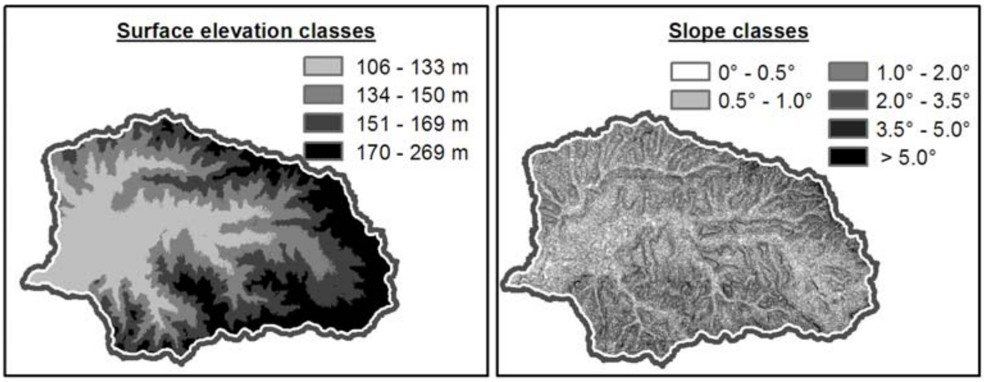

Figure 5-15 – Elevation and slope classes used for the Tamne basin

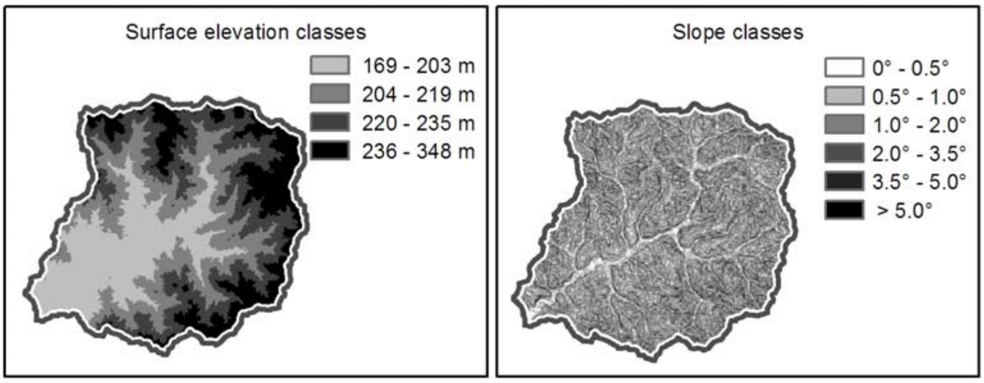

5.1.4.3 Comparison of estimation methods

For both selected basins, the first two interpolation methods yielded comparable potentiometric surfaces although the estimated groundwater flow pattern is more consistent with topography for the second one. The third method yielded potentiometric surfaces that follow topographical features much more closely than for the other two methods. For both basins, the difference between estimated and measured groundwater levels at available wells is on average much lower for the third method than it is for the other two methods (Table 5-3). For wells located in areas characterized by steep slopes and in elevated areas (e.g. at the head of the basin), the differences are higher still. The resolution at which calculations were carried out for the first and second methods (1 km; limited by quantity and coverage of data) is however much lower than for the third method (90 m; same as that of DEM) and thus more likely to show large errors between estimated and measured groundwater levels.

Figures 5-18 and 5-19 present the surface elevation and three estimated potentiometric surfaces for selected cross sections in both basins (N.B.: trace of cross sections shown in Figures 5-16 and 5-17). The figures show that potential discharge areas (i.e. where potentiometric surfaces are above surface elevation) and depth to groundwater estimated from the third method would be more realistic when considering the measured groundwater levels.

Results tend to show that the third estimation method would match the measured groundwater levels more closely than other methods. In a recent study in the Nabogo basin (Lutz *et al.*, 2007), a potentiometric surface was also simulated through the use of a groundwater flow numerical model developed with MODFLOW.

Figure 5-16 – Surface elevation and estimated potentiometric surfaces (Nabogo basin)

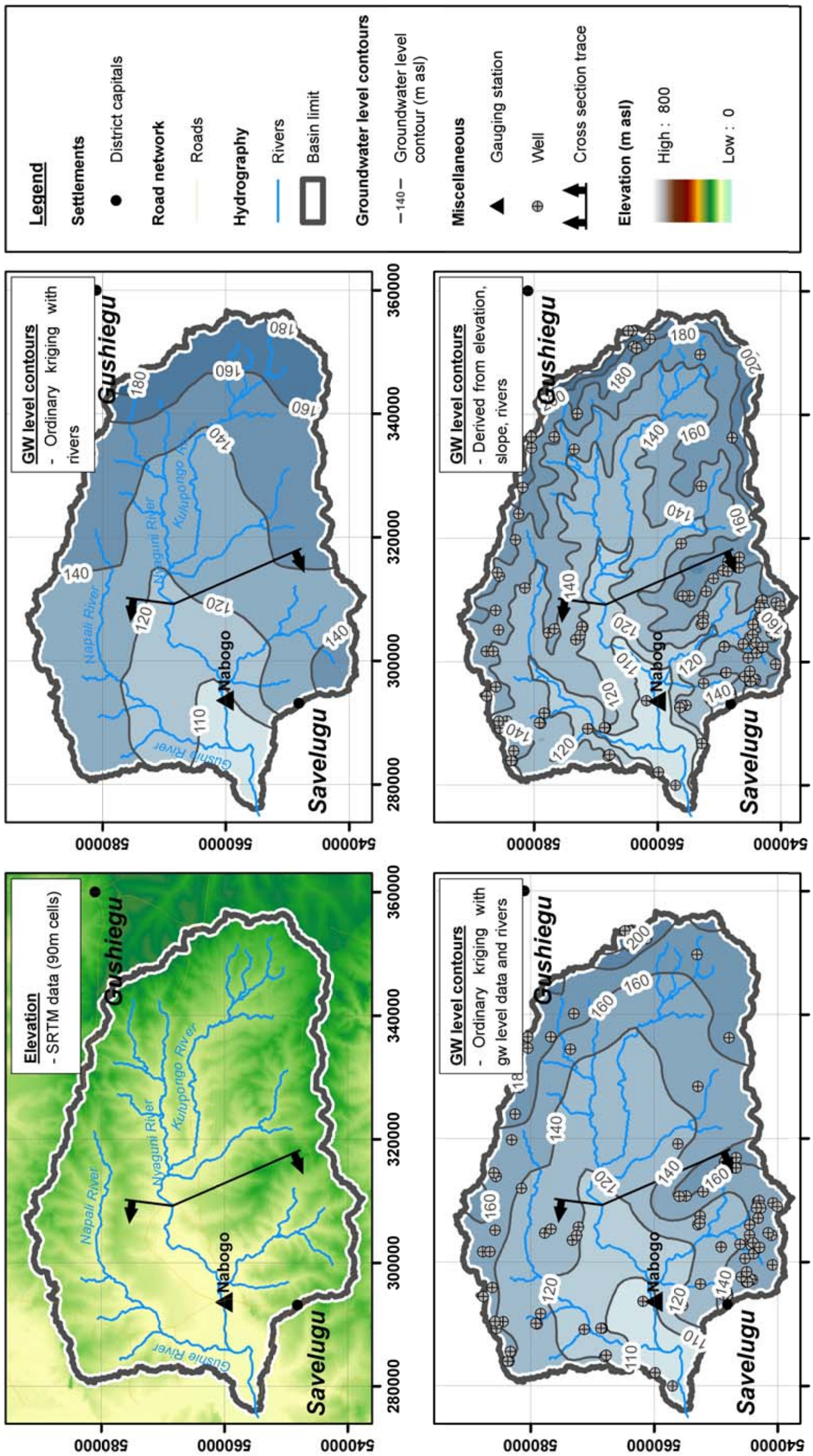

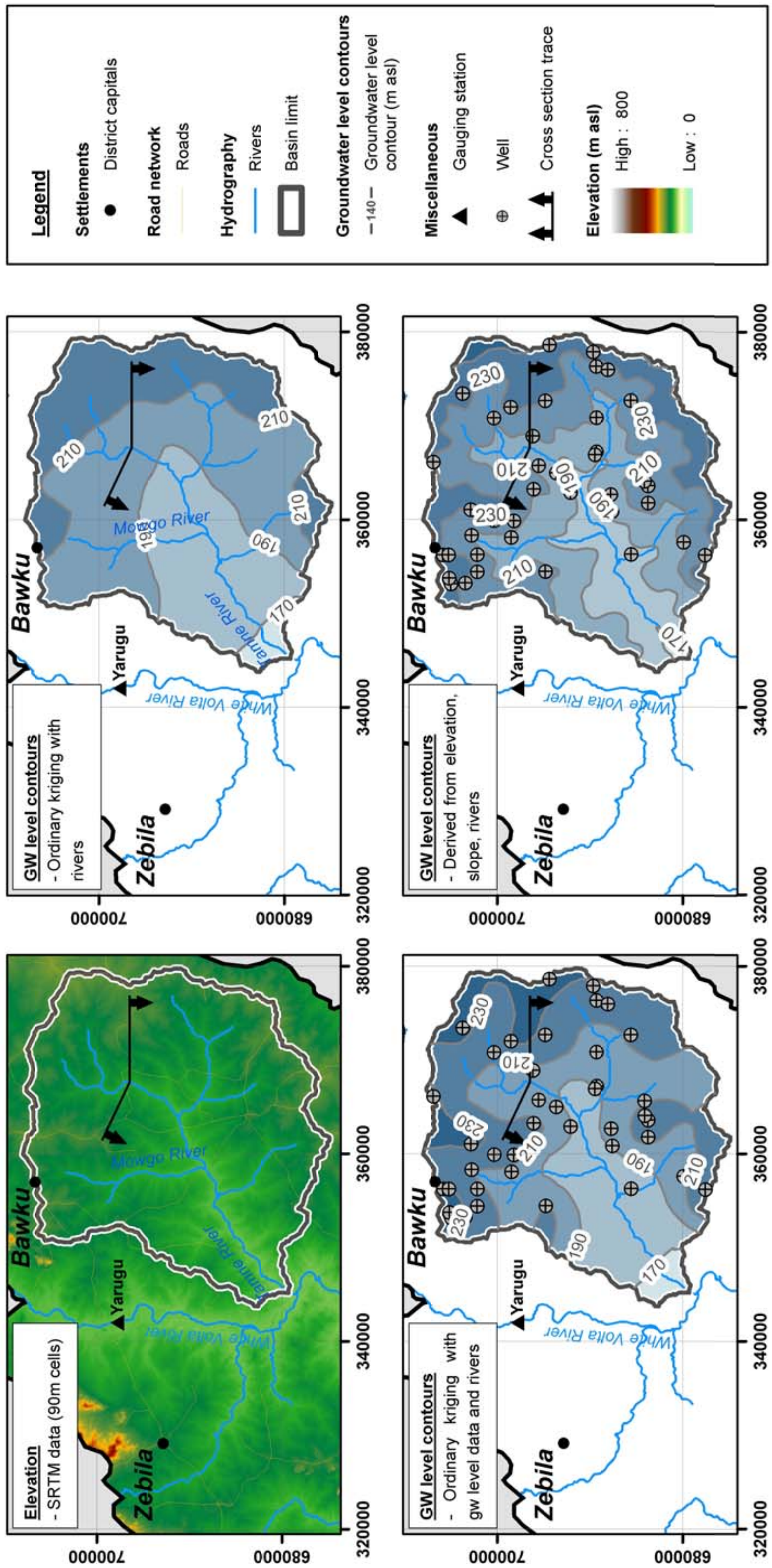

Figure 5-17 – Surface elevation and estimated potentiometric surfaces (Tamne basin)

The calibrated model from Lutz *et al.* (2007) yielded simulated groundwater levels that matched measured groundwater levels relatively well, with a root mean square error (RMSE) of less than 10 % of the difference between highest and lowest measured groundwater levels. The RMSE is somewhat higher for the third estimation method used in this study, i.e. about 17 %. While the number and location of wells used in this study are different and thus bound to generate differences with the results from Lutz *et al.* (2007), the high RMSE could suggest that some of the groundwater levels used were not representative of the regional trend or were affected locally at the time of measurement (e.g. pumping at or near well). Available groundwater levels were measured at different times of the year and often not in the same year so that groundwater level differences could sometime be misinterpreted. For most wells, casing height info was also lacking, thus introducing another source of error. Recent and reliable groundwater levels could thus potentially improve the estimated potentiometric surfaces.

Table 5-3 – Average differences between measured and estimated groundwater levels at available well locations

		First estimation method	Second estimation method	Third estimation method
Nabogo basin	Avg. and range of measured groundwater level (m bgl)	9.13 (2.1-32.5)		
	Avg. difference (m)	14.3	5.6	3.9
	Standard deviation (m)	10.7	4.2	3.5
Tamne basin	Avg. and range of measured groundwater level (m bgl)	6.1 (0.6-12.7)		
	Avg. difference (m)	16.4	5.3	2.9
	Standard deviation (m)	9.8	3.2	2.3

Figure 5-18 – Cross sections with estimated potentiometric surfaces (Nabogo basin)

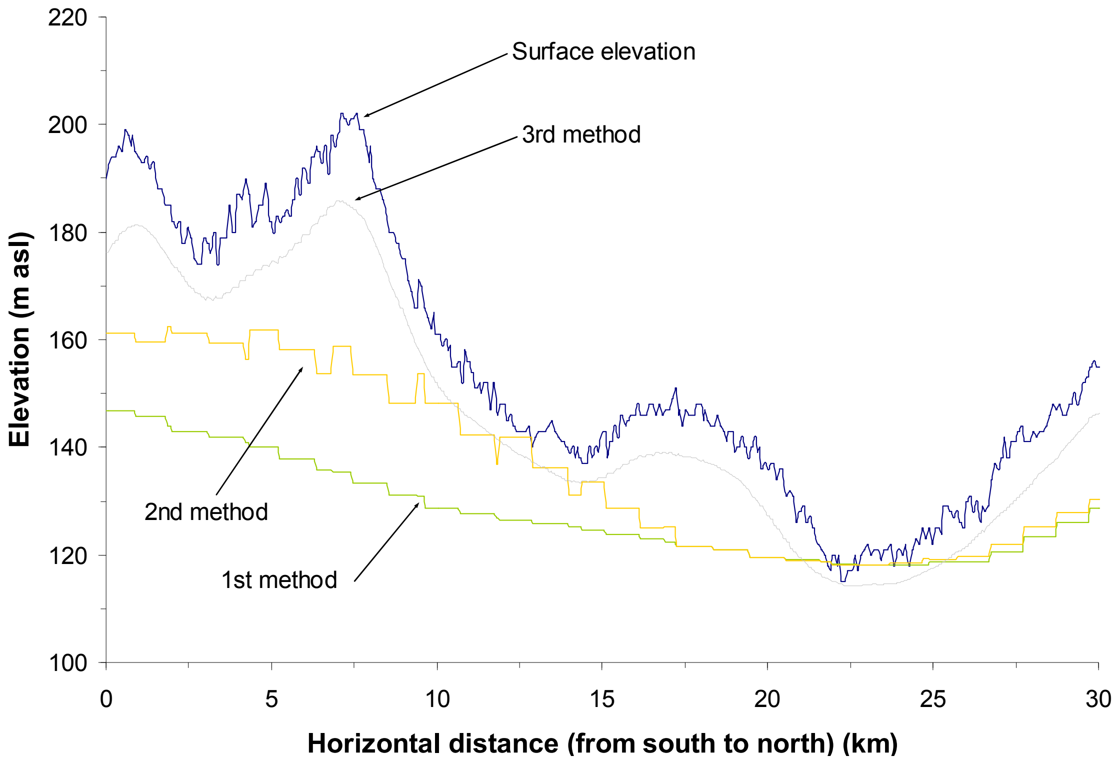

Figure 5-19 – Cross sections with estimated potentiometric surfaces (Tamne basin)

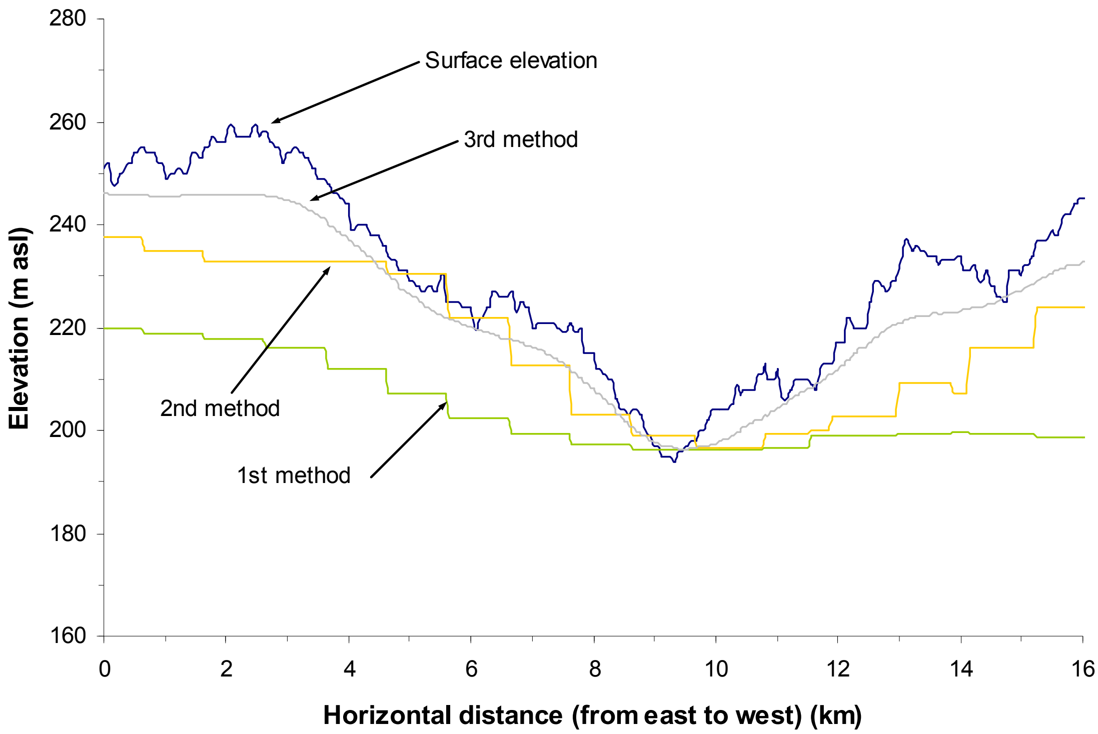

5.2 Groundwater production potential

5.2.1 Well and aquifer characteristics

The content of the HAP consolidated database was used to provide general statistics on borehole depth, static water level, yield, specific capacity and transmissivity. The distribution of each of these characteristics was assessed for the three northern regions and the different hydrogeological contexts. Statistics were computed from boreholes with reliable coordinates. As available groundwater level measurements were usually taken at different periods of the year (i.e. usually only once, immediately after borehole construction), depth to groundwater statistics presented here are only representative of average annual conditions. Available data were also used to compute statistics for typical well installations.

5.2.1.1 Typical boreholes

For the main hydrogeological contexts, typical boreholes are generally cased through unconsolidated material and grouted above the screened (or open-hole) section. The borehole is usually completed with a concrete pad at the surface for protection against preferential infiltration. For most rural water supply projects, screened sections made of slotted PVC are preferred over open-hole design. Figures 5-20 and 5-21 illustrate the average borehole characteristics of open-hole and lined boreholes for the two main hydrogeological contexts. The number of boreholes used to derive statistics presented on these figures is limited (see note on figures) so that values stated may not be locally representative. Analysis of statistics provided in Figures 5-20 and 5-21 reveals more variable characteristics for the VSB than for the PCB. The regolith overlying the Voltaian rocks is also generally thinner and slightly deeper groundwater levels are observed. In complement to statistics presented in Figures 5-20 and 5-21, general statistics on borehole depth and static water level were computed for all types of boreholes. Table 5-4 presents borehole depth statistics by hydrogeological context.

Figure 5-20 – Average borehole (bh) characteristics (Precambrian basement)

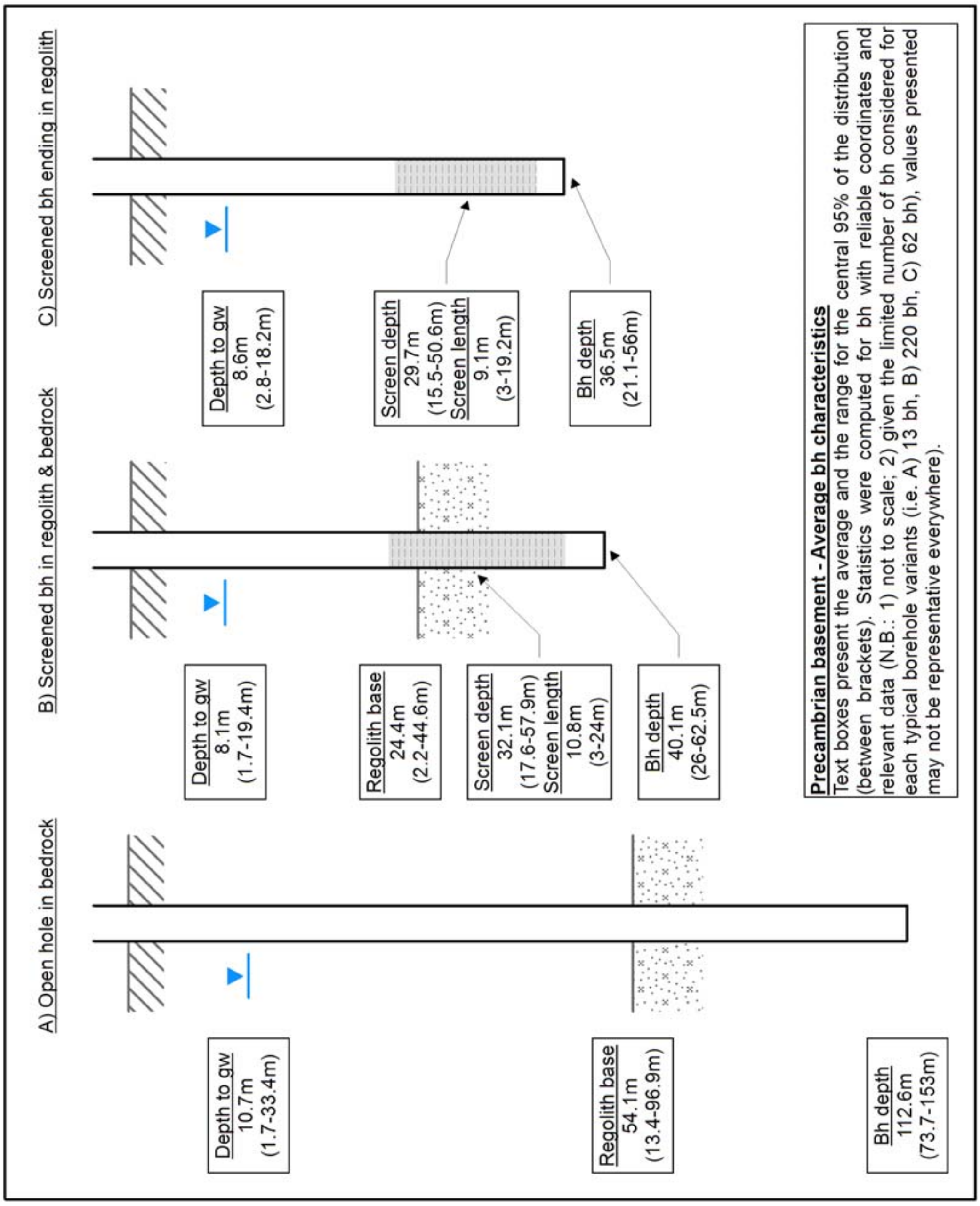

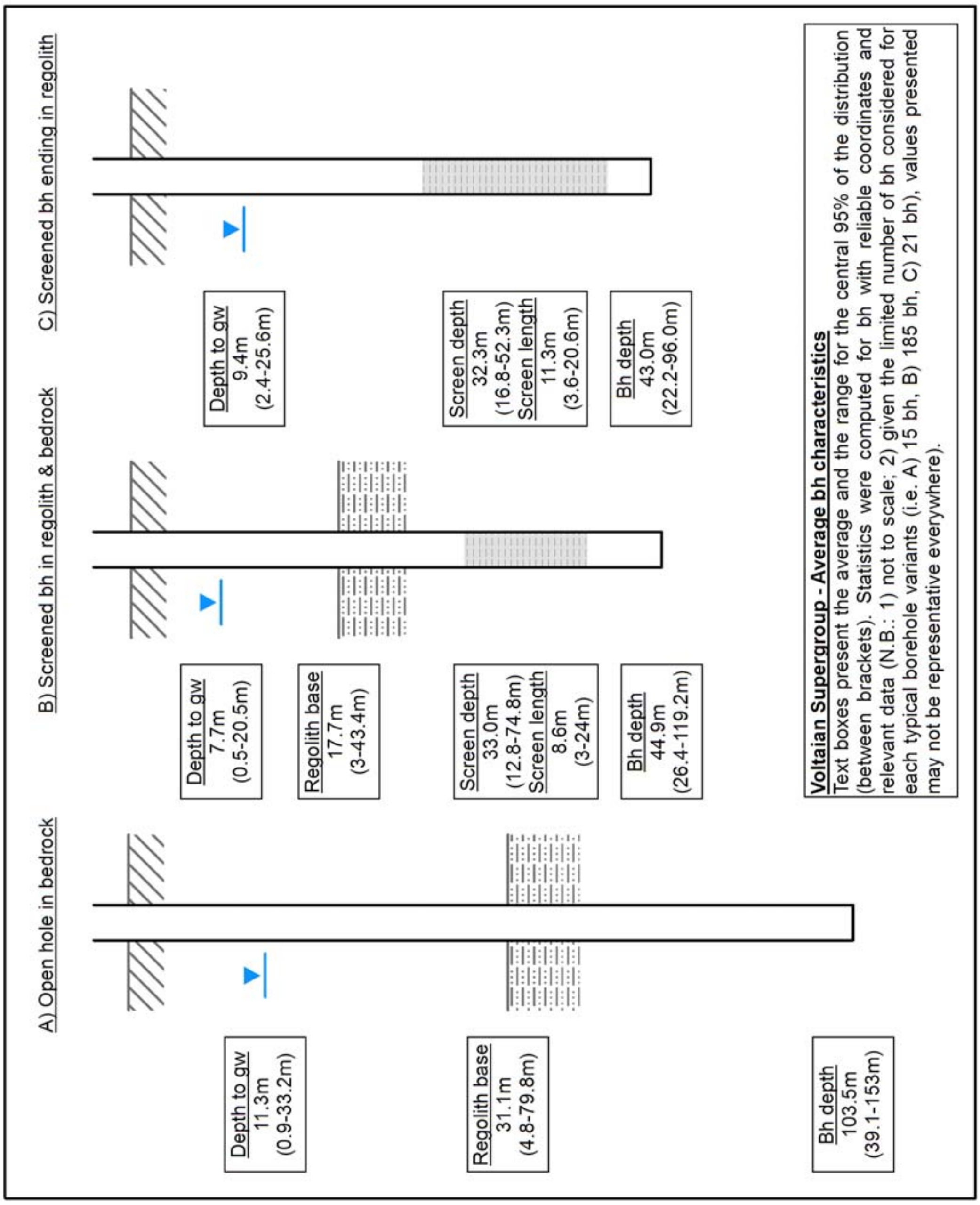

Figure 5-21 – Average borehole (bh) characteristics (Voltaian)

Table 5-4 – Borehole depth statistics by hydrogeological context

Hydrogeological contexts		All	Precambrian Basement				Voltaian Supergroup			
		All	All	Birimian & Tarkwaian	Intrusive rocks	Buem	All	Obosum	Pendjari-Oti	Kwahu-Morago
Total boreholes [1]		7874	4195	2019	2159	17	3679	828	2065	786
Boreholes with depth data		4860	1484	869	598	17	3376	811	1955	610
Distribution of borehole depth	<20m	94	47	24	23	0	47	8	35	4
	20-40m	1428	664	336	322	6	764	131	527	106
	40-60m	1884	581	382	194	5	1303	274	760	269
	>60m	1454	192	127	59	6	1262	398	633	231
Total depth range (m)		0.9-180	1.3-180	1.3-128	2.7-153	33.7-72	0.9-180	0.9-180	1.7-166	3 - 166
Probable depth range (95%) (m) [2]		22.3-90	19.5-90	20-78.3	16.4-72.2	33.8-69.7	25-91.3	27.4-104.3	22-77.1	29 - 99
Mean depth (m)		51	43.9	45.7	41.1	49.5	54.1	59.6	51.1	56.4
Median depth (m)		49.9	42.4	44	38	49	54	60	50.3	54.9
Standard deviation (m)		18.4	15.5	15	16	12.8	18.7	20.1	17.4	18.9

Notes:
(1) : Only unique boreholes with reliable coordinates were considered
(2) : Borehole depth range for the middle 95% of the distribution

Depth of boreholes drilled in Birimian and Tarkwaian rocks (~ 21 % of project area) range from about 20 m to 78 m (N.B.: probable range for the central 95 % of the distribution) with an average of 46 m. This compares relatively well with figures from Agyekum (2004) which reports a depth range of 35 m to 62 m with an average of 42 m. For areas underlain by intrusive rocks (~ 20 % of project area), borehole depths are similar, although slightly more shallow, ranging from approximately 16 m to 72 m with an average of 41 m. Boreholes in the Voltaian sedimentary basin are on average slightly deeper than those in the Precambrian basement. Borehole depths would range from about 25 m to 91 m with a mean depth of 54 m. Again these values are similar to those provided in Agyekum (2004), who stated a range of 45 m to 75 m with a mean depth of 55 m. Hand-dug wells, which tap the regolith aquifer in some areas, are not thoroughly discussed here as data on such wells were not systematically recorded until recently, through local inventories carried out by various organizations. An inventory recently performed in the Atankwidi catchment in the Upper East Region revealed that average depth of traditional hand-dug wells would be around 6 m while that of modern hand-dug wells would be around 10 m (Martin, 2006), the latter being deeper due to the use of explosives and/or machinery assisted excavation. Modern hand-dug wells are differentiated from traditional ones as they are generally constructed with NGOs support and are usually deeper and lined with concrete. Previous work in the Northern Region also revealed that average hand-dug well depth would range from 2 to 20 m (Kwei, 1997). In some areas, hand-dug wells are however not considered a good option as water levels are typically below the surface of the relatively hard bedrock.

Table 5-5 presents depth to groundwater statistics by hydrogeological context. Average depth to groundwater computed from available data is similar in both the Precambrian basement and the Voltaian sedimentary basin, with respective values of 9.3 m and 9.4 m. This is not consistent with typical descriptions found in literature (see references quoted in section 5.1.2.1) that usually suggest a deeper groundwater table for contexts such as the VSB, which are usually characterized by thinner regolith that is unable to store significant amounts of water. While the quality of data used to derive statistics could be questioned in regards to this discrepancy with the literature, there are no previous regional figures for depth to groundwater in northern Ghana that could be used for comparison. Additional data such as vertical gradient data from multi-level wells and groundwater level measurements taken at the same period of the year could help verify the statistics derived for Table 5-5. Within the VSB, depth to groundwater is relatively variable. The largest part of the Voltaian in northern Ghana is occupied by the Pendjari-Oti Group for which the groundwater table is slightly shallower with an average of 8.9 m compared to 9.7 m and 10.6 m in the Obosum and Kwahu-Morago Groups. Table 5-5 also shows that the range of depths to groundwater for the Voltaian is broader than for the Precambrian, suggesting more variable conditions.

5.2.1.2 Representative borehole yield

Table 5-6 presents statistics computed for borehole yield. The table also includes the number of dry or technically negative boreholes (e.g. faulty wells or poor groundwater quality) and the categories used to assess yield distribution are based on the suggested minimum yield for rural community water supply (i.e. 13 L/min; Dapaah-Siakwan and Gyau-Boakye, 2000) and the minimum required yield for mechanized pumping (i.e. 70 L/min; Kwei, 1997). In the Precambrian basement, borehole yields[9] for the Birimian Supergroup and Tarkwaian Group are generally low, ranging from 10 to 200 L/min with an average of 50 L/min. The average borehole yield given in literature (Dapaah-Siakwan and Gyau-Boakye, 2000) is higher at 160 L/min, but this value concerns all of Ghana. For areas underlain by intrusives, yields are slightly higher, ranging from 10 to 230 L/min with an average of 53 L/min. Again, this figure is lower than the one stated in literature, i.e. about 67 L/min (Darko and Krasny, 2000). Differences in degree of weathering and fracturing could partly explain lower yield values for intrusive rocks.

[9] Yield values from the consolidated database include values for boreholes tapping the regolith aquifer or fractured bedrock aquifer or both; in most cases, boreholes are reported to tap both aquifers.

Table 5-5 – Depth to groundwater statistics by hydrogeological context

Hydrogeological contexts		All	Precambrian Basement				Voltaian Supergroup			
		All	All	Birimian & Tarkwaian	Intrusive rocks	Buem	All	Obosum	Pendjari-Oti	Kwahu-Morago
Total boreholes [1]		7874	4195	2019	2159	17	3679	828	2065	786
Boreholes with depth to groundwater data [2]		1998	781	433	331	17	1217	204	814	199
Distribution of depth to groundwater	<5m	463	163	68	91	4	300	47	211	42
	5-10m	818	334	186	138	10	484	81	323	80
	10-15m	420	163	95	66	2	257	41	180	36
	>15m	297	121	84	36	1	176	35	100	41
Total depth to groundwater range (m)		-0.7-44.5	0.2-37.1	0.2-37.1	0.6-25.1	3.5-21.3	-0.7-44.5	0.4-38.1	-0.7-41.3	0.2 - 44.5
Probable depth to gw range (95%) (m) [3]		1.5-23.9	1.9-21.8	2.6-22.9	1.5-20.9	3.8-18.4	1.3-25.4	1.8-24	1-23.2	1.6 - 31.8
Mean depth to groundwater (m)		9.3	9.3	10.2	8.3	7.8	9.4	9.7	8.9	10.6
Median depth to groundwater (m)		7.9	8	8.8	7.3	6.2	7.8	8.5	7.7	7.9
Standard deviation (m)		5.9	5.4	5.6	4.9	4.4	6.3	6.2	5.7	8.0

Notes:
(1) : Only unique boreholes with reliable coordinates were considered
(2) : Groundwater level meas. were taken at different time of the year and derived statistics are thus only representative of avg. yearly conditions
(3) : Depth to groundwater range for the middle 95% of the distribution

Table 5-6 – Borehole yield statistics by hydrogeological context

Hydrogeological contexts		All	Precambrian Basement				Voltaian Supergroup			
		All	All	Birimian & Tarkwaian	Intrusive rocks	Buem	All	Obosum	Pendjari-Oti	Kwahu-Morago
Total boreholes [1]		7874	4195	2019	2159	17	3679	828	2065	786
Dry or tech. negative boreholes [2]		1916	423	238	185	0	1493	485	812	196
Boreholes with yield data [3]		1444	576	322	242	12	868	143	579	146
Distribution of yield (L/min)	<13	235	63	44	19	0	172	55	94	23
	13-70	855	393	217	171	5	462	66	318	78
	70-180	236	95	47	41	7	141	12	102	27
	>180	118	25	14	11	0	93	10	65	18
Total yield range (L/min)		1-830	2-300	7-300	2-300	30-130	1-830	4-720	1-830	5 - 360
Probable yield range (95%) (L/min) [4]		8-300	10-200	10-200	9.9-229.3	30-127.3	8-300	6.6-338	9-304.4	7.3 - 240
Mean yield (L/min)		62	52.2	50.4	53.3	78.3	68.5	54.6	72.2	67.2
Median yield (L/min)		30	30	28.9	30	90	30	16.7	30	36
Standard deviation (L/min)		85.7	55.7	55.3	56.8	34.9	100	106.8	104.6	72.4

Notes:
(1) : Only unique boreholes with reliable coordinates were considered
(2) : Dry and technically negative boreholes sometime have yield data (from bh constr.) even though they are now considered unsuccessful.
(3) : Only boreholes with pumping test data were considered (i.e. boreholes with only airlift data were left out of statistical analysis)
(4) : Yield range for the middle 95% of the distribution

Figure 5-22 – Experimental and model variograms for kriging of borehole yield

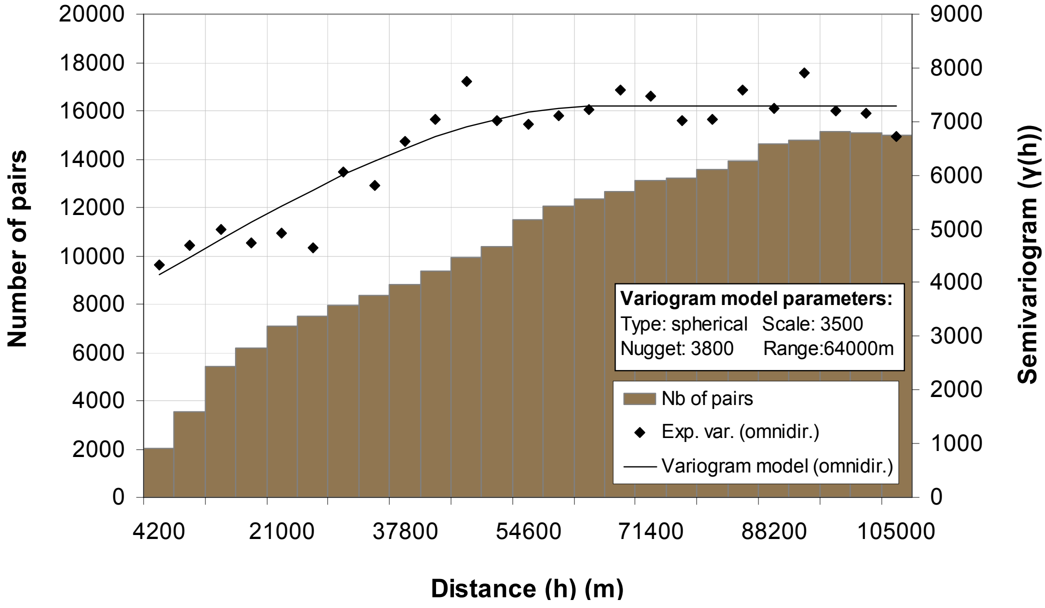

Figure 5-23 – Interpolated borehole yield

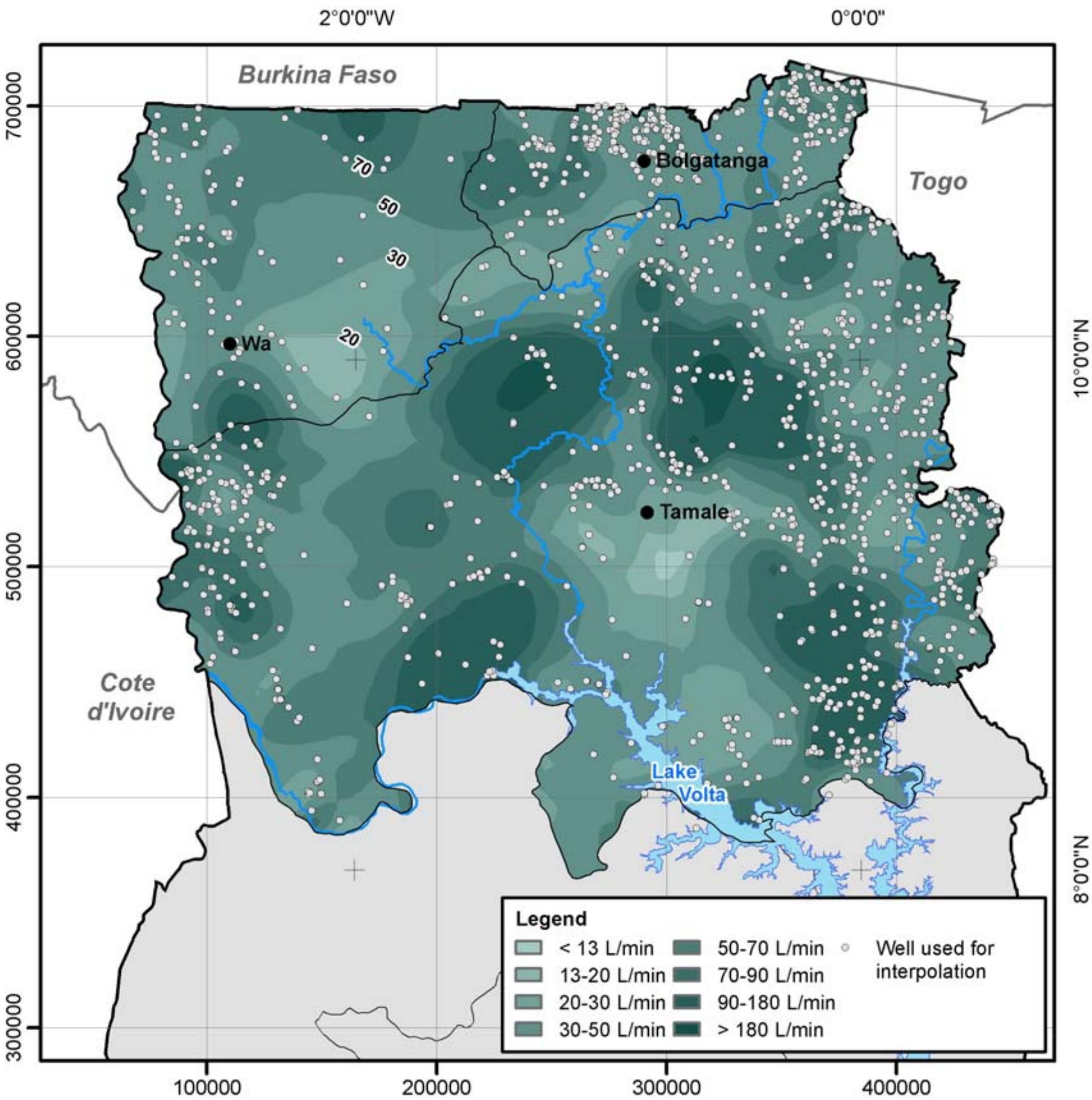

Available data reveal that fractured rock aquifers of the VSB generally have a low to moderate productivity, with borehole yields ranging from 8 to 300 L/min with an average of 69 L/min. As for the Precambrian basement, literature provides a higher average yield of about 125 L/min. To explain variability of borehole yields in the Voltaian, Acheampong and Hess (1998) suggest that water-bearing structures would be discrete entities with variable production rates. This would support assumptions that groundwater occurrence is mainly controlled by geologic structures in the Voltaian (Nathan and Harris, 1970).

Available yield values from wells with reliable coordinates were interpolated for the study area to provide an overview of regional trends. The interpolation was carried out by kriging using reliable boreholes for which pumping test data were available, that is 1 393 in total when excluding probable anomalous values. Matlab was used to interpolate values by ordinary kriging on a 5 km grid. The experimental and model variograms used for kriging are presented in Figure 5-22 along with the variogram model parameters. As for kriging of regolith thickness, only omnidirectional variograms are shown as directional variograms computed (0°, 45°, 90°, 135°) did not reveal the presence of anisotropy.

Interpolated values were exported in ArcGIS for graphical representation. As Figure 5-23 shows, there are obvious spatial data gaps so that, while interpolated values presented are generally representative, they could be inaccurate locally. With that caveat, the areas of lowest and highest estimated yield are respectively located southeast and northeast of Tamale.

5.2.1.3 Specific capacity and transmissivity

Table 5-7 presents the specific capacity statistics by hydrogeological context. Statistics were computed from specific capacities already in the HAP consolidated database and those added subsequently to the consolidation process for wells that had pumping test data by dividing pumping rate by drawdown. Data from Table 5-7 show that, on average, wells in the Voltaian are slightly more productive than those in the Precambrian basement with an average specific capacity of 12.9 L/min•m compared to 9.4 L/min•m. Values are again more variable for the VSB with a probable range of 0.3-76 L/min•m compared to 0.5-52 L/min•m for the Precambrian basement.

Transmissivity data were only available for some of the monitoring wells that are part of the WRC monitoring network as they were the only wells for which complete pumping test data were available. The values obtained are summarized in Table 5-8 along with other pumping test data. For monitoring wells installed in Precambrian basement rocks, transmissivity ranges from 0.1 to 143.3 m^2/d with an average of 16.6 m^2/d, while it ranges from 0.1 to 3294 m^2/d with an average of 183.8 m^2/d for wells located in the VSB. As values reported in the literature (Agyekum, 2004) are lower (7.4 m^2/d for Birimian Supergroup and Tarkwaian Group, 6.6 m^2/d for granitoid intrusions and 11.9 m^2/d for VSB), complementary data were used to derive transmissivity estimates.

In this project, as in many hydrogeological projects, it is not unusual that data on specific capacity (S_c) are more numerous than data on transmissivity (T), as specific capacity is easier to obtain from commonly available field data. Previous studies have thus developed various empirical relations between these two parameters in order to provide estimates of transmissivity when pumping test data are not available (Huntley *et al.*, 1992; Razack and Huntley, 1991; Razack and Lasm, 2006; Wladis and Gustafson, 1999; Yidana *et al.*, 2008). A similar relation was developed from the 35 monitoring wells for which pumping test data were available (i.e. existing WRC wells and newly constructed HAP wells). The following relation was obtained:

$$T = 0.67 S_c^{1.138} \qquad [5.3]$$

Table 5-7 – Specific capacity statistics by hydrogeological context

Hydrogeological contexts		All	Precambrian Basement				Voltaian Supergroup			
		All	All	Birimian & Tarkwaian	Intrusive rocks	Buem	All	Obosum	Pendjari-Oti	Kwahu-Morago
Total boreholes [(1)]		7874	4195	2019	2159	17	3679	828	2065	786
Boreholes with specific capacity data		1279	555	303	240	12	724	122	470	132
Distribution of specific capacity (L/min•m)	<5	752	319	185	130	4	433	94	263	76
	5-10	219	112	53	56	3	107	16	71	20
	10-25	191	85	46	35	4	106	10	71	25
	>25	117	39	19	19	1	78	2	65	11
Total specific capacity range (L/min•m)		0.1-720	0.1-223	0.2-180	0.1-223	2.6-36.1	0.1-720	0.2-126	0.1-720	0.2 - 221
Probable specific capacity range (95%) (L/min•m) [(2)]		0.3-65.1	0.5-52.1	0.5-41.1	0.5-65.1	2.6-31.3	0.3-76.1	0.3-21.3	0.5-85.5	0.4 - 39.9
Mean specific capacity (L/min•m)		11.4	9.4	8.5	10.3	10.9	12.9	4.8	15.8	10.1
Median specific capacity (L/min•m)		3.8	4	3.5	4.1	7	3.5	1.5	4	4.3
Standard deviation (L/min•m)		35.4	18.6	17.2	20.5	9.7	44.2	12.6	53	21.9

Notes:

(1) : Only unique boreholes with reliable coordinates were considered

(2) : Depth to groundwater range for the middle 95% of the distribution

Table 5-8 – Transmissivity and specific capacity for pump tested monitoring wells

Well ID	Airlift yield (L/min)	Pumping test date	Pumping test yield (L/min)	Static water level (m bgl)	Dynamic water level (m bgl)	Specific capacity (L/min•m)	Transmissivity (m^2/d)	Hydrogeol. context
WVB01	20	2005-11-03	10	2.34	44.2	0.239	0.820	Precambrian
WVB02	40	2005-11-05	30	15.9	25.5	3.125	1.440	Precambrian
WVB03	500	2005-11-07	200	8.59	40.2	6.329	5.400	Precambrian
WVB04	170	2005-11-10	150	4.79	25.3	7.306	26.400	Precambrian
WVB05	200	2005-11-14	170	1.4	13.2	14.370	29.800	Precambrian
WVB06	45	2005-11-12	30	5.44	15.9	2.876	3.960	Precambrian
WVB07	20	2005-11-15	20	2.17	14.5	1.625	0.670	Precambrian
WVB08	300	2005-11-16	100	3.2	37.4	2.922	0.890	Precambrian
WVB09	12	2005-11-02	10	5.65	21.6	0.627	0.620	Precambrian
WVB10	450	2005-11-08	200	19.5	33.8	13.957	35.100	Voltaian
WVB11	9	2005-11-03	9	8.63	38.5	0.301	0.340	Voltaian
WVB12	120	2005-11-21	150	8.42	13.3	30.550	30.400	Voltaian
HAP01	320	2007-08-13	200	29.2	36.9	26.042	40.852	Voltaian
HAP04	180	2007-08-14	140	10.1	38.9	4.871	2.679	Voltaian
HAP05-2	4	2007-09-06	5	7.65	34.1	0.189	0.096	Voltaian
HAP07	260	2007-08-17	160	5.37	13.2	20.382	10.617	Voltaian
HAP08	20	2007-08-18	15	25.5	35.3	1.542	3.277	Voltaian
HAP10	20	2007-08-23	15	2.11	23.7	0.695	2.600	Voltaian
HAP11	30	2007-08-15	24	8.21	24.3	1.492	5.243	Voltaian
HAP12	3	2007-08-22	6	11.8	39.5	0.217	1.311	Voltaian
HAP13	360	2009-10-26	290	1.12	10.6	30.655	143.25	Precambrian
HAP14	17	2009-10-25	19	3.42	34.8	0.605	0.235	Voltaian
HAP15	5.5	2009-10-23	10	9.14	28	0.531	0.38	Voltaian
HAP16	360	2009-10-27	6	20.7	62.4	0.144	0.0404	Precambrian

Table 5-8 – Transmissivity and specific capacity for pump tested monitoring wells (cont'd)

Well ID	Airlift yield (L/min)	Pumping test date	Pumping test yield (L/min)	Static water level (m bgl)	Dynamic water level (m bgl)	Specific capacity (L/min•m)	Transmissivity (m^2/d)	Hydrogeol. context
HAP17	240	2009-11-18	200	6.45	16.07	20.790	9.35	Voltaian
HAP18	360	2009-10-24	200	12.52	19.85	27.285	48.31	Voltaian
HAP19	11	2009-11-19	15	7.23	23.06	0.948	0.347	Voltaian
HAP20	360	2009-11-21	300	6.27	26.7	14.684	6.85	Voltaian
HAP21	14	2009-10-22	9	23.22	69.19	0.196	0.107	Voltaian
HAP22	360	2009-11-17	230	3.76	40.4	6.277	21.2	Precambrian
HAP23	67.5	2009-11-15	50	11.29	20.37	5.507	5.6	Precambrian
HAP24	18	2009-11-14	18	9.37	16.5	2.525	8.355	Precambrian
HAP25	431	2009-11-20	400	0.51	1.86	296.3	3294	Voltaian
HAP26	288	2009-10-28	140	20.52	31.24	13.060	12.8	Precambrian
HAP27	216	2009-11-16	138	11.34	34.86	5.867	4.82	Precambrian
Average	166.6	-	104.8	9.51	28.72	16.14	107.38	
Median	120	-	50	8.21	26.70	3.13	4.82	
Std deviation	159.4	-	103.8	7.23	13.80	48.95	547.10	
Range	3 - 500	-	5 - 400	0.51 - 29.2	1.86 - 69.19	0.14 - 296.3	0.04 - 3294	

Table 5-9 – Comparison of transmissivities estimated from specific capacity data and derived from pumping test data

Well ID	Specific capacity (L/min•m)	Transmissivity derived from pumping test data (m^2/d)	Transmissivity estimated with empirical relation (m^2/d)	Transmissivity estimated with Matlab program (m^2/d)	Hydrogeol. context
WVB01	0.239	0.82	0.200	0.23	Precambrian
WVB02	3.125	1.44	3.726	3.972	Precambrian
WVB03	6.329	5.4	8.316	8.605	Precambrian
WVB04	7.306	26.4	9.791	10.683	Precambrian
WVB05	14.37	29.8	21.136	21.942	Precambrian
WVB06	2.876	3.96	3.391	3.749	Precambrian
WVB07	1.625	0.67	1.770	1.965	Precambrian
WVB08	2.922	0.89	3.452	3.796	Precambrian
WVB09	0.627	0.62	0.599	0.654	Precambrian
WVB10	13.957	35.1	20.446	20.621	Voltaian
WVB11	0.301	0.34	0.260	0.286	Voltaian
WVB12	30.55	30.4	49.848	50.075	Voltaian
HAP01	26.042	40.852	41.568	41.051	Voltaian
HAP04	4.871	2.679	6.174	6.664	Voltaian
HAP05-2	0.189	0.096	0.153	0.181	Voltaian
HAP07	20.382	10.617	31.456	31.512	Voltaian
HAP08	1.542	3.277	1.668	1.886	Voltaian
HAP10	0.695	2.6	0.674	0.78	Voltaian
HAP11	1.492	5.243	1.607	1.82	Voltaian
HAP12	0.217	1.311	0.179	0.211	Voltaian
HAP13	30.655	143.3	50.043	50.052	Precambrian
HAP14	0.605	0.235	0.575	0.624	Voltaian
HAP15	0.531	0.380	0.496	0.521	Voltaian
HAP16	0.144	0.040	0.112	0.019	Precambrian

Table 5-9 – Comparison of transmissivities estimated from specific capacity data and derived from pumping test data (cont'd)

Well ID	Specific capacity (L/min•m)	Transmissivity derived from pumping test data (m^2/d)	Transmissivity estimated with empirical relation (m^2/d)	Transmissivity estimated with Matlab program (m^2/d)	Hydrogeol. context
HAP17	20.790	9.350	32.173	32.192	Voltaian
HAP18	27.285	48.310	43.834	43.771	Voltaian
HAP19	0.948	0.347	0.959	1.104	Voltaian
HAP20	14.684	6.850	21.663	21.938	Voltaian
HAP21	0.196	0.107	0.159	0.053	Voltaian
HAP22	6.277	21.200	8.238	8.820	Precambrian
HAP23	5.507	5.600	7.098	7.676	Precambrian
HAP24	2.525	8.355	2.923	3.339	Precambrian
HAP25	296.3	3,294	660.9	1131.1	Voltaian
HAP26	13.060	12.800	18.958	19.313	Precambrian
HAP27	5.867	4.820	7.629	8.210	Precambrian
Average	16.1	107.4	30.3	44.0	
Median	3	4.82	3.73	3.97	
Std deviation	49.0	547.1	109.2	187.0	
Range	0.14 - 296.3	0.04 - 3294	0.11 - 660.9	0.02 - 1131.08	

Transmissivities obtained from this relation are compared with the ones derived from pumping test data in Table 5-9. Monitoring wells used for this exercise are presented on Figure 5-24 according to their hydrogeological contexts. The empirical relation presented above compares relatively well with other selected empirical relations from previous studies that are also shown on Figure 5-24. Another approach based on work by McLin (2005) was also used to estimate transmissivity from specific capacity data while correcting for aquifer partial penetration and well efficiency. Aside from specific capacity data, the Matlab program provided by McLin (2005) to carry out calculations requires screen length, borehole radius and storage coefficient. The first two inputs were known from well construction details, but data on storage coefficient were scarce. As a first order approximation, a value of 0.005 was used as storage coefficient for both contexts. This is within the 0.003-0.008 range proposed by Bannerman and Ayibotele (1984). While the Matlab program provides a relatively good approximation of transmissivity (Table 5-9), transmissivity values derived from pumping test data should be preferred.

Figure 5-24 – Empirical relation between specific capacity and transmissivity

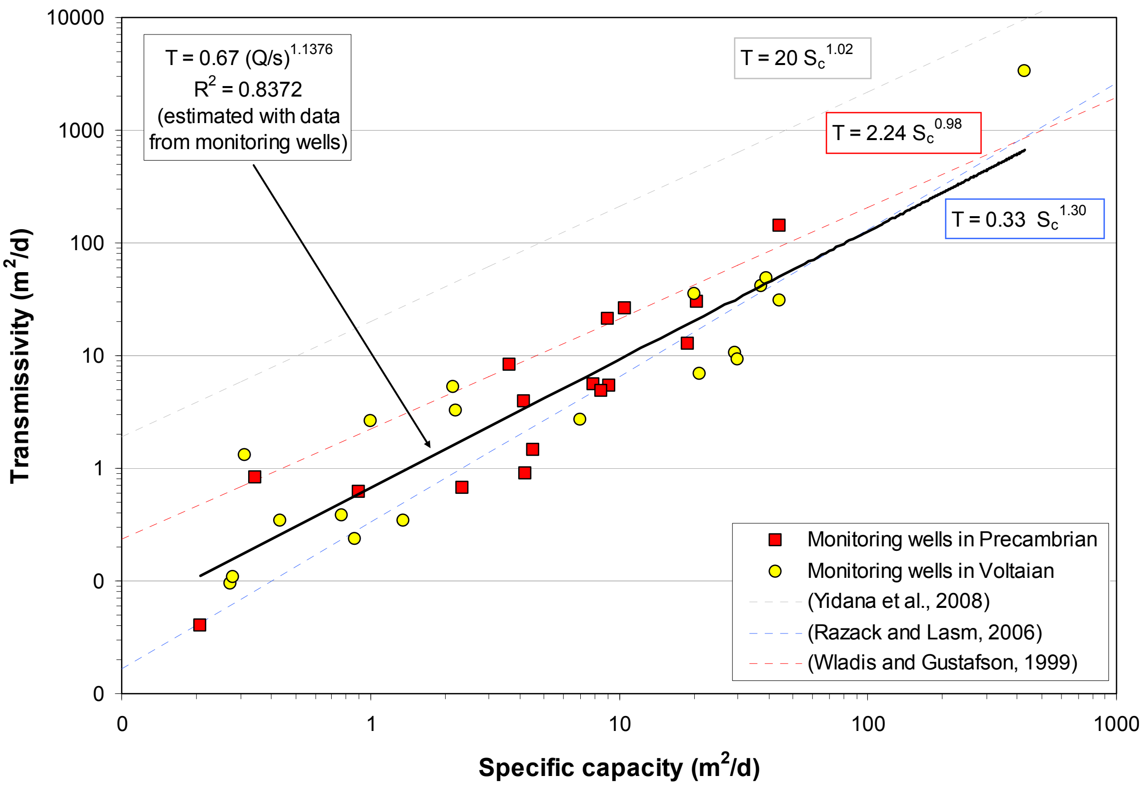

5.2.2 Groundwater exploration success potential

While well and aquifer characteristics presented in previous sections can provide useful information for planning and implementing groundwater supply projects in northern Ghana, the potential drilling success (see end of chapter 2 for definition) is still regarded as key information for project costing by many water sector stakeholders in northern Ghana. Consequently, the potential drilling success was estimated by hydrogeological context and region using data from the HAP consolidated database. However, as there was an obvious bias in favour of successful boreholes in the databases consolidated under HAP, representative success rates were subsequently estimated from local hydrogeological or water supply project reports collected under HAP. For districts with more than one data source, average rates were estimated with data from all reports concerned. Table 5-10 presents the drilling success rates by hydrogeological context. Based on the representative success rates and available yield data, the normalized proportions of borehole yields for each yield category are also presented in Table 5-10.

As stated in previous studies (Dapaah-Siakwan and Gyau-Boakye, 2000; Kwei, 1997), representative drilling success rates are lower for the VSB than for the Precambrian basement. They are also lower than rates calculated from the consolidated database, thus confirming that there is a bias in favour of successful wells in collected databases.

Data gathered from existing reports were also used to illustrate potential drilling success by district (Figure 5-25). Values presented on the figure may not be representative everywhere in the districts, but they still give an idea of the distribution of drilling success rates in northern Ghana. The lowest rates are found in the centre of the VSB (Tamale) while the highest are found in the Precambrian basement (Bawku East & Lawra).

Figure 5-25 – Potential drilling success by district in northern Ghana

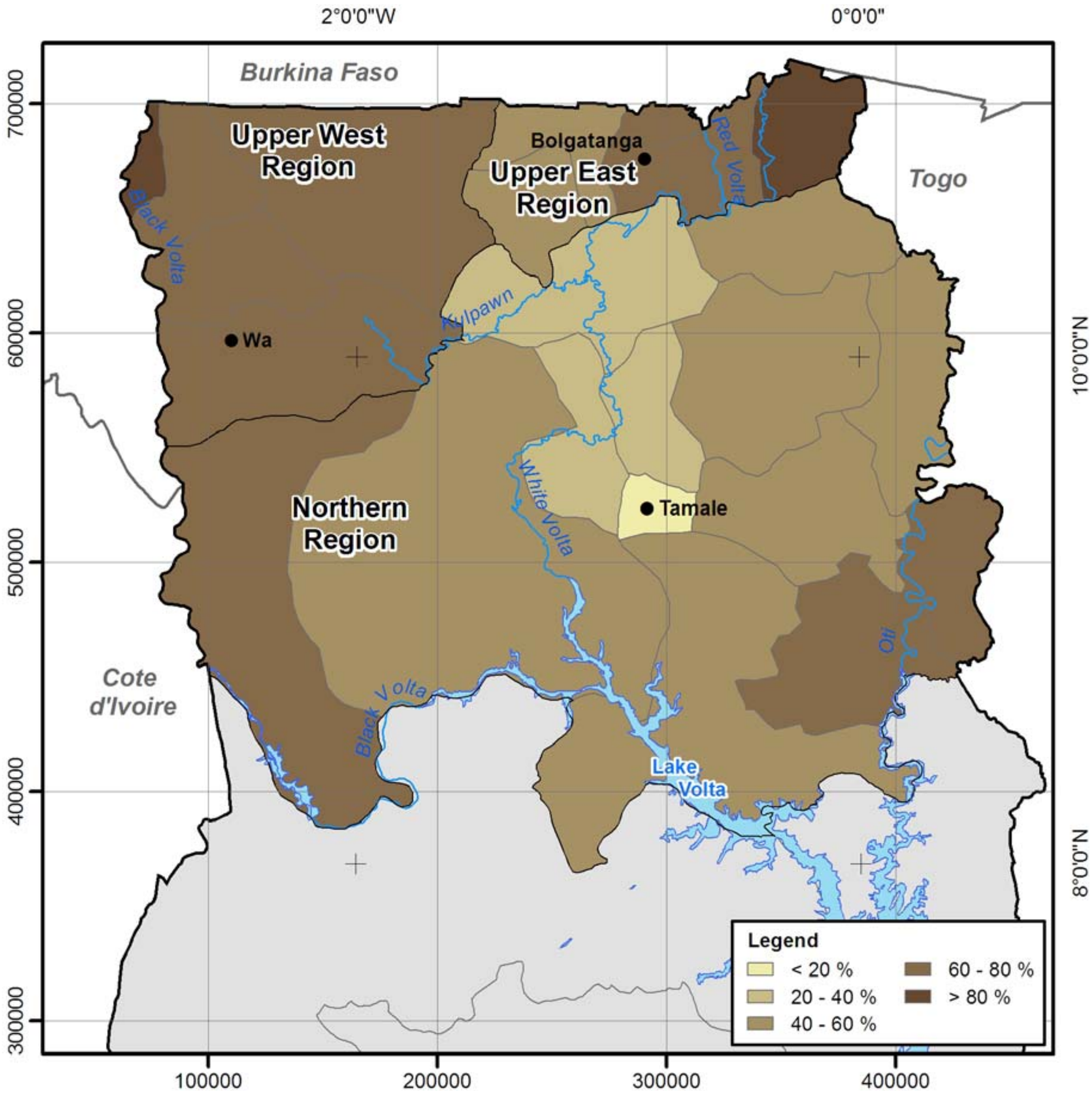

Table 5-10 – Potential drilling success statistics by hydrogeological context

Hydrogeological contexts		All	Precambrian Basement				Voltaian Supergroup			
		All	All	Birimian & Tarkwaian	Intrusive rocks	Buem	All	Obosum	Pendjari-Oti	Kwahu-Morago
Total boreholes (from database) [(1)]		7874	4195	2019	2159	17	3679	828	2065	786
Dry or tech. negative boreholes [(2)]		1916	423	238	185	0	1493	485	812	196
Successful boreholes (%) (from database)		75.7%	89.9%	88.2%	91.4%	100%	59.4%	41.4%	60.7%	75.1%
Representative success rates (%) (from reports) [(3) (4)]		58.5%	69.2%				50.2%			
Total boreholes considered for rates from reports		4169	1615				2159			
Data source (report number) [(5)]		(all)	1, 3, 4b, 8, 10, 11, 20, 27, 31b, 36, 37b, 44b, 47, 48, 50, 53, 167, 170b, 172b, 318, 347, 349, 351, 352, 372, 382, Binder 23				62, 66, 69, 70, 86, 129, 140, 146, 166, 204, 279, 318, 322, 343, 356, 359			
Normalized proportions of borehole yields (based on representative success rates) (L/min)	Dry or tech. neg.	41.5%	30.8%				49.8%			
	<13	9.5%	7.6%				10.1%			
	13-70	34.8%	47.6%				26.6%			
	70-180	9.6%	11.2%				8.3%			
	>180	4.6%	2.8%				5.2%			

Notes:
(1) : Only unique boreholes with reliable coordinates were considered
(2) : Dry and technically negative boreholes sometime have yield data (from bh constr.) even though they are now considered unsuccessful
(3) : Representative success rates were estimated from local hydrogeological or water supply project reports collected in HAP's first phase
(4) : Success rates presented here may not be representative everywhere in the districts considered as they were derived from local studies
(5) : The report numbers refer to the HAP report metadatabase created during the collection of existing reports (see digital library in Appendix D)

5.2.3 Overview of geophysical exploration methods for groundwater

Prior to the inception of the HAP, there had been little prior work on the evaluation of the use of geophysical exploratory methods for regional hydrogeological assessments on a large or even medium scale. Rather, due to the needs of rural and urban water supply projects, the use of geophysical methods has tended to focus on the specific goal of finding exact locations for drilling of water supply boreholes. This is in contrast to the use of the technology for delineation of aquifer zones on a large or medium scale assessment.

Nonetheless, a dominant methodology has been refined over the past decades in the HAP study area by local practitioners centered on the use of existing (often limited) data in conjunction with field geophysical techniques for reconnaissance and location of borehole drilling targets. While the overall methodology remains largely the same, the advent of new geophysical techniques holds the promise of increased drilling success rates as these new techniques build up the data from ongoing drilling results.

The approach is carried out in two phases: 1) collection of existing data and reconnaissance field visit, followed by 2) geophysical field work, as described below.

5.2.3.1 Data collection and reconnaissance

Borehole drilling site selection is carried out through a holistic approach incorporating data collection and review, site reconnaissance and geophysical surveys. Existing hydrogeological data are identified and collected for examination, including available aerial photographs, and the undertaking of a desktop study to develop an initial appreciation of the terrain features and layout of the project area. Potential sources of information may include local government agencies, bilateral aid agencies, NGOs, universities, and any other consultants who may have some knowledge of the local hydrogeological conditions. The additional types of information to be sought include soil survey, geological, hydrogeological and hydrological maps and reports, water quality information, and, if available, satellite imagery encompassing or including the area of interest.

A reconnaissance site visit based on the review of available data is undertaken by the practitioner to obtain or confirm information on the general depth to groundwater, the location and composition of rock outcrops and, where applicable, the availability and general quality of surface water. The local stratigraphy and general hydrogeological conditions are evaluated with respect to the fracture patterns of the rock in order to develop a better understanding of the positioning of the existing boreholes, permeability of the overburden and weathered bedrock, and groundwater recharge characteristics. Based on the data available on geological conditions, specific zones in the area of each proposed monitoring borehole location are delineated for future geophysical surveys. This delineation is based on identification of fracture traces from the aerial photographs and reconnaissance site visit, review of local topographical conditions, and examination of any available information regarding previous borehole construction activities in the area, including dry holes, and generally target fracture intersections where they can be identified.

5.2.3.2 Traditional geophysical field investigations (EM and VES)

The traditional approach for geophysical surveys of the selected siting areas to be investigated for borehole drilling is the combination of electro-magnetic (EM) and resistivity methods, while recent water supply projects have included the use of strictly resistivity methods, specifically, 2D resistivity imaging. However, more recently, the use of EM as a reconnaissance tool has diminished, especially in large parts of the Voltaian sedimentary basin due to the lack of clear anomalous features and the relatively shallow penetrating power of the instrument (no clear magnetic contrasts between rocks/materials).

Vertical Electrical Soundings (VES) using the resistivity method is still the most common geophysical exploratory technique used in northern Ghana. VES surveys are carried out along a (typically) straight line within the area of interest, with the most positive sites in terms of resistivity values and previous drilling (empirical method) selected for actual test drilling. While the interpretation methods vary from practitioner to practitioner, in general the apparent specific resistivity values are plotted against the half current electrodes distance on a diagram to obtain so-called "sounding curves" (see Figure 5.26). Whether by using existing computer software or through practitioner experience in the region, the geological situation is deduced by correlating each curve with solution curves that best represent the structure of the formation below the target site. The main instrument arrays used in Ghana are dipole-dipole and Schlumberger, with preference for each largely dependent on the practitioner's own preference and experience with regards to site conditions.

Figure 5-26 – Theoretical resistivity sounding graph (left) with typical apparent resistivity ranges for different types of material (right)

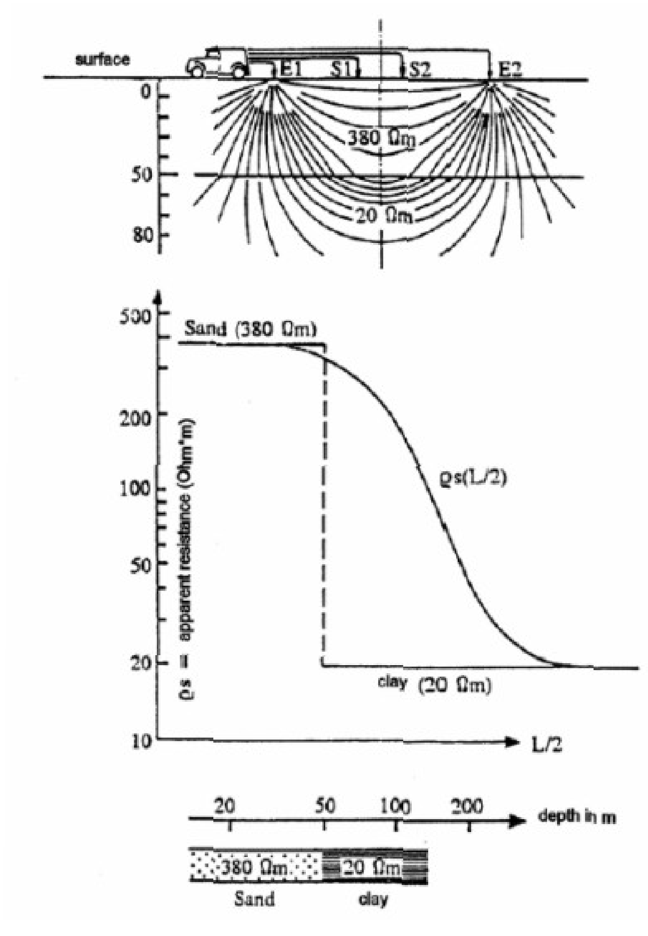

rock type	specific resistance (Ohm*m)
clay, marl	3 ... 30
clay, sandy	8 ... 40
sand, clayey	20 ... 100
sand, gravel	100 ... 2000
limestone, gypsum	100 ... 2000
sandstone	100 ... 5000
magmatic rocks	300 ... 10^5

The limitations of VES are very apparent in the HAP study area, especially in areas where existing borehole stratigraphic logs are not available to "calibrate" the data collected at a potential site. In addition, the nature of the method does not allow a full appreciation of the underlying structure in any direction other than below the target site itself, which is often critical in areas where primary permeability is structurally controlled. While multiple VES along a profile is possible and often done to provide this additional dimension, it is costly and time consuming, rendering an optimum number of VES unfeasible for water supply projects that have limited time and resources available for a given area.

5.2.3.3 Recent geophysical investigation approaches

As VES yield information related to individual points (i.e. straight down below the potential site), recent technology has been introduced to essentially allow multiple VES along a profile line with one "set up" called 2-D resistivity imaging. In essence, a computer controlled switching unit allows the compilation of resistivity data from the array along a lateral surface, which completes the function of many single VES (see Figure 5.27).

Figure 5-27 – Schematic vertical electrical sounding setup for 2D resistivity imaging

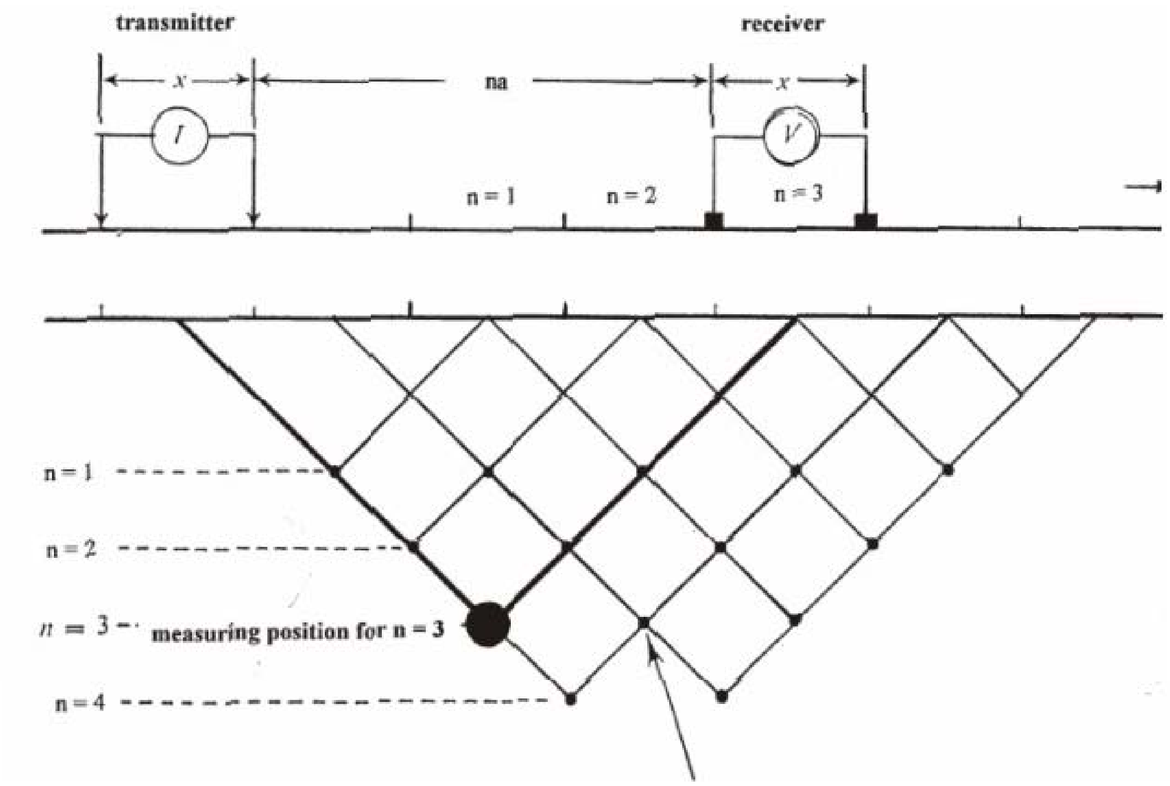

Through recent field work in the study area, this approach has been found to provide the needed lateral dimension allowing better interpretation of structural and layered features below a target area (i.e. thickness of overburden, lateral variation of resistivity). This technique provides true resistivity sections to a depth of approximately 100 m. Through its use on two recent water supply projects including the siting location of new HAP monitoring boreholes, the method was proven cost effective in data gathering and interpretation and in providing increased understanding of subsurface features While greatly increasing the amount of data that can be collected relative to VES, the cost of the equipment for 2-D resistivity imaging is still prohibitive to a vast majority of practitioners in Ghana. Moreover, it is likely too soon to tell if the 2-D resistivity imaging approach can provide an increased success rate for borehole drilling, given the very limited data (and regional bias) obtained using this method to date.

5.2.3.4 The way forward

The key to approaching a standardized methodology for borehole siting is to compare traditional method results with the results from new techniques, specifically the successful drilling of boreholes yielding adequate water supplies. In addition to the 2-D resistivity imaging system recently introduced to northern Ghana, other promising methods are being piloted in the region. In other countries with similar environments, new geophysical techniques such as nuclear magnetic resonance (NMR) seem to have a promising future in groundwater exploration (Wyns *et al.*, 2004; Lubczynski and Roy, 2004; Legchenko *et al.*, 2006). NMR is particularly interesting since its geophysical response, contrary to other geophysical techniques, is directly related to the amount of water itself. As the results of the new techniques becoming available, it will be critical for practitioners to share and discuss the results in an open forum to allow maximum synergy of experience and inputs. At this time, there is a clear need to strengthen the methods by which practitioners can share experience, and thereby contribute to a more standardized approach and interpretation methodology.

5.3 Groundwater recharge

While groundwater recharge is one of the most important parameters required to support sustainable management of groundwater resources, it is one of the most difficult to accurately assess, due to the numerous factors involved in recharge processes. Various methods exist to estimate recharge, each with their own advantages and limitations. Reviews of methods applicable to semi-arid and arid environments state the importance of using a variety of independent techniques, as they can complement each other in terms of time intervals and spatial scales at which they are applicable (Scanlon *et al.*, 2006; Kinzelbach *et al.*, 2002; Simmers, 1988).

Given the constraints of this project, two recharge estimation methods, the soil moisture balance and the chloride mass balance (unsaturated and saturated zone approaches), were selected and implemented. The soil moisture balance (SMB) method was first implemented to provide initial estimates as it only required readily available climate data. While it is relatively easy to implement, it however does not account for preferential recharge. Local direct recharge was later evaluated with the unsaturated zone chloride mass balance (CMB) method, using Cl concentrations from porewater samples. The latter method was chosen to provide independent estimates as it has been widely used in semi-arid regions and is relatively low-cost and easy to implement. The interpretation of the resulting chloride profiles can however be complicated by soil heterogeneities. Also, this method does not allow the assessment of the indirect portion of recharge through preferential pathways. Consequently, another approach of the CMB method, using Cl concentrations from groundwater, was also implemented to allow estimation of spatially averaged recharge values.

Other methods have been considered to complement the ones mentioned above but could not be satisfactorily implemented with the available or newly acquired data, given the project timeframe.

More specifically, the water table fluctuation (WTF) method could not be used to estimate recharge for many monitoring wells as transducers failures generated significant data gaps in the well hydrographs. For the few monitoring wells presenting fairly continuous datasets, it was not possible to apply the method within the project timeframe. Therefore, exploitable groundwater level datasets should be revisited after a few years of continuous data acquisition (i.e. in the order of 5 years) to interpret them in terms of recharge magnitude and processes. One difficulty in the interpretation of these data will however be the estimation of representative specific yield values that are needed to estimate recharge from changes in water levels. These data will also be important in showing the timing of recharge events and should thus help validate if there is a single yearly event or if recharge occurs more continuously. In addition, hydrographs could show if preferential recharge is likely to occur. Variations in water levels could thus provide indications on aquifer conditions (confined or unconfined) as well as aquifer dynamics.

River hydrographs and baseflow separation is another way to obtain representative global recharge estimates for a basin or sub-basin, but which HAP did not address due to data constraints. However, the following section cites other work that used river hydrographs to obtain water balance components, such as runoff, and recharge. These previous studies were used to validate the recharge estimates obtained from our study.

Since chloride mass balance in the unsaturated zone was used to estimate recharge in our study, it could have been possible to complement the results obtained with other environmental tracers, notably tritium. However, this method could not be implemented as the cost of the transport and analysis for all profiles was prohibitive.

Finally, infiltration modeling (e.g. HELP or similar models) (Croteau *et al.*, 2005) could not be implemented systematically since its application requires a good knowledge of the distribution of materials in the subsurface, which could not be reliably derived at the regional scale of our study given the data available.

5.3.1 Previous studies on recharge

In northern Ghana, few studies have investigated groundwater recharge (Table 5-11). Recently, Martin (2006) estimated groundwater recharge in the Atankwidi catchment (~ 20 km northeast of Navrongo) using three methods, namely chloride mass balance (CMB), water table fluctuation (WTF) and soil moisture balance (SMB). Comparison of results revealed recharge rates varying from 1.8 to 13 % of annual rainfall for 2003 and 2004 (i.e. 20 mm to 147 mm). In the Northern Region of Ghana, Pelig-Ba (2004) investigated groundwater recharge using stream hydrograph separation (Bui-Lawra and Nawuni-Pwalugu catchments) and chloride mass balance (Tamale) with results ranging from 1.7 to 4.9 % of annual rainfall (i.e. 18 mm to 44 mm). Another study carried out in the Kompienga Dam basin area in Burkina Faso (~ 85 km northeast of Bawku) revealed an average recharge rate of 5.3 % of rainfall (i.e. 44 mm) based again on chloride mass balance, water table fluctuation and water balance (Sandwidi, 2007). A more regional figure was estimated for the Volta River basin by Martin and van de Giesen (2005). Based on a linear regression of recharge rates from previous work done in West Africa, they estimated the recharge rate within the area of the basin that falls within the borders of Ghana and Burkina Faso at 3.7 % of rainfall (i.e. ~ 31.5 mm). For well field design purposes in the upper regions, groundwater recharge estimates of 2.5 % of the average annual rainfall (i.e. ~ 25 mm) (Bannerman and Ayibotele, 1984) and of 3-4 % (i.e. ~ 28-37 mm) (Apambire, 1996) were respectively recommended for the Wa and Bawku well fields. Other studies throughout West Africa provide groundwater recharge rates of similar magnitude (Table 5-11).

Estimated recharge rates in northern Ghana are generally low, with high spatial and temporal (from year to year) variations. Due to the nature and amount of rainfall events in northern Ghana (i.e. short, intense rainstorms occurring over a relatively short rainy season), recharge rates are largely influenced by rainfall but also by runoff, evapotranspiration, thickness of weathering, soil characteristics, vegetation, land use and topography. Significant recharge generally occurs towards the end the rainy season as a combination of direct and indirect infiltration. Although the contribution of both these infiltration processes to overall recharge is difficult to quantify, recharge from soil matrix infiltration is generally considered small when compared to recharge from indirect infiltration (e.g. from fractures or from temporary drainage networks such as pools and streams) (Leduc *et al.*, 1997; Desconnets *et al.*, 1997; Acheampong, 1996; Martin, 2006; Edmunds *et al.*, 2002; Sandwidi, 2007).

5.3.2 Soil moisture balance

The soil moisture balance is one of most commonly used water balance methods due to its low cost and use of usually readily available climate data. It is used to estimate a component of the water balance, usually groundwater recharge, as the residual of all other fluxes that can be measured or estimated more easily (Lerner *et al.*, 1990). The general relation between fluxes (i.e. precipitation (P), surface runoff (Q), evapotranspiration (ET), groundwater recharge (R) and change in water storage in the saturated and unsaturated zones (ΔS)) consists of:

$$P = Q + ET + R \pm \Delta S \qquad [5.4]$$

The basis of the soil moisture balance method for estimating recharge is that the soil becomes free draining when the moisture content of the soil reaches a limiting value called field capacity; excess water then generates infiltration towards the aquifer.

Table 5-11 – Annual recharge rates from selected previous studies in West Africa

Study area	Rainfall (mm/y)	Recharge		Method	Source
		(% rainfall)	(mm)		
Northern Ghana (Atankwidi basin)	910-1138	1.8-13 %	20-147	Water balance, CMB, WTF	Martin, 2006
Northern Ghana (White Volta basin)	800-1140	2.2-18.5 %	22-183	WTF, CMB, hydrological modelling	Obuobie, 2008
Northern Ghana (Northern Region)	729-1048	1.7-4.9 %	18-44	CMB, stream hydrograph	Pelig-Ba, 2004
Ghana & Burkina Faso (Volta River basin)	~ 850	3.7 %	31.5	Linear regression	Martin and van de Giesen, 2005
Ghana (Volta River basin)	1000-1600	13.4-16 %	151-205	Water balance	GEF-UNEP, 2002
Central Ghana (Afram Plains)	1400	12 %	185	Water balance	Acheampong, 1996
South central Ghana (Pra River basin)	1170-1490	3.9 %	51	Hydrological modelling	Darko and Krasny, 2003
South central Ghana (Birim River basin)	1578	10.8%	172	Stream hydrograph	Asomaning, 1992
Central Burkina Faso	690	3.3-6.5 %	23-45	Hydrological modelling	Thiery, 1988
Central Burkina Faso	720	14.8 %	107	Soil moisture modelling	Milville, 1991
South Burkina Faso (Kompienga Dam)	834	5.3 %	43.9	Water balance, CMB, WTF	Sandwidi, 2007
Southwest Niger	419-620	~ 10 %	~ 50-60	WTF	Leduc *et al.*, 1997
Southwest Niger	564	2.3 %	13	CMB	Bromley *et al.*, 1997
Northeast Nigeria	519	12.5 %	65	Soil moisture modelling	Rushton *et al.*, 2006
Northeast Nigeria	320-400	4.4-15.3 %	14-49	CMB	Edmunds *et al.*, 2002
Range for selected previous studies	**320-1600**	**1.7-18.5 %**	**13-205**		

Different conceptual models have been previously developed to represent soil water storage in the upper layer of soil, but an improved soil moisture balance model (Rushton *et al.*, 2006) was used with the daily climate dataset for the estimation of groundwater recharge. While similar in essence to the classical model, this improved model notably introduces a modification for near surface soil storage of water (NSSS). The aim of the NSSS is to retain a certain amount of water after a significant rainfall event when soil moisture deficit is greater than the readily available water. This allows a more realistic estimated response by making some water available for evapotranspiration on subsequent days instead of being all allocated to reduce soil moisture deficit. The model uses an empirical factor to define the proportion of the increase in moisture content which becomes NSSS. This improved model also takes into account soil water stress by considering soil moisture distribution in terms of total and readily available water, which allows the adjustment of transpiration and evaporation rates as soil water is depleted. This evapotranspiration adjustment notably depends on soil and crop properties. As available information on the upper soil layer was minimal, typical average values of field capacity and wilting point were selected from literature (Allen *et al.*, 1998) with respect to soil texture at each meteorological station. A conservative value was used for rooting depth since such information was not available for the different crops. While this model can also take into account the influence of the different characteristics of each crop (i.e. length of crop development stages, crop height, crop distribution & density), the lack of readily available data on crops did not allow such an adjustment.

Calculations were carried out with the daily climate dataset obtained through contacts with the Global Change in the Hydrological Cycle Project (GLOWA-Volta). The daily climate dataset, in the form of MS Excel files, originally came from the Ghana Meteorological Service Department (MSD) and includes the following climate variables:

- Mean, maximum and minimum temperature
- Rainfall
- Relative humidity at 06h00, 09h00, 12h00, 15h00
- Wind speed, wind run and wind direction
- Sun hours

Data were available for eight meteorological stations: Navrongo, Wa, Bole, Tamale, Yendi (all inside the northern regions), Kete-Krachi (Volta Region), Wenchi and Sunyani (both in Brong-Ahafo Region) (N.B.: stations names in bold on Figure 3-5). Coordinates and elevation of these stations are summarized in Table 5-12 (N.B.: data source is United States National Weather Service Telecommunication Gateway (http://www.weather.gov/tg/siteloc.shtml)). The dataset covered the 2000-2005 period (N.B.: the first three or four months of 2006 were also available, but were not considered for calculations). For some years, the files were incomplete (from daily to monthly gaps) so that gap filling was necessary to obtain a continuous dataset. Data gaps were filled using measurements from nearest neighbouring stations and monthly average data observed at the gap filled station. The method followed a constant ratio correction for all climate variables (Gong, 2004).

Table 5-12 – Location information for the meteorological stations considered

Station location	Coordinates (decimal degrees)		Elevation (m)
	Longitude	Latitude	
Bole	-2.48	9.03	299
Kete-Krachi	-0.03	7.82	122
Navrongo	-1.10	10.90	201
Sunyani	-2.33	7.33	309
Tamale	-0.85	9.50	173
Wa	-2.50	10.05	323
Wenchi	-2.10	7.75	339
Yendi	-0.02	9.45	195

Calculations were carried out in MS Excel for each meteorological station (see Appendix D on USB flash drive). Inputs were also computed with values taken directly at the station location (i.e. no spatial data interpolation). Consequently, results are representative of conditions at the station only. The following sections describe required inputs and associated outputs for the daily soil moisture balance. Calculations were also made on a monthly basis since the monthly climate dataset was obtained earlier in the project. Results obtained with the monthly data are not discussed in detail here but are illustrated in Appendix C for comparison and are also detailed in Appendix D (USB flash drive).

5.3.2.1 Inputs

The precipitation (*P*) values used here are daily precipitation values from the 2000-2005 period. As mentioned earlier, observed data gaps in the precipitation data were filled for that period using data from neighbouring stations.

For reasons stated in section 3.3, the Penman-Monteith method was applied to daily climate data to estimate potential evapotranspiration (*pET*). The Penman-Monteith general equation is expressed as follows (Allen *et al.*, 1998):

$$pET = \frac{0.408\Delta\left(R_n - G\right) + \gamma\left(\frac{900}{T+273}\right)u_2\left(e_s - e_a\right)}{\Delta + \gamma\left(1 + 0.34u_2\right)} \quad [5.5]$$

where *pET* = mean daily potential (or reference) evapotranspiration (mm/d), Δ = slope of vapour pressure curve (kPa/°C), R_n = net radiation at crop surface (MJ/m^{2}d), *G* = soil heat flux density (MJ/m^{2}d), γ = psychometric constant (kPa/°C), *T* = mean air temperature (°C), u_2 = wind speed at 2 m height (m/s), e_s = saturation vapour pressure (kPa), e_a = actual vapour pressure (kPa). This equation allows the calculation of potential evapotranspiration for a reference surface which Allen *et al.* (1998) define as a grass crop with an assumed crop height of 0.12 m, a fixed surface resistance of 70 s/m and an albedo of 0.23. Crop evapotranspiration, which accounts for the variability of these crop characteristics (i.e. crop height, crop resistance, albedo …) was not computed here because of the unavailability of these and other specific data on crops (i.e. characteristics and distribution) in the northern regions. The complete calculation procedure used for each station is documented in Appendix A.

For the purpose of this study, a constant runoff coefficient (*Q*) of 12.5 % was used to evaluate the portion of precipitation that does not infiltrate the soil since readily available information did not allow a more detailed and reliable estimation of runoff. This coefficient was estimated from results of previous studies summarized in Table 5-13.

Table 5-13 – Summary of available runoff coefficients from previous studies in Ghana

Study area	Region(s)	Runoff coefficient (% of rainfall)	Reference
Atankwidi River basin	Upper East Region	10-17 %	Martin, 2006
Afram Plains	Eastern Region	13 %	Acheampong, 1996
Pra River basin	Ashanti, Eastern and Central regions	6-9 %	Darko and Krasny, 2003
Volta River basin	Mostly all central northern regions	11 %	Friesen *et al.*, 2005
		10 %	Shahin, 2002
		8 %	Andreini *et al.*, 2000

Two estimation methods have been tested in parallel to provide a basis of comparison for runoff values obtained with this constant coefficient: 1) a runoff value derived from the Curve Number method and 2) a runoff value derived from tabulated coefficients based on precipitation and soil moisture deficit values. Since many input values had to be estimated or taken from the literature to use these methods, their results were not used for more than comparison. Calculation details and results are presented in Appendix D (USB flash drive).

5.3.2.2 Model parameters

For the model used here, the daily infiltration (*I*) is defined as the amount of precipitation that does not run off at the surface plus the amount of water retained for near surface soil storage on the previous day ($NSSS_{pr}$). It is given by the following equation:

$$I = P - Q + NSSS_{pr} \qquad [5.6]$$

where *I* = infiltration (mm), *P* = precipitation (mm), *Q* = runoff (mm) and $NSSS_{pr}$ = near surface soil storage for previous day (mm).

The near surface soil storage (*NSSS*) can be obtained from the following equations:

$$NSSS = FRACSTOR \bullet (I - pET) \quad (I > pET) \qquad [5.7]$$

$$NSSS = 0 \quad (I \le pET) \qquad [5.8]$$

where *NSSS* = near surface soil storage (mm), *I* = infiltration (mm), *FRACSTOR* = coefficient for *NSSS* and *pET* = potential evapotranspiration (mm). As information on soil response to significant rainfall events was not available to determine *FRACSTOR*, an average empirical factor of 0.4 was selected from literature on the basis of soil texture (Rushton *et al.*, 2006).

The soil moisture deficit (*SMD*) is defined as the amount of water required to bring the soil water content up to field capacity. It can be obtained from the following equations:

$$SMD = 0 \quad (SMD_{pr} - I + NSSS + aET \le 0) \qquad [5.9]$$

$$SMD = SMD_{pr} - I + NSSS + aET \quad (SMD_{pr} - I + NSSS + aET > 0) \qquad [5.10]$$

where *SMD* = soil moisture deficit (mm), SMD_{pr} = soil moisture deficit for previous day (mm), *I* = infiltration (mm), *aET* = actual evapotranspiration (mm) and *NSSS* = near surface soil storage (mm).

The actual evapotranspiration (*aET*) refers to the portion of potential evapotranspiration that is truly utilized given soil moisture conditions and vegetation characteristics. It can be obtained from the following equations:

$$aET = I \quad (SMD_{pr} > TAW \text{ and } I < pET) \qquad [5.11]$$

$$aET = I + K_s (pET - I) \quad (RAW < SMD_{pr} < TAW \text{ and } I < pET) \qquad [5.12]$$

$$aET = pET \quad (SMD_{pr} < RAW \text{ or } I > pET) \qquad [5.13]$$

$$\text{with} \quad K_s = (TAW - SMD_{pr}) / (TAW - RAW) \qquad [5.14]$$

where *aET* = actual evapotranspiration (mm), *pET* = potential evapotranspiration (mm), SMD_{pr} = soil moisture deficit for previous day (mm), *I* = infiltration (mm), *TAW* = total available water (mm) and *RAW* = readily available water (mm). The latter two variables which are related to soil water stress effect can be obtained from:

$$TAW = 1000\left(\theta_{FC} - \theta_{WP}\right)Z_r \qquad [5.15]$$

$$RAW = pTAW \qquad [5.16]$$

where TAW = total available water (mm), RAW = readily available water (mm), θ_{FC} = field capacity (m^3/m^3), θ_{WP} = wilting point (m^3/m^3), Z_r = rooting depth (m) and p = depletion fraction. As suggested by Allen *et al.* (1998), a conservative value of 2.0 m was used for rooting depth since information on crops was not available. For the depletion factor, which corresponds to the average fraction of *TAW* that can be depleted from the root zone before soil water stress occurs, an average value of 0.5, also suggested by Allen *et al.* (1998) for many crop types, was used. Due to the lack of data, it was not possible to determine seasonal variations of either the rooting depth or the depletion factor.

The recharge component (R) of the soil moisture balance corresponds to the amount of infiltrated water that percolates to recharge groundwater. It only occurs when the soil moisture deficit is zero:

$$R = 0 \qquad \left(SMD \geq 0\right) \qquad [5.17]$$

$$R = -\left(SMD\right) \qquad \left(SMD < 0\right) \qquad [5.18]$$

where R = groundwater recharge (mm) and SMD = soil moisture deficit (mm).

5.3.2.3 Results

The average annual results for each of the components of the soil moisture balance are summarized in Table 5-14. The daily values obtained for two of the eight meteorological stations considered are shown in Figure 5-28.

Table 5-14 – Summary of soil moisture balance annual results

		Soil moisture balance Average annual values for the 2000-2005 period									
Station	Region	pET		P		Q		aET		R	
		(mm)	(%)	(mm)	(%)	(mm)	(%)	(mm)	(%)	(mm)	(%)
Navrongo	Upper E.	1 968	-	963	100	120	12.5	758	78.7	84	8.8
Wa	Upper W.	1 767	-	1 040	100	130	12.5	891	85.7	19	1.8
Tamale	Northern	1 944	-	1 040	100	130	12.5	862	82.9	48	4.6
Yendi	Northern	1 642	-	1 291	100	161	12.5	919	71.2	205	15.9
Bole	Northern	1 670	-	1 157	100	145	12.5	970	83.9	36	3.1
Kete-Krachi	Volta	1 582	-	1 353	100	169	12.5	915	67.6	268	19.8
Sunyani	Brong-Ahafo	1 551	-	1 197	100	150	12.5	1 006	84.0	34	2.8
Wenchi	Brong-Ahafo	1 472	-	1 258	100	157	12.5	1 071	85.1	12	1.0
Standard deviation range		19-74	-	111-203	-	14-25	-	42-111	-	16-147	-

Legend: pET: potential evapotranspiration; P: precipitation; Q: runoff (constant coefficient of 12.5 %); aET: actual evapotranspiration; R: recharge)

Climate profiles obtained are typical of semi-arid regions, with the evapotranspiration component dominating over other components (71.2-85.7 % of average annual rainfall for the five stations in the northern regions). As expected, profiles for stations in the northern regions reveal only one rainy season preceded by high potential evapotranspiration values. As the rainy season advances, actual evapotranspiration generally increases to reach a high proportion of the potential evapotranspiration and the soil moisture deficit starts to decrease. Groundwater recharge occurs at the end of the rainy season, during a relatively short period. For stations located in the project area, recharge values range from 19-205 mm (i.e. 1.8-15.9 % of average annual rainfall) with standard deviations ranging from 16 to 147 mm (see appendix D-12 for SD values by station). It can be observed from the graphs on Figure 5-28 that the occurrence and amount of recharge is notably influenced by the distribution of precipitation events, rather than only by their absolute magnitude.

Figure 5-28 – Soil moisture balance results at selected meteorological stations for the 2000-2005 period

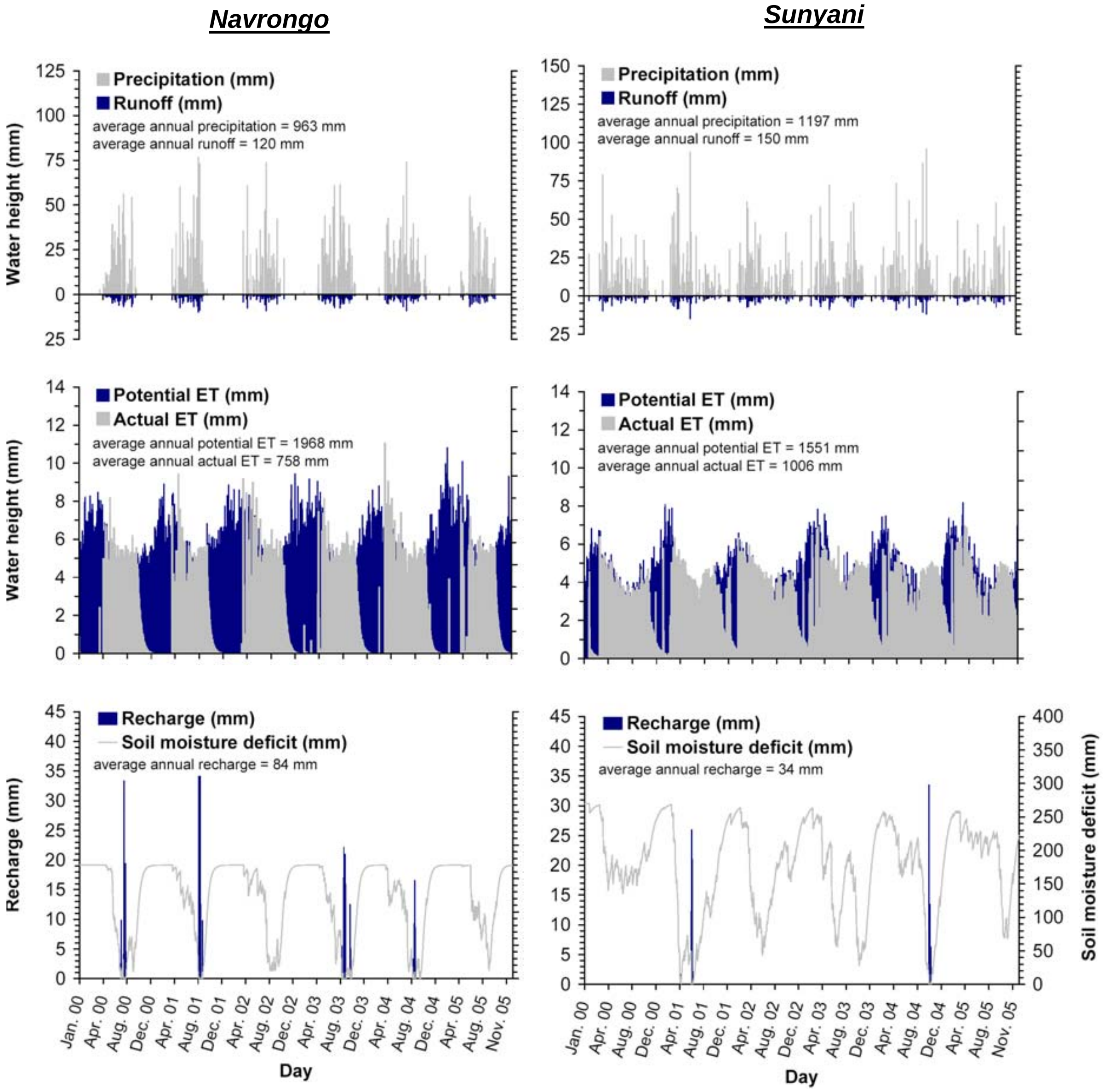

Comparison of results with those obtained from the monthly calculation (Appendices D-12 and D-13) reveals similar values for each component of the soil moisture balance. Slight differences observed between estimated values from the monthly and daily datasets can mainly be attributed to the period considered (i.e. 2000-2005 as opposed to 1971-2001) and the use of an improved soil moisture model with a daily time step. The pattern of the evapotranspiration is generally similar to that obtained with the monthly calculation but the introduction of a correction for soil water stress in the daily calculation is noticeable during the dry season where a slower decrease in actual evapotranspiration is observed. The change in relative duration of the dry and rainy season is also more apparent when northern stations (e.g. Navrongo) are compared to stations south of the project area (e.g. Sunyani).

The estimated duration of the recharge period shown in Figure 5-28 (i.e. generally < 1 month, but up to 2-3 months) is consistent with data from hydrographs obtained from the monitoring wells (Figure 4-4). As available well hydrographs do not cover the period considered for SMB calculations (i.e. 2000-2005), it was not possible to compare measured groundwater response to the corresponding estimated recharge in time. However, the average daily groundwater recharge estimated at the Navrongo meteorological station for the 2000-2005 period was compared to the 2006 groundwater levels from the hydrograph of monitoring well WVB04 (near Bonia) in Figure 5-29. The latter shows that the well hydrograph for 2006 matches relatively well the estimated recharge, with a time lag, even though the period considered is different.

Figure 5-29 – Comparison of WVB04 hydrograph and estimated recharge from SMB at Navrongo station

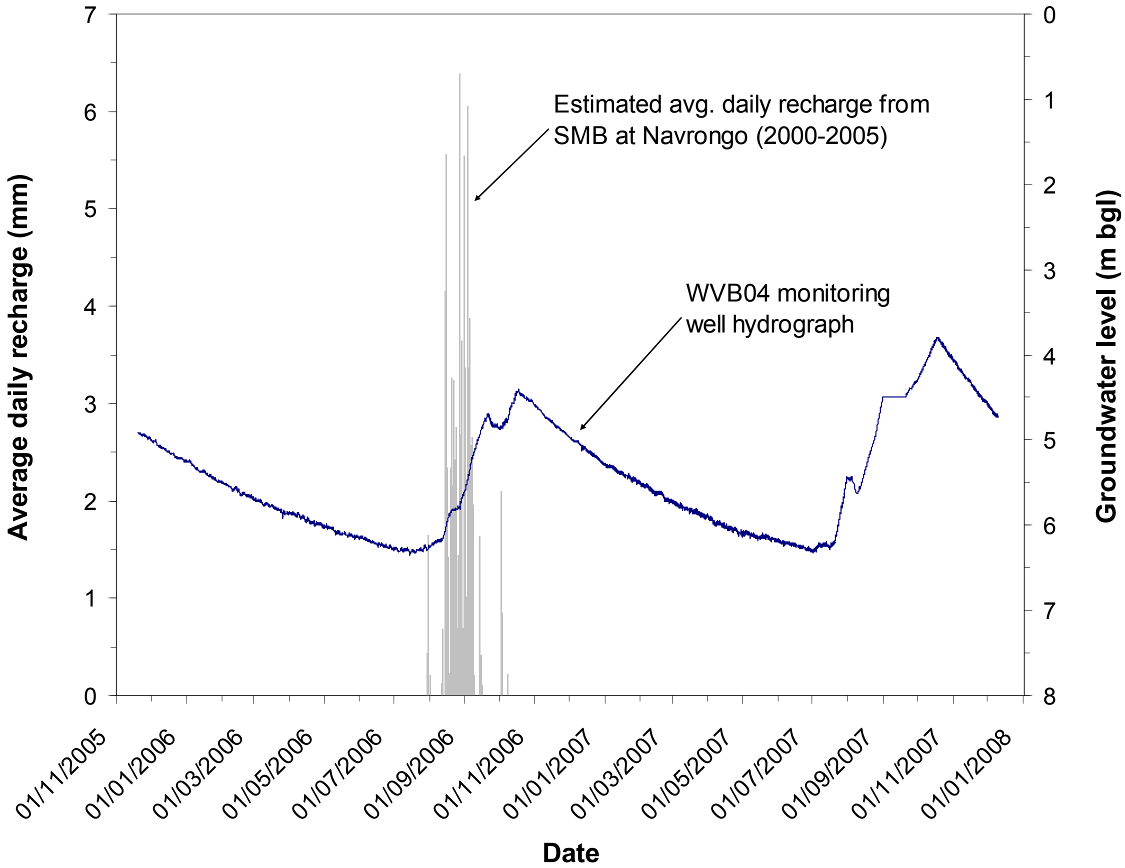

General spatial trends were evaluated for the main climate variables estimated with the soil moisture balance. As the soil moisture balance was computed for only five stations in the northern regions, linear trends were considered more appropriate than contour maps for spatial representation. The spatial linear trends presented here are basically flat planes representing the average gradient. The planes were generated in ArcGIS by the interpolation of climates variables with a global first-order polynomial function.

The trend map for **precipitation** (Figure 5-30) reveals decreasing values from southeast to northwest. This is consistent with observations at the continental scale, which indicate that precipitation diminishes towards the Sahel region. The inclination towards the west may be caused by the lack of data points in the extreme northwest of Ghana.

Potential evapotranspiration generally increases with latitude with a slight tendency towards northeast. Again, the trend is in agreement with the increase of global radiation with latitude in West Africa. Ojo (1969) produced a general contour map for potential evapotranspiration in West Africa that supports this observation.

Figure 5-30 – General spatial trends for main climate variables based on SMB results at eight meteorological stations

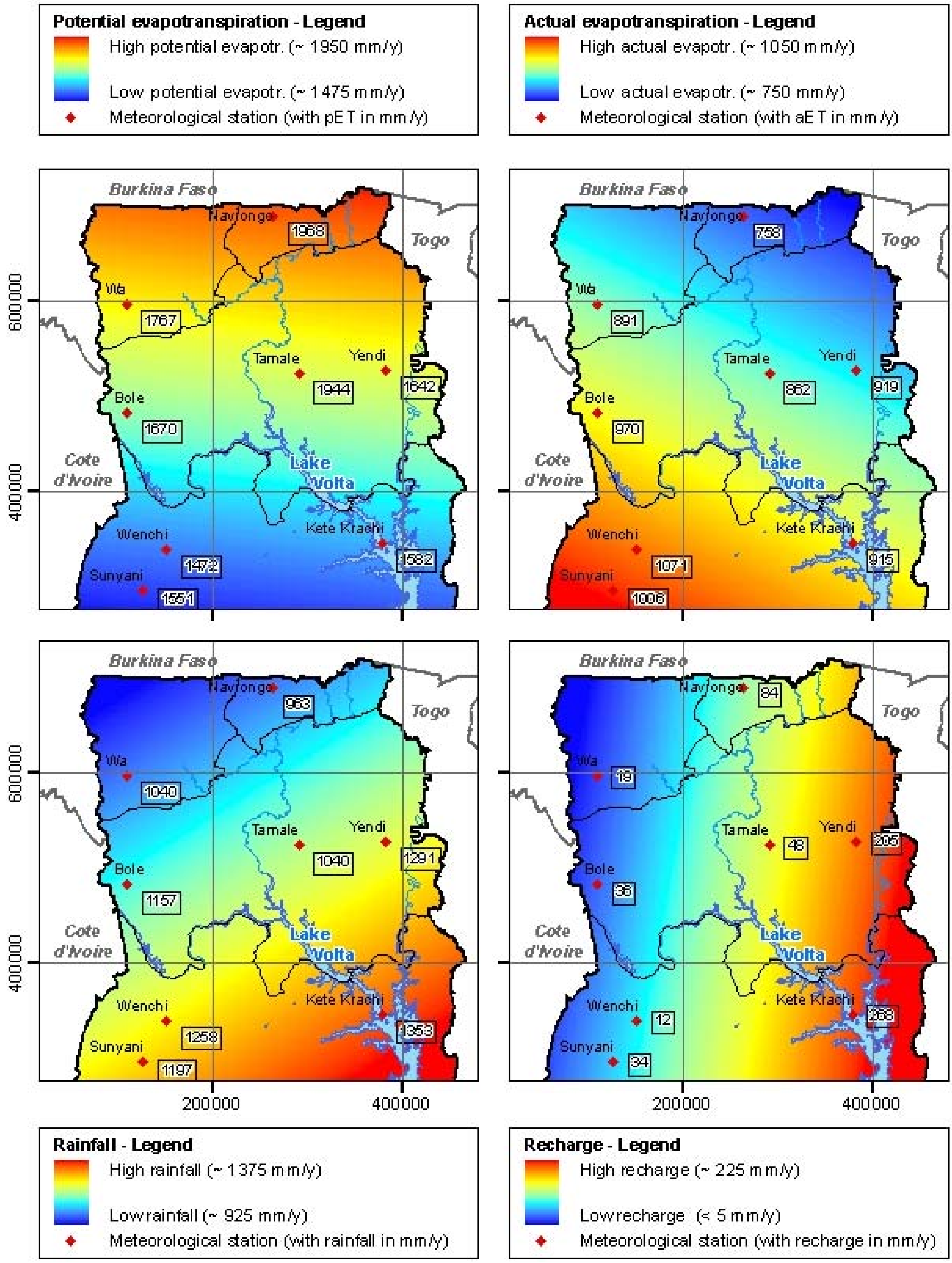

The **actual evapotranspiration** trend diminishes from south-southwest to north-northeast. Since the actual evapotranspiration estimates depend mainly on the precipitation and potential evapotranspiration data, its trend will vary accordingly to the combined influence of these climate variables. There is however no available data on spatial variation of the actual evapotranspiration in Ghana for comparison.

Figure 5-30 reveals a decreasing **recharge** trend from east-southeast to west-northwest. While there is little information on recharge at regional scale to assess the validity of the trend, estimated recharge at the stations considered seem to be in agreement with available values from previous studies.

Examination of the estimated values notably shows that recharge at the Navrongo station is relatively high when compared to recharge at Wa, Tamale and Bole stations. This can be partially explained by the higher potential evapotranspiration rates at the Wa and Tamale stations. However, the intensity, duration and amount of rainfall events during the rainy season can also cause important variations in the amount of runoff thus influencing the amount of water potentially available for recharge (Lerner *et al.*, 1990).

In addition, the number of days between consecutive rainfall events can affect soil water storage and recharge. At the Navrongo station, the amount of rainfall measured during the rainy season (~ late May to October) represents approximately 90 % of total rainfall, whereas at the Wa, Tamale and Bole stations it varies from 74 % to 80 %. While this difference does not explain by itself the variation of recharge values observed at these stations, it does suggest that the distribution of rainfall events throughout the year has a significant influence. This is also noticeable when comparing stations with different amounts of rainfall and different annual distributions of rainfall events. For example, the Sunyani and Navrongo stations respectively have 1 197 and 963 mm/year of rainfall but the latter is distributed over an average of 70 wet days/y while total rainfall in Sunyani is spread out over 105 wet days/y. In addition, rainfall events in Navrongo are more clustered together throughout the year than they are at Sunyani where only 53.4 % of total annual rainfall occurs from late May to October. This relation between recharge and the amount of rainfall in the rainy season is illustrated in Figure 5-31, which shows a relatively good correlation between variables (determination coefficient of 0.76).

Figure 5-31 – Relation between estimated recharge and bulk of rainfall in rainy season

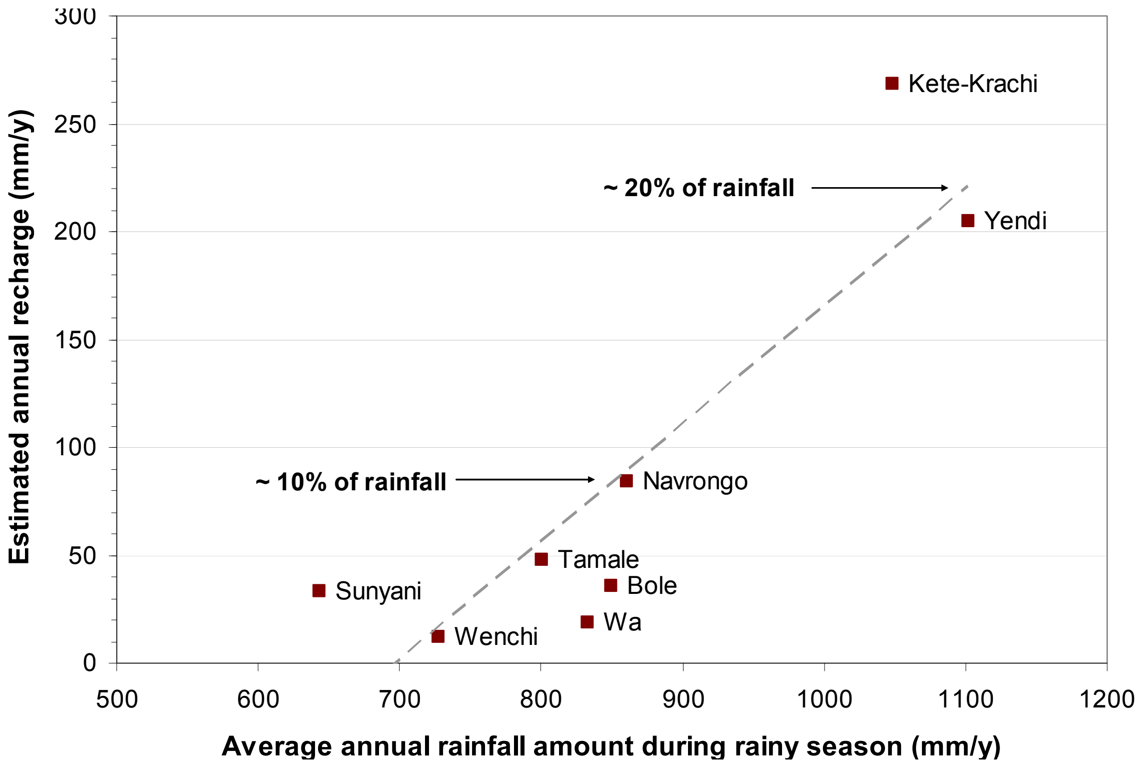

5.3.3 Chloride mass balance

The chloride mass balance (CMB) method uses chloride (Cl) as a natural conservative tracer to distinguish downward soil-water flux from evapotranspirative loss as it does not evaporate from soil surface nor does vegetation take up significant quantities. Input of Cl occurs at the soil surface both as dry fallout and rainfall. For this study, it was assumed that Cl remains inert during atmospheric processes and that only solutes deposited during the rainy season (both wet and dry deposition) form the effective solute load for CMB calculations (Edmunds and Gaye, 1994). Dry deposition during the dry season is likely to be in a quasi-steady state, in which the amount of dust deposited is equal to that taken up (Edmunds *et al.*, 2002). Thus, the application of the CMB method involves the following assumptions (Wood, 1999):

- Flow is 1D, vertically downward, piston-type (i.e. no preferential flow and dispersion & diffusion are negligible compared to vertical convection)
- Cl in porewater originates only from atmospheric Cl flux (i.e. Cl input from run-on/run-off and underlying or adjacent aquifers is unaccounted for)
- Cl is conservative in the system
- Cl mass flux is in steady state

Only wet deposition (i.e. from rainfall) was directly considered for data collection to facilitate field work. According to Martin (2006), neglecting dry deposition of chloride would underestimate recharge by less than 10 %. Considering all assumptions are verified, recharge (*R*) can be estimated as follows:

$$R = P\frac{Cl_P}{Cl_W} \qquad [5.19]$$

where P is the average annual rainfall (mm/year), Cl_P is the average Cl concentration in rainfall (mg/L) and Cl_W is either the average porewater Cl concentration (mg/L) when the unsaturated zone CMB approach is used or the average groundwater Cl concentration (mg/L) for the saturated CMB approach. The latter allows estimation of spatially averaged recharge considering both diffuse and localized input while the unsaturated zone CMB provides local direct recharge estimates. The CMB method has been used before in West Africa and in other semi-arid regions of the world and a detailed description can be found in the literature (Allison *et al.*, 1994; Cook *et al.*, 1992; Murphy *et al.*, 1996; Eriksson and Khunakacem, 1969; Wood, 1999).

Field work related to CMB involved sampling and analysis of rain water for the determination of atmospheric chloride input, sampling of shallow wells for the saturated zone approach and, sampling of soil above the water table for the unsaturated zone approach. The latter also involved soil water extraction and analysis (see section 4.3.5). The following sections present results from these activities.

5.3.3.1 Atmospheric chloride input

Atmospheric Cl deposition was estimated from rainfall samples collected at 8 meteorological stations in northern Ghana for the 2007-2010 period (section 4.3.5.1). A weighted average Cl was used to estimate atmospheric chloride input at each station using the following equation:

$$Weighted\ Cl_{P\ total} = \Sigma\left(\frac{P_{event}\ Cl_{P\ event}}{P_{total}}\right) \qquad [5.20]$$

where $Cl_{P\ event}$ is the Cl concentration measured for individual rainfall events (mg/L), P_{event} is the rainfall of the individual event (mm) and P_{total} is the total sampled rainfall for the rainy season (mm). A summary of weighted average Cl concentrations in rainfall is provided in Table 5-15 for each station considered and calculation details are provided in Appendix D (USB flash drive). Annual rainfall values are derived from daily rainfall data provided by the MSD for 2007-2010. Chloride concentrations used to derive weighted averages range from < 0.1 to 6.7 mg/L and the regional weighted average Cl value is 0.40 mg/L. The weighted averages calculated here are comparable to those obtained by Martin (2006) in northern Ghana (0.20 mg/L), Obuobie (2008) in the Volta Basin (0.80 mg/L) and Bromley *et al.* (1997) in Niger (0.62 mg/L).

Figure 5-32 illustrates the chloride concentrations in rainfall over the 2007-2010 period for all stations considered. Results show a generally decreasing trend in Cl concentrations from the beginning of the rainy season towards the end. This trend is not as obvious in 2007 as the first rain events of that year were not sampled. Additionally, results suggest that chloride concentrations are higher on average for years with higher annual rainfall. A longer dataset would however be required to support this observation. Results for the few samples analyzed for nitrate (NO_3) range from undetected to 3.55 mg/L, with an average of 0.60 mg/L. As the number NO_3 results is relatively low, reliable comparison with Cl values was not possible.

Table 5-15 – Weighted average Cl values for 2007-2010 rainfall at selected stations

Station	Annual rainfall (mm)	Annual rainfall sampled (%)	Weighted average Cl concentration (mg/L)
Bole	1 159.4	72.7	0.31 ± 0.05
Kete-Krachi [(1)]	1 149.6	46.8	0.30 ± 0.11
Navrongo	1 082.1	79.1	0.55 ± 0.10
Sunyani	1 333.0	62.9	0.36 ± 0.05
Tamale	1 126.2	57.4	0.36 ± 0.05
Wa	1 111.6	79.8	0.43 ± 0.09
Wenchi	1 319.5	67.6	0.46 ± 0.08
Yendi	1 378.7	75.6	0.43 ± 0.06
Regional average	1 251.5	67.8	0.40 ± 0.07

Notes:
[(1)] : As mentioned in section 4.3.5.1, samples for Kete-Krachi station were only collected for 2007.

Figure 5-32 – Chloride concentrations in rainfall for selected stations in 2007-2010

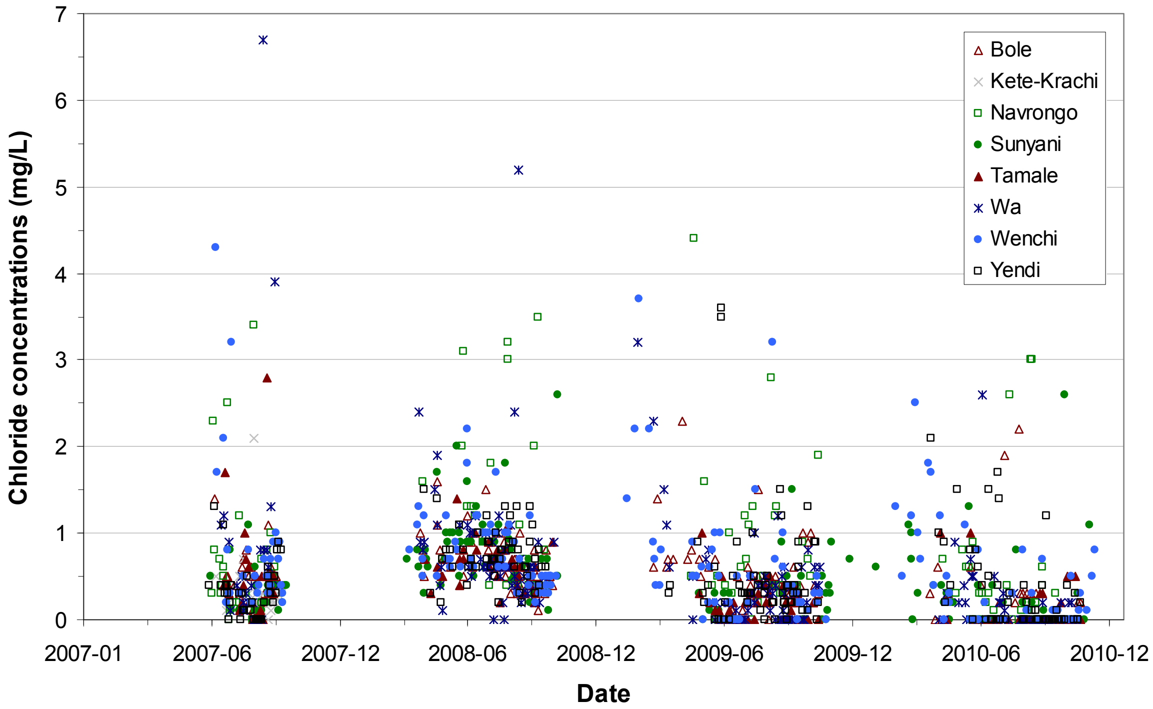

5.3.3.2 Recharge estimation from unsaturated zone profiles

As stated in section 4.3.5.2, only 12 out of the 18 unsaturated zone profiles that were drilled are considered for interpretation. The six other profiles were left out of recharge calculations as they ended inside the assumed evapotranspirative zone.

Variations in moisture content revealed that the evapotranspirative zone would range from 0.9 to 3.1 m in thickness, with an average of 1.7 m. This is consistent with the average value of 2 m proposed in literature (Edmunds *et al.*, 2002; Murphy *et al.*, 1996). Gravimetric moisture content varies between 2 and 25 %wt, with an average around 8.7 %wt. Moisture content would be slightly higher in the VSB (9.5 %wt) than in the Precambrian basement (7.6 %wt), which could suggest a weathered layer with a finer soil texture on average in the VSB. This is supported by particle size analyses (PSA) that were carried out on selected samples from 4 unsaturated zone profiles.

Figures 5-33 and 5-34 present results for selected samples collected in profiles CMB13 (VSB) and CMB18 (Precambrian basement). The average particle size (D_{50}: maximal diameter for 50 % of the particle content) is much lower on average for samples of CMB13 (0.14 mm against 0.57 mm for samples of CMB18), thus indicating finer grained material for this profile. On average, the uniformity coefficient ($C_u = D_{60}/D_{10}$) for samples of CMB18 is larger than that of CMB13 (28.2 against 9.1), suggesting that samples from the latter are better sorted. Particle size analyses were also carried out on selected samples for profiles CMB04 and CMB15. Results for the average particle size are coherent with those of profiles CMB13 and CMB18, with of D_{50} values 0.28 mm (CMB04) and 0.52 mm (CMB15). As for the uniformity coefficients, average values are 27.5 for CMB04 and 18.9 for CMB15.

According to the USDA classification, samples from CBM 13 would mostly range from silty loam to sandy loam while samples from CMB18 would range from sandy loam to sand. Particle size analyses were also carried out on selected samples for two other profiles (CMB04 and CMB15). Results respectively suggest sandy loam (CMB04) and loamy sand (CMB15)

Figure 5-33 – Particle size analysis results for selected samples from profile CMB13

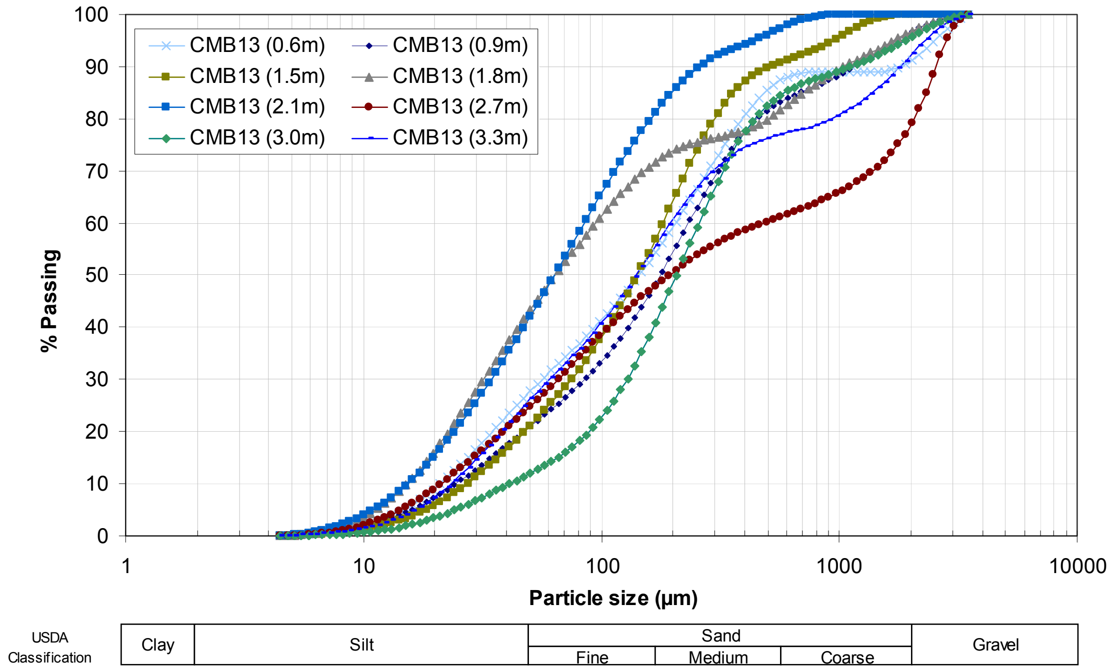

Figure 5-34 – Particle size analysis results for selected samples from profile CMB18

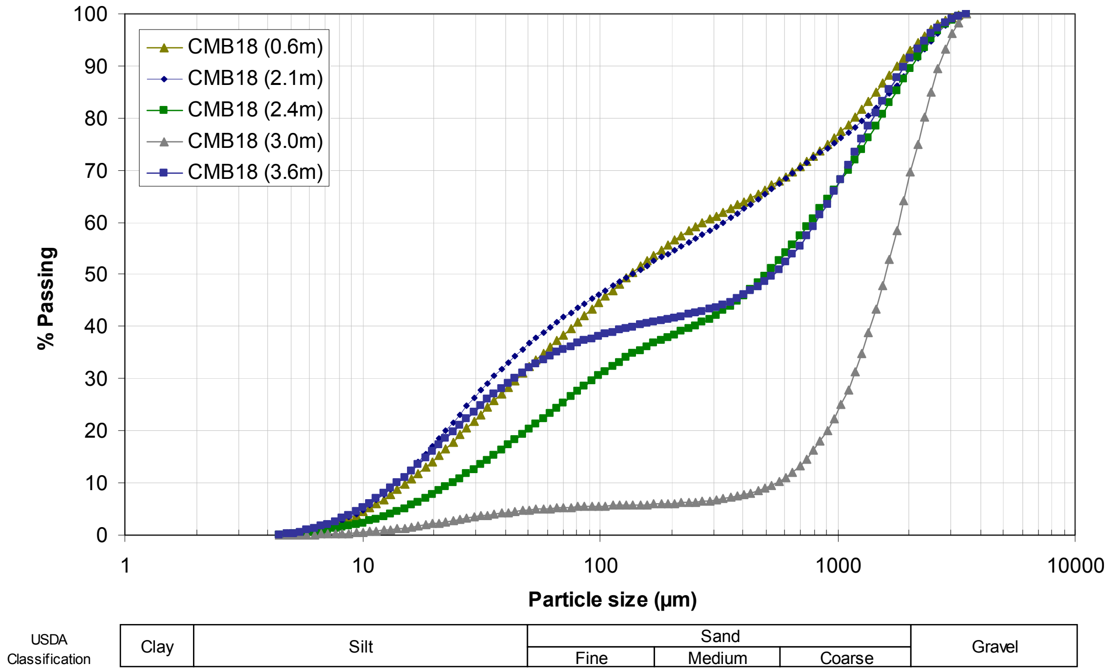

Two methods, elutriation and centrifugation, were used to extract porewater from soil samples for analysis of chloride and nitrate (see section 4.3.5.2 for details). Figures 5-35 and 5-36 compare results for samples analyzed with both methods for Cl and NO_3. Correlation of chloride concentrations between the two methods is relatively low with a correlation coefficient of about 0.25. On average, Cl concentrations obtained for centrifuged samples are slightly higher than those from elutriation (i.e. 14.2 mg/L compared to 10.2 mg/L). For some samples, duplicate analyses revealed heterogeneity in particle size and moisture content within a single sample. Results from the duplicates revealed that these heterogeneities mostly influenced centrifuged sample results in terms of quantity and solute content of porewater recovered.

Figure 5-35 – Comparison of chloride concentrations obtained from elutriation and centrifugation methods

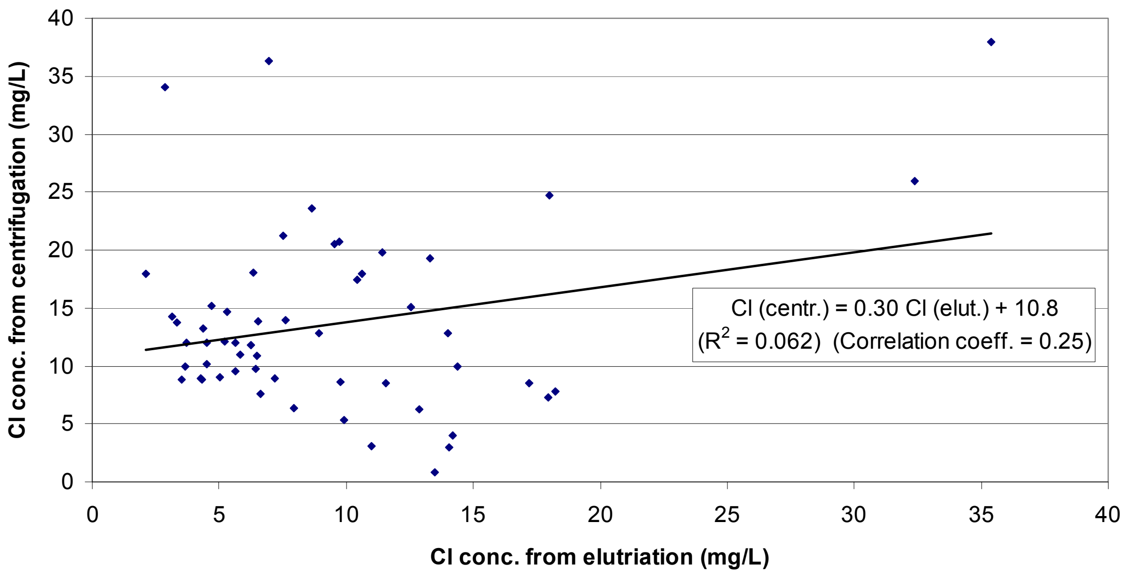

Figure 5-36 – Comparison of nitrate concentrations obtained from elutriation and centrifugation methods

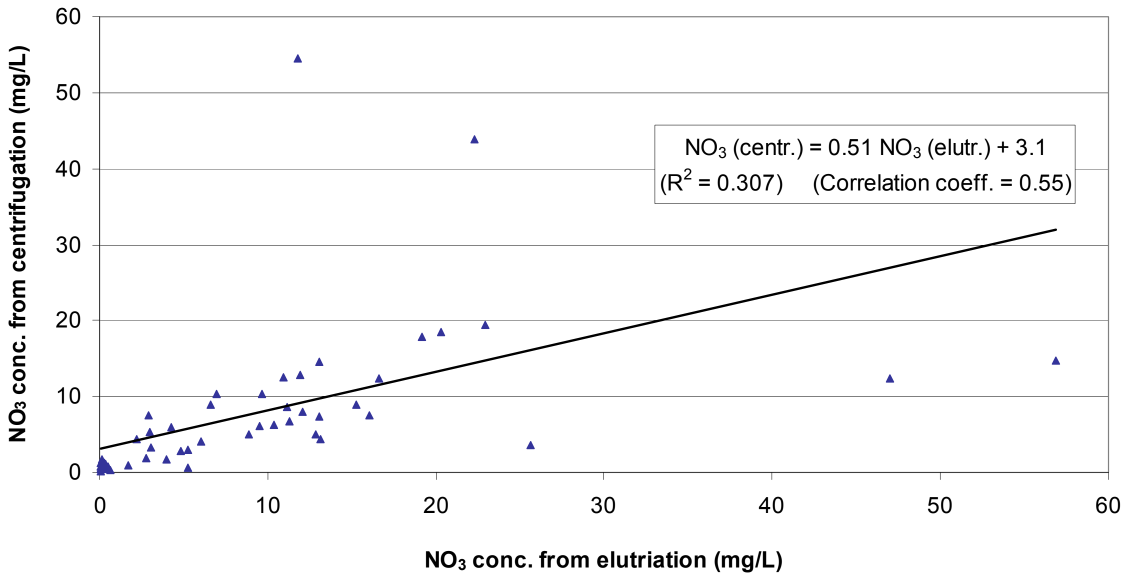

While this would suggest a larger error on centrifuged samples, potential errors on elutriated sample results were not properly assessed. For samples with a significant proportion of fine-grained sediments, the leaching ratio used in this study might not have allowed the maximum chloride extraction and thus, could potentially have introduced an error. However, one of the major drawbacks of the centrifugation method was that porewater could not be extracted by centrifugation for all samples since moisture content was too low or particle size too fine to allow significant recovery. For this reason and considering that duplicate values obtained by centrifugation were more variable (SD of 2.1 mg/L versus 0.9 mg/L for elutriation), results obtained from elutriation were used for recharge calculations. All further reference to Cl and NO_3 concentrations thus concern concentrations obtained from elutriation.

Two of the twelve profiles selected for interpretation are presented in Figure 5-37. The depth of the interpreted profiles ranges from 2.7 m to 6.6 m and the average Cl concentrations range from 5.4 to 38.7 mg/L for samples collected below the evapotranspirative zone. Some profiles reveal a high Cl concentration in this zone, which would likely be caused by enrichment of Cl by evapotranspiration (Sukhija *et al.*, 2003). Such a feature has also been associated to near surface mineralization that is released through elutriation (Gaye and Edmunds, 1996). As figure 5.37 shows, profiles can also exhibit relatively large fluctuations of Cl concentrations with depth. These probably reflect the combined effects of Cl concentration variations and of rainfall amount and intensity fluctuations in time.

Average NO_3 concentrations show much more variation, ranging from 1.1 to 78.5 mg/L. They however mimic Cl concentrations for most profiles and thus support the assumption of conservative behaviour of Cl. For some profiles, NO_3 concentrations however tend to decrease with depth, which could suggest a higher input of NO_3 in recent years. As there is no historic record of NO_3 concentrations in rain, it is however difficult to determine the origin of additional NO_3 input (i.e. rain, anthropogenic …). High NO_3 values can however be partly explained by nitrogen fixation by vegetation in soils (Edmunds *et al.*, 2002).

For the profiles considered here, average recharge values were estimated with equation 5.19 using weighted average Cl of the station closest to the profile. Results are summarized in Table 5-16 and calculation details are provided in Appendix D (USB flash drive). Annual rainfall values used for recharge estimation were extracted from the interpolated rainfall map (Figure 3.5, derived from the 1971-2007 rainfall dataset provided by the MSD) at each profile location. Assuming runoff is negligible, chloride concentrations in porewater would translate into an estimated recharge range of 1.1 % (12 mm) to 7.8 % (80 mm) of average annual rainfall at profile locations. Typically, recharge estimates would be slightly higher in the Precambrian basement (4.8 % or 47 mm) than in the VSB (3.7 % or 38 mm). While this could imply that the upper layer of the regolith in the Precambrian basement comprises more permeable material than in the VSB, additional and/or independent data with a much better spatial distribution would be required to support this assumption. The uncertainty related to average recharge estimates was evaluated through the standard deviation with the following equation:

$$SD\ R = R\sqrt{\left(\frac{SD\ P}{P}\right)^2 + \left(\frac{SD\ Cl_P}{Cl_P}\right)^2 + \left(\frac{SD\ Cl_W}{Cl_W}\right)^2} \qquad [5.21]$$

where the prefix *SD* denotes the standard deviation of a variable (e.g. *SD R* is the standard deviation of the recharge estimate (mm/year)), *R* is the recharge estimate (mm/year), *P* is the average annual rainfall (mm/year), Cl_P is the average Cl concentration in rainfall (mg/L) and Cl_W is the average porewater Cl concentration (mg/L). Resulting standard deviations are presented in Table 5-16. Average porewater chloride concentrations generally have the highest standard deviations, and would thus have a more significant influence of recharge estimates uncertainty. Other notable sources of uncertainty include the assumption that no run-on/runoff occurs at each site. While profiles were sited carefully to avoid areas characterized by high runoff, this assumption could induce an error in the order of the estimated runoff coefficient (i.e. 12.5 %).

Figure 5-37 – Selected unsaturated zone profiles showing moisture content, chloride and nitrate in porewater

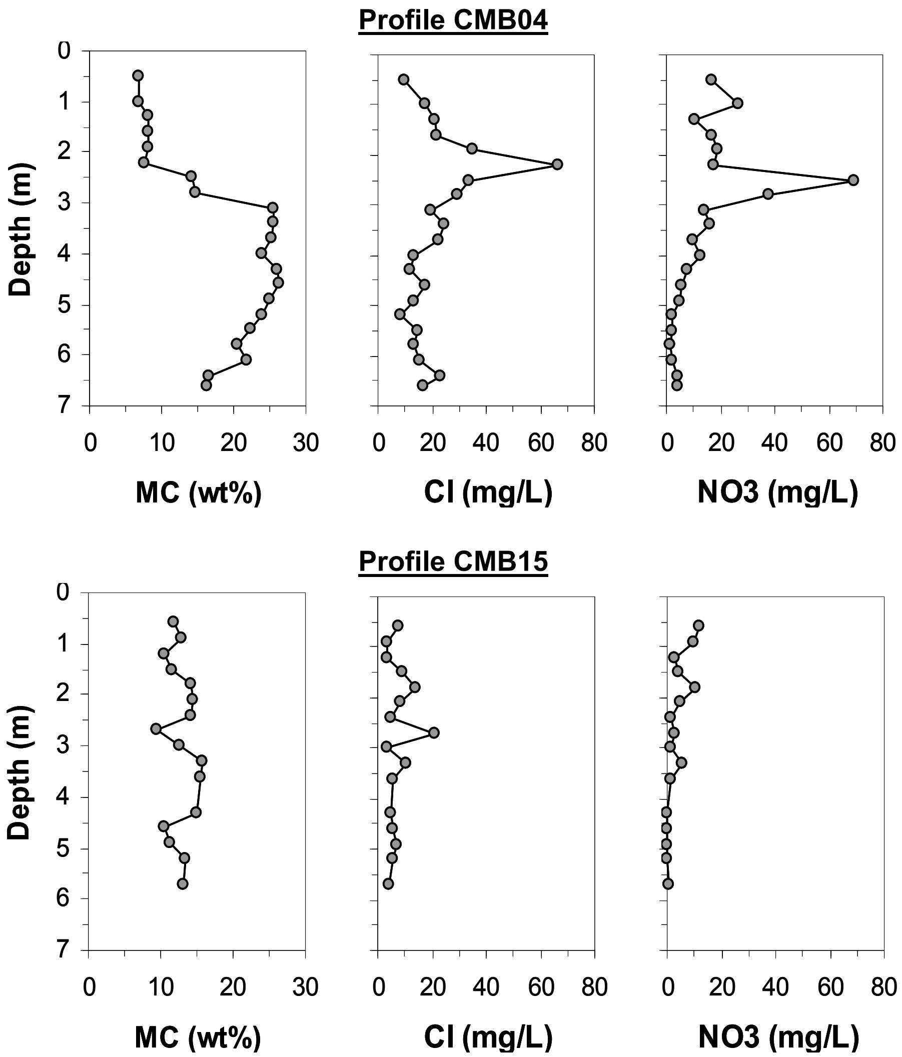

Table 5-16 – Summary results for recharge estimation from selected unsaturated zone profiles in northern Ghana

Profile ID	Hydrogeol. context	Predominant soil texture	Sampling date	Profile depth (m)	Weight. avg. Cl (mg/L)	Est. annual rainfall (mm)	Avg. porewater Cl (mg/L)	Est. annual recharge (mm and % of rainfall)
CMB01	Voltaian	N/A	2008-01-30	4.2	0.31 ± 0.05	1052 ± 173	9.9 ± 13.7	33 ± 46 (3.1 % ± 4.4)
CMB04	Voltaian	Sandy loam	2007-12-13	6.6	0.36 ± 0.05	1034 ± 157	16.6 ± 4.6	23 ± 8 (2.2 % ± 0.8)
CMB05	Voltaian	N/A	2008-02-07	4.8	0.36 ± 0.05	1002 ± 180	5.4 ± 0.8	68 ± 19 (6.8 % ± 1.9)
CMB07	Voltaian	N/A	2008-01-17	2.9	0.43 ± 0.06	1184 ± 183	14.2 ± 4.3	35 ± 13 (3 % ± 1.1)
CMB12	Voltaian	N/A	2008-01-09	3	0.55 ± 0.1	980 ± 184	20.4 ± 2.1	26 ± 7 (2.7 % ± 0.8)
CMB13	Voltaian	Silty/sandy loam	2008-01-10	3.9	0.55 ± 0.1	979 ± 176	13.3 ± 3.2	40 ± 14 (4.1 % ± 1.5)
CMB14	Precambrian	N/A	2008-02-10	2.7	0.55 ± 0.1	922 ± 154	11.1 ± 1.6	46 ± 13 (4.9 % ± 1.4)
CMB15	Precambrian	Loamy sand	2008-02-08	5.7	0.55 ± 0.1	938 ± 154	7.5 ± 4.9	69 ± 48 (7.3 % ± 5.2)
CMB16	Precambrian	N/A	2008-02-04	3	0.55 ± 0.1	974 ± 163	13.0 ± 5.6	41 ± 20 (4.2 % ± 2.1)
CMB17	Precambrian	N/A	2008-02-02	3.3	0.43 ± 0.09	1016 ± 162	5.5 ± 1.7	80 ± 33 (7.8 % ± 3.2)
CMB18	Precambrian	Loamy sand	2008-02-03	4.2	0.43 ± 0.09	1016 ± 172	12.2 ± 8.9	36 ± 28 (3.5 % ± 2.7)
CMB19	Precambrian	N/A	2008-02-01	2.7	0.43 ± 0.09	1052 ± 174	38.7 ± 6.1	12 ± 4 (1.1 % ± 0.3)

Note: the predominant soil texture was obtained from particle size analysis of selected samples.

5.3.3.3 Groundwater residence time estimation from unsaturated zone profiles

Groundwater residence time estimation and reconstruction of recharge history were carried out using the conventional CMB method, i.e. assuming (quasi-) steady state with constant chloride deposition and exclusively piston flow conditions in the unsaturated zone. As these assumptions may not be valid everywhere considering the extent and the variable conditions encountered in the study area, results from this exercise should be taken as first order estimates to be validated or revisited as new data become available. Principles underlying this exercise are only summarized below but are discussed more thoroughly in Cook *et al.* (1992), Scanlon (2000) and Ginn and Murphy (1997).

As chloride is considered an inert solute, it is assumed that variations in Cl concentration in the unsaturated zone, corresponding to recharge events, will persist as water and solutes move downward. However, depending on moisture content and recharge rates, only variations occurring over a large time scale will persist as diffusion in the unsaturated zone will reduce the original Cl concentration with time. For example, variations with a 5-year time scale would persist about 50 years with a minimum recharge rate of 20 mm/year. Thus, annual variations in recharge rates are not likely to persist. The residence time of groundwater at a given depth *z* in the profile can be calculated with the following equation, assuming that atmospheric chloride input remains constant (Edmunds *et al.*, 2002):

$$t = \frac{\int_0^z Cl_S(z)\,\theta(z)\,dz}{Cl_P P} \qquad [5.22]$$

where t is the groundwater residence time (year), P is the average annual rainfall (m/year), Cl_P is the average Cl concentration in rainfall (mg/m^3) and Cl_S is the average unsaturated zone Cl concentration (mg/m^3), θ is the volumetric moisture content (m^3/m^3) and z is the depth (m). The volumetric moisture content was estimated with the following relation:

$$\theta(z) = \frac{w(z)\,\rho_s\left(1-n\right)}{\rho_w} \qquad [5.23]$$

$$\text{with} \quad \rho_s = \frac{\rho_b - n\rho_w}{1-n} \qquad [5.24]$$

where is w the gravimetric moisture content (kg/kg), ρ_s is the density of solids (kg/m^3), n is the porosity (m^3/m^3), ρ_w is the density of water (kg/m^3) and ρ_b is the bulk density (kg/m^3). Porosity and bulk density were estimated from previous work in northern Ghana (Martin, 2006; Agyare, 2004) and in similar environments (Dethier and Lazarus, 2006; Kuma and Younger, 2001). The respective range of values used for both parameters are 0.35-0.45 m^3/m^3 and 1 500-1 900 kg/m^3.

The resulting residence times are presented in Table 5-17 and range from 6 to 60 years. They were used, with the average groundwater recharge estimated in the previous section, to model recharge history and compare it with available rainfall values. Both porosity and bulk density were allowed to vary in order to calibrate groundwater residence time with historical rainfall from the closest meteorological station (see calculation details in Appendix D). The porosity and bulk density values presented in Table 5-17 were mainly estimated on the basis of moisture content, soil texture and particle size distribution when available. Figure 5-38 presents the resulting recharge history for one selected unsaturated zone profiles (CMB04), excluding recharge values from recent years (corresponding to Cl in the assumed evapotranspirative zone). For comparison purposes with the recharge history, both the annual and moving 5-year average rainfall derived from the monthly rainfall dataset (1961-2005) are presented in Figure 5-38.

Table 5-17 – Summary results for groundwater residence time for selected unsaturated zone profiles in northern Ghana

Profile ID	Profile depth (m)	Avg. bulk density (kg/m^3)	Avg. porosity (-)	Avg. annual Cl mass deposited (mg/m^2y)	Est. annual recharge (mm)	Est. residence time (year)	Est. downward velocity (m/y)
CMB01	4.2	1 700	0.45	325.5	33.0	10.3	0.41
CMB04	6.6	1 500	0.45	377.2	22.8	60.3	0.11
CMB05	4.8	1 700	0.45	365.4	68.3	10.0	0.48
CMB07	2.9	1 575	0.45	504.7	35.4	9.3	0.31
CMB12	3	1 625	0.40	537.9	26.4	12.5	0.24
CMB13	3.9	1 600	0.40	537.3	40.5	14.4	0.27
CMB14	2.7	1 700	0.40	505.9	45.6	7.1	0.38
CMB15	5.7	1 550	0.45	515.1	69.0	10.9	0.52
CMB16	3	1 550	0.40	534.6	41.1	10.0	0.30
CMB17	3.3	1 750	0.40	436.2	79.6	6.0	0.55
CMB18	4.2	1 875	0.40	436.3	35.9	36.0	0.12
CMB19	2.7	1 900	0.35	451.7	11.7	31.1	0.09

While recharge peaks derived from Cl concentrations below the assumed evapotranspirative zone generally match the rainfall peaks relatively well, obvious discrepancies are observed in some profiles. The main sources of error that could originate from the assumptions or approximations made are summarized below:

- variable atmospheric Cl input in time
- presence of preferential pathways for groundwater recharge
- presence of soil texture heterogeneity
- sampling intervals too large
- inaccuracy of the rainfall record for profiles located at distance from stations

The relatively short period for which Cl concentrations in rainfall are available along with soil texture heterogeneity are likely to be the greatest sources of error.

Figure 5-38 – Historical estimated recharge and annual rainfall variations for selected unsaturated zone profiles

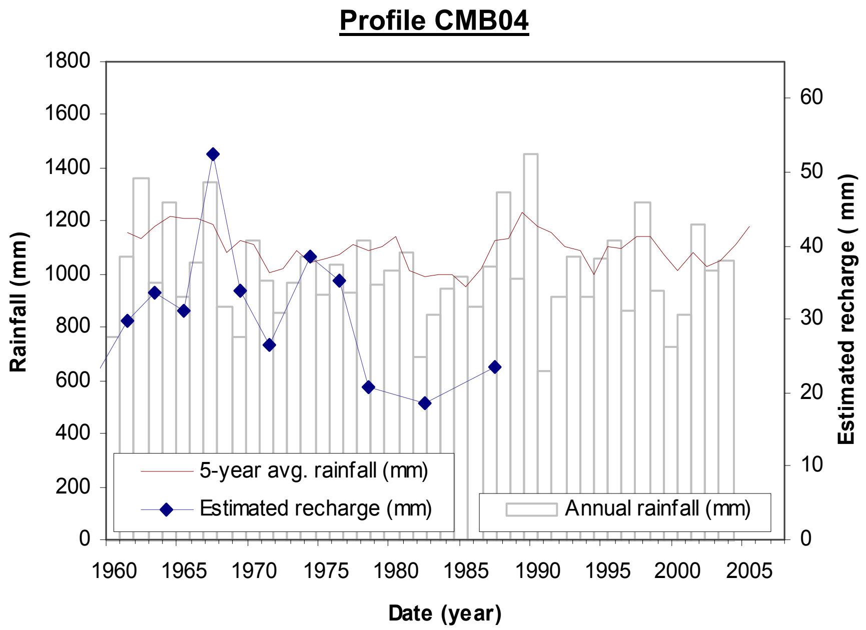

5.3.3.4 Recharge estimation from shallow groundwater samples

The saturated zone CMB, which was applied to samples collected from hand-dug wells, was selected as complementary method to provide recharge estimates integrating both diffuse and localized recharge but also information on the spatial variations in recharge rates over the study area. However, as the number of hand-dug wells sampled was lower than initially proposed (23 instead of 90), results were insufficient to carry out a representative evaluation of spatial variations of recharge. Consequently, recharge estimates obtained with this method were simply used to evaluate the reliability of estimates from the SMB and unsaturated zone CMB.

Chloride concentrations from the sampled hand-dug wells range from 1.2 to 87.5 mg/L with a median of 11.6 mg/L. The general spatial trend reveals increasing Cl concentrations from south to north. Nitrate concentrations, which show a similar trend, range from 1.3 to 101.7 mg/L with a median of 18.0 mg/L. The source of the high nitrate concentrations could not be identified with available information, although contamination of anthropogenic nature (e.g. fertilizers or inadequate sanitation facilities) is considered a likely cause. Higher concentrations could also be the result of groundwater evaporation from the well if it was unprotected and unused.

Recharge estimates were obtained with equation 5.19 using the weighted average chloride concentration of the nearest station and annual rainfall values extracted from the interpolated rainfall map (Figure 3.5, derived from the 1971-2007 rainfall dataset provided by the MSD) at each hand-dug well location. . Results are summarized in Table 5-18 and calculation details are provided in Appendix D (USB flash drive). As for the unsaturated zone CMB, runoff is assumed to be negligible. The resulting recharge estimates range from 0.5 % (5 mm) to 36.5 % (389 mm) of average annual rainfall with an average of 9.3 % (92 mm). As opposed to the unsaturated zone CMB results, recharge estimates are generally higher for wells located in the VSB (10.2 % or 101 mm) than for wells in the Precambrian basement (8.3 % or 82 mm).

Table 5-18 – Summary results for recharge estimation from shallow groundwater samples in northern Ghana

Well ID	Hydrogeol. context	Groundwater Cl conc. (mg/L)	Weighted avg. Cl in rain (mg/L)	Avg. annual rainfall (mm)	Estimated annual recharge (mm)
10113	Precambrian	9.0 ± 0.1	0.55 ± 0.1	940 ± 152	57 ± 14 (6.1 % ± 1.5)
10114	Precambrian	3.7 ± 0.1	0.55 ± 0.1	944 ± 155	140 ± 34 (14.8 % ± 3.6)
10115	Precambrian	3.4 ± 0.1	0.55 ± 0.1	941 ± 157	150 ± 37 (15.9 % ± 3.9)
10116	Precambrian	87.5 ± 0.1	0.55 ± 0.1	893 ± 148	6 ± 1 (0.6 % ± 0.2)
10117	Precambrian	4.3 ± 0.1	0.55 ± 0.1	926 ± 149	119 ± 29 (12.9 % ± 3.1)
10118	Precambrian	4.7 ± 0.1	0.43 ± 0.09	919 ± 175	84 ± 24 (9.1 % ± 2.6)
10119	Precambrian	14.5 ± 0.1	0.55 ± 0.1	990 ± 167	38 ± 9 (3.8 % ± 0.9)
10120	Precambrian	15.1 ± 0.1	0.43 ± 0.09	990 ± 163	28 ± 8 (2.8 % ± 0.8)
10121	Precambrian	11.6 ± 0.1	0.43 ± 0.09	1022 ± 156	38 ± 10 (3.7 % ± 1)
10122	Precambrian	2.2 ± 0.1	0.55 ± 0.1	925 ± 159	232 ± 59 (25.1 % ± 6.4)
10123	Precambrian	26 ± 0.1	0.55 ± 0.1	949 ± 162	20 ± 5 (2.1 % ± 0.5)
10124	Voltaian	12.7 ± 0.1	0.55 ± 0.1	985 ± 170	42 ± 11 (4.3 % ± 1.1)
10125	Voltaian	2.1 ± 0.1	0.55 ± 0.1	960 ± 172	247 ± 64 (25.7 % ± 6.6)
10126	Voltaian	12.5 ± 0.1	0.55 ± 0.1	983 ± 176	43 ± 11 (4.4 % ± 1.1)
10127	Voltaian	73.1 ± 0.1	0.36 ± 0.05	994 ± 177	5 ± 1 (0.5 % ± 0.1)
10128	Voltaian	10.9 ± 0.1	0.55 ± 0.1	997 ± 177	50 ± 13 (5 % ± 1.3)
10129	Voltaian	21.7 ± 0.1	0.36 ± 0.05	1043 ± 161	18 ± 4 (1.7 % ± 0.3)
10130	Voltaian	14.5 ± 0.1	0.43 ± 0.06	1185 ± 206	35 ± 8 (2.9 % ± 0.6)
10131	Voltaian	19.2 ± 0.1	0.43 ± 0.06	1056 ± 201	23 ± 5 (2.2 % ± 0.5)
10132	Voltaian	1.2 ± 0.1	0.43 ± 0.06	1066 ± 202	389 ± 97 (36.5 % ± 9.1)
10133	Voltaian	1.3 ± 0.1	0.36 ± 0.05	1014 ± 158	278 ± 61 (27.4 % ± 6)
10134	Voltaian	13.7 ± 0.1	0.36 ± 0.05	1045 ± 165	28 ± 6 (2.7 % ± 0.6)
10135	Voltaian	7.6 ± 0.1	0.36 ± 0.05	1124 ± 176	54 ± 11 (4.8 % ± 1)
Regional average		**16.2 ± 0.1**	**0.40 ± 0.07**	**995 ± 169**	**92 ± 23 (9.3 % ± 2.3)**

5.3.3.5 Comparison of results from SMB and CMB

For the study area, the estimated recharge for the unsaturated zone CMB method ranges from 12 mm to 80 mm while it is of 19 mm to 205 mm for the SMB and of 5 mm to 389 mm for the saturated CMB (Table 5-19). This compares relatively well with estimates from previous studies stated in Table 5-11. On average, recharges estimates from the saturated zone CMB are higher than those obtained with the other two methods. This could suggest that preferential recharge occurs in the project area (e.g. by infiltration under streams or in depressions where ponding can occur) and is not captured by the other two estimation methods. A potential indication of such preferential recharge could also be the changes in groundwater level observed shortly (i.e. ~ 2 months) after the recharge events indicated by the SMB (Fig. 5.29). Since the groundwater residence times through the unsaturated zone were estimated to be in the order of several years (Table 5-17), there should be no such response of groundwater level following recharge events if recharge were only diffuse through the unsaturated zone. Alternatively, higher saturated zone CMB estimates could be the result of anomalous or invalid Cl concentrations. Low chloride concentrations (i.e. < 2 mg/L) observed in some samples could notably have been diluted by recent rain events. Additional shallow groundwater samples with an improved spatial distribution would however be required to validate or invalidate these hypotheses.

It can also be observed that recharge estimates from the 12 unsaturated zone profiles considered for interpretation are lower than those obtained from the soil moisture balance. Average annual rainfall values used for the SMB (daily data for 2000-2005) are generally higher than the average annual rainfall values used for the CMB (monthly data for 1961-2005), which could partly explain the observed differences. For most of the meteorological stations inside the study area (Tamale, Bole, Navrongo, Wa), there is a relatively good correlation between recharges estimates from both SMB and unsaturated zone CMB methods, except for the Yendi station, where there is a significant difference. Discrepancies observed for these two methods could notably be caused by differences in spatial and temporal scales considered and uncertainties in the determination of parameters (e.g. input estimates for SMB or unsaturated CMB may not be as representative in Yendi as they are elsewhere).

According to Rushton *et al.* (2006), the SMB method would only be able to indicate if recharge occurs but would not provide precise numerical estimates. The SMB results are however helpful in analyzing the variability of recharge with respect to climate data. The method notably illustrated the importance of rainfall events distribution on the occurrence of recharge. Comparison of SMB results at Navrongo station with available WVB04 well hydrograph also showed that this method can predict the period of occurrence of recharge relatively well.

Supposing that all assumptions are verified for the unsaturated zone CMB, this method can provide more reliable and long term averages in comparison to the SMB method that was only applied to the 2000-2005 period in this study. This is supported by lower standard deviations associated to unsaturated zone CMB recharge estimates. However, the unsaturated zone CMB only accounts for diffuse recharge and does not consider localized or preferential recharge. Consequently, both these methods would underestimate overall recharge rates as SMB cannot account for localized recharge either (Lerner *et al.*, 1990). As stated previously, the saturated zone CMB was implemented to address this limitation, as it provides complementary estimates integrating both diffuse and localized recharge. However, even when supposing all assumptions are met, results from this method are considered insufficient in term of quantity and coverage to form a statistically representative dataset to be used for reliable comparison.

Despite the limitations of each method used, recharge estimates were interpolated to provide an overview of regional trends for northern Ghana. The interpolation was carried out by kriging using reliable estimates from the SMB (8 stations), the unsaturated zone CMB (12 profiles) and the saturated zone CMB (23 hand-dug wells). To complement these estimates in terms of spatial distribution, the saturated zone CMB method was also tentatively applied to groundwater samples collected from 97 boreholes as part of the groundwater geochemical characterization (Section 4.3.5). Matlab was used to interpolate values by ordinary kriging on a 5 km grid. Interpolated values were exported in ArcGIS for graphical representation. Figure 5-

39 shows the distribution of recharge estimates used for interpolation along with the resulting regional trend. As mentioned previously, interpolated values for such an exercise should be generally representative but they might not accurate locally. With that caveat, areas of lowest and highest estimated recharge are respectively located in the middle of the VSB (east of Tamale) and in the northeastern part of the PCB (southeast of Bawku).

Figure 5-39 – Distribution of groundwater recharge estimates from CMB and SMB

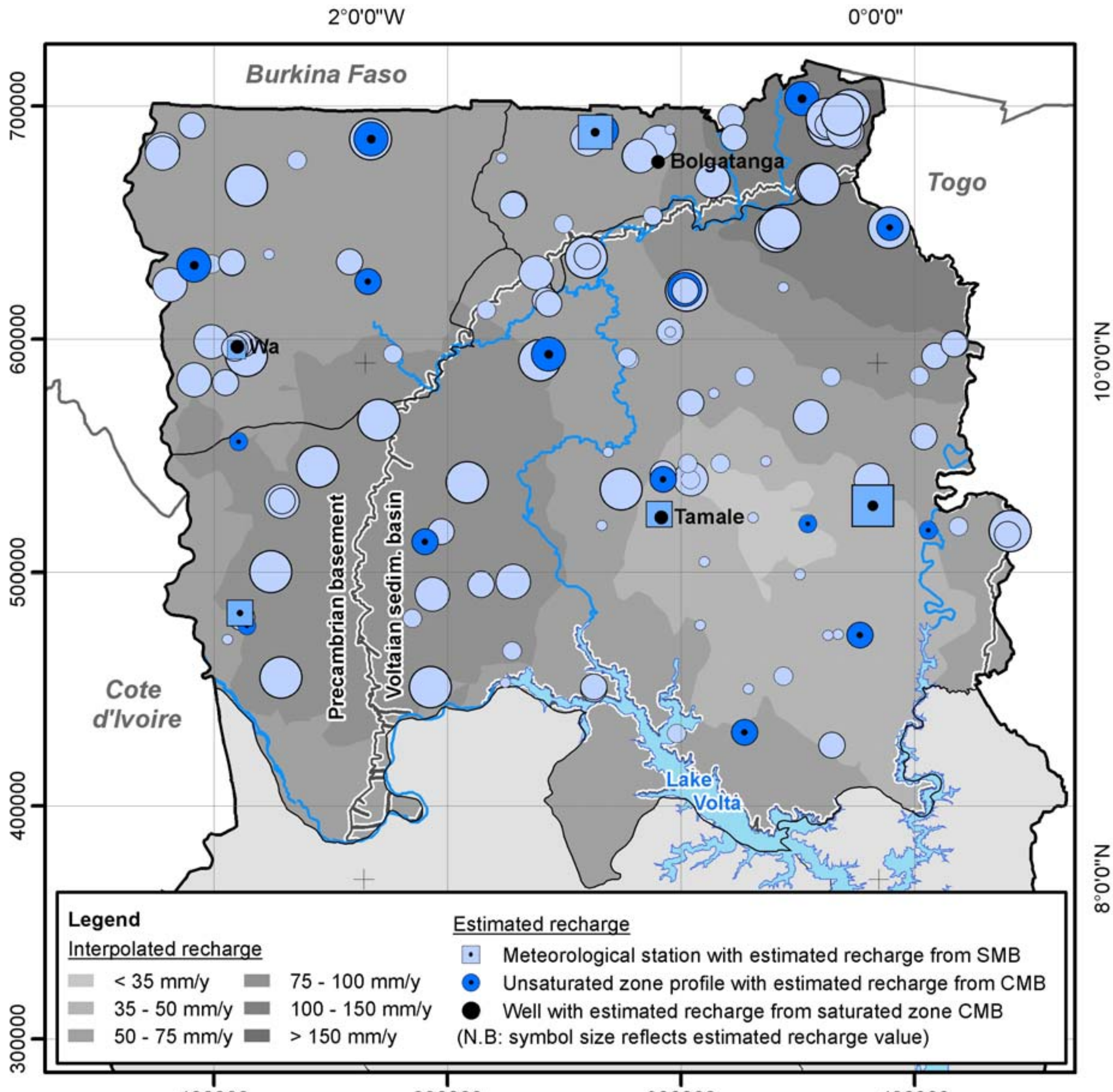

Table 5-19 – Groundwater recharge estimates obtained from CMB and SMB

Method	Avg. annual rainfall (mm)	Estimated groundwater recharge (mm and % of rainfall) ± standard deviation	
		Average	Range
Soil moisture balance	1 098 (1)	78 (6.8 %) ± 59	19-205 (1.8-15.9 %) ± 16-147
Chloride mass balance (UZ)	1 012 (2)	42 (4.2 %) ± 21	12-80 (1.1-7.8 %) ± 4-48
Chloride mass balance (SZ)	995 (2)	92 (9.3 %) ± 23	5-389 (0.5-36.5 %) ± 1-97

Notes:
(1) : Avg. annual rainfall values for the 5 meteo. stations in northern Ghana for 2000-2005
(2) : Avg. annual rainfall values extracted at 12 profile locations for 1971-2007

5.4 Groundwater geochemistry

Geochemical characteristics of groundwater are inherited from the various chemical, hydrological and, to a lesser extent, biological processes taking place along the groundwater flow path, from the recharge area to the sampling location (Hem, 1985; Appelo and Postma, 1993; Hounslow, 1995). The nature and physicochemical properties of the geological formations within which water flows and the transit time of water in them exert a major control over the solute and particulate content of groundwater. Depending on the nature of the rock mineralogy and Eh-pH conditions in the groundwater flow system, some chemical components of the rock matrix will dissolved into groundwater. As such, analysis of the geochemical characteristics of groundwater can assist in the development and validation of a conceptual model defining the hydrogeological and hydrogeochemical systems in northern Ghana, as well as for the understanding of groundwater recharge, storage and discharge processes. A geochemical characterization also has the benefit of highlighting the potential health risks and limitations of use of groundwater resources in the project area.

5.4.1 Overview of groundwater geochemistry

In semi-arid regions such as northern Ghana, major groundwater constituents originate mainly from chemical weathering of minerals during infiltration and flow through geological materials. Weathering is more intense in the unsaturated zone, where oxygen and carbon dioxide are generally more abundant. To a lesser extent, other processes in soils (e.g. adsorption and subsequent oxidation of gaseous compounds) can also affect the chemical composition of groundwater. A few elements such as chloride and iodine can also be deposited in small amounts by rainfall from the atmosphere (Larsson, 1984). Minor constituents such as heavy metals, metalloids or non-metals in trace concentration are also largely derived from weathering of minerals, although the proportion coming from the regolith is generally smaller than the one from unweathered bedrock (Apambire *et al.*, 1997). Aside from lithology, the relative proportion of groundwater constituents also depends on climate and aquifer characteristics.

As a consequence of the generally low recharge and high evapotranspiration prevailing in northern Ghana, solute concentrations are relatively high. In general, pH, total dissolved solids (TDS) and bicarbonate (HCO_3^-) increase with depth and with distance from recharge areas as a result of increasing residence time and reactions with minerals (Smedley, 1996). Weathering of primary minerals commonly produces ferric oxide, kaolinite, montmorillonite and, depending on solute content and conditions (pH, P_{CO2} …), calcium carbonate may also be formed. Previous geochemical studies in northern Ghana and other Ghanaian regions provide detailed assessments of geochemical processes (Acheampong and Hess, 1998; Kortatsi, 2007; Yidana, 2008, 2010, 2011; Anku *et al.*, 2009; Ahialey *et al.*, 2010). The analysis of the HAP geochemical characterization data is mostly qualitative. Besides chemical components, isotopic analyses of HAP geochemical samples for stable isotopes (^{2}H and ^{18}O) and radioactive ^{14}C also provided further insights on geochemical processes and groundwater residence time.

Groundwater in northern Ghana is generally of good chemical quality and thus suitable for drinking or other uses. Quality issues related to drinking water withdrawn from boreholes are however encountered in some areas of northern Ghana. In particular, high concentrations in fluoride, iron and manganese, and nitrate have been reported in several wells and boreholes. These high concentrations represent potential health hazards and may also restrain groundwater use for aesthetical reasons (i.e. color, odor and taste). Therefore, water quality issues must be considered and included in the planning process for long-term groundwater resource management.

5.4.2 Approach for geochemical data analysis and interpretation

5.4.2.1 Source of hydrogeochemical data

Development of the HAP consolidated database allowed the collection and compilation of existing geochemical data related to groundwater in northern Ghana. These data generally consist in analytical results from laboratory analysis of groundwater samples, although occasionally *in situ* field measurements also complement laboratory analyses. However, the spectrum of analytical results available for any given groundwater sample and sampling location varies considerably, due to the diversity of origins and intended groundwater collection purposes. In addition, reliability of existing geochemical data could generally not be fully assessed, although careful examination of the consistency of analytical results and metadata was carried out prior to data interpretation.

Only existing samples for which at least one result for either iron, manganese, chloride, nitrate or fluoride was available were considered to derive geochemical characteristics of groundwater and evaluate groundwater quality. Those parameters are the compounds most commonly found in groundwater for which the World Health Organization (WHO) specifies quality standards. Geochemical data from the most recently collected samples were the ones considered in instances where the same monitoring well or borehole had been sampled more than once. In total, 1659 existing entries from the database, each corresponding to a single groundwater sample and sampling location, were thus considered for geochemical data interpretation.

Analytical results from new samples collected under the three groundwater sampling campaigns carried out in the course of the HAP were also integrated into the database to be used along with existing data. These three sampling campaigns took place, respectively, in August-September 2010, January-February 2011 and April-May 2011. These results represent groundwater geochemistry data obtained from a total of 121 additional wells (97 boreholes and 24 hand-dug wells) . A full interpretation was only made of results from HAP's first monitoring campaign, encompassing 107 of these 121 wells, which were utilized in conjunction with the 1659 pre-HAP entries to assess groundwater geochemical characteristics and evolution. Since carbon isotopes (^{14}C and ^{13}C) analyses were only available for the second sampling campaign, ^{14}C and stable isotope (^{2}H and ^{18}O) data from this campaign were used, along with other geochemical data, to complete the geochemical interpretation.

5.4.2.2 Statistical analysis of hydrogeochemical data

Preliminary assessment of the geochemistry of groundwater in the project area consisted in the calculation of descriptive statistics related to concentrations of major ions. The chemical parameters selected were the following:

- Calcium, magnesium, sodium, potassium, chloride, bicarbonate and sulphate.

Occurrence of these ions and their concentrations were studied on the basis of three criteria: main geological contexts, geological groups and watersheds. Analytical results of groundwater samples were pooled in exclusive subsets, each corresponding to a sub-category of a given criteria, and descriptive statistics were calculated for each subset of data. Discriminative criteria and associated sub-categories were defined as follows:

- Geological contexts and groups: Precambrian basement (comprising Birimian Supergroup, Buem Structural Unit and Tarkwanian Group), intrusive rocks (comprising Eburnean Plutonic Suite, Mesozoic intrusives, Tamnean Plutonic Suite) and Voltaian sedimentary basin (comprising Kwahu-Morago, Obosum and Oti-Pendjari groups);
- Main surface water basins or watersheds: Black Volta, Lower Volta, Oti River and White Volta.

The average content, maximum and minimum concentrations, standard deviation and variance were estimated for these parameters from the database according to the related criteria. Limited statistical analysis was carried out on the data because several geochemical parameters had only a few available results in the field considered. The purpose of this exercise was to evaluate the typical content and range (distribution) in values for each chemical parameter within each group of analysis, and thus identify areas for additional investigation of potential groundwater quality issues.

More detailed descriptive statistics were prepared for parameters that can pose environmental or human health concerns: arsenic, fluoride, iron, manganese, lead, nitrates and nitrites. Details are provided in section 5.4.7.

5.4.2.3 Spatial analysis of hydrogeochemical data

Spatial distribution of an array of geochemical parameters was investigated earlier in the project through the production and/or updating of concentration maps. As new data were collected later in the project, this approach was refined by examining the groundwater evolution of major ions within the hydrogeological systems. A usual approach to study hydrogeochemical characteristics and groundwater evolution consists in the preparation of Piper trilinear diagrams (Piper, 1944).

A Piper diagram allows the representation of the content in major cations and anions as a percentage of several groundwater samples on a single graph. This type of diagram facilitates the identification of clusters or trends in water sample analyses (Hounslow, 1995; Güler *et al.*, 2002; Cloutier *et al.*, 2008). This diagram can also help identify a mixture of two different waters that will plot as a straight line joining the 2 end-members. Piper diagrams are also useful for the identification of hydrogeochemical facies. The latter are defined as distinct zones that have cation and anion concentrations describable within distinct compositions categories (Freeze and Cherry, 1979).

Piper diagrams were prepared for all geological contexts and groups for which sufficient data were available. Since the diagram represents the proportions of each major ion, an ionic balance was carried out on the geochemical data in order to verify the reliability of the analyses. Only reliable results with a satisfying ionic balance (i.e. 136 samples) were used in the preparation of the Piper diagrams. The interpretation of the Piper diagrams allows the development of conceptual geochemical models of the origin and evolution of the chemical species found in groundwater.

5.4.2.4 Evaluation of water quality

The quality of groundwater was evaluated for the purpose of the current study on the basis of WHO drinking-water recommended guideline values (WHO, 2008). However, since the quantity of parameters analyzed included in the database is limited, only critical chemical parameters were retained for comparison with WHO guideline values. These parameters are pH, electrical conductivity, arsenic, fluoride, iron, manganese, lead, copper, zinc, nitrates and nitrites. Insufficient microbiological data were available for interpretation. The relative impact of high concentrations within these geochemical parameters varies according to its use. Arsenic, fluoride, lead, nitrates and nitrites can represent major health hazards. Excess copper or zinc can also pose a significant threat to human health. Iron and manganese are typically aesthetical parameters limiting the use of groundwater.

5.4.3 Groundwater geochemical characteristics

As discussed in section 5.4.2, 1766 existing and newly collected samples were examined according to their location within the various geological groups and watersheds encountered in the project area. The analysis was carried out for geology only on data reported in the geological unit field included in the database; and for watershed only on data reported under the basin field. The chemical species examined in this section are the major cations and anions included in the database.

5.4.3.1 Geological contexts

The concentrations in major ions measured in groundwater samples from boreholes drilled in distinct geological contexts (Precambrian basement, Intrusive rocks and Voltaian sedimentary basin (or VSB)) were used for the estimation of descriptive statistics. Table 5-20 presents the results of the statistical analysis. As shown in the table, the quantity of analytical results available for each geochemical parameter is quite variable.

Preliminary assessment of the major ion content in groundwater displays some patterns in the data. Typically, average values for Ca, Mg, Na, Cl, HCO_3 and SO_4 are in the same order of magnitude in groundwater from the Precambrian basement and Intrusive rocks contexts, as opposed to average values in groundwater from the VSB context.

Na, Cl and SO_4 average concentrations are much higher in VSB groundwaters. On the contrary, Ca, Mg, and HCO_3 average concentrations are much lower. The K average concentration is slightly higher in the Intrusive rocks context. There is also a larger variability observed in the VSB data for Na, Cl and SO_4. Variability in HCO_3 is also greater in all contexts.

The primary explanation for these trends could be related to the composition of the parent rocks within the geological contexts. Indeed, the lithologies found in these contexts are expected to vary, and additional data are needed in order to validate this assumption. Consequently, it is assumed that a more detailed analysis is required at the level of geological groups in order to improve the identification of patterns and trends in the geochemical data relative to the geological contexts.

Table 5-20 – Descriptive statistics of major ions in groundwater within geol. contexts

	Ca	Na	Mg	K	Cl	HCO_3	SO_4
	mg/l	mg/l	mg/l	mg/l	mg/l	mg/l	mg/l
Precambrian basement							
number	50	46	49	39	395	39	257
average	**32.02**	**40.19**	**10.24**	**4.45**	**10.35**	**224.4**	**13.17**
maximum	113	117.8	33.5	10.5	187	450	668
minimum	0.52	1.21	0.56	0.11	0.01	2.67	0.00
standard deviation	19.40	26.35	8.20	2.98	20.10	90.94	48.47
variance	376.2	694.3	67.2	8.9	403.8	8270.6	2349.8
Intrusive rocks							
Number	52	50	50	40	335	40	235
Average	**33.15**	**39.49**	**7.42**	**11.88**	**6.88**	**211.57**	**9.88**
Maximum	65.81	100.6	28.2	84.4	98	451.4	169
Minimum	1.84	1.88	0.58	0.04	0.02	4.61	0.02
standard deviation	15.67	26.05	7.10	17.32	14.04	90.03	20.86
Variance	245.60	678.34	50.37	299.84	197.14	8105.20	434.97
Voltaian sedimentary basin							
number	216	179	215	181	750	181	593
average	**14.006**	**92.121**	**3.6424**	**3.757**	**135.3**	**133.01**	**21.808**
maximum	226	1513	108	95.9	26344	976	2496
minimum	0.16	0.27	0.038	0	0.003	0.32	0.021
standard deviation	28.26	210.65	9.26	10.36	1043.74	203.18	109.61
variance	798.5	44374.0	85.8	107.3	1089392.0	41283.0	12014.0

Note:
Fields of average concentrations for dominant cations and anions are highlighted.

5.4.3.2 Geological groups

The groundwater geochemical data were also examined in greater detail within the geological contexts according to some of the main geological groups included in the consolidated database. These geological groups are the Birimian Supergroup, Buem Structural Unit and Tarkwaian Group for the Precambrian basement; the Eburnean and Tamnean plutonic suites and Mesozoic intrusives for the Intrusive rocks; and the Kwahu-Morago, Obosum and Oti-Pendjari groups for the Voltaian sedimentary basin.

The descriptive statistics of major ions within each main geological group are presented in Table 5-21. Not all the geochemical parameters examined were available for analysis in each group (i.e. Buem and Tarkwaian), and the quantity of existing data also varied for each chemical parameter. Despite these limitations, some general observations and patterns can still be drawn on the basis of statistical results.

Table 5-21 – Descriptive statistics of major ions in groundwater within geol. groups

	Ca	Na	Mg	K	Cl	HCO_3	SO_4
	mg/l	mg/l	mg/l	mg/l	mg/l	mg/l	mg/l
PRECAMBRIAN BASEMENT							
Birimian Supergroup							
Number	50	46	49	39	375	39	241
Average	**32.02**	**40.19**	**10.24**	**4.45**	**10.35**	**224.40**	**12.76**
Maximum	113.00	117.80	33.50	10.50	187.00	450.00	668.00
Minimum	0.52	1.21	0.56	0.11	0.01	2.67	0.00
Standard deviation	19.40	26.35	8.20	2.98	20.46	90.94	49.90
Variance	376.2	694.3	67.2	8.9	418.8	8270.6	2489.5
Buem Structural Unit							
number	--	--	--	--	10	--	10
average	**--**	**--**	**--**	**--**	**10.16**	**--**	**28.3**
maximum	--	--	--	--	15	--	39
minimum	--	--	--	--	4	--	8
standard deviation	--	--	--	--	3.68	--	11.84
variance	--	--	--	--	13.5	--	140.2
Tarkwaian Group							
number	--	--	--	--	10	--	6
average	**--**	**--**	**--**	**--**	**10.37**	**--**	**4.38**
maximum	--	--	--	--	55	--	5.9
minimum	--	--	--	--	0.1	--	2.9
standard deviation	--	--	--	--	16.20	--	1.22
variance	--	--	--	--	262.5	--	1.5

Note:
Fields of average concentrations for dominant cations and anions are highlighted, when possible.
--: not available (insufficient data)

Table 5-21 – Descriptive statistics of major ions in groundwater within geological group (cont'd)

	Ca	Na	Mg	K	Cl	HCO_3	SO_4
	mg/l	mg/l	mg/l	mg/l	mg/l	mg/l	mg/l
INTRUSIVE ROCKS							
Eburnean plutonic suite							
Number	26	26	26	17	171	17	137
Average	**33.58**	**40.53**	**8.61**	**13.74**	**8.92**	**200.91**	**12.92**
Maximum	65.81	100.60	24.30	84.40	87.54	366	169
Minimum	1.84	1.88	0.76	0.04	0.02	4.61	0.02
Standard deviation	17.78	29.49	6.89	23.52	16.62	100.15	26.06
Variance	316.2	869.3	47.4	553.2	276.1	10031.0	679.1
Mesozoic intrusives							
number	2	2	2	2	4	2	2
average	**41.45**	**37.35**	**4.91**	**8.15**	**2.60**	**249.5**	**5.55**
maximum	55.77	38.9	4.93	10.3	3.6	292.8	9.82
minimum	27.14	35.8	4.88	6	1	206.2	1.28
standard deviation	20.25	2.19	0.03	3.04	1.19	61.24	6.04
variance	409.8	4.8	0.001	9.2	1.4	3749.8	36.4
Tamnean plutonic suite							
number	24	22	22	21	160	21	96
average	**32.00**	**38.46**	**6.25**	**10.73**	**4.80**	**216.60**	**5.62**
maximum	63.43	91.2	28.2	49.4	98	451.4	40
minimum	4.2	3.4	0.58	2.10	0.03	73.20	0.02
standard deviation	13.25	23.34	7.57	11.66	10.47	85.59	8.17
variance	175.5	544.8	57.3	136.0	109.6	7326.1	66.8

Note:
Fields of average concentrations for dominant cations and anions are highlighted, when possible.

The average values of each geochemical parameter are similar in all geological groups of the Precambrian basement and Intrusive rocks. In addition, the range of variability for any given ion within any given geological group and, from a geological group to the other, is small. The highest average HCO_3 concentration is recorded in Mesozoic intrusives, although differences with groundwaters of other groups of the Precambrian basement and Intrusive rocks are small.

Results of the chemical analyses in the VSB suggest that groundwater within the Obosum Group display higher average values in Na, Cl and SO_4; and a larger variability in these parameters as well for Ca and HCO_3. Groundwater in the Oti-Pendjari displays large concentrations in Cl and Na, although lower than those recorded in groundwater samples from the Obosum Group. Samples from the Oti-Pendjari Group also display lower average in Ca, Mg and HCO_3, in comparison with other groups. The results also indicate a large variability in Cl and HCO_3 concentrations.

Table 5-21 – Descriptive statistics of major ions in groundwater within geological group (cont'd)

	Ca	Na	Mg	K	Cl	HCO_3	SO_4
	mg/l	mg/l	mg/l	mg/l	mg/l	mg/l	mg/l
VOLTAIAN SEDIMENTARY BASIN							
Kwahu-Morago Group							
Number	24	24	24	24	101	24	83
Average	**10.93**	**37.83**	**3.87**	**3.02**	**34.67**	**125.63**	**15.24**
Maximum	40.1	320	28.3	16.6	1393	732	142
Minimum	0.24	0.27	0.05	0.04	0.003	1.80	0.11
Standard deviation	13.21	88.11	6.79	4.20	142.52	220.13	27.93
Variance	174.4	7762.6	46.1	17.68	20311	48458	780.3
Obosum Group							
number	63	48	62	49	141	49	118
average	**24.16**	**169.94**	**5.57**	**3.79**	**420.91**	**171.62**	**40.54**
maximum	226	1513	53.4	40.5	26344	603	2496
minimum	0.2	0.27	0.04	0.003	0.03	0.32	0.02
standard deviation	45.16	298.23	9.07	7.68	2297.2	186.07	230.51
variance	2039.4	88943	82.4	59.0	5276936	34622	53135
Oti-Pendjari Group							
number	129	107	129	108	508	108	392
average	**9.62**	**69.39**	**2.67**	**3.90**	**76.03**	**117.13**	**17.56**
maximum	65.80	1200	108	95.90	6165	976	450
minimum	0.16	0.31	0.04	0.00	0.01	0.44	0.02
standard deviation	15.82	171.65	9.65	12.25	346.42	206.28	44.65
variance	250.2	29462	93.1	150.1	120006	42551	1993.9

Note:
Fields of average concentrations for dominant cations and anions are highlighted, when possible.

5.4.3.3 Watersheds

Finally, groundwater chemistry was examined according to the regional watersheds present within the project area. The latter comprise the Black Volta, White Volta, Lower Volta and Oti River watersheds. Sufficient data were available for calculation of statistics for each watershed. The descriptive statistics of major ions within each watershed are presented in Table 5-22.

Groundwater in the Black Volta watershed presents high average concentration values in Mg, K and HCO_3 in comparison with the other watersheds. Large variability is also estimated in HCO_3 concentrations.

Results of the chemical analyses in the Lower Volta watershed suggest that groundwater displays typically higher averages in Ca, Na, Cl, HCO_3 and SO_4, and large variability in all these parameters.

Groundwater in the Oti River watershed presents typically lower average values in Ca, Na, K and HCO3 in comparison with other watersheds. Large variability in Mg and Cl is also observed in the data.

Groundwater in the White Volta watershed presents average values within the extreme values previously discussed. The parameters concerned are: Ca, Na, Cl, HCO_3 and SO_4. Large variability was also observed in the data.

The types of lithologies and the geological diversity found within a given watershed would act as major controls over the geochemistry of groundwater. The relationships between geology and the geochemical evolution of groundwater are investigated in the following section.

Table 5-22 – Descriptive statistics of major ions in groundwater within watersheds

	Ca	Na	Mg	K	Cl	HCO_3	SO_4
	mg/l	mg/l	mg/l	mg/l	mg/l	mg/l	mg/l
Black Volta River							
Number	58	57	58	44	355	44	239
Average	**29.32**	**60.02**	**11.26**	**5.30**	**11.44**	**284.42**	**13.59**
Maximum	63.30	380	33.50	25.10	187	976	668
Minimum	3.10	3.40	0.14	0.80	0.01	70.80	0.01
Standard deviation	14.66	82.73	8.85	4.36	21.94	195.78	46.23
Variance	215.0	6844.1	78.3	19.0	481.5	38329.2	2137.5
Lower Volta River							
number	25	23	24	63	133	24	96
average	**39.19**	**189.25**	**4.87**	**3.60**	**358.16**	**182.63**	**43.67**
maximum	226	849	21.9	32.8	26343.92	603	2496
minimum	0.4	0.709	0.165	0.008	0.03	0.721	0.069
standard deviation	53.50	221.95	5.97	6.51	2334.72	172.70	255.05
variance	2862.7	49263.1	35.6	42.4	5450911.6	29825.2	65048.5
Oti River							
number	41	40	42	40	325	40	240
average	**9.21**	**45.24**	**4.01**	**1.92**	**76.59**	**71.50**	**15.59**
maximum	57.10	929	108	13.6	6165	536.8	400
minimum	0.24	0.709	0.039	0.003	0.01	0.48	0.042
standard deviation	15.21	151.61	16.54	3.72	395.21	139.06	32.76
variance	231.4	878.0	273.6	13.8	156194.8	19338.4	1073.5
White Volta River							
number	193	155	190	152	667	152	510
average	**17.01**	**69.22**	**3.78**	**6.13**	**46.89**	**139.88**	**14.62**
maximum	216	1513	53.4	95.9	2897	927.2	450
minimum	0.16	0.27	0	0	0.003	0.32	0
standard deviation	24.51	187.90	6.08	14.23	242.57	169.74	40.28
variance	600.6	35304.8	37.0	202.4	58841.6	28813.2	1622.6

Note:
Fields of average concentrations for dominant cations and anions are highlighted, when possible.

5.4.4 Groundwater geochemical evolution

5.4.4.1 Major ions related to geological contexts and groups

Typical content in major ions in groundwater was assessed in the previous section on the basis of concentrations measured in groundwater samples collected from boreholes and wells located in distinct geological formations and watersheds. However, the estimation of the statistics for the major ions in groundwater only indicated general trends within the specific unit examined without any consideration to the location of the sample along the groundwater flow path. Isotopic analyses, discussed later in section 5.4.4.4, allow the assessment of geochemical patterns in groundwater related to groundwater dynamics and geochemical evolution in the project area. Prior to the discussion of isotopic data, but the definition of hydrogeochemical water types can be done to define the relationship between water types and geology (see following subsections). In the next section (5.4.4.2), the spatial distribution of these water types will be described. These descriptions of groundwater geochemistry will set the stage for an initial interpretation of the geochemical evolution of groundwater, which will be discussed in section 5.4.4.3. The variations in the groundwater major ions between geological units will be described using Piper diagrams (Piper, 1944).

As previously discussed in section 5.4.2.3, a single Piper diagram can present the proportions of major cations and anions of numerous groundwater samples. This representation facilitates the identification of clusters or patterns in water geochemistry. Such patterns can also indicate mixing between water types. Piper diagrams are also used for the determination of hydrogeochemical facies (Güler *et al.*, 2002; Cloutier *et al.*, 2008).

As opposed to the estimation of statistics, it was necessary to examine in details the chemical analysis results of each sample to prepare reliable Piper diagrams. Only complete chemical analysis results with an ionic balance, or electro-neutrality, lower than 10% (most of the samples were below 5%) have been retained for the preparation of the diagrams. This limit (10%) was decided with the objective of maximizing the number of data for each geological group, without compromising data quality and reliability. A total of 136 groundwater samples were considered on the basis of this criterion. Of this number, 91 samples were collected during the first geochemical characterization sampling phase of the HAP, in August-September 2010. Analytical results from 45 samples collected as part of other studies outside HAP were also included in the data set.

Results are presented hereafter in Figures 5-40 and 5-41 for each group of analysis, respectively geological groups and geological contexts. No distinction was made between the various units of the Birimian Supergroup due to the complex and heterogeneous nature of their spatial distributions, as well as the small number of sampling locations in some units. Also, as no samples with an electro-neutrality lower than 10% were available in the Tarkwaian Group and Buem Structural Unit, the Birimian Supergroup represents the only geological group within the geological context of the Precambrian basement.

The ellipses shown on the diagrams represent potential paths of groundwater evolution. The Piper diagrams have been prepared using the AquaChem 5.1® software packages formerly distributed by Waterloo Hydrogeologic Software (now Schlumberger Water Services, www.swstechnology.com).

Efforts to identify specific hydrogeochemical facies or evolution trends on the basis of location within given watersheds did not yield any conclusive results. Such efforts only highlighted the lithological control that the various geological units have on groundwater geochemistry. Geochemical differences between groundwaters of given watersheds seemed to essentially depend on the geological units found in different watersheds.

5.4.4.1.1 Birimian Supergroup

As seen from Figure 5-40, hydrogeochemical facies encountered in groundwater from wells located in the Birimian Supergroup are generally within the HCO_3 type. Dominating cations vary between Ca, Na and Mg, and cations assemblages correspond to “mixed cations” types, as they always include one or two of the former as secondary (and tertiary) cation(s). The Piper diagram for the Birimian Supergroup displays two distinctive evolution paths for groundwater. One consists in the gradual increase in the Na relative concentration, starting from an original Ca-Na-HCO_3 facies, which potentially corresponds to recharge water. Na enrichment occurs through dissolution of Na-feldspar and cation exchange reactions as water percolates and flows through the regolith and fractured rock. The second evolution path consists in the gradual increase in Mg relative concentration from the recharge water facies. This path could be associated with Fe-Mg-silicates weathering, which results in the dissolution of Mg ions in percolating/flowing groundwater. The relative proportion of Na or Mg cations is inferred to increases with the residence time of groundwater in the geological formations, as indicated by increased total dissolved solids. As such, it is an indication of the evolution stage of groundwater in the Birimian Supergroup.

The fact that most Mg water types correspond to groundwater sampled outside of the project framework could be related to the geological nature of the terrains covered by these previous sampling campaigns. These campaigns took place over a relatively limited domain exclusively located within the Northern region. It is possible that sampled groundwater were representative of only very specific rock type(s) and/or mineralogy. This is supported by the fact that all Mg-dominated water types were collected in locations underlain by metamorphic protoliths. Integrity of these samples prior to analysis and representativeness of the analytical results with respect to actual groundwater geochemistry may also be sub-par in comparison to HAP groundwater samples.

Figure 5-42 displays the spatial distribution of the various water types identified in sampled wells of the study area. It appears that a majority of groundwater samples exhibiting Ca dominated facies (Ca-Na-HCO_3, Ca-Mg-HCO_3, Ca-Na-Mg-HCO_3) were collected in wells positioned in relative proximity (< 5 km) to the upgradient boundary of the watershed or catchment within which they are located. This suggests that these groundwaters would represent a relatively early stage of geochemical evolution. As groundwater flows farther down gradient within the watershed and towards discharge areas, water geochemistry would be expected to shift towards Na and Mg dominated water types in areas underlain by Birimian formations.

Chloride is found as a secondary anion in a total of 4 groundwater samples. HCO_3-Cl water types would reflect a certain degree of groundwater evolution. These water types would emerge as the result of either mineral build-up under the effect of progressive evaporation or rock matrix-groundwater interactions. The relatively low electrical conductivity of most of these samples (between 311 and 655 µS/cm) however suggests a rather moderate evolution stage, and a proportionally short residence time for groundwater.

5.4.4.1.2 Eburnean Plutonic Suite

Similar to the Birimian Supergroup, hydrogeochemical facies characterizing groundwater in wells installed in Eburnean Plutonic Suite formations essentially correspond to the HCO_3 water type. A certain proportion of the samples collected also display an evolution towards the Cl end point. HCO_3 nevertheless remains the dominating anion in all but one instance. In terms of cations, groundwaters from the Eburnean Plutonic Suite display a mixed cations signature, with Ca and Na being either the dominating or secondary cation.

Groundwater evolution in the Eburnean Plutonic Suite formations appears to be following two major paths. One corresponds to a gradual enrichment in Na without any significant increase in Cl relative concentration, which would occur as the result of Na-feldspar weathering. Such an evolution would apparently be of a moderate extent, as maximal Na (+K) relative proportion remains lower than 70 %. The second evolution path corresponds to Na enrichment occurring concurrently with Cl enrichment. Total dissolved solids (TDS) concentrations generally undergo significant increase along this path, which would be the result of both evaporative processes and rock matrix-groundwater interactions. Both processes concur to generate groundwater composition where Na/Cl ratios generally tend towards 1. From a global standpoint, evolution of groundwater along the second path appears to reach higher stages, indicating a longer residence time for groundwater. No distinctive spatial pattern nevertheless arises in relation to this evolution trend. Some mixing of groundwater along the two major evolution paths would also occur.

5.4.4.1.3 Tamnean Plutonic Suite

Groundwater sampled from wells installed in Tamnean Plutonic Suite formations mainly correspond to the HCO_3 water type. Dominant hydrogeochemical facies are Ca-Na-HCO_3 and Na-Ca-HCO_3. Three groundwater samples also bear a significant proportion of Mg (between 20 and 60 %). Groundwater found in the Tamnean Plutonic Suite hence corresponds to the mixed cations water type.

Two evolution paths characterize groundwater from the Tamnean Plutonic Suite. The first one consists in Na-enrichment in response to Na-feldspar weathering and cation exchange along groundwater flow paths. The second one corresponds to Mg-enrichment in response to weathering of Fe/Mg-silicates. Low TDS and small relative proportions of Na or Mg indicate that the evolution stage of groundwater found in the Tamnean Plutonic Suite is generally early. Most sampled wells would thus be located in relative proximity to potential groundwater recharge zones. Flow paths and residence time of groundwater in Tamnean Plutonic Suite formations would hence be relatively short.

5.4.4.1.4 Mesozoic intrusives

Only two samples collected from wells installed in Mesozoic intrusives were available for hydrogeochemical facies analysis and determination. Both samples correspond to HCO_3 water type. One groundwater sample can be associated with Ca-Na-HCO_3 hydrogeochemical facies, while the other corresponds to Na-Ca-HCO_3 facies. Both samples fall within the mixed cations water type.

Relative proportions of Na versus Ca suggest that the sample exhibiting a Na-Ca-HCO_3 facies would have been subjected to certain enrichment in Na, which would have occurred in response to either Na-feldspar weathering or cations exchange reactions. Low TDS concentrations of both samples (< 200 mg/l) indicate that sample groundwater are at an early stage of evolution, and that sampled wells would be located in relative proximity to local recharge zones.

5.4.4.1.5 Kwahu-Morago Group

All groundwater samples collected from wells installed in Kwahu-Morago Group formations belong to the HCO_3 water type. Cations assemblages found in groundwater samples are quite diverse, highlighting a diversity of processes involving groundwater within formations of the geological group. Ca-HCO_3 and Ca-Na-HCO_3 facies would correspond to recharge waters or groundwater which has undergone very limited geochemical evolution, and hence small-scale flow. This is supported by the fact that most of these samples exhibit very low (< 50) TDS. K-Ca-HCO_3 facies corresponds to groundwater which has undergone a certain geochemical evolution, where K-feldspar weathering in sandstones contributed to enrichment in K. Only one sample however displays this geochemical pattern.

Two groundwater samples exhibit Na-HCO_3 facies. The sodic nature of these samples is related to relatively elevated TDS (> 350 mg/l), which suggests that groundwater of this type has undergone significant geochemical evolution. Na-feldspar weathering and cations exchange reactions contributed to enrichment in Na and near-complete substitution of Ca ions.

Wells where the two samples were collected lie at a long distance (> 10 km, measured along the corresponding flow line) from the up gradient boundary of their respective local-scale watersheds. This suggests an important distance from local recharge areas, which implies a long residence time for groundwater in the area.

Three groundwater samples display enrichment in Mg, corresponding to Mg-Ca-HCO_3 and Ca-Mg-Na-HCO_3 facies. The sample corresponding to Mg-Ca-HCO_3 facies originates from a well located in a direct down gradient position from terrains belonging to the Birimian Supergroup. Groundwater flows from Birimian formations to Kwahu-Morago Group formations. It likely already has an advanced level of evolution upon penetrating the latter formations. Groundwater geochemistry at this location is therefore indicative of processes taking place in Birimian formations, where Fe/Mg-silicate weathering would occur. Cations exchange reactions and, to a lesser extent, Fe/Mg-silicate weathering in sandstones of the Kwahu-Morago Group would be responsible for local-scale Mg enrichment in groundwater further away from Precambrian basement formations.

5.4.4.1.6 Obosum Group

Groundwater sampled from wells installed in Obosum Group formations display a wide variety of hydrogeochemical facies. With the exception of one sample, Na is the dominating cation in all groundwater samples. Groundwater of the Obosum Group is hence clearly sodic in nature, which reflects a relatively high degree of geochemical evolution. The dominating anion groundwater of the Obosum Group is HCO_3. However, a number of samples correspond to the Cl water type.

The most frequently encountered facies is Na-HCO_3. Na enrichment of groundwater is probably driven both by Na-feldspar weathering and cations exchange reactions within sandstones, mudstones and shale. Sustained exposure between rock and water, related to long residence time and significant distance from recharge areas, would allow groundwater to reach a high level of mineralization and geochemical evolution. Less frequently observed facies such as Na-Ca-HCO_3 would be indicative of a lower stage of evolution, shorter residence time and greater proximity with local recharge zones.

The second and third most frequently encountered facies are Na-Cl-HCO_3 and Na-Cl, respectively. An important proportion of groundwater flowing in Obosum Group formations evolves towards enrichment in Cl. This enrichment takes place either concurrently with enrichment in Na or in conjunction with the mixing of groundwater that is already enriched in Na. Increases in relative concentrations of Cl observed in the Obosum Group occur as groundwater reaches an advanced stage of evolution. Concurrent increases in TDS are observed as well. Very elevated TDS (> 1200 mg/l) are measured in groundwater samples of the Na-Cl facies. These samples exhibit Na/Cl ratio lower than 0.90, suggesting that processes such as reverse softening may be active in groundwater at the corresponding locations.

Cl concentrations reached in samples corresponding to facies Na-Cl-HCO_3 and Na-Cl reflect a very long residence time of groundwater in the geological formations. Evapotranspiration losses that occurred along the flow paths could be responsible for the increase in relative and absolute Cl concentrations in groundwater. Some diffusion of solutes from pore water may also be active in enriching groundwater in Cl (and Na). A certain number of these samples originate from wells located a great distance from up gradient watershed or catchment limits and potential recharge zones, which would imply long groundwater residence time and flow paths. A number of these samples were rather collected in wells located relatively close (< 5 km) to up gradient watershed or catchment limits, which suggests a shorter residence time for groundwater. As most of the wells displaying elevated Cl concentrations are located in cultivated areas, it is also possible that infiltration of water dedicated to livestock watering and irrigation contribute to local salinization of soils and groundwater, and concurrent increase in Cl.

SO_4 identified in relative proportions above 40 % in two samples could be related to contamination of well water from activities taking place at surface.

Figure 5-40 – Piper diagrams for the various geological groups studied

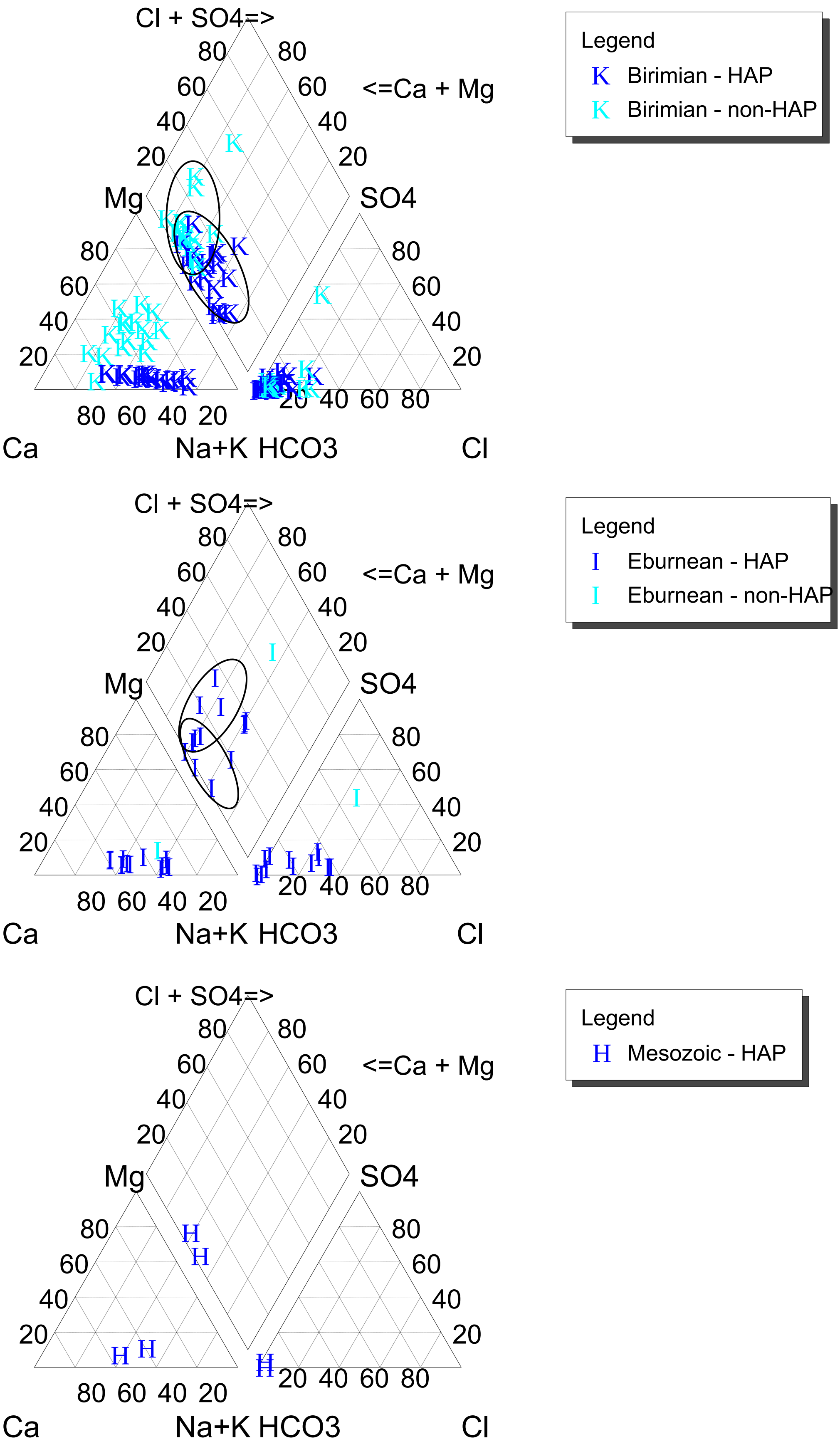

Figure 5-40 – Piper diagrams for the various geological groups studied (cont'd)

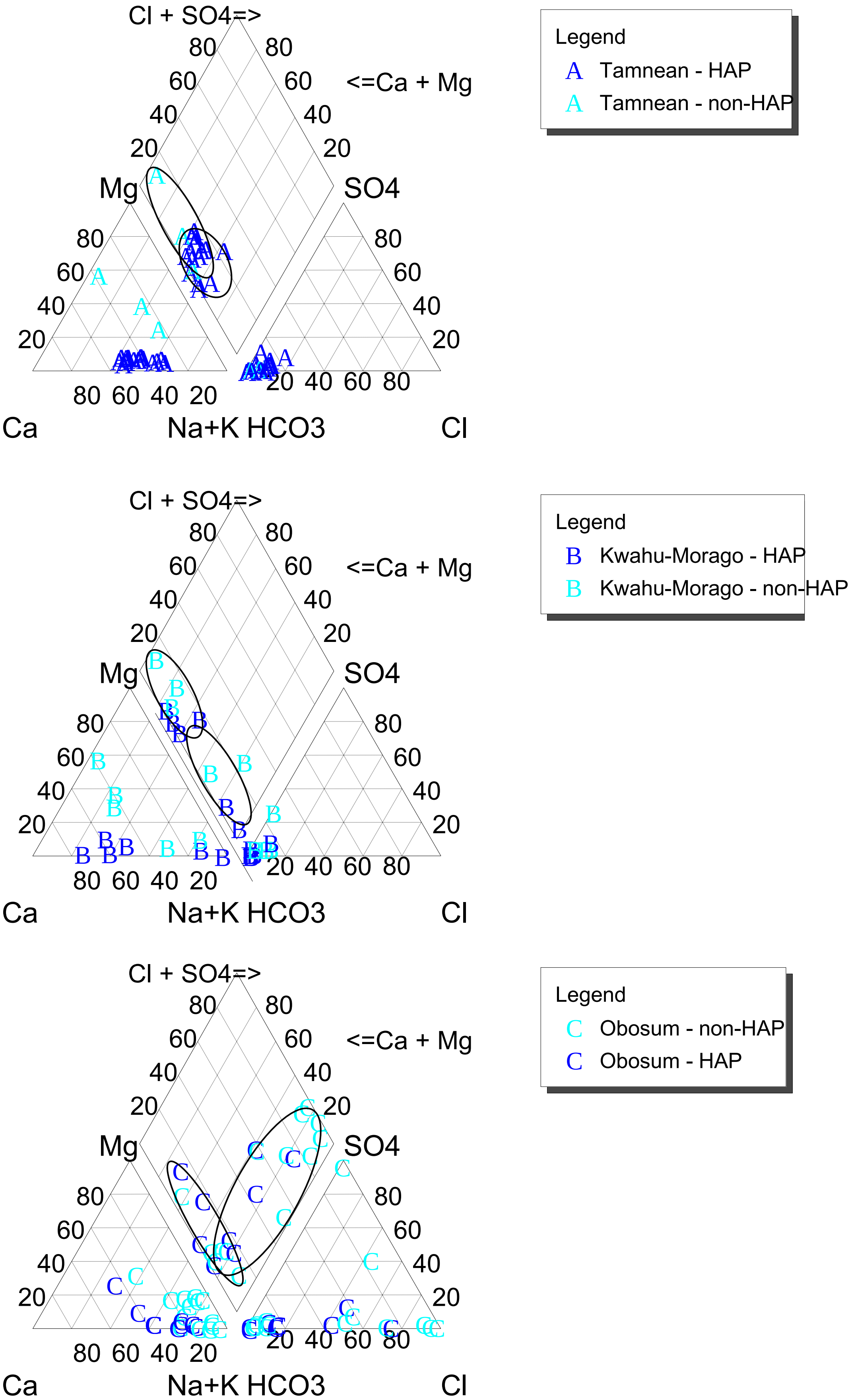

Figure 5-40 – Piper diagrams for the various geological groups studied (cont'd)

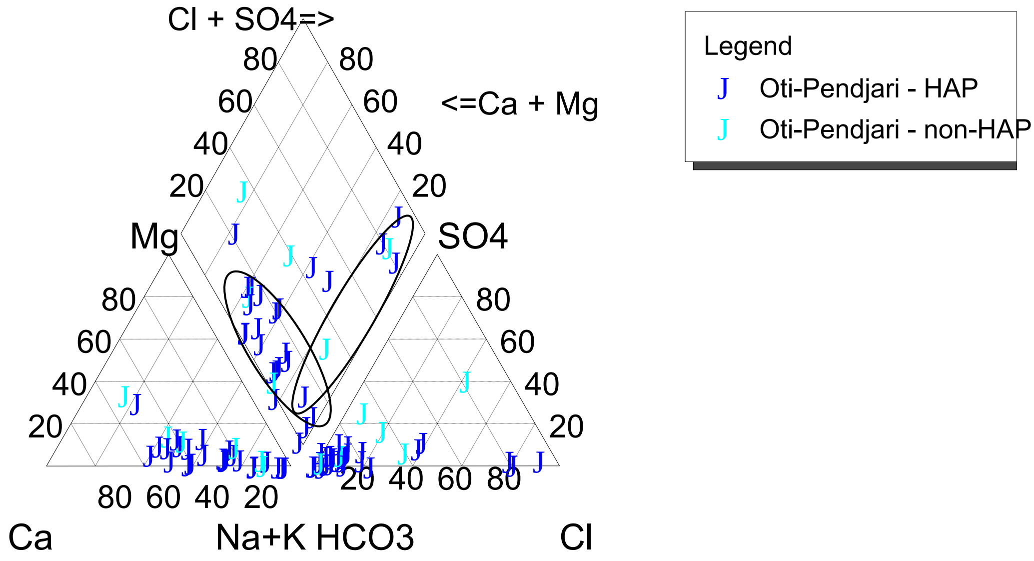

5.4.4.1.7 Oti-Pendjari Group

Groundwater sampled from wells installed in Oti-Pendjari Group formations generally corresponds to HCO_3 water type. Na is the dominating cation, which translates to sodic water type. Many samples include Ca as a secondary cation, while for some samples, Ca will be the dominating cation. K is also present in relative proportions above 20 % in four samples.

The most commonly found hydrogeochemical facies is Na-Ca-HCO_3, followed by Na-HCO_3. Ca-Na-HCO_3 facies also characterizes three groundwater samples collected from Oti-Pendjari Group formations. These various facies corresponds to intermediate, advanced and early groundwater evolution stages, respectively. They are essentially related to the intensity and extent of water mineralization as Na-feldspar weathering and cation exchange reactions at the rock matrix interface progressively modify the geochemical make-up of groundwater. The occurrence of K cations in groundwater together with Na would be related to weathering of K-feldspar.

Early stages of evolution would be indicative of short residence time of groundwater within the geological formations while advanced stages would correspond to long residence time. Similar to the other geological groups of the VSB, groundwaters corresponding to Na-HCO_3 facies are generally found in locations down gradient with respect to local groundwater, and in proximity with streams or rivers, which likely may act as discharge zones.

A second evolution path corresponds to the shift from HCO_3 water type to Cl water type. This pattern would reflect an even more advanced evolution stage for groundwater that may be subjected to evapotranspiration processes, which would result in the concentration of Cl anions in water. Three groundwater samples exhibit Na-Cl facies, which represents the ultimate stage of evolution in the VSB environment. Very high TDS (> 1300 mg/l) are recorded in these samples, emphasizing the significant level mineralization of this type of groundwater. Similar to locations where Na-HCO_3 waters are observed, Na-Cl type waters are confined to the low portions of local watersheds or catchments, near the ending points of local groundwater flow paths. Again, there is also a possibility that elevated Cl concentrations would be caused in part by the infiltration of water utilized for agricultural purposes. Groundwater samples exhibiting Na-Ca-HCO_3-Cl facies could be indicative of mixing between waters evolving towards the Na and Cl types respectively. SO_4 identified in relative proportions above 20 % in two samples could be related to contamination of well water from activities taking place at surface.

5.4.4.1.8 Intrusive rocks

Integration of Eburnean Plutonic Suite, Mesozoic Intrusives and Tamnean Plutonic Suite on a single Piper diagram is presented in Figure 5-41. A high level of concordance appears between dominant water types and hydrogeochemical facies of the Eburnean and Tamnean plutonic suites and Mesozoic Intrusives as well. This resemblance suggests that similar geochemical processes would be active in groundwater percolating through and flowing in the various geological units of this geological context

One of the main discrepancies concerns the occurrence of HCO_3-Cl water type in the Eburnean, while it is absent in the Tamnean Plutonic Suite (and Mesozoic Intrusives). This would indicate that Cl enrichment through evaporative processes and rock matrix-groundwater interactions is not a significant process in the geochemical evolution of groundwater in the Tamnean Plutonic Suite, and Mesozoic Intrusives. Explanations for this discrepancy could have a physiographic origin rather than a lithological origin, although no obvious pattern was identified in that regard.

Figure 5-41 – Piper diagrams for Intrusive rocks and VSB contexts

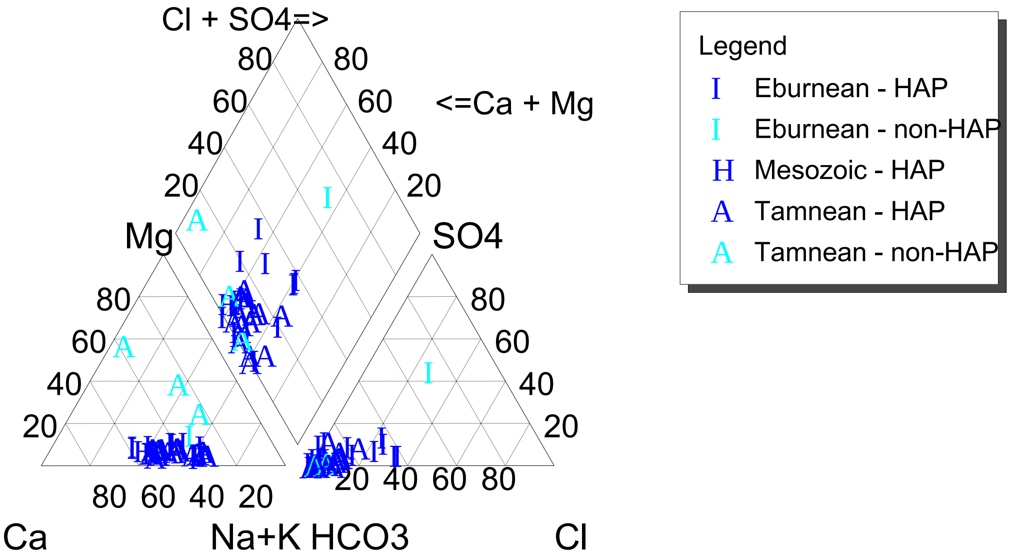

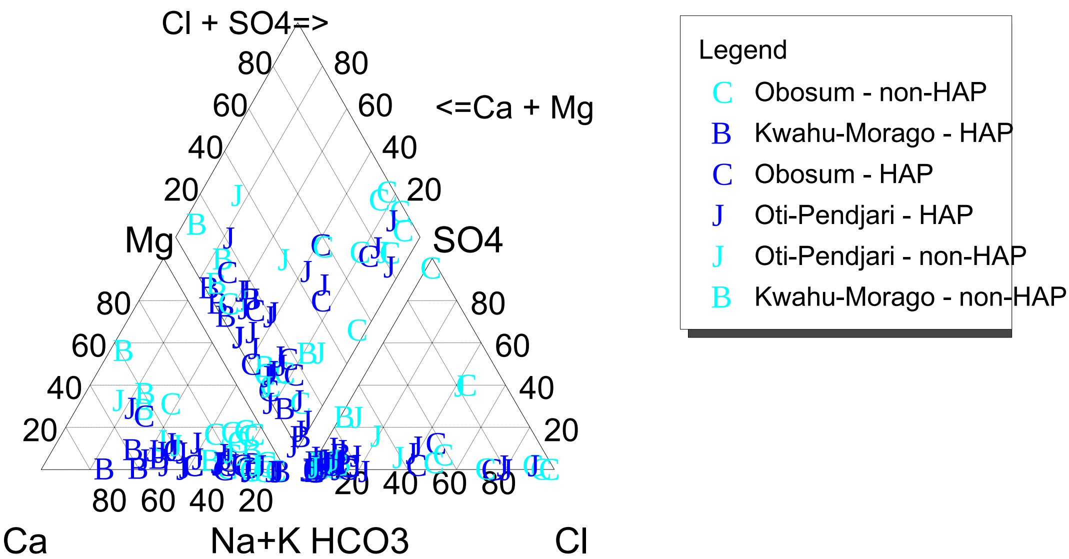

Another difference would be the enrichment in Mg of some groundwater samples from Eburnean Plutonic Suite, although no indication of such enrichment appears for any groundwater sample from the Tamnean Plutonic Suite or Mesozoic Intrusives. Active weathering of Fe/Mg-silicates, which is likely responsible for this enrichment, would thus be essentially limited to the Eburnean Plutonic Suite. Differences in the mineralogy of these various intrusive rocks could explain the existence or absence of this process.

5.4.4.1.9 Voltaian sedimentary basin

Comparison of water types and hydrogeochemical facies determined for groundwater samples from the Kwahu-Morago, Obosum and Oti-Pendjari groups also shows a high level of resemblance. Most of the same geochemical processes would be active in all three groups. One emerging difference is the absence of Cl enrichment processes in groundwater of the Kwahu-Morago Group. Comparison of geological and topographical data indicates that mean surface slope is generally greater in areas where the Kwahu-Morago Group is found, compared to areas of the Obosum or Oti-Pendjari groups. As piezometric surfaces generally mimic ground surface in the northern regions of Ghana, this means that higher hydraulic gradients would prevail, on average, in formations of the Kwahu-Morago Group. This would likely translate into shorter residence time for groundwater and hence, less advanced geochemical evolution. Impact of human activities on the geochemical make-up of groundwaters in the Obosum and Oti-Pendjari groups cannot be ruled out either.

Table 5-23 – Occurrence and spatial distribution of water types

Group	Water types	N (%)	Class	Spatial distribution	N (%)
Ca-Mg-HCO_3	Ca-HCO_3 Ca-Mg-HCO_3 Mg-Ca-HCO_3	7 (5.1 %)	Mixed cations and bicarbonate water types	Dominant in basement hydrogeological context	88 (64.7 %)
Ca-Mg-Na-HCO_3	Ca-Mg-Na-HCO_3 Mg-Ca-Na-HCO_3 Mg-Na-Ca-HCO_3 Ca-Na-Mg-HCO_3 Ca-Na-HCO_3 Ca-K-HCO_3 Ca-Na-K-HCO_3 Mg-Na-Ca-HCO_3 Mg-Na-HCO_3	37 (27.2 %)			
Na-Ca-Mg-HCO_3	Na-Ca-HCO_3 Na-Ca-Mg-HCO_3 Na-Mg-Ca-HCO_3 Na-Mg-HCO_3	44 (32.4 %)			
Na-HCO_3	Na-HCO_3 K-Na-HCO_3 K-Ca-HCO_3-CO_3	17 (12.5 %)	Sodium and bicarbonate water types	Only found in Voltaian hydrogeological context	17 (12.5 %)
Na-Ca-SO_4-Cl-HCO_3	Na-HCO_3-SO_4 Ca-Na-SO_4-HCO_3 Na-Ca-SO_4-Cl-HCO_3 Na-Ca-SO_4 Na-Cl-SO_4	7 (5.1 %)	Mixed cations and sulfate water types	Rare group mostly found in Voltaian hydrogeological context	7 (5.1 %)
Ca-Na-HCO_3-Cl	Ca-Mg-HCO_3-Cl Ca-Na-HCO_3-Cl Na-Ca-HCO_3-Cl Na-Ca-K-HCO_3-Cl Na-Ca-Mg-HCO_3-Cl	13 (9.6 %)	Sodium and chloride water types	Abundant in basement hydrogeological context (Na-Cl water type only found in Voltaian)	24 (17.6 %)
Na-Cl	Na-Ca-Cl-HCO_3 Na-Cl-HCO_3 Na-Cl	11 (8.1 %)			
	Total	**136 (100%)**			**136 (100%)**

5.4.4.2 Spatial distribution of water types

Table 5-23 summarizes the occurrence and spatial distribution of groups of water types related to the sampling points that are shown on Figure 5-42. Water facies (or types) are assembled into groups of similar geochemistry. These groups are listed in order of increased groundwater geochemical evolution, from Ca-HCO_3 facies to Na-Cl facies. Mixed cations and bicarbonate facies (groups 1, 2 and 3) are largely dominant, representing 65% of samples. As discussed in the previous section, these facies are dominant in the Precambrian basement geological groups (Figure 5-42). Sodium-dominated and chloride-dominated facies (groups 4 and 7) are only found in the Voltaian sedimentary basin geological groups, whereas facies with mixed cations and anions (groups 5 and 6) are both found in the PCB and VSB geological groups.

Figure 5-42 – Spatial distribution of groundwater geochemical facies groups

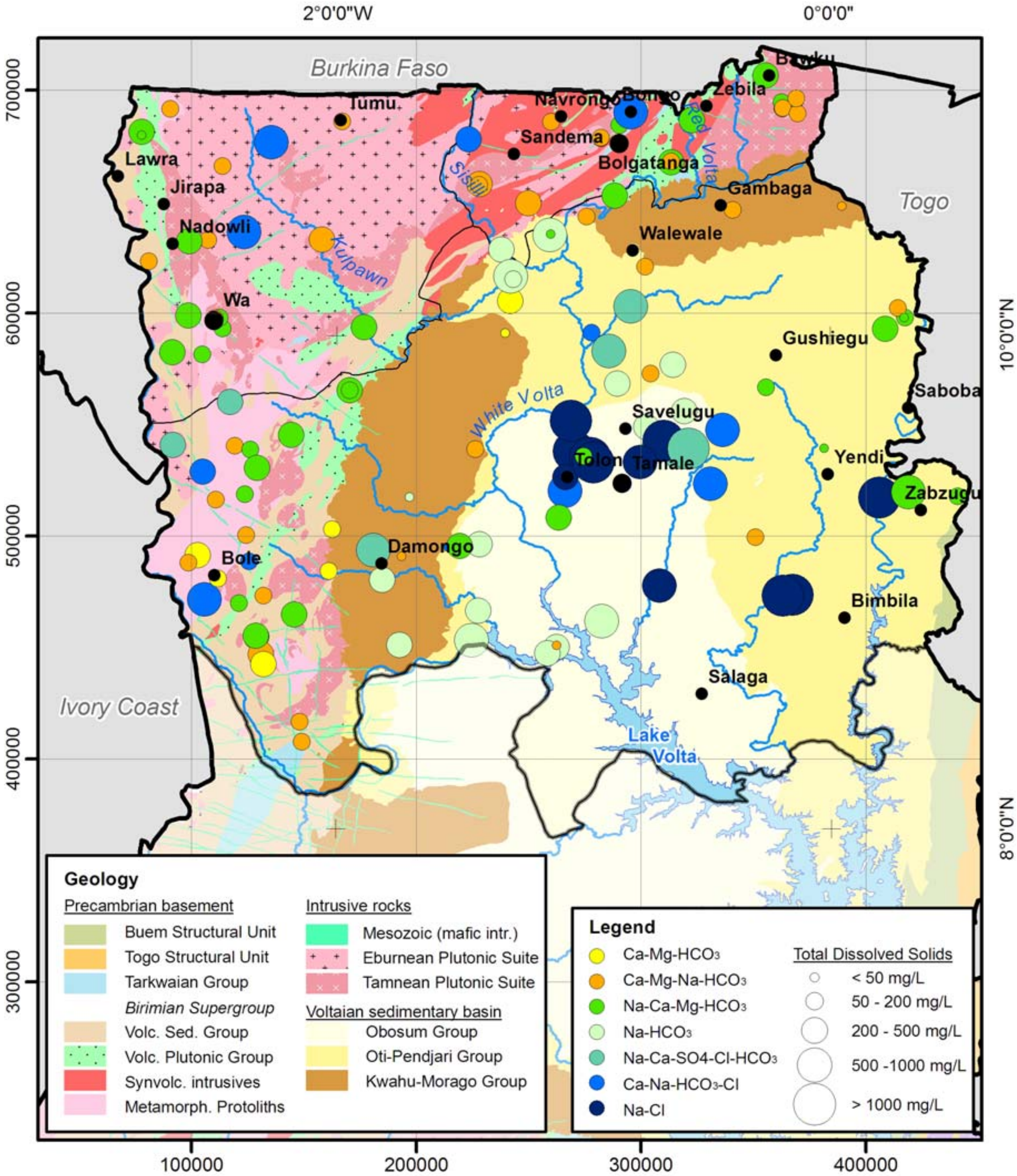

Similarly to the Piper diagram, Figure 5-43 is a Chadha diagram (Chadha, 1999) that provides a global overview of the relative proportions of cations and anions in groundwater found in the Precambrian basement and Voltaian sedimentary basin geological groups. As mentioned previously, although some of the geochemical facies are similar in the two hydrogeological contexts, sodium and chloride are more abundant in the Voltaian, which indicates more evolved groundwaters with longer residence times, as confirmed also by higher TDS.

Figure 5-43 – Proportions of cations and anions in Precambrian and Voltaian

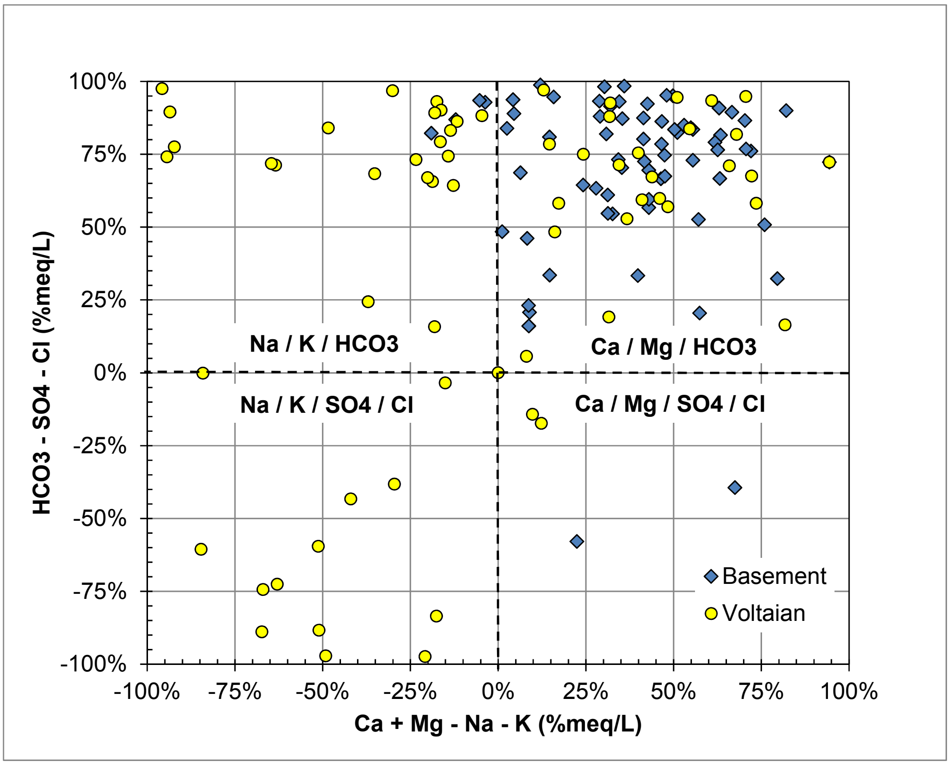

5.4.4.3 Major ions as indicative of geochemical processes

This section provides relationships among geochemical parameters supporting the geochemical processes indicated by trends of major ions on Piper diagrams. The following section 5.4.4.4 completes the interpretation of geochemical processes on the basis of isotopic analyses. The same high quality data set of 136 chemical analyses used in the previous section is also used in this section. The quality of these analyses was indicated by an imbalance of cations and anions lower than 10%. The coherence of this data set is also shown by the excellent fit between global geochemical parameters such as electrical conductivity and total dissolved solids (TDS) (Figure 5-44).

Figure 5-45 is a Gibbs diagram showing that most groundwater compositions can be related to processes of rock weathering. However, some data also plot along the evaporative trend, which may be an indication that more evolved groundwaters with higher TDS may have been subjected to evaporative processes. Section 5.4.4.4 provides stable isotope evidence of such evaporative processes.

Figure 5-44 – Correlation of electrical conductivity with total dissolved solids (TDS)

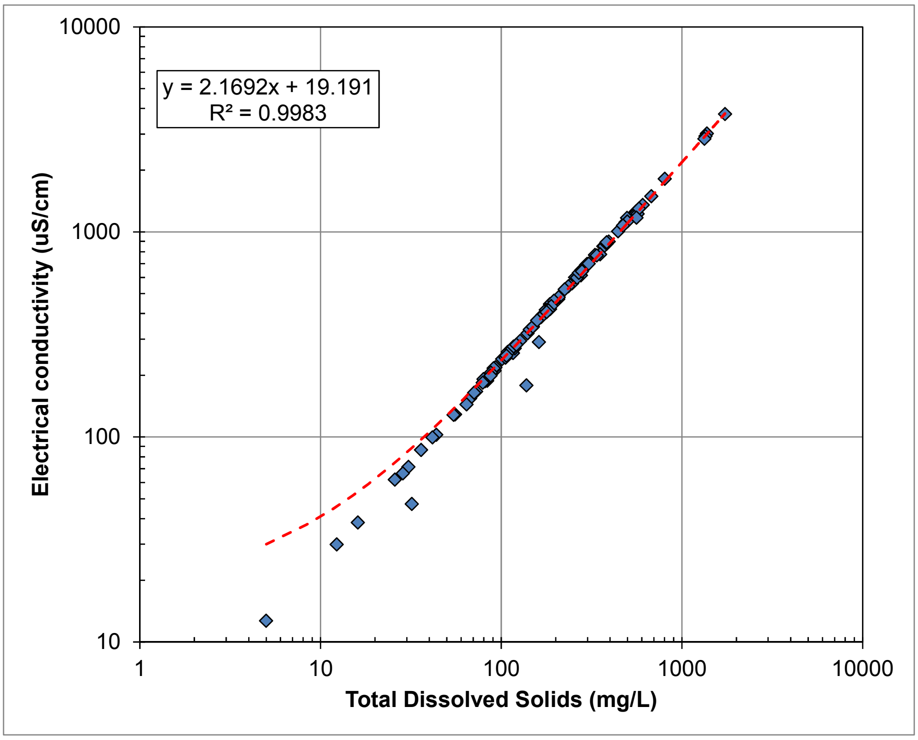

Figure 5-45 – Gibbs diagram (Gibbs, 1970)

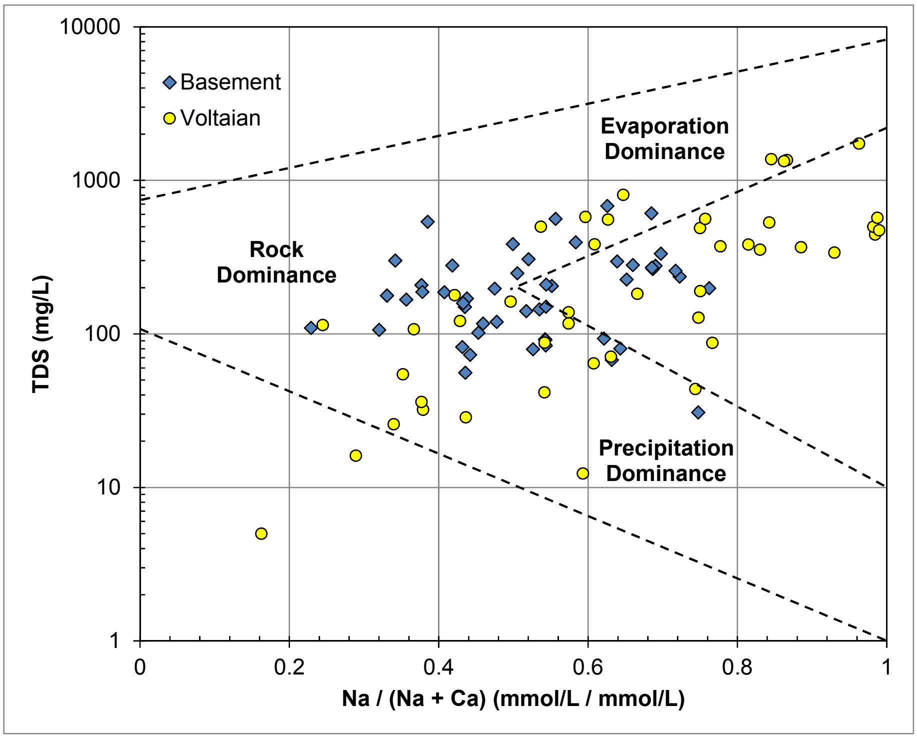

Besides indications provided by the Piper diagrams presented before, there are other strong indications of the importance of ion exchange on groundwater geochemistry. Figure 5-46 regroups four diagrams providing a comparison between the groundwater geochemistry of the Precambrian basement (PCB) compared to the Voltaian sedimentary basin (VSB) as well as indications of the effect of ion exchange. On the graph of Na vs Cl, the much higher concentrations of Na compared to Cl for most of the groundwater samples shows that most of the Na was acquired along groundwater flow paths without adding Cl. The higher proportion of Na in many of the VSB samples compared to the PCB provides further indications of greater evolution and residence times in the Voltaian. Even though most of the samples are higher than the 1:1 Na/Cl line, some of the highest concentrations of Na and Cl in the Voltaian do plot on the 1:1 line. This could be an indication that some of the Na-Cl waters found in that hydrogeological context also originate from halite dissolution. Similarly, on the graph of Ca+Mg vs HCO3+SO4, the higher proportion of HCO3 and SO4 compared to Ca and Mg (in meq/L) points out to the effect of ion exchange, which effect is especially strong in some Voltaian groundwaters. On the graph of the Na/Ca ratio vs TDS, the increase of the Na/Ca ratio as TDS increases provides strong evidence of the replacement of Ca by Na as groundwater evolves farther along flow paths (which corresponds to increased TDS). Finally, on the graph of pH vs Na, the increase in pH related to higher Na concentrations is a strong indication of ion exchange.

Besides the more evolved nature of groundwater found in the Voltaian context compared to the Basement (Figure 5-46), Figure 5-47 shows that these context impart quite distinct proportions of major cations to groundwater. The proportion of Mg compared to Ca is much higher in the Voltaian than the Precambrian. Likewise, evolved Voltaian groundwaters have much higher proportions of Na relative to K than what is found in the Basement context.

Figure 5-46 – Geochemical graphs providing indications of ion exchange

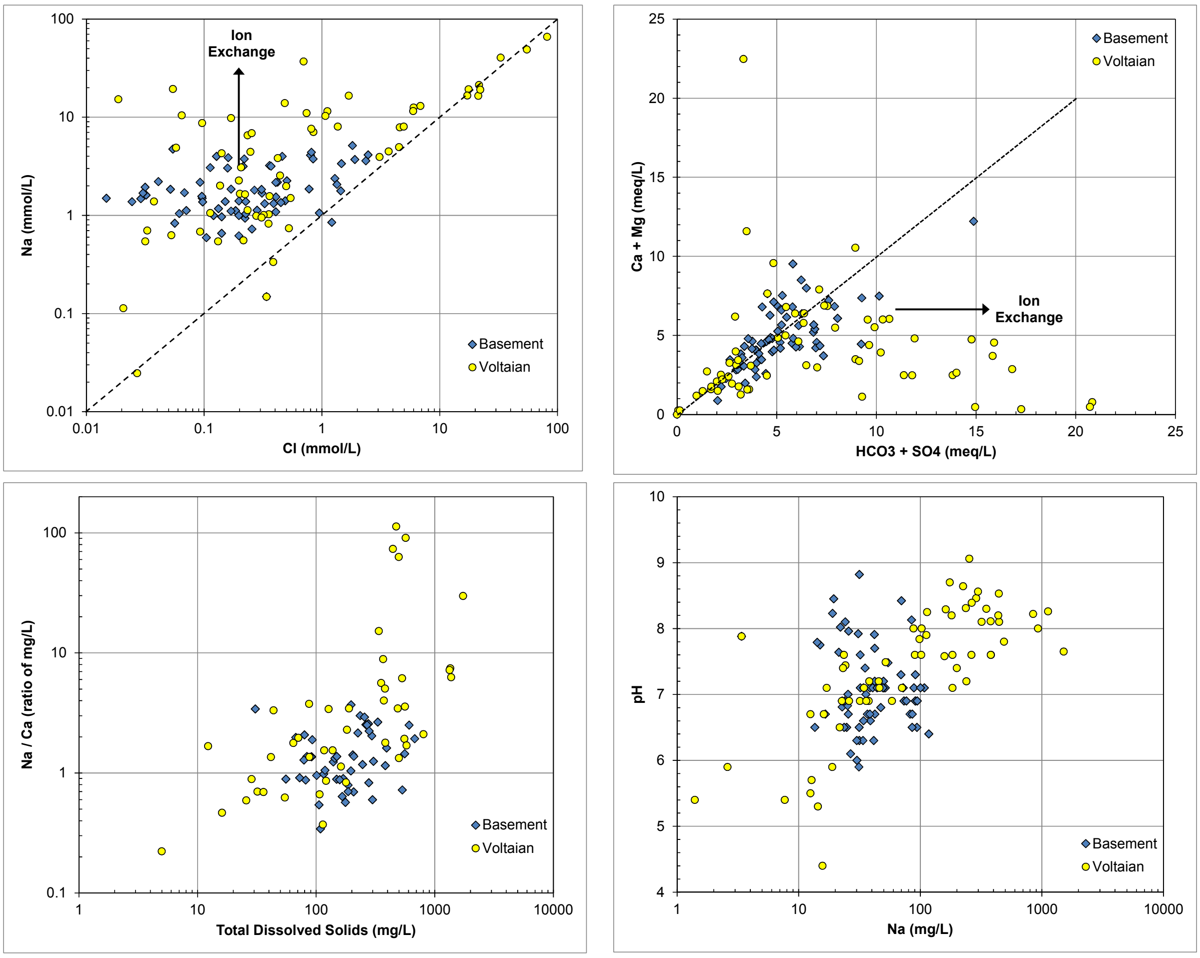

Figure 5-47 – Comparison of major cations in the Voltaian and Basement contexts

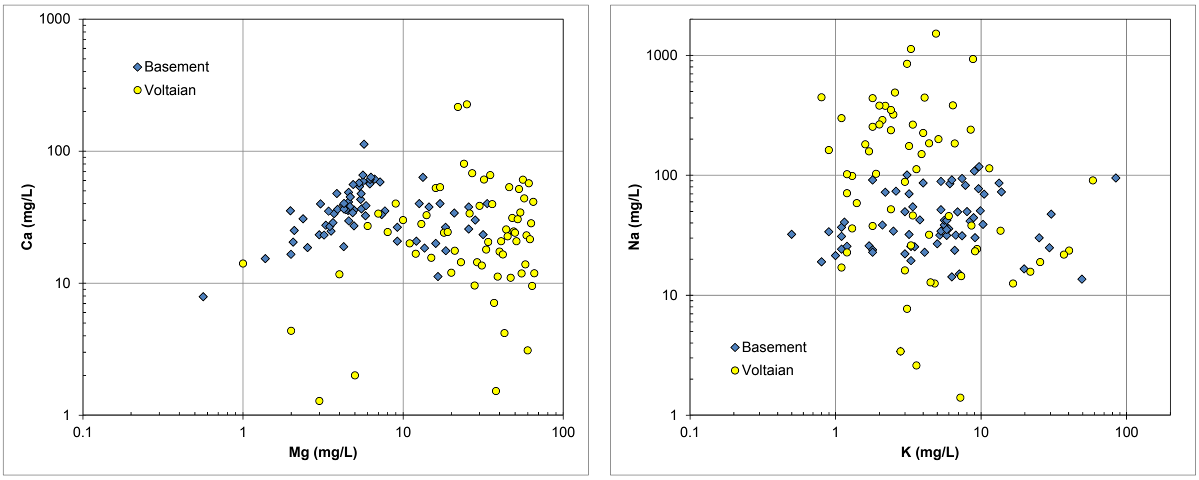

Figure 5-48 provides some insight on factors that may exert a control on the concentrations of two groundwater quality issues, nitrate (NO_3) and fluoride (F). Although WHO guideline for nitrate is 10 mg/L (N in NO_3), concentrations exceeding 1 mg/L are considered resulting from anthropogenic effect (i.e. exceed normal natural levels) and groundwater protection "actions" should normally be undertaken when concentrations rise above 3 mg/L, in order to avoid a degradation up to the WHO guideline. Both for the Voltaian and Basement contexts, N in NO_3 concentrations above 1 mg/L are found over a wide range of TDS values, showing that human impact on groundwater quality can occur over wide ranging groundwater conditions. However, the larger concentrations were found in the Basement context.

In the case of fluoride (F), Figure 5-48 shows that concentrations exceeding the WHO guideline are only found in groundwater having relatively high TDS (above 100 mg/L), which is both the case for high F in Voltaian or Basement contexts. So, high F concentrations are mostly a concern for evolved groundwaters, especially water types 3, 4, 5, 6 and 7.

Figure 5-48 – Concentrations of NO_3 and F versus TDS

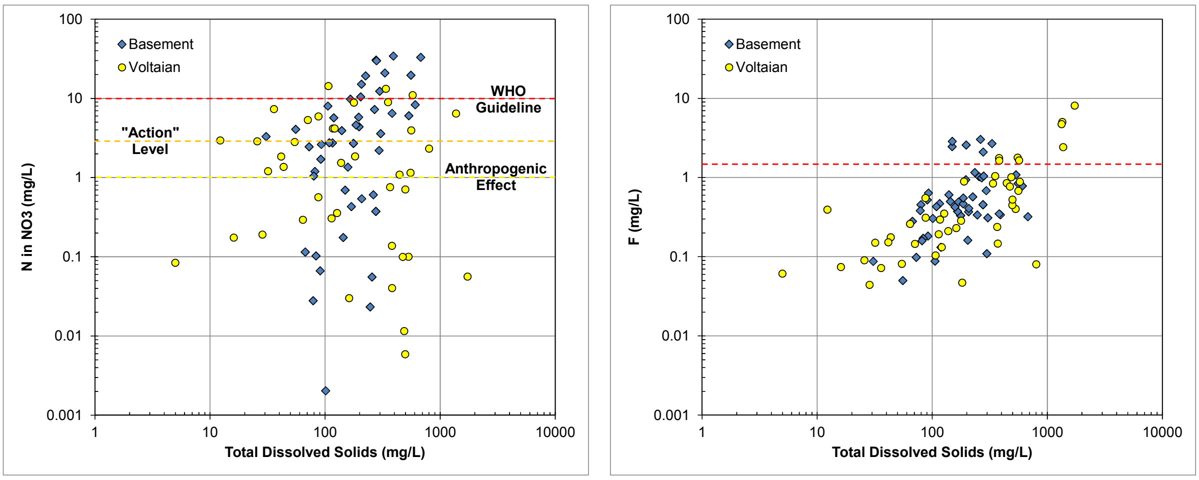

5.4.4.4 ^{14}C and stable isotopes as indicative of geochemical processes

This section documents the interpretation of isotopic analyses that were used to provide further indications on the geochemical processes identified in the previous section on the basis of major ions (Piper diagrams). Furthermore, isotopic analyses can also provide clues about the dynamics of groundwater flow in the northern regions of Ghana. The previous section used data from the first HAP groundwater sampling campaign, whereas this section uses data from the second sampling campaign for which carbon (^{14}C and ^{13}C) and stable (^{2}H and ^{18}O) isotopes were available. In order to relate the interpretation of isotopic analyses to results of the previous section on major elements, water types were reassigned to all samples of the second HAP sampling campaign. In most cases the water types were the same as for the first sampling campaign, with some switches in dominant cations (mostly Ca or Na) compared to the previous sampling campaign, and more rarely a switch in dominant anions (mostly HCO_3 and Cl). The interpretation thus focuses on determining the isotopic signature of water types as well as the major geological contexts of northern Ghana (Basement and Voltaian). To avoid duplication with the previous section, this section is restricted to the additional understanding obtained from the interpretation of isotopic data, compared to the interpretation geochemical processes on the basis of major ions (Piper diagram) and water types.

Figure 5-49 shows stable isotope data in groundwater that are available from 121 samples for the second HAP sampling campaign. The graph distinguishes samples from the Basement and Voltaian geological contexts. Groundwater data are compared to rainfall analyses from the Bobo-Dioulasso station (southwest Burkina Faso) that were obtained from the IAEA (2006) web site. These data were used to obtain a Bobo-Dioulasso meteoric water line (BMWL) that is considered representative of northern Ghana. The BMWL derived is quite similar to the one obtained by Dakoure (2003) who analyzed the rain stable isotope data in more details. Figure 5-49 focuses on the groundwater data and does not show all available rainfall points. The full range of ^{2}H and ^{18}O values in rain is wider and from about -60 to 20 for ^{2}H and -8 to 1 for ^{18}O. Groundwater stable isotope values occupy the central part of the range of rainfall data points.

There is an overlap of stable isotope for samples from the Basement and Voltaian contexts. A broader range of recharge conditions appears for Voltaian groundwater samples. The spreading of these points along the BMWL indicates that groundwater originates from the mixing of precipitation initially having a relatively wide range of isotopic values. This could be an indication that recharge events can occur under varied conditions (temperature) or seasons. Besides mixing, there is another trend away from the BMWL that could be related to evaporation (indicated by dashed lines). Samples from the Basement context appear more clearly influenced by evaporation than samples from the Voltaian context.

Figure 5-49 – Stable isotopes in rainfall and groundwater

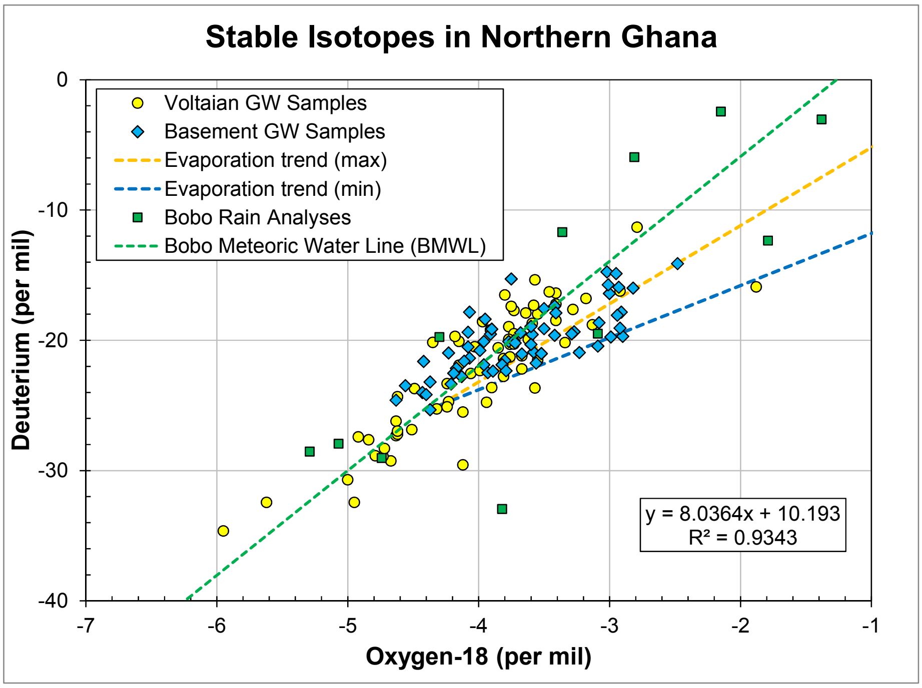

Even though groundwater stable isotopes from the Basement and Voltaian contexts overlap, some Voltaian samples have a wider negative extension than Basement samples. Figure 5-50 shows that Voltaian and Basement samples were collected from areas with distinct topographies, the Basement wells being located at higher elevations than Voltaian wells. ^{2}H data show a distribution that is quite similar to the one of ^{18}O presented on Figure 5-50. Voltaian isotopic data also appear to be influenced by topographic elevation, whereas the Basement data show no correlation. This effect may reflect a difference in the actual isotopic signature of precipitation in the low-lying central areas of the Voltaian Basin compared to its generally higher periphery. The lower part of Figure 5-50 shows that the distinct distribution of Voltaian and Basement stable isotope signature has remained similar over the entire range of groundwater ages found in northern Ghana. Even though the temporal trend is weak, it also appears that the stable isotope signature has slightly shifted over time, which may reflect a gradual change in groundwater recharge temperatures related to a climatic evolution.

Figure 5-50 – ^{18}O versus elevation (top) and apparent ^{14}C groundwater age (bottom)

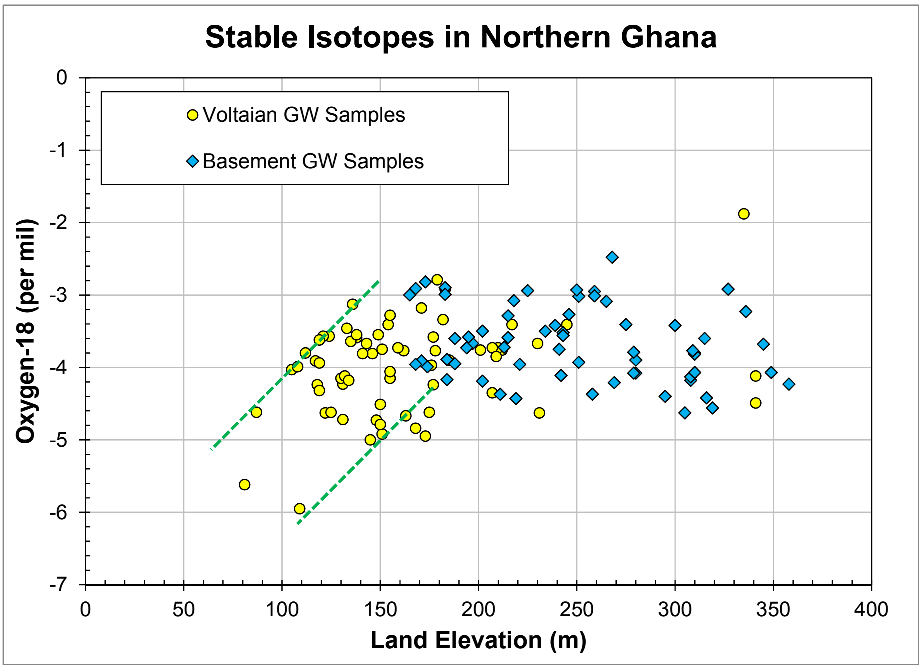

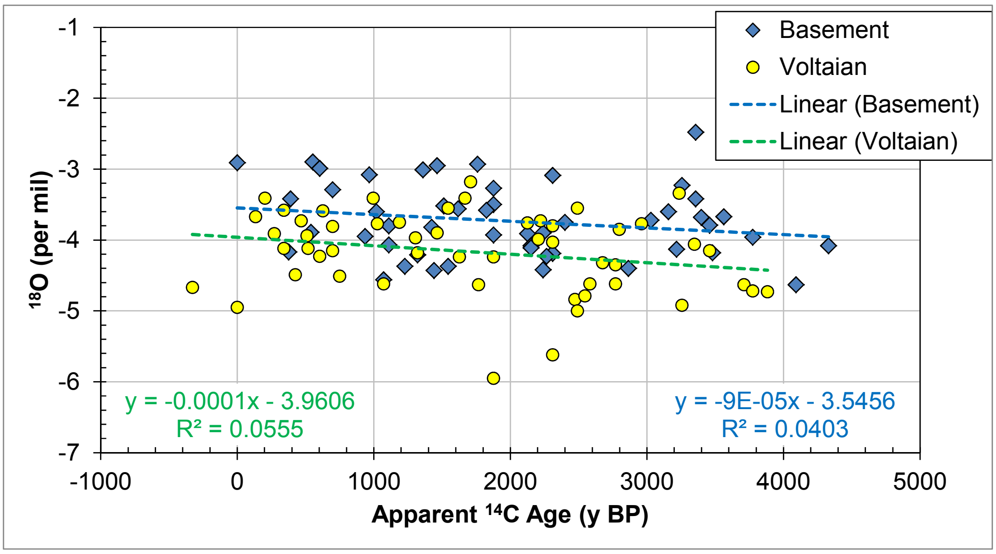

Tables 5-24 and 5-25 present the distribution and descriptive statistics of carbon isotopes (^{14}C and ^{13}C) for groundwater samples of the second sampling campaign. The number of samples for which these analyses are available is 103, as not all 121 water samples taken could be analyzed for carbon isotopes. Tables 5-24 and 5-25 provide an overview of results, considering all samples and also subgroups originating from the PCB and VSB geological contexts. Table 5-24 provides the distribution of ^{14}C apparent groundwater age (or residence time) in terms of number of samples and percentages. Table 5-25 provides descriptive statistics for both the percent of modern carbon (pmc) and ^{14}C apparent. The information presented in these tables is illustrated and discussed below. No water samples with carbon isotope data had Water Types 1 or 5; there are thus no statistics for these water types. Furthermore, Water Types 4 and 7 were only found within the VSB, so there are no statistics for these water types for the PCB.

Table 5-24 – Distribution of apparent ^{14}C groundwater age among hydrogeological contexts and water types

All water types						
Range	**All**	**Basement**	**Voltaian**	**All**	**Basement**	**Voltaian**
^{14}C Age (y)	**N**	**N**	**N**	**%**	**%**	**%**
< 500	12	3	9	11.7%	6.0%	17.0%
500-1500	30	16	14	29.1%	32.0%	26.4%
1500-2500	33	17	16	32.0%	34.0%	30.2%
2500-3500	21	10	11	20.4%	20.0%	20.8%
> 3500	7	4	3	6.8%	8.0%	5.7%
Total:	**103**	**50**	**53**	**100.0%**	**100%**	**100%**
Water Type 2: Ca-Mg-Na-HCO_3						
Range	**All**	**Basement**	**Voltaian**	**All**	**Basement**	**Voltaian**
^{14}C Age (y)	**N**	**N**	**N**	**%**	**%**	**%**
< 500	3	2	1	10.0%	10.0%	10.0%
500-1500	12	7	5	40.0%	35.0%	50.0%
1500-2500	8	5	3	26.7%	25.0%	30.0%
2500-3500	5	4	1	16.7%	20.0%	10.0%
> 3500	2	2	0	6.7%	10.0%	0.0%
Total:	**30**	**20**	**10**	**100.0%**	**100%**	**100%**
Water Type 3: Na-Ca-Mg-HCO_3						
Range	**All**	**Basement**	**Voltaian**	**All**	**Basement**	**Voltaian**
^{14}C Age (y)	**N**	**N**	**N**	**%**	**%**	**%**
< 500	5	0	5	10.6%	0.0%	22.7%
500-1500	14	8	6	29.8%	32.0%	27.3%
1500-2500	15	10	5	31.9%	40.0%	22.7%
2500-3500	10	5	5	21.3%	20.0%	22.7%
> 3500	3	2	1	6.4%	8.0%	4.5%
Total:	**47**	**25**	**22**	**100.0%**	**100.0%**	**100.0%**
Water Type 4: Na-HCO_3						
Range	**All**	**Basement**	**Voltaian**	**All**	**Basement**	**Voltaian**
^{14}C Age (y)	**N**	**N**	**N**	**%**	**%**	**%**
< 500	1	0	1	11.1%		11.1%
500-1500	2	0	2	22.2%		22.2%
1500-2500	4	0	4	44.4%		44.4%
2500-3500	2	0	2	22.2%		22.2%
> 3500	0	0	0	0.0%		0.0%
Total:	**9**	**0**	**9**	**100.0%**		**100.0%**

Table 5–24 – Distribution of apparent ^{14}C groundwater age among contexts and water types (cont'd)

Water Type 6: Na-Ca-HCO_3-Cl						
Range	**All**	**Basement**	**Voltaian**	**All**	**Basement**	**Voltaian**
^{14}C Age (y)	**N**	**N**	**N**	**%**	**%**	**%**
< 500	2	1	1	16.7%	20.0%	14.3%
500-1500	1	1	0	8.3%	20.0%	0.0%
1500-2500	5	2	3	41.7%	40.0%	42.9%
2500-3500	3	1	2	25.0%	20.0%	28.6%
> 3500	1	0	1	8.3%	0.0%	14.3%
Total:	**12**	**5**	**7**	**100.0%**	**100.0%**	**100.0%**
Water Type 7: Na-Cl						
Range	**All**	**Basement**	**Voltaian**	**All**	**Basement**	**Voltaian**
^{14}C Age (y)	**N**	**N**	**N**	**%**	**%**	**%**
< 500	0	0	0	0.0%		0.0%
500-1500	1	0	1	25.0%		25.0%
1500-2500	1	0	1	25.0%		25.0%
2500-3500	1	0	1	25.0%		25.0%
> 3500	1	0	1	25.0%		25.0%
Total:	**4**	**0**	**4**	**100.0%**		**100.0%**

Table 5-25 – Descriptive statistics for percent modern carbon (pmc) and apparent ^{14}C groundwater age (y BP)

All Water Types	All Samples	All Samples	Basement	Voltaian
Descriptive stats	**pmc**	**^{14}C Age (y BP)**	**C-14 Age**	**C-14 Age**
Min	70	-328	0	-328
Mean	96	1859	2001	1725
Max	125	4330	4330	3883
10th percentile	78.68	435	600	342
25th percentile	86.5	1008	1140	699
Median (50th perc.)	96	1826	1877	1709
75th percentile	106	2630	2988	2546
90th percentile	113.68	3391	3463	3253
Water Type 2		**All Samples**	**Precambrian**	**Voltaian**
Descriptive stats		**^{14}C Age (y BP)**	**C-14 Age**	**C-14 Age**
10th percentile		504	536	487
25th percentile		1004	1101	703
Median (50th perc.)		1505	1711	1246
75th percentile		2235	3227	1712
90th percentile		3407	3489	2277

Table 5–25 – Descriptive statistics for percent modern carbon (pmc) and apparent ^{14}C groundwater age (y BP) (cont'd)

Water Type 3		All Samples	Basement	Voltaian
Descriptive stats		**^{14}C Age (y BP)**	**C-14 Age**	**C-14 Age**
10th percentile		444	969	279
25th percentile		1046	1441	540
Median (50th perc.)		1826	2152	1487
75th percentile		2914	3029	2717
90th percentile		3399	3420	3339
Water Type 4		All Samples	Basement	Voltaian
Descriptive stats		**^{14}C Age (y BP)**	**C-14 Age**	**C-14 Age**
10th percentile		494		494
25th percentile		750		750
Median (50th perc.)		2311		2311
75th percentile		2491		2491
90th percentile		2808		2808
Water Type 6		All Samples	Basement	Voltaian
Descriptive stats		**^{14}C Age (y BP)**	**C-14 Age**	**C-14 Age**
10th percentile		518	621	1164
25th percentile		1462	966	1876
Median (50th perc.)		2218	1759	2311
75th percentile		2556	2311	2565
90th percentile		2837	2643	3103
Water Type 7		All Samples	Basement	Voltaian
Descriptive stats		**^{14}C Age (y BP)**	**C-14 Age**	**C-14 Age**
10th percentile		1586		1586
25th percentile		1984		1984
Median (50th perc.)		2440		2440
75th percentile		2951		2951
90th percentile		3446		3446

The apparent ^{14}C groundwater age can be obtained from the following relation (Domenico and Schwartz, 1990):

$$^{14}\text{C Age} = \frac{\text{Half-life}}{\ln(2)} \cdot \ln\left(\frac{^{14}C_o}{^{14}C_s}\right)$$

Where the half-life of ^{14}C, which undergoes decay, is 5 568 years (by convention), $^{14}C_o$ is the normal activity of ^{14}C in a standard and $^{14}C_s$ is the activity in the sample. The apparent ^{14}C age is reported before “present”, which is defined as 1950. Numerous and complex corrections need to be applied to apparent ^{14}C age in order to make it representative of the actual residence time, especially the integration of “dead” carbon from the dissolution of carbonates (Domenico and Schwartz, 1990; Clark and Fritz, 1997). In this report, we have only considered the activity of ^{14}C in the groundwater recharge and no corrections for mineral dissolution were made. The ^{14}C age reported here is not the conventional ^{14}C age but a partly corrected apparent ^{14}C age. Figure 5-51 explains part of the reasons for this choice. The histogram shows that the highest values of the analyzed percent of modern carbon are actually quite higher than 100%. The conventional calculation of age using 100% of modern carbon as a reference would thus greatly underestimate age. We thus made the choice to use 120% as a “source” value of percent modern carbon. We did not make a correction for carbonate dissolution even though Figure 5-52 shows that there appears to be some effect of mineral dissolution on the carbon isotopic signature. This implies that reported apparent ^{14}C ages should be considered as maximum values, and actual ages should be expected to be lower. Figure 5-52 also shows that the apparent range of soil gas ^{14}C at the origin of the recharge groundwater has a wide range of ^{13}C values that are also higher than those reported for temperate northern hemisphere conditions, besides having percent modern carbon values higher than 100%. Figure 5-52 shows that away from the presumed range of ^{14}C in soil, groundwater samples show both effects of ^{14}C radioactive decay and mineral dissolution. Quite similar trends are seen for samples from Basement and Voltaian contexts.

Figure 5-51 – Proportion of modern carbon in groundwater analyses

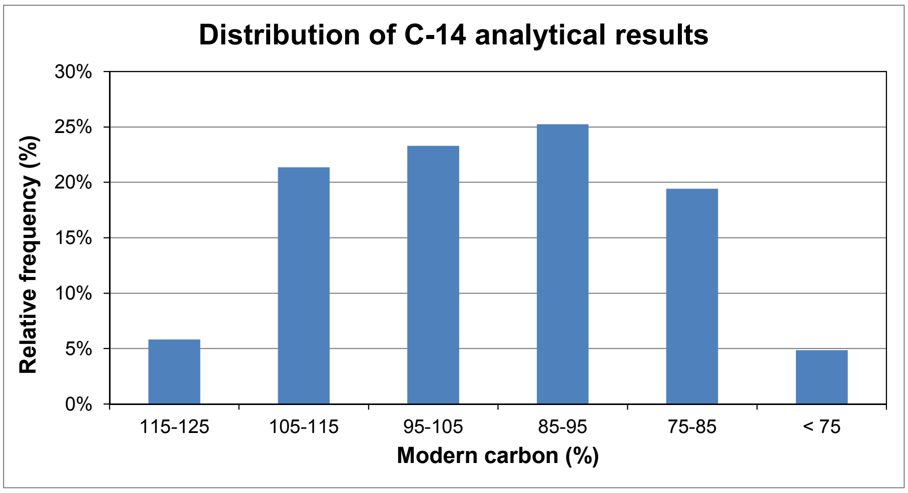

Figure 5-52 – Interpretation of the origins of ^{14}C in groundwater samples

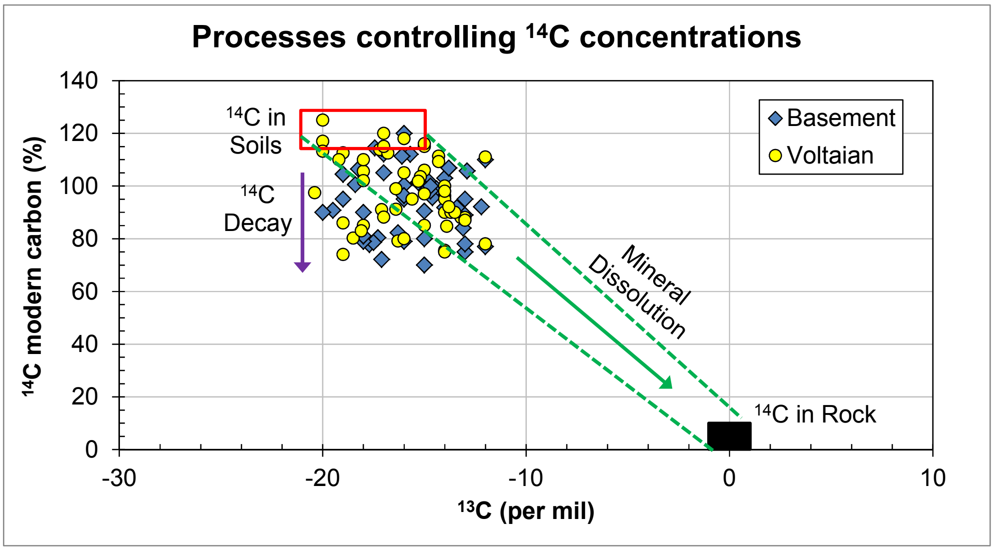

However, even though there is an apparent effect of mineral dissolution, the graphs of Figure 5-53 show that such an effect may be limited. The graphs show that increases in dissolved inorganic carbon (HCO_3) and TDS, which should be indicators of groundwater evolution, do not lead to great shifts in ^{13}C signature. However, the ^{13}C is in the upper range of presumed soil ^{13}C source for more evolved groundwaters. No data could be used to consider the potential effect of mixing of young recharge groundwater with older waters along flow paths. Such contributions of young waters could alter the residence time indications provided by ^{14}C data.

Figure 5-53 – Trends in ^{13}C with groundwater evolution (as indicated by HCO_3 & TDS)

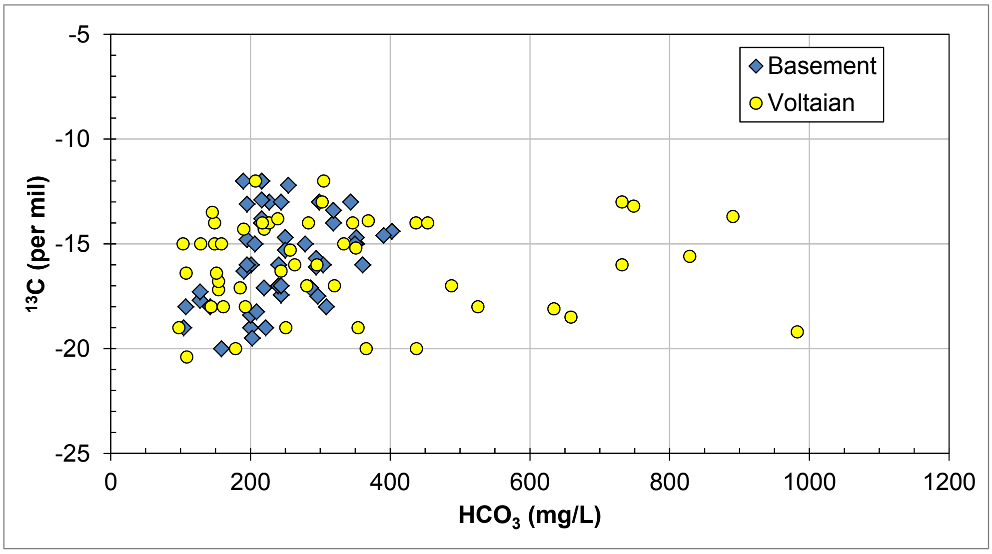

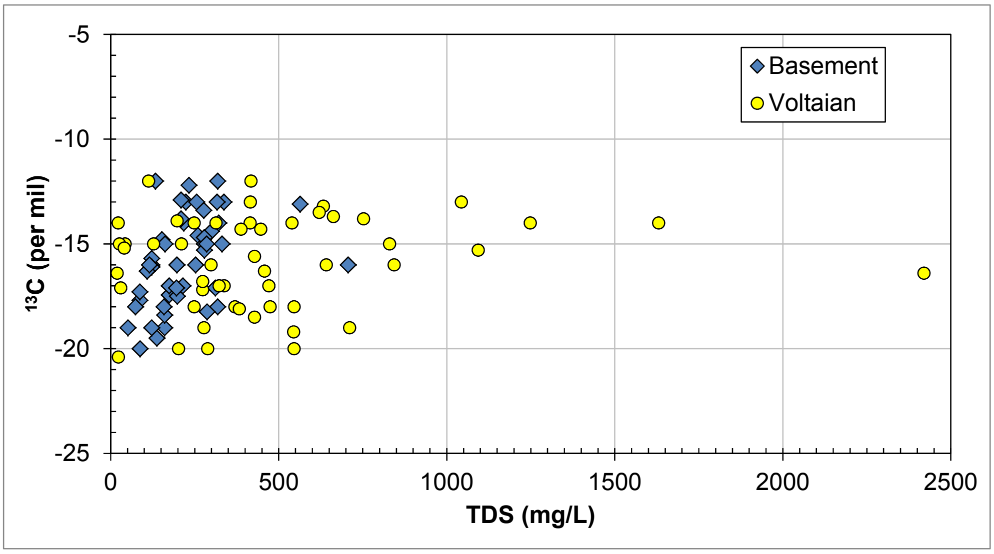

Figure 5-54 displays the distribution of calculated apparent ^{14}C ages for all samples and for the samples of the Basement and Voltaian contexts. Globally, the distributions of ages are quite similar. These apparent ages ranging mostly between 500 and 3500 years would indicate relatively long residence times, which would be compatible with the low recharge rates, relatively modest aquifer transmissivity and relatively flat topography of northern Ghana, which together should lead to slow moving groundwater. Figure 5-55 shows no clear trend in age with well depth, shallower wells actually having the greatest ages. Such shallow wells could be located in groundwater dischage zones located at the end of groundwater flow paths.

Figure 5-54 – Distribution of apparent (uncorrected) ^{14}C groundwater ages for all samples (top) and by geological contexts (bottom)

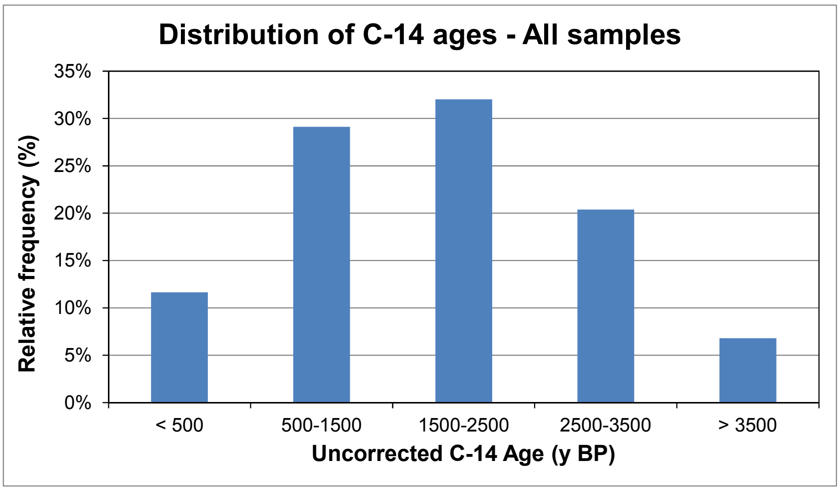

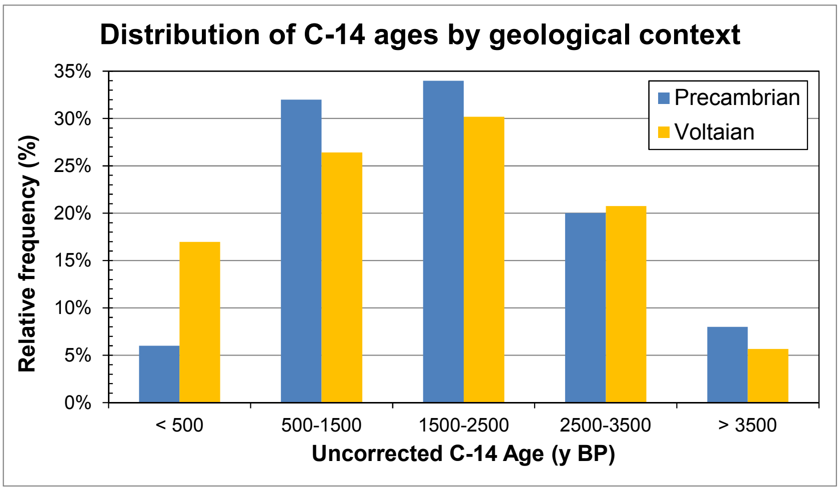

Figure 5-55 – Apparent ^{14}C groundwater ages versus well depth

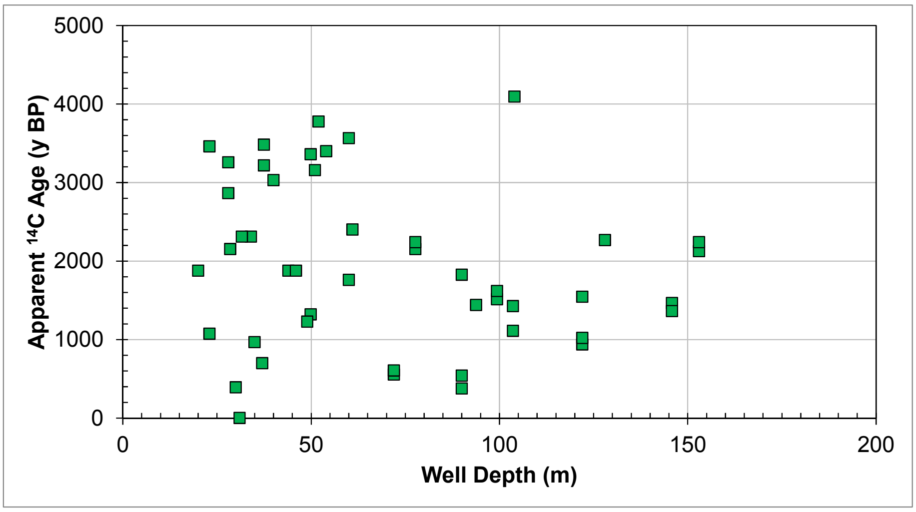

Figure 5-56 shows the distribution of apparent ^{14}C ages by water types for all samples as well as per geological context. In general, the proportions of less evolved water types are more important in younger ^{14}C age groups, whereas more evolved water types are more represented in older age groups.

Figure 5-56 – Apparent ^{14}C groundwater ages by water types for all samples (top), Precambrian (Basement) samples (middle) and Voltaian samples (bottom)

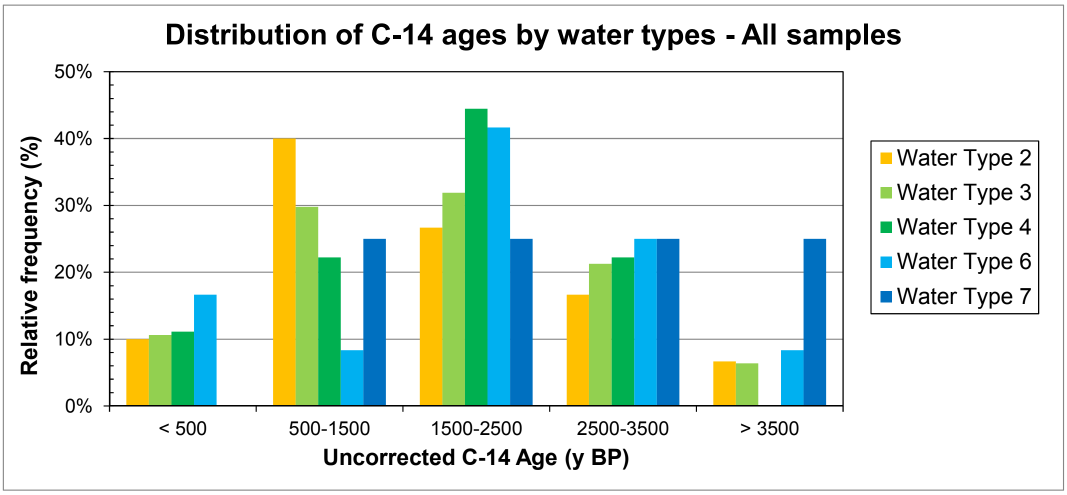

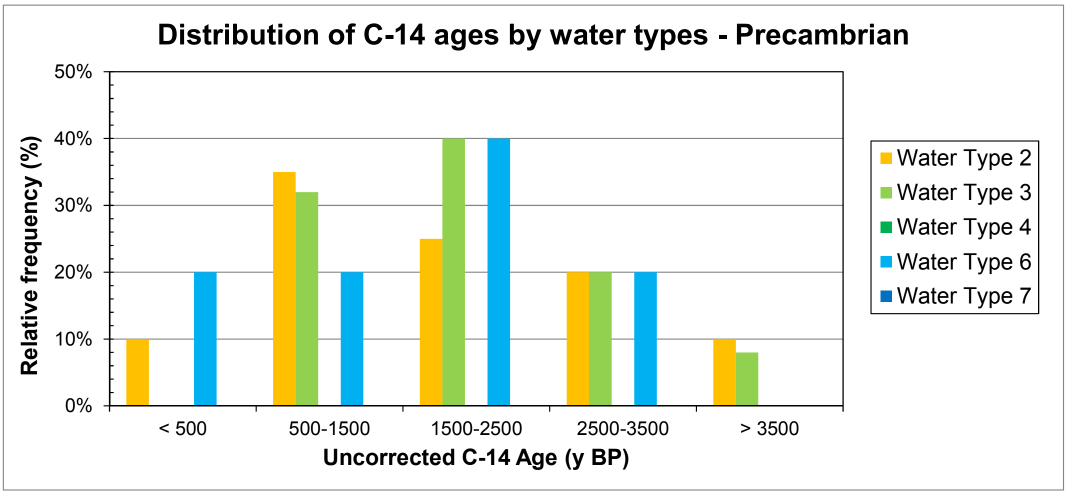

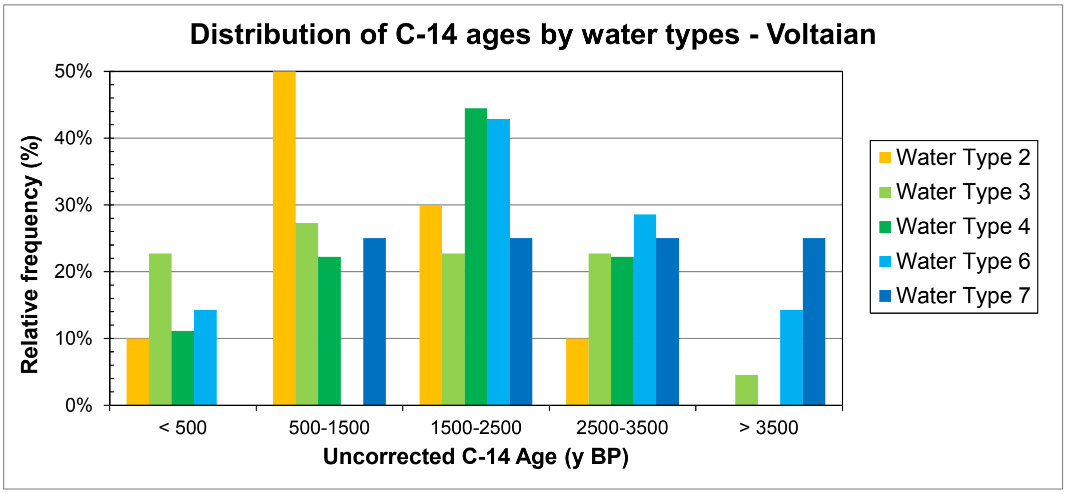

Figure 5-57 actually shows more clearly that median ages increase from less to more evolved water types. This trend is actually more apparent for samples from the Voltaian context, which are better represented in more evolved water types, i.e. water types dominated by Na and Cl.

^{14}C ages thus strongly support the interpretation made on the basis of major ions and water types regarding the existence of more evolved water types.

Figure 5-57 – Apparent ^{14}C groundwater ages distribution by water types for all samples (top), Precambrian (Basement) samples (middle) and Voltaian samples (bottom)

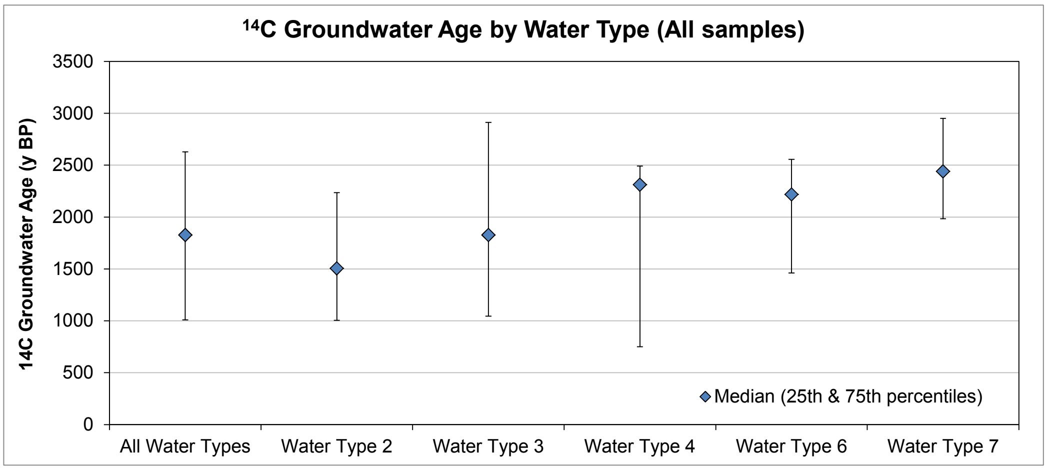

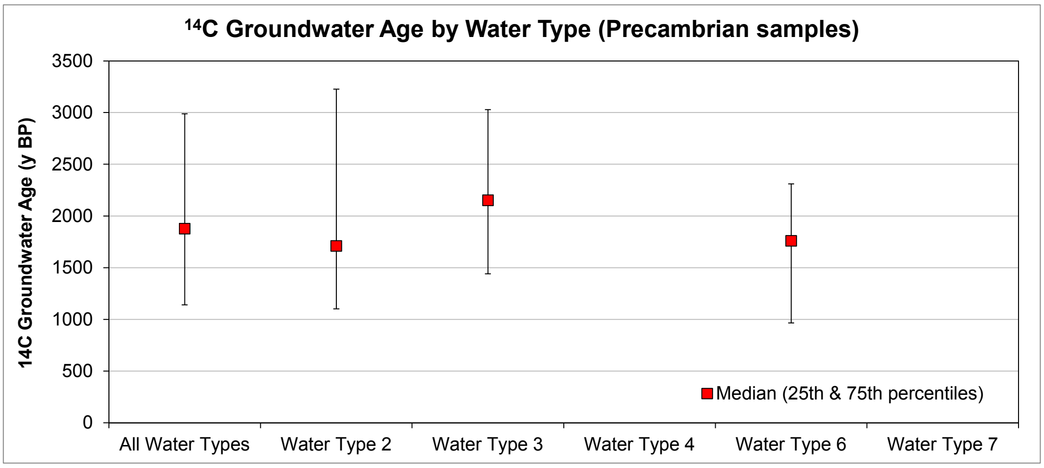

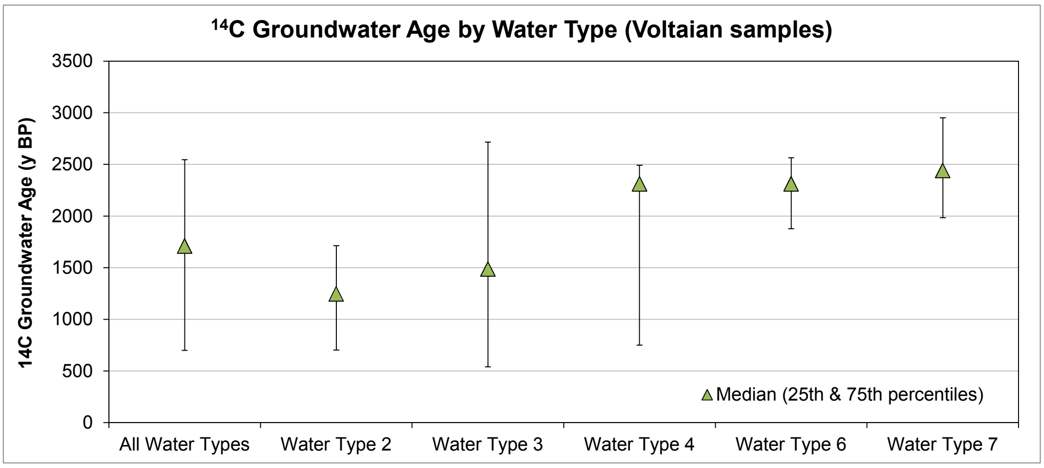

The ages do indicate that these evolved water types have had longer residence times in the aquifer system. Besides having a higher median value, the range of ^{14}C ages obtained for the most evolved water types (6 and 7) is also more restricted, which may indicate that groundwater of these types is less prone to mixing with younger groundwater recharge. This may be an indication that these water types are present either at the end of flow path where groundwater is mostly emerging, or that confined conditions prevail to restrict recharge. On the contrary, Water Types 2 and 3 have a wide range of ages that could indicate significant mixing between recharge and groundwater along flow paths where these water types are found.

The age data thus support the conceptual model of shorter residence time in the Basement context where topography is more rugged and the longer residence times due to long flow paths in the low relief Voltaian context.

5.4.5 Temporal variations in groundwater chemistry

Natural groundwater chemical content is closely related to the nature of the rock minerals and to some physicochemical characteristics within the hydrogeological setting (i.e. dissolved oxygen, redox conditions, etc.). Typically, these conditions do not significantly vary seasonally in hydrogeological systems, and therefore the geochemical composition of groundwater remains often similar all year long. However, the natural geochemistry of groundwater in some areas can vary through the course of the year according to some characteristics of the groundwater setting. For instance, it is recognized that shallow groundwater and water from wells in recharge areas can present significant seasonal variability in physicochemical parameters. This issue is therefore interesting to investigate in a groundwater resource assessment program. It is important to stress that some of the chemical variability observed from one sampling campaign to another could also be related to variations in sampling or analytical conditions

A specific objective of the groundwater geochemical assessment consisted in documenting temporal variations occurring over the course of a year. Three groundwater sampling phases took place between August 2010 and May 2011 in a total of 121 wells. Two of these wells were sampled only once. As such, analytical results obtained from these two samples were not considered for the assessment of temporal variation of groundwater chemistry.

Conclusions that may be drawn regarding the annual variability of groundwater chemistry on the basis of a single year of records remain limited, as the representativeness of the records is directly dependent upon the hydrological and meteorological conditions that prevailed during that year and the similarity/deviation of these conditions with respect to historical averages. It nevertheless provides an indication of how groundwater chemistry might vary over a given year. While actual concentrations measured and intra-annual variations in absolute concentrations will fluctuate from year to year, the assumption is made that geochemical results obtained through HAP groundwater sampling during 2010-2011 reflect seasonal trends normally observed in northern Ghana.

Temporal variations in the occurrence of natural elements or compounds and contaminants in groundwater was assessed by comparing median concentrations recorded in samples from each of the three monitoring campaign. Contrary to average values, medians bear the advantage of not being affected or biased by the existence of one or a few extreme value(s) or outlier(s) in the dataset. A distinction was made between results from the three regional geological contexts (Precambrian basement, Intrusive rocks and Voltaian sedimentary basin), in order to detect potential trends that would be specific to these contexts. Comparison between median concentrations of various geochemical parameters over the three sampling campaigns is shown in Figure 5-58.

Figure 5-58 – Median concentrations of selected chemical parameters for the three sampling campaigns

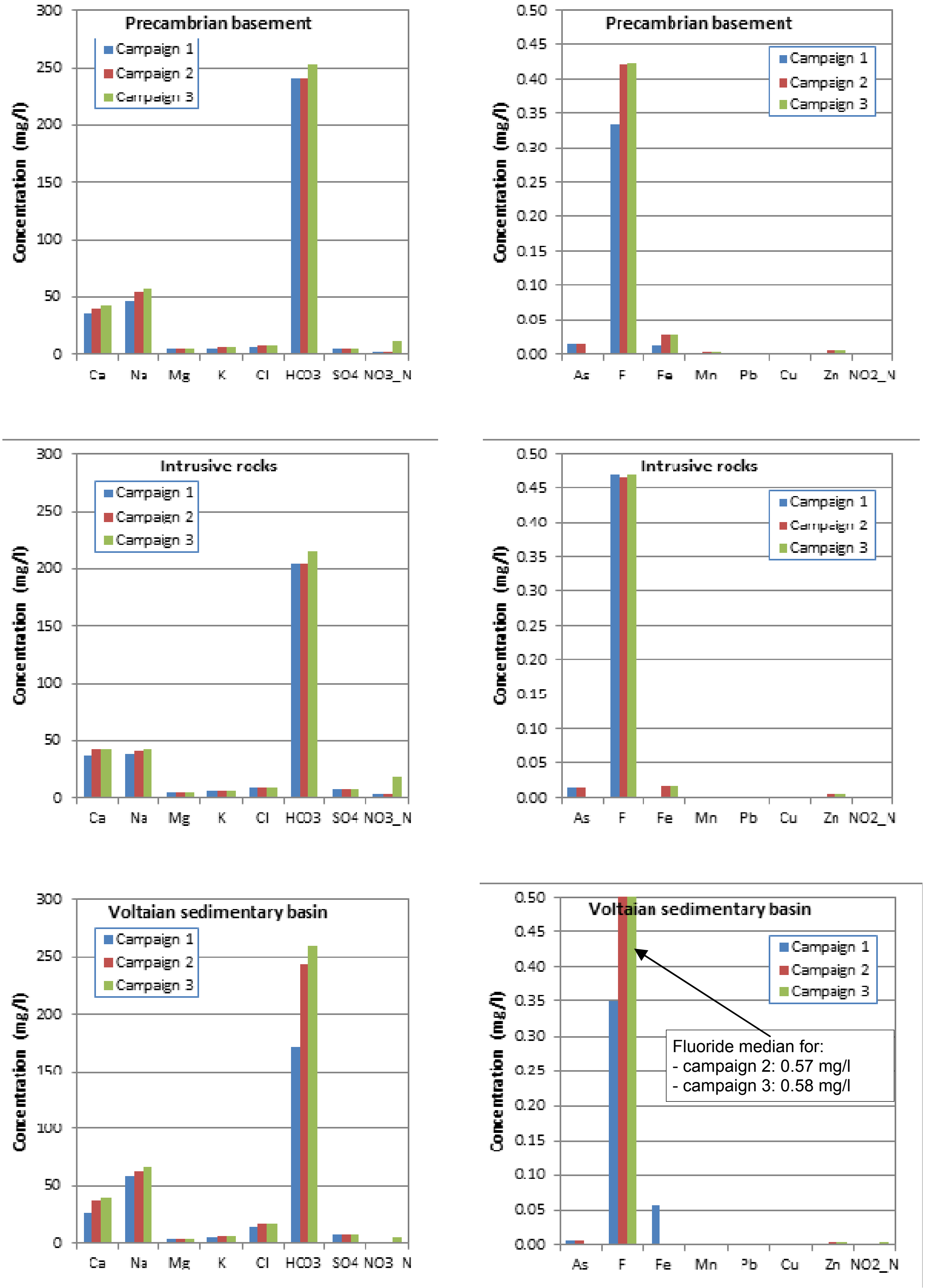

From a global perspective, median elements or compound concentrations measured in groundwater display an increase between campaign 1 and campaign 2, and again, although to a lower extent, between campaign 2 and campaign 3 for a majority of the considered parameters. Increase of the median concentration ranges between 0 and 1550 %. This latter figure relates to the increase of median zinc concentration in Precambrian basement rocks, which in turn correspond to a change of 0.3 to 5.0 µg/l in absolute median concentrations. Zinc concentrations aside, the compound with the greatest relative increase from campaign 1 to 3 is nitrates. While median nitrate concentrations exhibit a slight decrease between campaign 1 and 2 for all geological contexts, the median concentrations increased between 365 and 438 % from campaign 2 to campaign 3.

The variation range of median concentrations for major ions from one campaign to the other spans between -4 and 43 %. Most major ions exhibit sustained median concentrations increase throughout the three monitoring campaigns. Sulfate median concentrations display a different pattern, as a decrease is observed between campaigns 1 and 2 in wells installed in all three geological contexts. The highest increases in major ions concentrations are generally observed in groundwaters of the Voltaian sedimentary basin, between campaigns 1 and 2, for an average of 19 %. In contrast, lower increases are generally observed in groundwater found in intrusive rocks, again between campaigns 1 and 2, with an average increase of 4 %. Major ions concentrations from samples collected in wells of the Precambrian basement indicate an average increase of 9 % between campaigns 1 and 2. Major ions concentrations variations between the second and third monitoring campaigns are relatively similar from one geological context to the other, as they all average between 5 and 6 %.

Arsenic concentrations recorded in samples collected during campaign 1 and 2 are deemed as being erroneous, since they displayed a quasi-systematic bias of very similar magnitude and narrow variation range. Magnitude and spread of concentrations measured in samples from campaign 3 do not show any bias and are consistent with historical data available for arsenic in groundwater in the study area. They are thus deemed as being representative of the actual chemistry of groundwater. Median concentrations for arsenic in campaign 3 samples from Precambrian basement and Intrusive rocks wells ranks at 0 mg/l, while it is equal to 0.001 mg/l in campaign 3 samples from Voltaian sedimentary rocks wells.

Significant increase is observed for fluoride concentrations in groundwaters of the Precambrian basement and Voltaian sedimentary basement between campaigns 1 and 2, while median fluoride concentrations remain relatively constant in groundwater flowing in intrusive rocks. Median concentrations also display increase between campaigns 1 and 2 for manganese, zinc and iron (in Precambrian basement and intrusive rocks wells for the latter), while they stay constant between campaigns 2 and 3. For their part, lead and copper median concentrations remained equal to zero throughout the three sampling phases, indicating both a low-magnitude occurrence and a stability of occurrence in groundwater for these two elements.

Regarding nitrites, only median concentration obtained for samples of the third monitoring campaign in wells of the Voltaian sedimentary basin ranked above 0 mg/l.

There could be potential natural causes for the general increase in compounds or elements concentrations over the sampling periods. However, it is difficult to explain why groundwater geochemistry would seasonally change for water types involving long residence times. In that perspective, the fact that the highest concentrations increases are recorded in groundwater flowing in the Voltaian sedimentary basin could be related more to natural variability of the groundwater geochemistry within the aquifer than to the effect of changes in seasonal conditions. The occurrence of sulfate, nitrates and nitrites, which are potentially related to surface contamination in the study area, appears to be independent from any seasonality effect. We need to stress that variations in geochemical parameters could also be partly related to variations in sampling or analytical conditions, which would not be related to natural variability of the groundwater geochemistry. Long-term sampling and analyses of the WRC monitoring wells would provide a way to determine if there are real seasonal changes in groundwater geochemistry, or some non-seasonal variability, or long-term evolution trends.

5.4.6 Groundwater geochemistry issues

Outstanding issues related to groundwater geochemistry include the relative concentrations of magnesium in samples collected in certain wells installed in Birimian Supergroup formations and, to a lesser extent, Eburnean Plutonic Suite formations in sampling campaigns carried out as part of studies predating the HAP. Uncertainties persist about the representativeness of analytical results for magnesium, as they generally differ from those obtained for groundwater samples collected in the course of the HAP. While magnesium concentrations in groundwater are not an environmental or quality issue, the possibility of analytical drift or improper sample collection or handling may cast a doubt on the representativeness of other analytical results obtained for those samples.

Greater geochemical uniformity observed for samples collected in the Birimian Supergroup in the course of the HAP suggests that analytical results yielded for major ions would be representative of actual groundwater geochemistry. Monitoring and laboratory procedures implemented for the purpose of the HAP as well as geochemical data produced would thus appear more reliable, from a global perspective. Reproduction and optimization of these procedures over the course of future sampling campaigns should insure the quality of geochemical data over the long-term, in addition to the detection of possible seasonal variations or long-term trends that may be accountable for a certain degree of variability in analytical results related to geochemical data from projects carried out prior to HAP.

5.4.7 Groundwater quality

5.4.7.1 Overview of groundwater quality

Existing data indicate that groundwater is generally of good natural quality (microbiological and chemical) in the HAP area. However, some natural chemical components of groundwater do not always meet international water quality standards. Indeed, it was reported that groundwater exhibits aggressive characteristics and large concentrations in some chemical species in some areas of northern Ghana. More specifically, iron, manganese, fluoride and chloride were measured in groundwater in concentrations exceeding WHO recommended guideline values. It was also reported that the quality of water generally deteriorates closer to areas where human activities take place, due in part to the occurrence of latrines, the use of manure for agriculture, or the disposal of domestic wastes. Some chemical analyses displaying high nitrate concentrations have been reported locally. These high concentrations can represent potential health risks for local people and also limit the use of groundwater for aesthetical reasons (e.g. odor, taste).

A preliminary interpretation of existing chemical analyses compiled in the consolidated HAP database highlighted the characteristics of several physicochemical parameters, such as pH, electric conductivity (EC), iron (Fe), manganese (Mn), chloride (Cl), fluoride (F), and nitrates (NO_3); along with an assessment of the limitations of the data. Additional analyses were carried out on these existing data in order to examine the possible existence of geochemical trends related to specific geological contexts or watersheds.

The updated groundwater quality assessment presented herein includes both existing data and geochemical data obtained through the HAP targeted sampling program. Results from the third monitoring campaign were considered for the latter, as only one entry (or data from a specific sampling phase) per well was retained for assessment of groundwater quality. The third campaign corresponds to the campaign where recorded concentrations were generally the highest. As such, it represents the most conservative conditions with respect to potential restrictions in groundwater uses.

For the purpose of this discussion, it is assumed that As, F, Fe and Mn concentrations are related to natural content in groundwater, whereas NO_2 and NO_3 have typically an anthropogenic origin resulting from surface contamination from human activities. Consequently, the interpretation presented in this report was carried out according to these assumptions.

5.4.7.2 Natural content

Physicochemical parameters

Available data from the consolidated HAP database suggest that relatively aggressive groundwater is encountered in northern Ghana, notably in some areas of the Precambrian basement. This observation was also reported in earlier studies that investigated pH values in Precambrian basement rocks (Langenegger, 1994; Pelig-Ba, 1998). pH values included in the database are in the range of 4 to 11.8 with an average of 7.5. Extreme values are generally observed in sedimentary rock formations. The lowest pH values (< 5) are measured in sandstones of the Kwahu-Morago Group of the VSB, and the highest values are found in the Obosum and Oti-Pendjari groups.

There is no health-based WHO guideline for pH. However, optimum operational range recommended is 6.5-8.0 in order to minimize technical problems, such as corrosion. Approximately 32 % of pH values in the database fall outside this range, with approximately 9 % of the values below and 23 % above.

Electrical conductivity values included in the consolidated database range from 0.1 µS/cm to 68 700 µS/cm with an average of 732 µS/cm. Typically, conductivity is lower and more constant in groundwater from wells drilled in the Precambrian basement compared to those located in the VSB. There is also no guideline value proposed by WHO for electric conductivity, but the parameter is indicative of total dissolved solids in water (TDS), which also provide an indication of water potability.

The relationship between electrical conductivity (EC) and TDS was defined with data from the HAP consolidated database. Linear regression between the two parameters yielded an excellent correlation ($R^2=0.9983$) (similar to Figure 5-44 based on a smaller set of data). The corresponding equation is:

$$EC\ (\mu S/cm) = 2.1694 * TDS\ (mg/L) + 19.083$$

On the basis of this relation, average TDS concentrations would correspond to 329 mg/L. WHO does not issue definitive quality standard for TDS in drinking water. However, it states that the presence of levels of TDS greater than 1200 mg/L (or 2622 µS/cm) in drinking water may be objectionable to consumers. Approximately 3 % of groundwater samples collected in the northern regions of Ghana exhibit electrical conductivities above this threshold value.

<u>Arsenic</u>

Arsenic is widely distributed throughout the earth crust. Typically, arsenic occurrence in natural groundwater is related to the dissolution of As-bearing minerals and ores. Some arsenic can also originate from industrial effluents, alloying agents and wood preservation.

Several igneous and metamorphic rocks have average arsenic concentrations between 1 and 10 mg/kg. Similar concentrations are measured in carbonate minerals and carbonate rocks (Plant *et al.*, 2004). Arsenic concentrations in other sedimentary rocks can be more variable. In these rocks, arsenic is concentrated in clays and other fine-grained sediments. Higher concentrations are typically found in organic-rich and sulphide-rich shales, sedimentary ironstones, phosphatic rocks, and some coals (Smedley and Kinniburgh, 2002). The average concentration of arsenic in shale is reported to be an order of magnitude larger than concentrations measured in sandstones, limestones and carbonate rocks.

Table 5-26 – Descriptive statistics for arsenic in groundwater

Data group	As (WHO guideline value ≤ 0.01 mg/l) (1)							Analyses exceeding WHO guideline
	Number of analyses	Average	Minimum	25 perc.	Median	75 perc.	Maximum	
Northern Ghana	183	0.008	0	0	0.001	0.002	**0.700**	10 (5 %)
Geological context								
Precambrian	25	0.003	0	0	0.001	0.002	**0.015**	**4 (16 %)**
Intrusive	35	0.001	0	0	0	0.001	**0.013**	**1 (3 %)**
Voltaian	123	**0.012**	0	0.001	0.001	0.002	**0.700**	**5 (4 %)**
Geological group								
Birimian	25	0.003	0	0	0.001	0.002	**0.015**	**4 (16 %)**
Buem	-	-	-	-	-	-	-	-
Tarkwaian	-	-	-	-	-	-	-	-
Eburnean	17	0.002	0	0.001	0.001	0.002	**0.013**	**1 (6 %)**
Mesozoic	3	0	0	0	0	0	0	0
Tamnean	15	0	0	0	0	0	0.002	0
Kwahu-Morago	29	0.001	0	0	0.001	0.001	0.004	0
Obosum	19	0.002	0	0	0.001	0.002	**0.014**	**1 (5 %)**
Oti-Pendjari	75	**0.018**	0	0.001	0.002	0.003	**0.700**	**4 (5 %)**
Watershed								
Black Volta	25	0.001	0	0	0	0.002	**0.013**	**1 (4 %)**
Lower Volta	16	0.001	0	0.001	0.001	0.002	0.004	0
Oti	27	**0.029**	0	0.001	0.002	0.003	**0.700**	**3 (11 %)**
White Volta	115	0.006	0	0	0.001	0.002	**0.500**	**6 (5 %)**

Notes:
(1) : Numbers are in bold when exceeding WHO guideline value for parameter of concern.

The concentration of arsenic estimated in most groundwaters is typically below 0.01 mg/L, and often below the detection limit. Arsenic is strongly adsorbed by oxides of iron, aluminum and manganese, as well as by some clay, leading to its enrichment in ferromanganese nodules and manganiferous deposits (Plant *et al.*, 2004). Processes controlling arsenic mobility in aquifers are variable, complex and poorly understood, although some of the key factors leading to high groundwater arsenic concentrations are known.

Typically, arsenic mobility can occur under strongly reducing conditions where arsenic, mainly as As(III), is released by desorption from or dissolution of iron oxides. Reducing conditions for arsenic mobility have been reported most frequently in young alluvial, deltaic sediments characterized by complex patterns of sedimentation and rapid burial of large amounts of sediment together with fresh organic matter. Plant *et al.* (2004) reported that thick sequences of young sediments often contain groundwater with high arsenic concentrations. High concentrations of arsenic are also encountered in oxidizing conditions where groundwater pH values are high (>8) (Smedley and Kinniburgh, 2002). In these environments, inorganic As(V) predominates and arsenic concentrations are positively correlated with those of other anion-forming species, such as HCO_3 and F. Groundwater with high arsenic concentrations is also usually found in arid or semi-arid regions where groundwater salinity is high. Evaporation was suggested as an important additional cause of arsenic accumulation in some arid areas (Welch and Lico, 1998). High concentrations of arsenic have also been found in groundwater from areas of bedrock and placer mineralization, which are often the sites of mining activities.

Table 5-26 presents the summary statistics for As concentrations measured in groundwater and reported in the HAP consolidated database while Figure 5-59 presents the distribution of these concentrations. The statistics are presented here according to geology and watershed. Joint analysis of pre-HAP geochemical data and analytical results obtained through HAP's third monitoring campaign showed that 5 % of all arsenic concentrations considered (183 chemical analyses) exceed the WHO guideline value. Both maximum concentration and highest average concentration are recorded in samples from the Oti-Pendjari Group. It should be stressed that statistics calculated for arsenic in groundwaters of the Oti-Pendjari Group are heavily influenced by two single results (0.50 and 0.70 mg/l) that may be outliers, as the third highest arsenic concentrations in the complete dataset is at 0.020 mg/l. The 75^{th} percentile concentration for arsenic is nevertheless highest for samples from the Oti-Pendjari Group, indicating that concentrations are generally higher in groundwater flowing in rocks of this Group.

As previously discussed, the occurrence of mudstone, shale and carbonate rocks reported in the Oti-Pendjari Group, potentially containing larger organic matter content in comparison with geological groups dominated by sandstone formations, may in part contribute to the presence of the high As concentrations encountered in some of the groundwater samples.

According to available data, the frequency of occurrence of WHO guideline exceedances for arsenic in groundwater is greater in formations of the Birimian, especially Oti-Pendjari, Obosum and Eburnean Groups. No WHO guideline exceeding was recorded in groundwaters of the Mesozoic, Tamnean or Kwahu-Morago Groups. The small number of analytical results available in most geological groups implies that spatial coverage and statistical representativeness of arsenic results might be too limited. Care should thus be paid to potentially high arsenic concentrations in groundwater, despite the low frequency of occurrence documented in Intrusive rocks formations as well as units of the Kwahu-Morago and Obosum Groups. This is also true for groundwater in formations of the Buem and Tarkwaian Groups, since no data for arsenic were available for either of them.

Lastly, high content of arsenic has also been reported in groundwater typically in southern regions of Ghana (Smedley, 1996). These high concentrations are however associated to mining activities carried out in the southern region.

Figure 5-59 – Groundwater quality – Distribution of As values

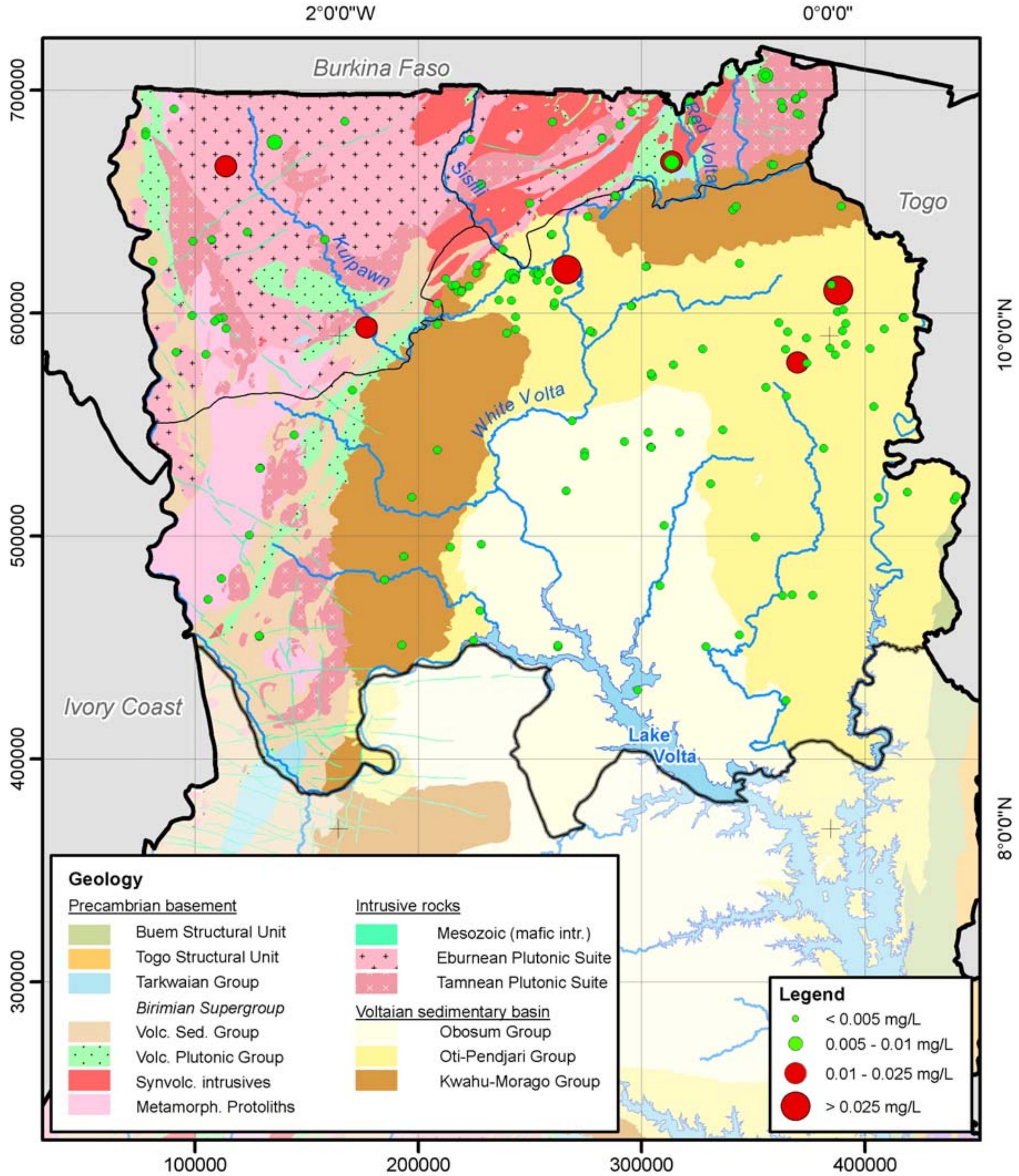

Fluoride

Among all the chemical parameters identified in groundwater in the project area, fluoride represents a significant threat to human health because large concentrations are quite common. The health concern related to fluoride is that its excess in a diet can cause bone fluorosis. The WHO guideline value for fluoride in drinking water is 1.5 mg/L, and mottling of teeth may occur above this value. Fluoride concentrations between 3 and 6 mg/L in water may cause skeletal fluorosis, and continued consumption of water with fluoride in excess of 10 mg/L can result in crippling fluorosis (Apambire *et al.*, 1997).

Fluorine is a common element in the earth crust, and it is encountered in the form of fluorides in several minerals. The most common fluorine-bearing minerals are fluorite, apatite and micas.

Igneous and volcanic rocks have a fluorine concentration from 100 mg/kg (ultramafic) to more than 1000 mg/kg (alkaline) (Frencken, 1992). Sedimentary rocks have a fluorine concentration from 200 mg/kg (limestone) to more than 1000 mg/kg (shales). Clastic sediments have higher fluorine concentrations as the fluorine is concentrated in micas and illites in the clay fractions. High concentrations may also be found in sedimentary phosphate beds or volcanic ash layers. Finally, metamorphic rocks have a fluoride concentration from 100 mg/kg (regional metamorphism) to more than 5000 mg/kg (contact metamorphism).

During weathering and circulation of water in rocks and soils, fluorine can be leached out and dissolved in groundwater. The fluoride content of groundwater varies greatly depending on the geological settings and type of rocks. Consequently, fluoride problems tend to occur in places where fluorine-bearing minerals are most abundant in the host rocks.

The concentration of fluoride in groundwater typically depends on the reaction time with aquifer minerals. High fluoride concentrations can be measured in groundwaters which have long residence times, i.e. usually groundwater associated with deep aquifer systems and/or slow velocity. This was confirmed to be the case in northern Ghana, as high fluoride concentrations are associated with more evolved groundwater with high TDS concentrations (Figure 5-48), which were shown by ^{14}C apparent ages to have had longer residence times (Figure 5-57). As opposed, shallow aquifers which contain recently infiltrated rainwater usually have low fluoride. High-fluoride groundwaters are mainly associated with a sodium-bicarbonate water type and relatively low calcium and magnesium concentrations. Such water types usually have pH values above 7.

Arid regions are prone to high fluoride concentrations, and the fluoride contents of water may increase during evaporation. Stable isotope data in northern Ghana have indicated some influence of evaporation, especially for the Basement geological context (Figure 5-49). Dissolution of evaporative salts deposited in arid zone may be an important source of fluoride. Fluoride increase is less pronounced in humid tropics, because of high rainfall inputs and their diluting effect on the groundwater chemical composition (Frencken *et al.*, 1992).

Table 5-27 presents the summary statistics for F concentrations measured in groundwater and reported in the consolidated database while Figure 5-60 presents the distribution of these concentrations. Here again, the statistics are presented according to geology and watershed.

Existing data suggest that about 12% of all fluoride concentrations included in the statistical analysis (1084 chemical analyses) exceed the 1.5 mg/L WHO guideline value. Fluoride concentrations generally range from undetected to about 8 mg/L with an average of about 1.0 mg/L. The highest fluoride concentrations are encountered in the rocks of the Oti-Pendjari Group, although large concentrations are measured in other geological groups (sedimentary and crystalline rocks).

Groundwaters from crystalline rocks, especially alkaline granites, tend to display high fluoride concentrations. Some high concentrations ranging from 0.11 mg/L to 4.6 mg/L have been reported in some areas underlain by granitoids (Apambire, 1996; Apambire *et al.*, 1997; Apambire, 2000) and, more recently, in rocks of the VSB (Lutz *et al.*, 2007). These concentrations would originate mainly from the dissolution of fluorite minerals, notably found in the Bongo Granite. No information was available concerning the origin of fluoride concentrations in wells located in the VSB, except perhaps the observation that higher fluorine content are often measured in clastic rocks. Also, as previously discussed, long groundwater flow paths and evaporation are conditions that favor high fluoride concentrations (Figure 5-48).

Lastly, since large fluoride concentrations are measured in all watersheds, it is difficult to propose any relationship between F content and watershed.

Table 5-27 – Descriptive statistics for fluoride in groundwater

Data group	F (WHO guideline value ≤ 1.5 mg/l) [1]							Analyses exceeding WHO guideline
	Number of analyses	Average	Minimum	25 perc.	Median	75 perc.	Maximum	
Northern Ghana	1084	1.046	0.001	0.230	0.500	0.930	**125.0**	**131 (12 %)**
Geological context								
Precambrian	268	0.578	0.007	0.300	0.445	0.700	**3.200**	**12 (4 %)**
Intrusive	244	0.687	0.001	0.198	0.462	0.760	**5.350**	**25 (10 %)**
Voltaian	572	1.289	0.001	0.200	0.590	1.295	**125.0**	**94 (16 %)**
Geological group								
Birimian	250	0.587	0.007	0.293	0.480	0.758	**3.200**	**11 (4 %)**
Buem	10	0.373	0.250	0.370	0.395	0.423	**0.430**	0
Tarkwaian	8	0.550	0.100	0.300	0.450	0.600	**1.600**	**1 (12.5 %)**
Eburnean	112	0.940	0.001	0.235	0.535	1.210	**5.350**	**21 (19 %)**
Mesozoic	4	0.556	0.323	0.376	0.444	0.624	**1.010**	0
Tamnean	128	0.469	0.001	0.123	0.400	0.600	**2.800**	**4 (3 %)**
Kwahu-Morago	83	0.345	0.008	0.053	0.192	0.400	**2.500**	**3 (4 %)**
Obosum	94	1.101	0.011	0.263	0.600	1.343	**8.400**	**17 (18 %)**
Oti-Pendjari	395	**1.532**	0.001	0.275	0.670	1.387	**125.0**	**74 (19 %)**
Watershed								
Black Volta	224	0.638	0.001	0.290	0.445	0.710	**4.800**	**14 (6 %)**
Lower Volta	95	1.346	0.059	0.400	0.800	**1.719**	**8.400**	**25 (26 %)**
Oti	270	1.362	0.001	0.263	0.610	1.373	**125.0**	**46 (17 %)**
White Volta	495	0.851	0.001	0.123	0.450	0.800	**69.500**	**46 (9 %)**

Notes:
(1) : Numbers are in bold when exceeding WHO guideline value for parameter of concern.

Figure 5-60 – Groundwater quality – Distribution of F values

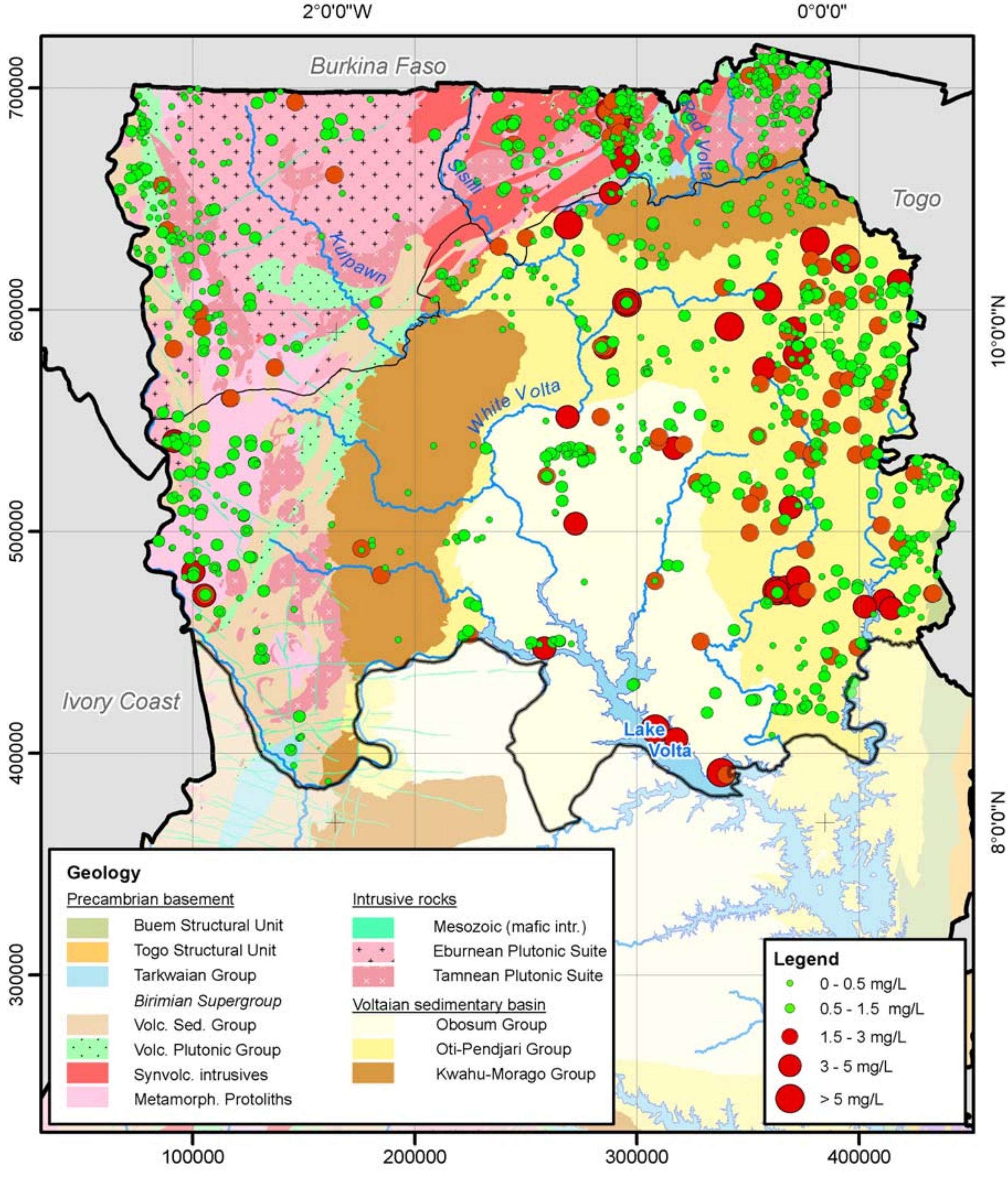

Iron and manganese

Iron and manganese are among the most abundant chemical species. The most common sources of iron and manganese in groundwater are from the result of weathering Fe-Mn-bearing minerals and rocks. Iron and manganese can also originate from industrial effluents, acid-mine drainage and sewage and landfill leachate. Typically, iron and manganese are not considered a health risk, but rather an aesthetical parameter. They can cause staining of plumbing fixtures or laundry, and an unpleasant appearance and taste.

In the HAP area, concentrations of iron and manganese have not been found to be correlated with a specific geology. High iron and manganese concentrations are often reported to be associated with aggressive groundwater (Ofosu, 2005). This would mostly affect areas where total dissolved solids values are low (i.e. areas with low electrical conductivity), thus allowing dissolution of additional solutes under low pH groundwater.

Concentrations presented in the consolidated database generally range from undetected (< 0.001 mg/L) to about 20 mg/L for Fe and about 6 mg/L for Mn. Fe concentrations close to 65 mg/L have been reported. Average concentrations for Fe and Mn are respectively of 0.20 mg/L and 0.15 mg/L. For comparison, Gill (1969) reported Fe concentrations ranging from 0.3 mg/l to 4.2 mg/L in the Precambrian basement, while a study conducted in the upper regions by Pelig-Ba (1998) reported Fe and Mn average concentrations of 0.8 mg/L and 0.04 mg/L, respectively.

Table 5-28 and 5-29 respectively present the summary statistics for iron and manganese concentrations measured in groundwater samples according to geology and watershed while Figure 5-61 and 5-62 present the distribution of these concentrations.

There is no WHO guideline value for iron regarding health hazards. Only a suggested value of 0.3 mg/L exists for taste and color. Table 5-28 indicates that 8% of all the results considered (1190 chemical analysis) present concentrations exceeding the guideline value.

Table 5-28 indicates that iron concentrations generally exceed the 0.3 mg/L guideline value in some groundwater samples in most of the groups examined. However, the average iron concentration value and the highest iron concentration measured are only encountered in the rocks of the Kwahu-Morago Group, although large concentrations are measured in other geological groups (sedimentary and crystalline rocks). The Kwahu-Morago Group consists mainly of sandstone formations.

The health-based WHO guideline value for manganese is 0.4 mg/L. Table 5-27 indicates that 6% of all the results considered (1090 chemical analysis) present concentrations exceeding the guideline value.

The results presented in Table 5-29 indicate that average manganese concentrations in groundwater samples are lower than the 0.4 mg/L guideline value in all the groups examined. However, exceeding manganese concentrations have been measured in some groundwater samples in almost each group.

The occurrence of iron and manganese in several groundwater samples would suggest an origin related to Fe-Mn-bearing minerals in the various aquifers encountered in the project area. While the highest Fe and Mn concentrations are usually found in the same areas as those characterized by aggressive groundwater, correlation between available low pH values and high iron-manganese concentrations is poor. This could be partly explained by the fact that iron concentrations can come from corrosion of hand pump parts as well as from steel casings utilized for borehole construction.

Table 5-28 – Descriptive statistics for iron in groundwater

Data group	Fe (WHO guideline value ≤ 0.3 mg/l) [1]							Analyses exceeding WHO guideline
	Number of analyses	Average	Minimum	25 perc.	Median	75 perc.	Maximum	
Northern Ghana	1190	0.204	0	0.010	0.040	0.120	**63.900**	**92 (8 %)**
Geological context								
Precambrian	300	0.224	0	0.020	0.050	0.130	**20.000**	**22 (7 %)**
Intrusive	270	0.127	0	0.010	0.030	0.100	**5.500**	**16 (6 %)**
Voltaian	620	0.225	0	0.010	0.040	0.110	**63.900**	**54 (9 %)**
Geological group								
Birimian	284	0.233	0	0.019	0.050	0.140	**20.000**	**22 (8 %)**
Buem	10	0.070	0	0.035	0.070	0.090	**0.120**	0
Tarkwaian	6	0.047	0	0.033	0.045	0.058	**0.080**	0
Eburnean	151	0.168	0	0.010	0.039	0.110	**5.500**	**11 (7 %)**
Mesozoic	4	0.042	0	0.008	0.039	0.073	**0.091**	0
Tamnean	115	0.075	0	0.004	0.020	0.080	**1.750**	**5 (4 %)**
Kwahu-Morago	96	**0.832**	0	0.010	0.040	0.110	**63.900**	**9 (9 %)**
Obosum	112	0.167	0	0.005	0.065	0.223	**1.630**	**17 (15 %)**
Oti-Pendjari	412	0.099	0	0.010	0.040	0.090	**5.100**	**28 (7 %)**
Watershed								
Black Volta	288	0.281	0	0.030	0.080	0.183	**20.000**	**32 (11 %)**
Lower Volta	108	0.139	0	0.020	0.040	0.162	**2.800**	**13 (12 %)**
Oti	264	0.104	0	0.020	0.050	0.103	**2.800**	**19 (7 %)**
White Volta	530	0.222	0	0.005	0.020	0.080	**63.900**	**28 (5 %)**

Notes:
(1) : Numbers are in bold when exceeding WHO guideline value for parameter of concern.

Figure 5-61 – Groundwater quality – Distribution of Fe values

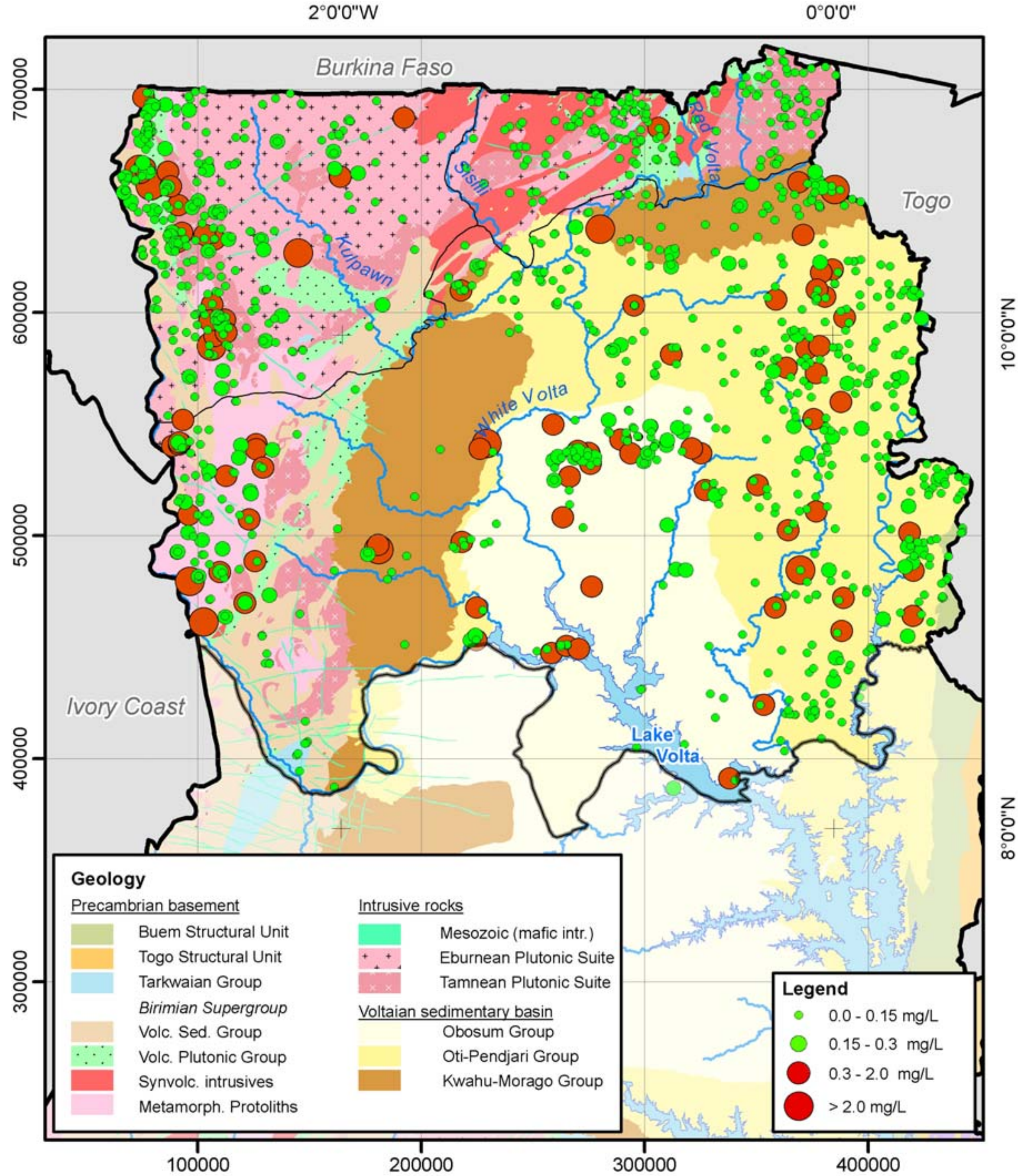

Table 5-29 – Descriptive statistics for manganese in groundwater

Data group	Mn (WHO guideline value ≤ 0.4 mg/l) [1]							Analyses exceeding WHO guideline
	Number of analyses	Average	Minimum	25 perc.	Median	75 perc.	Maximum	
Northern Ghana	1090	0.150	0	0.015	0.100	0.200	**6.100**	**68 (6 %)**
Geological context								
Precambrian	229	0.175	0	0.032	0.100	0.200	**2.790**	**18 (8 %)**
Intrusive	244	0.188	0	0.015	0.100	0.200	**3.190**	**19 (8 %)**
Voltaian	617	0.119	0	0.006	0.054	0.132	**6.100**	**31 (5 %)**
Geological group								
Birimian	222	0.177	0	0.033	0.100	0.200	**2.790**	**18 (8 %)**
Buem	1	0.001	0.001	0.001	0.001	0.001	**0.001**	0
Tarkwaian	6	0.132	0.020	0.058	0.115	0.143	**0.350**	0
Eburnean	139	0.162	0	0.012	0.100	0.200	**1.000**	**10 (7 %)**
Mesozoic	3	0.022	0.002	0.012	0.023	0.032	0.041	0
Tamnean	102	0.228	0	0.019	0.110	0.300	**3.190**	**9 (9 %)**
Kwahu-Morago	130	0.137	0	0.011	0.100	0.200	**1.400**	**10 (8 %)**
Obosum	108	0.091	0	0.010	0.044	0.100	**0.500**	**7 (6 %)**
Oti-Pendjari	379	0.121	0	0.005	0.054	0.122	**6.100**	**14 (4 %)**
Watershed								
Black Volta	251	0.188	0	0.031	0.100	0.200	**3.190**	**19 (8 %)**
Lower Volta	111	0.110	0	0.012	0.060	0.122	**1.400**	**6 (5 %)**
Oti	234	0.115	0	0.016	0.085	0.168	**0.900**	**12 (5 %)**
White Volta	494	0.148	0	0.006	0.100	0.200	**6.100**	**31 (6 %)**

Notes:

(1) : Numbers are in bold when exceeding WHO guideline value for parameter of concern.

Figure 5-62 – Groundwater quality – Distribution of Mn values

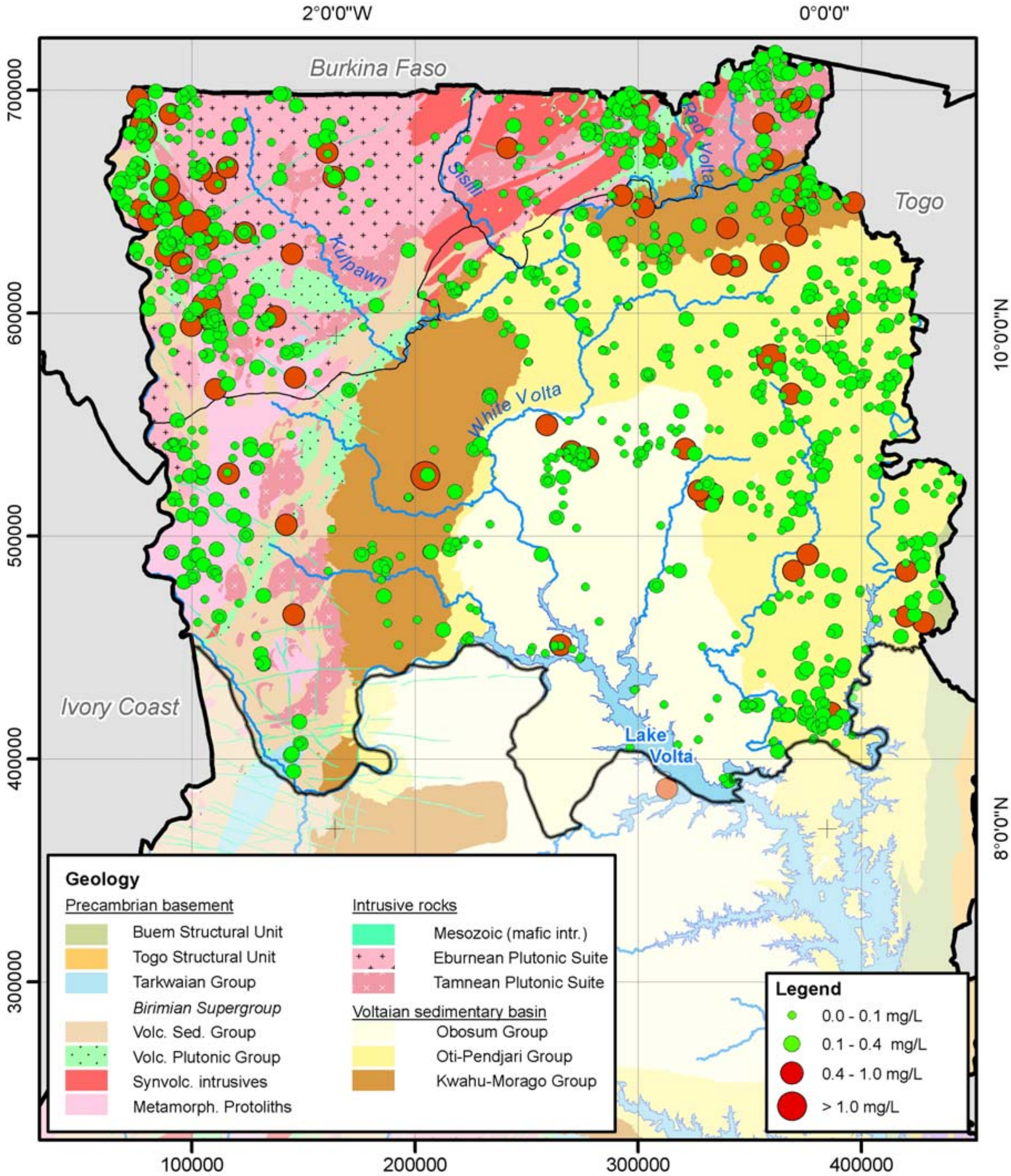

Lead

Natural occurrence of lead (Pb) in groundwater is generally limited. At neutral or alkaline pH, the solubility of Pb in groundwater is low. Oxidizing conditions such as those prevailing near the water table interface would however favor dissolution of Pb-bearing minerals. Lead is usually found in ore in the form of galena, often in combination with copper and zinc sulfides. It may also be present in sedimentary or metasedimentary formations that initially formed in reducing environments.

Little literature exists regarding the occurrence of lead in groundwaters in Ghana. Pelig-Ba *et al.* (1991) and Pelig-Ba (1999) report lead concentrations that were occasionally in excess of WHO guideline for drinking water (0.01 mg/L) in samples collected in the northern part of the

Precambrian shield and in the Voltaian basin. Pelig-Ba (1998) found lead concentrations that were generally low in groundwaters from the upper regions of Ghana (average concentration of 0.005 mg/L).

Table 5-30 present the summary statistics for lead concentrations measured in groundwater samples according to geology and watershed while Figure 5-63 presents the distribution of these concentrations.

Table 5-30 indicates that 11% of all the results considered (273 chemical analyses) present concentrations exceeding the WHO guideline value. The maximal lead concentration is recorded in a sample from the Obosum Group, while highest average concentrations are recorded in Tarkwaian and Obosum Groups. Groundwaters found in formations of the Birimian Supergroup and Oti-Pendjari Group may also display lead concentrations above WHO guideline for drinking water. Maximal lead concentration recorded in groundwater from the Tarkwaian Group ranks equal to the corresponding WHO guideline.

Based on the available data, it is not possible to determine the exact origin of lead found in groundwaters of the Precambrian basement and Voltaian sedimentary basin. WHO guideline exceedances recorded nonetheless call for the inclusion of this parameter in any groundwater quality monitoring or characterization targeting wells installed in Birimian, Obosum, Oti-Pendjari and Tarkwaian groups.

Chloride

Table 5-31 present the summary statistics for chloride concentrations measured in groundwater samples according to geology and watershed while Figure 5-64 presents the distribution of these concentrations.

Only a few number of wells (3% of the 1 486 wells considered) presented chloride concentrations above the 250 mg/l aesthetic WHO guideline value. There is no health-based guideline value. Cl concentrations generally range from undetected to about 1 000 mg/l, although a concentration as high as 21 491 mg/l was recorded in one groundwater sample. Average chloride concentration in groundwater ranks at 63.6 mg/l.

The groundwater samples with the highest concentrations have been collected in wells located in the VSB, more specifically in the rocks of the Obosum group (sandstone, mudstone and shale). Sustained evaporative processes affecting water percolating and flowing in these formations and long transit time would be the main causes of chloride ions concentration in groundwater, although other origins such as agriculture could also be involved. Groundwaters in rocks of the Oti-Pendjari group (sandstone, mudstone, shale and carbonate) and, to a lesser extent, Kwahu-Morago group (sandstone) also display high maximal chloride concentrations. In addition to Cl concentration processes mentioned previously, basal salt deposits in the Oti-Pendjari group could also be a source of Cl for groundwaters in these formations, as suggested by Kwei (1997) and further demonstrated on the basis of geochemical graphs (Figure 5-46).

Table 5-30 – Descriptive statistics for lead in groundwater

Data group	Pb (WHO guideline value ≤ 0.01 mg/l) [1]							Analyses exceeding WHO guideline
	Number of analyses	Average	Minimum	25 perc.	Median	75 perc.	Maximum	
Northern Ghana	273	0.005	0	0	0.005	0.005	**0.100**	**29 (11 %)**
Geological context								
Precambrian	75	0.006	0	0	0.005	0.005	**0.026**	**10 (13 %)**
Intrusive	45	0.001	0	0	0	0	**0.005**	**0**
Voltaian	153	0.006	0	0	0.005	0.005	**0.100**	**19 (12 %)**
Geological group								
Birimian	71	0.005	0	0	0.008	0.026	**0.026**	**10 (14 %)**
Buem	-	-	-	-	-	-	-	-
Tarkwaian	4	0.008	0.005	0.005	0.005	0.010	**0.010**	0
Eburnean	24	0.002	0	0	0	0.005	**0.005**	0
Mesozoic	3	0	0	0	0	0	**0**	0
Tamnean	18	0.001	0	0	0	0	**0.005**	0
Kwahu-Morago	17	0.001	0	0	0	0.005	**0.005**	0
Obosum	68	0.008	0	0.001	0.005	0.01	**0.100**	**11 (16 %)**
Oti-Pendjari	68	0.004	0	0	0	0.005	**0.038**	**8 (12 %)**
Watershed								
Black Volta	88	0.005	0	0	0.005	0.005	**0.026**	**10 (11 %)**
Lower Volta	47	0.009	0	0	0.005	0.010	**0.100**	**8 (17 %)**
Oti	17	0.003	0	0	0	0.001	**0.038**	**1 (6 %)**
White Volta	121	0.003	0	0	0	0.005	**0.040**	**10 (8 %)**

Notes:
(1) : Numbers are in bold when exceeding WHO guideline value for parameter of concern.

Figure 5-63 – Groundwater quality – Distribution of Pb values

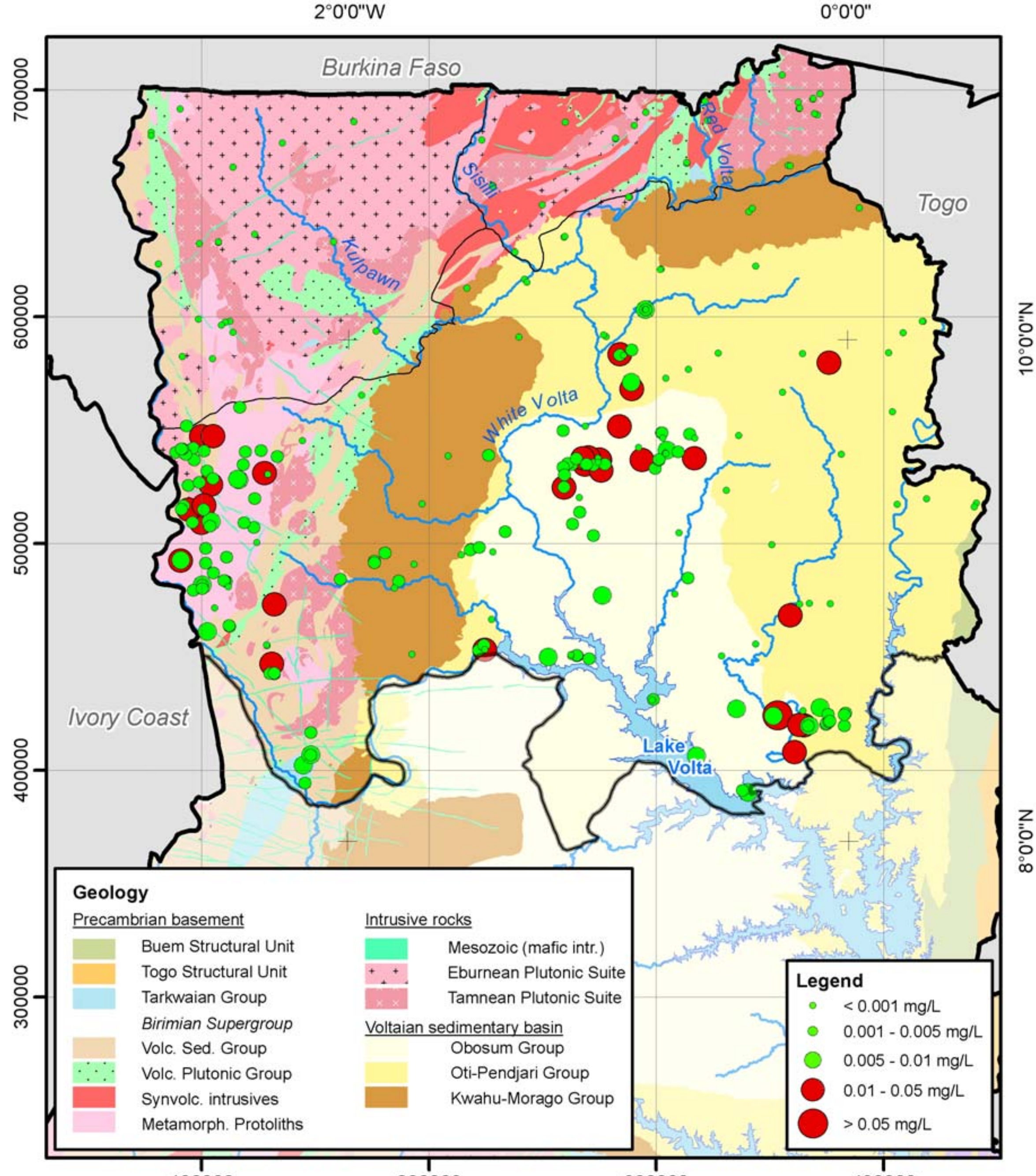

Table 5-31 – Descriptive statistics for chloride in groundwater

Data group	Cl (WHO guideline value ≤ 250 mg/l) [1]							Analyses exceeding WHO guideline
	Number of analyses	Average	Minimum	25 perc.	Median	75 perc.	Maximum	
Northern Ghana	1486	63.6	0.003	1.157	7.9	20.0	**21490.6**	**46 (3%)**
Geological context								
Precambrian	388	10.7	0.10	1.0	5.0	10.9	**187.0**	0
Intrusive	341	6.9	0.020	0.6	1.7	6.6	**98.0**	0
Voltaian	757	116.2	0.003	5.0	15.0	31.0	**21490.6**	**46 (6 %)**
Geological group								
Birimian	368	10.7	0.010	1.0	4.6	10.9	**98.0**	0
Buem	10	10.2	4.0	8.0	8.8	13.5	**15.0**	0
Tarkwaian	10	10.4	0.10	1.9	6.5	7.9	**55.0**	0
Eburnean	173	8.9	0.020	0.9	2.0	7.8	**95.0**	0
Mesozoic	9	6.1	1.0	2.0	3.6	12.0	**15.4**	0
Tamnean	159	4.7	0.028	0.30	1.2	4.6	**98.0**	0
Kwahu-Morago	105	33.8	0.003	4.0	12.0	20.0	**1393.0**	**2 (2 %)**
Obosum	141	347.1	0.030	6.0	17.3	80.8	**21490.6**	**21 (15 %)**
Oti-Pendjari	511	69.4	0.010	4.5	15.6	31.2	**6165.0**	**23 (4.5 %)**
Watershed								
Black Volta	356	11.7	0.010	1.2	5.0	11.0	**187.0**	0
Lower Volta	133	273.5	0.030	10.0	18.0	60.0	**21490.6**	**15 (11 %)**
Oti	325	69.0	0.010	10.0	17.0	29.0	**6165.0**	**12 (4 %)**
White Volta	672	46.8	0.003	0.70	3.8	15.0	**2897.0**	**19 (3 %)**

Notes:
(1) : Numbers are in bold when exceeding WHO guideline value for parameter of concern.

Figure 5-64 – Groundwater quality – Distribution of Cl values

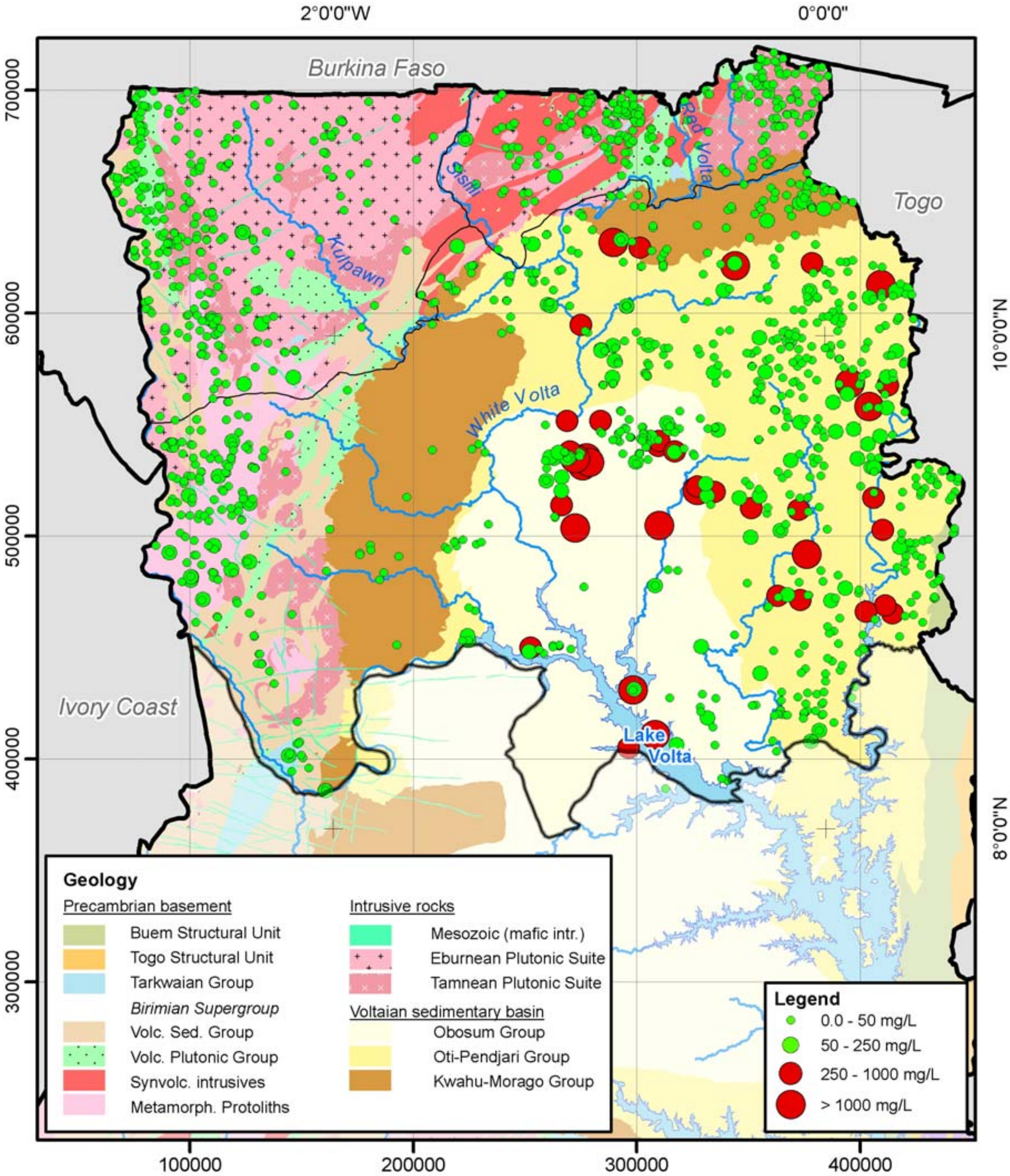

<u>Other natural geochemical parameters</u>

Geochemical data considered in the current analysis show that copper in concentrations above the WHO guideline for drinking water have been detected twice in a total of 365 groundwater samples and sampling locations. The two exceedances ranked at 2.5 and 5 mg/L, while the WHO guideline is set at 2 mg/L. They were recorded in wells installed in formations of the Birimian Supergroup. Average Cu concentration in groundwaters of the Birimian is equal to 0.12 mg/L, while average Cu concentration over the whole project area is equal to 0.07 mg/L. Cu detected in groundwater would likely originate from units with small and local concentrations of Cu-sulfides. As such Cu-bearing minerals are localized; the occurrence of high Cu concentrations in groundwater would be quite local and only affect areas of small extent. It would also be essentially concentrated in Birimian Supergroup.

Zinc in concentrations above the WHO guideline for drinking water was also detected twice, over a total of 633 groundwater samples and sampling locations. The two exceedances ranked at 5 and 24 mg/L, while the WHO guideline is set at 3 mg/L. They were recorded in wells installed in formations of the Oti-Pendjari Group. Average Zn concentration in groundwaters of the Oti-Pendjari is equal to 0.27 mg/L, while average Zn concentration over the whole project area is equal to 0.15 mg/L. Existence of elevated Zn concentration in groundwater may originate from the presence of units with small and local concentrations of Zn-sulfide, such as sphalerite. It could also be linked the presence of sphalerite in shales of the Oti-Pendjari Group. A concentration of 24 mg/L suggests the existence of a nugget effect that would rather correspond to a concentration of Zn-bearing minerals located in relative proximity with the monitoring point. Geochemical data indicate that, similar to Cu, high Zn concentrations would essentially be localized.

5.4.7.3 Groundwater contamination

Groundwater resources are potentially vulnerable to contamination from human activities. In northern Ghana, these activities include primary agriculture and the lack of efficient sanitation systems, but also some commercial and industrial activities. The latter can produce accidental oil spills, or metal leaching from the disposal of wastes (batteries, paint, and old household items) that could lead to groundwater contamination, if pollutants can infiltrate the soil and reach the water table.

Although numerous data on nitrate and nitrite concentrations are compiled in the consolidated database, limited microbiological parameters are available in order to address this groundwater contamination issues. An interpretation of existing data, updated with analytical results from samples collected in the first phase of groundwater sampling of the HAP, is presented hereafter.

Nitrates and nitrites

Nitrates (NO_3) are naturally occurring in the environment. They are present in all plants in various concentrations. Nitrites (NO_2) are less abundant, except in reducing environments, because nitrogen is more stable under the form of nitrates under oxidizing conditions. Nitrogen compounds in waters are typically the result of human contamination. More specifically, the application of inorganic nitrogenous fertilizers and manure in agriculture, wastewater disposal, and human and animal excrements are causes of nitrogen contamination, when nitrates are leached into groundwater. Thus, data on nitrate and nitrite content can provide some information regarding groundwater contamination of hydrogeological systems, as well as indications of the vulnerability of the groundwater supplies to surface contamination.

The WHO guideline value for nitrates is 50 mg/L (as NO_3), and 3 mg/L for nitrites (as NO_2). Although nitrates and nitrites are typically expressed in water quality studies as NO_3 and NO_2, they are also often expressed as their nitrogen content. For instance, the values included in the consolidated database are expressed as nitrate-nitrogen (NO_3-N), and nitrite-nitrogen (NO_2-N) concentrations. In this case, the WHO recommended guideline values for nitrate-nitrogen is 10 mg/L (as NO_3-N), and 1 mg/L for nitrites (as NO_2-N) (WHO, 2008).

Nitrate-nitrogen data in the consolidated database indicate concentrations generally below the 10 mg/L guideline value. Values range from undetected to concentrations of up to 171 mg/L. The average NO_3-N concentration is 3.9 mg/L for all existing data. The highest concentrations are generally observed near larger communities (Bole, Walewale, Bongo), which suggest sources of anthropogenic nature.

The consolidated database was examined again according to geology and watersheds. Descriptive statistics of nitrates and nitrites were calculated for each groups examined using the data included in the database. Table 5-32 and 5-33 present the results. Figure 5-65 presents the distribution of nitrate concentrations.

Table 5-32 – Descriptive statistics for nitrate in groundwater

Data group	NO_3-N (WHO guideline value ≤ 10 mg/l) (1)							Analyses exceeding WHO guideline
	Number of analyses	Average	Minimum	25 perc.	Median	75 perc.	Maximum	
Northern Ghana	1133	3.912	0	0.090	0.400	1.900	**171.0**	**99 (9 %)**
Geological context								
Precambrian	306	3.648	0.001	0.120	0.700	2.775	**155.757**	**26 (8 %)**
Intrusive	311	6.500	0.003	0.135	0.800	3.550	**171.0**	**41 (13 %)**
Voltaian	516	2.580	0	0.037	0.180	0.708	**92.348**	**32 (6 %)**
Geological group								
Birimian	296	3.721	0.006	0.120	0.700	2.800	**155.757**	**26 (9 %)**
Buem	2	0.071	0.001	0.036	0.071	0.105	**0.140**	0
Tarkwaian	8	1.850	0.140	0.273	1.355	2.590	**5.100**	0
Eburnean	158	7.319	0.004	0.123	0.800	3.175	**139.419**	**25 (16 %)**
Mesozoic	4	6.890	0.021	0.530	0.712	7.072	**26.114**	**1 (25 %)**
Tamnean	149	5.620	0.003	0.158	0.900	3.700	**171.0**	**15 (10 %)**
Kwahu-Morago	80	1.559	0	0.100	0.201	1.061	**19.483**	**4 (5 %)**
Obosum	121	3.202	0.002	0.011	0.120	0.800	**54.957**	**9 (7 %)**
Oti-Pendjari	315	2.600	0.001	0.037	0.200	0.700	**92.348**	**19 (6 %)**
Watershed								
Black Volta	294	3.944	0.003	0.120	0.500	1.800	**171.0**	**18 (6 %)**
Lower Volta	82	2.801	0.002	0.040	0.300	0.843	**54.957**	**6 (7 %)**
Oti	192	1.747	0.001	0.100	0.200	0.500	**57.483**	**8 (4 %)**
White Volta	565	4.857	0	0.053	0.500	3.040	**139.419**	**67 (12 %)**

Notes:

(1) : Numbers are in bold when exceeding WHO guideline value for parameter of concern.

Table 5-33 – Descriptive statistics for nitrite in groundwater

Data group	NO_2-N (WHO guideline value ≤ 1 mg/l) [1]							Analyses exceeding WHO guideline
	Number of analyses	Average	Minimum	25 perc.	Median	75 perc.	Maximum	
Northern Ghana	823	0.088	0	0.001	0.004	0.011	**23.0**	**10 (1 %)**
Geological context								
Precambrian	202	0.017	0	0.001	0.003	0.012	**0.495**	0
Intrusive	177	0.100	0	0.001	0.004	0.016	**6.100**	**4 (2 %)**
Voltaian	444	0.123	0	0.001	0.004	0.009	**23.0**	**6 (1 %)**
Geological group								
Birimian	188	0.018	0	0.001	0.003	0.013	**0.495**	0
Buem	8	0.004	0.002	0.003	0.004	0.006	**0.007**	0
Tarkwaian	6	0.001	0.001	0.001	0.001	0.001	**0.001**	0
Eburnean	93	0.116	0	0.001	0.004	0.020	**6.100**	**2 (2 %)**
Mesozoic	4	0.008	0	0	0	0.008	**0.031**	0
Tamnean	80	0.086	0	0.001	0.003	0.011	**3.780**	**2 (2.5 %)**
Kwahu-Morago	75	0.104	0	0.002	0.005	0.012	**6.350**	**1 (1 %)**
Obosum	72	0.079	0	0.001	0.001	0.001	**2.345**	**2 (3 %)**
Oti-Pendjari	297	0.138	0	0.002	0.005	0.009	**23.0**	**3 (1 %)**
Watershed								
Black Volta	180	0.036	0	0.001	0.002	0.020	**3.780**	**1 (1 %)**
Lower Volta	80	0.013	0	0.001	0.001	0.006	**0.501**	0
Oti	216	0.175	0	0.003	0.005	0.009	**23.0**	**2 (1 %)**
White Volta	347	0.087	0	0.001	0.004	0.012	**6.350**	**7 (2 %)**

Notes:

(1) : Numbers are in bold when exceeding WHO guideline value for parameter of concern.

Figure 5-65 – Groundwater quality – Distribution of NO_3-N values

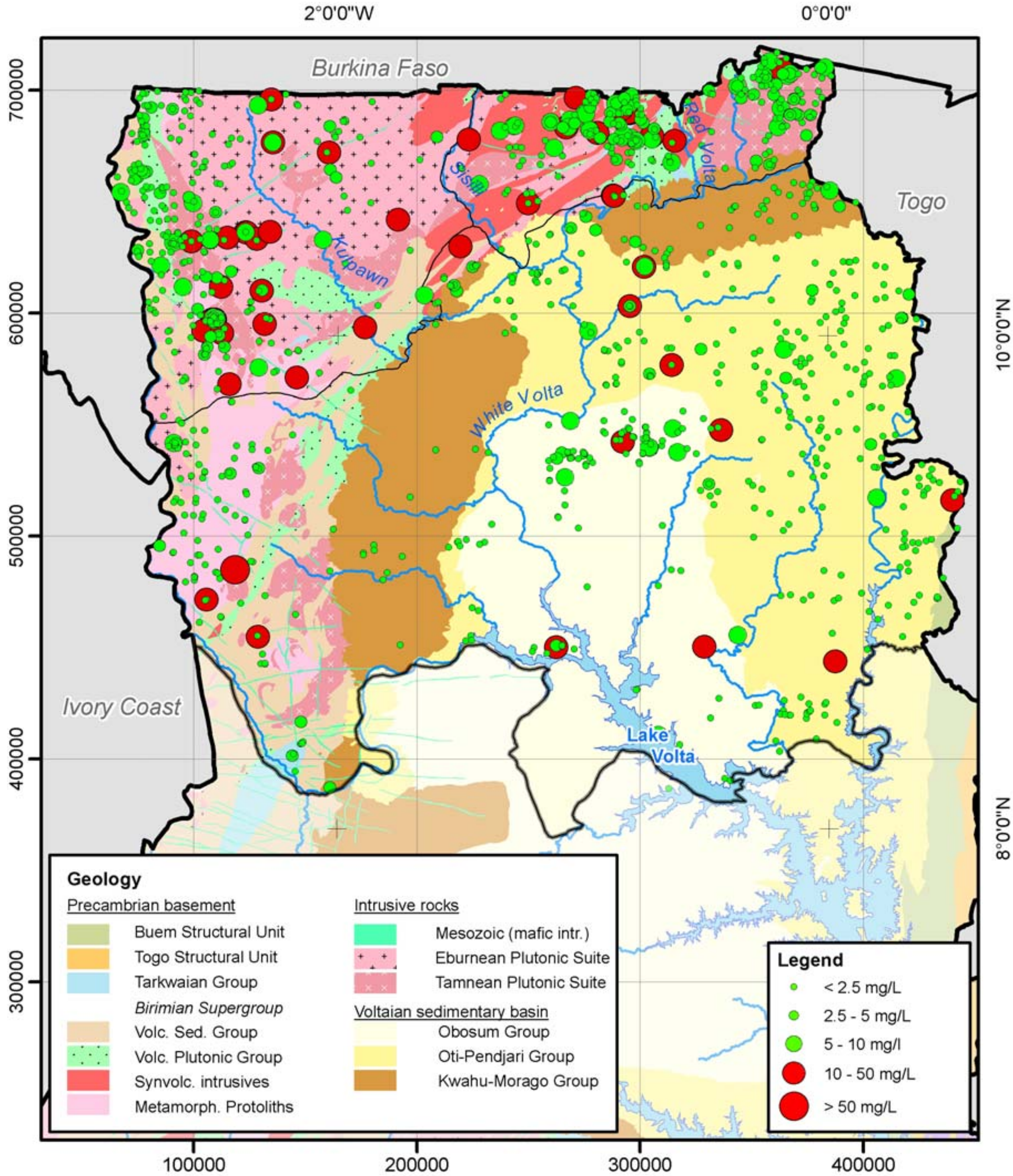

Table 5-32 shows that nitrate-nitrogen concentrations exceed the 10 mg/L WHO guideline value in a limited number of groundwater samples (8.7% of 1133 chemical analyses). The results from Table 5-33 also indicate that a very few groundwater samples (1.2% of 823 chemical analyses) display nitrite-nitrogen concentrations in excess of the 1 mg/L WHO guideline value. Average concentrations in NO_3-N and NO_2-N are all below the guideline values. The highest NO_3-N concentrations measured are encountered in the intrusive rocks of the Tamnean Plutonic Suite and the sedimentary rocks the Oti-Pendjari Group. The highest NO_2-N concentrations measured are encountered in this latter geological unit and, to a lesser extent, in sedimentary rocks of the Kwahu-Morago Group and intrusive rocks of the Eburnean Plutonic Suite.

Large NO_3-N and NO_2-N concentrations have been measured in the Black Volta, Oti River and White Volta watersheds. On the basis of available data, no relationship appears between nitrates or nitrites concentrations measured in groundwater samples and watersheds within which the monitoring stations are located.

Other geochemical parameters related to potential contamination

The consolidated database contains only a few results of analyses made for total coliforms (63 results) and E. coliforms (6 results). Furthermore, little details are included in the database on the methods used for sampling; sample preservation and transport; and analysis. Consequently, it is difficult to confirm if groundwater is in fact contaminated, because this type of analysis is very sensitive to the method of sampling and preservation.

As previously discussed, the poor sanitation coverage in the project area, the typical well setup and the lack of groundwater protection (i.e. wellhead protection areas) are conditions favorable for groundwater contamination from surface activities. This potential for surface contamination is suggested by the presence of nitrate concentrations mentioned in the previous section, especially near large communities. Due to the few number of analyses included in the database, the results are probably not adequately representing the groundwater quality regarding microbiological parameters. Therefore, it is recommended to carry out a more accurate analysis of potential microbiological contamination in future groundwater quality assessment programs. However, due to logistical limitations (transport, conservation), sensitive sites (e.g. near large wells supplying important communities) should be prioritized for groundwater sampling for microbiological parameters.

5.4.7.4 Additional controls on groundwater quality

Results of section 5.4.7.2 highlighted the control that geology and lithology have on the quality of groundwater. Alternatively, interpretations put forward in section 5.4.7.3 suggest that other factors, such as well depth, can also influence the occurrence and concentrations magnitude of specific elements or compounds in groundwater. Efforts have been made to investigate possible relationships between recorded concentrations in the various groundwater samples and a number of parameters that could impact or control geochemical processes up gradient from or in the vicinity of the monitored well (or borehole). Three parameters were considered for the analysis: regolith thickness, depth of the screened interval mid-point, and hydrostratigraphical units intersected by the well (or borehole). Where no screen was installed, the mid-point of the borehole portion open to geological formations was considered.

Quantitative and qualitative correlation analyses were carried out in order to detect potential trends between either one of these parameters and recorded concentrations for the various elements and compounds. The analysis aims at identifying possible relationships, pinpointing specific explanations for the existence, or absence, of any given relationship falls outside of its scope.

Table 5-34 summarizes the main findings of the quantitative and qualitative correlation analyses. Exposed results are discussed subsequently. Determination coefficients were calculated between regolith thickness at each sampling location (well or borehole) and concentrations recorded for the various elements and compounds of interest, on the basis of the geological unit from which groundwater sample was collected. The same procedure was carried out for the parameter “depth of the screened interval mid-point”. Calculated R^2 are presented for each geological unit where a certain relationship was detected. In the case of the hydrostratigraphical units, comparison was made between descriptive statistics of concentrations recorded in each of the three different units (RG: regolith; RG-RK: regolith-bedrock; RK: bedrock), on the basis of the various geological units. When similar in pattern, single geological units have been regrouped. Again, results are only presented for cases where coherent patterns were identified.

Table 5-34 – Correlation analysis results related to groundwater quality data

Element	Regolith thickness	Depth of the screened interval mid-point	Hydrostratigraphical unit
Arsenic	-	-	VSB: [RG] > [RG-RK] & [RK]
Fluoride	Tamnean: R^2 = 0.10 KM: R^2 = 0.09	Tamnean: R^2 = 0.11 Obosum : R^2 = 0.19	VSB: [RK] > [RG-RK] & [RG] Prec. & Intr.: [RG-RK] > [RG] & [RK]
Iron	-	-	KM: [RG-RK] > [RK] & [RG]
Manganese	Birimian: R^2 = 0.09	-	-
Lead	-	Birimian: R^2 = 0.10	-
Chloride	KM: R^2 = 0.20	-	[RK] > [RG-RK] & [RG]
Nitrates	Obosum: R^2 = 0.09	Obosum : R^2 = 0.15	VSB: [RG] > [RG-RK] > [RK] Prec. & Intr.: [RG-RK] > [RG] > [RK]
Nitrites	-	-	VSB & Birimian: [RG] > [RG-RK] > [RK]

Positive correlations were identified between regolith thickness and fluoride concentrations in samples from the Tamnean Plutonic Suite and Kwahu-Morago Group. Similar results were obtained for manganese concentrations, chloride concentrations and nitrates concentrations in samples from the Birimian Supergroup, the Kwahu-Morago Group and Obosum Group, respectively. Calculated R^2 ranges between 0.09 and 0.20. Such values can be considered as low in terms of the quality of the correlation. Construction of scatter plots for the various relations studied showed that a significant number of data pairs did not match the proposed correlation. It is suggested that a relationship between regolith thickness and concentrations recorded exists only in specific instances and under certain conditions. In other instances, regolith thickness would have no control over the geochemistry of groundwater flowing at a given well or borehole. The existence or absence of significant percolation in the vicinity of the sampled well or borehole could be a factor determining the existence or absence of such relationship.

Positive correlations were identified between depth of the screened interval mid-point and fluoride concentrations in samples from the Tamnean Plutonic Suite and Obosum Group. Similar results were obtained for lead and nitrates concentrations in samples from the Birimian Supergroup and the Obosum Group, respectively. Calculated R^2 range between 0.10 and 0.19 and correspond to a weak correlation. Constructed scatter plots for the various relations studied yielded the same observations as those highlighted for regolith thickness correlation analysis. Again, the existence or absence of significant percolation in the vicinity of the sampled well or borehole could be a factor determining the existence or absence a relationship between depth of the screened interval mid-point and concentrations recorded.

Groundwater samples collected from Voltaian sedimentary basin formations generally display higher arsenic concentrations when collected in wells open to the regolith (exclusively). In the case of fluoride, it is rather samples collected from bedrock that would display higher concentrations. In the case of Precambrian basement and Intrusive rocks contexts, it is samples originating from the regolith-bedrock interface that generally show the highest fluoride concentrations. The fact that regolith-bedrock interface in Precambrian basement and Intrusive rocks contexts is generally found at depths greater than in the VSB context could explain this discrepancy.

Iron concentrations in groundwaters of the Kwahu-Morago Group appear to be greater at the regolith-bedrock interface.

A trend that applies to all geological units is the occurrence of higher chloride concentrations in groundwater samples originating from bedrock. This suggests that accumulation of chloride in groundwater would proceed in a downward fashion, corresponding to more evolved groundwater, and that main flow paths of Cl-rich groundwaters are located in bedrock.

A strong vertical gradation in both nitrates and nitrites concentrations exists in VSB formations, where the highest concentrations are generally recorded in groundwaters of the regolith, while the lowest are recorded in groundwaters flowing in bedrock. The same trend exists for nitrites in Birimian Supergroup formations. These results underscore the facts that the two compounds originate from surface and that shallower units are more exposed to this type of contamination. In the case of nitrates in the Precambrian basement and Intrusive rocks, the highest concentrations are generally recorded at regolith-bedrock interface.

Although some trends have been highlighted with regard to possible control of the three parameters over groundwater quality, most are statistically non-significant, and their ability to explain the variability of elements/compounds concentrations in groundwater is limited at best. Such results underscore the fact that local lithology and mineralogy as well as hydrological and hydrogeological processes at the catchment scale exert the greatest control over groundwater chemistry.

5.4.7.5 Groundwater quality issues

The results included in the consolidated HAP database have demonstrated that the natural groundwater quality exceeds WHO guideline values for several physicochemical parameters in some areas of the project characterized by distinct geological groups, notably the sedimentary rocks from the VSB. For instance, groundwater in the Oti-Pendjari Group often displays poor quality in comparison with sedimentary formations of the Kwahu-Morago Group as well as intrusive and metamorphic formations of the Precambrian basement. The parameters of concern in the Oti-Pendjari Group are primarily arsenic, fluoride, chloride and nitrates. Some high fluoride concentrations have however been reported in all geological groups. Groundwaters in the Obosum Group may also display mediocre quality with regard to iron, lead and chloride.

Average iron and manganese concentrations have been measured at high levels in the Kwahu-Morago Group especially, although large concentrations are observed in almost all geological groups examined. It has been reported that iron and manganese could be associated with corrosion of well casing. Therefore, it will be required in further studies to examine natural iron and manganese concentrations in water with respect to well casing physical conditions.

The chemical results included in the consolidated database also suggest that groundwater quality in surface wells and boreholes can be affected by surface contamination. However, the results do not indicate major problems related to nitrates or nitrites in boreholes. There are also too few available analytical results to assess the situation regarding microbiological contamination.

Nitrate concentrations obtained from pore water analysis carried out for the CMB indicated that concentrations in a few locations are increasing at shallow depths, which suggest that groundwater quality issues related to nitrate could increase in the future. Following these observations and since adequate sanitation coverage in rural Ghana is relatively limited, nitrates and nitrites should be analyzed systematically in monitoring wells in addition with some microbiological analyses.

The determination of the natural geochemical characteristics and quality of groundwater in the project area is a critical part in the groundwater resource planning process. Indeed, the development of groundwater resources can be limited by the occurrence of high natural concentrations in some chemical species, or by poor water quality, which will affect the development of the resource. For instance, poor water quality may require the use of costly water treatment systems in order to be used as water supply. Poor water quality may also deteriorate faster pumping and distribution equipments, which increase the cost of development. Furthermore, the use of poor quality water may induce health problems on local people increasing the cost for healthcare.

Thus, the quality of the groundwater can influence water supply options, e.g. the selection between surface water (when available) and groundwater. Consequently, although numerous data has already been collected on some critical physicochemical parameters, these results need to be validated and completed in the most sensitive areas by continued monitoring. Amongst other objectives, future sampling campaigns should target the production of arsenic concentration results representative of actual groundwater chemistry.

5.5 Groundwater resources sustainability

The information and data that were collected and analyzed in the course of this hydrogeological synthesis are used in the present section to evaluate and compare current groundwater use to estimated groundwater recharge rates. This exercise is by no means a comprehensive assessment of groundwater resources sustainability and therefore cannot predict if aquifer mining will or will not occur locally. However, it is intended to provide estimates on the amount of recharge used at regional scale, which can be used by water sector stakeholders in groundwater resources management and development until more accurate figures become available. The following assumptions were considered for calculations: 1) pumping occurs under steady state conditions (i.e. no removal of water from storage) and 2) groundwater recharge is not significantly affected by pumping (Devlin and Sophocleous, 2005).

Data from the HAP consolidated database indicate that most boreholes in northern Ghana are equipped with Afridev Modified India Mark II or Nira 85 pumps for which the discharge rate ranges from 0.6 to 1.7 m^3/h. Thus, assuming an average discharge rate of 1.0 m^3/h (or ~ 17 L/min) and an average daily pumping duration of 8 h/day (Martin and van de Giesen, 2005), the annual average production for a typical borehole fitted with a handpump would be around 2 920 m^3/y. The total groundwater production from the 5 958 unique and reliable boreholes (excluding dry or technically negative boreholes) in HAP's consolidated database would therefore be around 17.4 Mm^3/y. As data on hand-dug wells and groundwater-fed piped systems were not available (i.e. number of installations, discharge rates, operation period …), production rates for such installations were estimated using data from Martin and van de Giesen (2005) for the Volta Basin in 2001. Assuming that groundwater production ratios (e.g. hand-dug well production over total groundwater production) were similar to those estimated in the study by Martin and van de Giesen (2005), production rates were respectively estimated to 4.1 and 2.3 Mm^3/y for hand-dug wells and piped systems. The resulting average abstraction rates per installation would be 0.8 m^3/h for hand-dug wells (4 h/day for 10 months per year) and 7.4 m^3/h for groundwater-fed piped systems (24 h/day all year). Considering abstraction from springs is not significant at regional scale, the total groundwater production would be around 23.8 Mm^3/y. Table 5-35 summarizes the groundwater production estimates.

Estimates from the soil moisture balance exercise reveal that groundwater recharge would vary between 1.8 % and 15.9 % of local rainfall or 1 856 and 20 029 Mm^3/y for the study area (i.e. 97 704 km^2). These values would suggest that the estimated groundwater production would be between 0.1 % and 1.3 % of annual estimated groundwater recharge. Natural groundwater discharge (e.g. to surface water bodies) would thus be between 1 833 and 20 006 Mm^3/y. Similar values could be derived from groundwater recharge estimates obtained from the chloride mass balance. In comparison, Martin and van de Giesen (2005) estimated that 0.7 % of average annual groundwater recharge was used by groundwater production installations in the Volta River basin. Lutz *et al.* (2007) also assessed groundwater resource sustainability in the Nabogo River basin using a numerical model developed in MODFLOW. The different scenarios simulated with the numerical model yielded ratios of annual groundwater recharge ranging from 0.2 to 2.5 %. Another recent study in southern Burkina Faso (Sandwidi, 2007) yielded a slightly higher ratio of 3 % of annual groundwater recharge.

Table 5-35 – Estimated groundwater production in northern Ghana based on data from the consolidated database and Martin and van de Giesen (2005)

Installation type	Number of installation	Estimated avg. abstraction rate per installation (m^3/h)	Estimated annual abstraction rate for study area (Mm^3/y)
Boreholes	5 958 (1)	1.0	17.4
Hand-dug wells	3 960 (2)	0.8	4.1 (3)
GW-fed piped systems	36 (2)	7.4	2.3 (3)
		Total	23.8

Notes:
(1) : Unique boreholes with reliable coordinates, excluding dry or tech. negative boreholes
(2) : Numbers taken from Martin and van de Giesen (2005) for Volta basin in 2001 (N.B.: only modern hand-dug wells are considered)
(3) : Rates estimated with gw production ratios in Ghanaian part of Volta basin from Martin and van de Giesen (2005), i.e. 73 %, 17 % and 10 % for bh, hand-dug wells and piped systems

While further investigations are needed in order to better estimate input parameters (i.e. number of groundwater production installations and their discharge rates), figures obtained on the proportion of recharge actually used are in the same order of magnitude as those estimated from previous studies. As mentioned in these studies, this suggests that renewable groundwater resources would not presently be overexploited at regional scale even though the number of wells drilled is rapidly increasing.

While the quantity of groundwater seems adequate for present needs at regional scale, other factors must also be considered for the sustainability of groundwater resources in northern Ghana. Locally, the quality of groundwater can be problematic as pointed out in the previous section. For certain areas, anthropogenic contamination, notably by nitrates from fertilizers used in agriculture or by inadequate sanitation facilities, can affect the quality of groundwater. Available data do not reveal any widespread problems related to nitrate, but hand-dug wells, which were not covered by this synthesis, could present higher nitrate concentrations as they are usually shallower and sometimes unprotected at the surface. Further investigations are thus needed to document the extent of this potential problem in space and time as little information is available concerning such aquifer contamination in northern Ghana. In general, the quality of groundwater is however superior to that of surface water.

Another issue concerns the sustainability of groundwater production installations. Many wells, mostly those constructed with open-hole design, are abandoned at some point for technical problems such as siltation, caving or increasingly low yield. As stated in Akudago *et al.* (2007), construction of open-hole wells may be relatively cheaper than lined wells but their life span is shorter (i.e. 15 years on average compared to 40 years for lined wells). While clogged-up wells can sometimes be rehabilitated, open-hole wells should not be encouraged as they cannot adequately serve the beneficiary community in terms of cost and long-term sustainability. Maintenance of the wells and handpumps is also of concern when assessing the sustainability of groundwater production. Efforts have been made in the past (1990's) to equip wells with the same four handpump models (Ghana Modified India Mark II, Afridev, Nira and Vernet) to facilitate spare part availability. However, as of 2002, spare parts provision were still subsidised to some level as commercial viability of handpump spares in Ghana was in doubt (Harvey *et al.*, 2002).

5.6 Reporting framework for state of groundwater resources

A thorough understanding of regional hydrogeology is the necessary basis for the sustainable management of groundwater resources. This is particularly true for semi-arid areas such as northern Ghana. The Hydrogeological Assessment Project (HAP) of the northern regions of Ghana thus aimed to improve the knowledge base as well as the capacity that would allow WRC to carry out informed groundwater resource management. As documented in this report, the HAP has contributed to the knowledge base through a wide range of activities: integration of existing groundwater data bases; compilation of reports and scientific papers relevant to Ghana groundwater resources; integration of geological, hydrogeological and groundwater quality data; compilation of weather and hydrologic data; development of a network of monitoring boreholes to follow both groundwater levels and quality; the measurement of chlorides in water from precipitation and extracted from soil from the vadose zone, which served as a basis for recharge estimation. These data allowed the development of the hydrogeological synthesis presented in this report. HAP also involved capacity development activities aimed both at the WRC and the Ghana water resources stakeholders.

On the basis of this knowledge base and enhanced capacity, WRC is in a better position to carry out the following core activities of groundwater resources management. These activities, which are already mostly part of the WRC mission, can be summarized as follows:

- Information archiving: the HAP produced a virtual library including a compilation of electronic reports and relevant scientific papers related to groundwater resources in Ghana. WRC could continue to digitize and compile the new reports received as well as key existing reports to insure their long-term preservation.
- Hydrogeological database update and maintenance: the WRC Water Resources Database is an important tool that will provide the necessary data to support the decision-making process regarding groundwater resources exploitation and protection. As such, this tool should not remain static, but should rather be continuously updated with new data extracted from reports submitted to the WRC. Present regulations impose the submission of reports but it would facilitate the integration of data in the database if the data were submitted to the WRC using a template compatible with the database structure and data fields. This would be especially important for large water supply projects that have the resources necessary to integrate their data in the template. Tentative data entry form templates that could be used for this purpose were developed under HAP (see Volume 2 of HAP Final Technical Report, titled Water Resources Database Development Report). These templates could be distributed to water supply projects to standardize data entry.
- Monitoring network: the groundwater monitoring network is a major infrastructure whose importance and worth will increase as continuous quality data are acquired over the long-term (over 15 years). The data from monitoring can be a source of increased understanding about aquifer dynamics and recharge. Monitoring will also identify the effect on resources of groundwater abstraction activities as well as climate change. Key questions that are difficult to address without sound monitoring data. Maintenance and use of the monitoring network involves a relatively heavy logistics and significant human and monetary resources to download and maintain divers and do regular groundwater sampling and analysis. Needed resources will be needed to maintain this key tool of sustainable groundwater resources management.
- Knowledge development: the HAP hydrogeological synthesis presented in this report offers an initial level of understanding about groundwater resources in northern Ghana. However, there are numerous possibilities for follow-up work based on HAP data and results, as well as other studies of interest. Such follow-up studies could include the following: further characterization of deep boreholes and the evaluation of the deep groundwater potential; further sampling and analysis (chloride and nitrate) of shallow hand-dug wells to enhance the spatial estimation of recharge; an integration and interpretation of water level data from the monitoring network after the acquisition over 5-year of data; development of numerical models of selected watersheds to better understand groundwater dynamics; enhanced

analysis of the HAP groundwater geochemical data; post-audit of the geophysical siting data available for monitoring wells installed by the HAP; local hydrogeological studies based on the WRC Groundwater Database in areas targeted for increased groundwater use to estimate the sustainable level of water use, especially in areas of interest for SADA.

- GW data sharing: the dissemination and sharing of data to other agencies of the water sector and to water supply projects is an important function of the WRC. The data can include borehole data from the database as well as maps and reports from the virtual library. This data sharing function could also be extended to the development of technical and scientific collaborations within Ghana and also internationally (within and outside Africa). Such collaborations would enhance the capacity of WRC and allow the sharing of its own competence and experience. Data sharing is a time consuming activity that could require dedicated resources and staff at the WRC.
- Regulations and permitting: the WRC is responsible for the development of regulations related to the sustainable management of groundwater resources as well as the permitting of activities related to water supply projects. These regulations also provide opportunities to favour the sustainable acquisition and preservation of new data in the WRC Groundwater Database. In turn, the data and knowledge in the custody of the WRC provide an informed base for its permitting and regulatory decisions.
- Reporting on the state of groundwater resources: even though the WRC already carries out a broad range of groundwater resources management activities, it should be provided with the resources required to regularly report on the state of water resources in Ghana, which could be done at 5 year intervals. Numerous countries in the world have for a long time recognized the need for such regular reporting, notable examples being Denmark, the United States, and especially Australia. Other countries or states are initiating such reporting, for example the province of Quebec in Canada is committed to such reporting and the Canadian Council of Academies (2009) has recently recommended that the Natural Resources Canada initiate regular reporting on the state of groundwater resources in Canada at 5-year intervals. In Ghana, such regular reporting should provide the WRC with an incentive as well as means to regularly integrate and analyse available data on surface water and groundwater resources availability and use in Ghana. Such reporting could form a basis for governmental actions related not only to quality water supply but also for economic development based on sustainable water resources. This reporting would also be a basis for WRC to define its priorities and actions. The remainder of this section describes the potential content of such regular reporting on water resources.

The present final HAP technical report could be thought as the first of such regular reports on the state of water resources in Ghana. However, the HAP can only provide part of the information needed as it focussed on groundwater resources only for northern Ghana. Initiatives similar to the HAP for southern Ghana as well as the integration of information on surface water resources would be needed to provide the information base needed to portray water resources for all of Ghana. Alternatively, initial reporting could also focus on groundwater resources in Northern Ghana and be solely based on the HAP as a starting point.

The United States, Denmark and Australia provide examples of activities related to the sustainable management of water resources, especially groundwater, at various levels of development. Even though these are developed countries, it is not all developed countries that have put in place approaches meant to provide the information base needed for water resources management. These mature programs cannot be duplicated in Ghana, but they provide a perspective for the development of a reporting framework on water resources in Ghana. In the USA, the U.S. Geological Survey USGS (2011) manages the Cooperative Water Program, which monitors and assesses water in every State, protectorate and territory of the USA in partnership with nearly 1,600 local, State and Tribal agencies. This program is thus of interest first because of its collaborative framework that involves water sector stakeholders. This program is also of interest for the type of knowledge that it develops and transfer relative to water resources: water availability and use, ecosystem health, water quality and drinking water, hazard risk and assessment, energy, climate and land-use change. The program thus provides information on the water resources itself but also on its relations with broader issues.

The water resources program of the Geological Survey of Denmark and Greenland (GEUS, 2011) provides an example of a mature scientific knowledge program in a country where a detailed assessment of water resources is already available. The importance of this program reflects the fact that groundwater is practically the sole source of water supply in Denmark. Research and advice of the GEUS concerning the exploitation and protection of water resources are among its main activities. These activities have been in large part dedicated to the study of threats on groundwater resources, such as landfills, industrial facilities, intensive farming and pesticides. Today, GEUS activities are concerned with the exploitation and protection of water resources as a whole in the perspective of sustainability, considering together issues such as water-supply, irrigation, preservation of ecosystems and industrial activities. Activities of the GEUS involve the development of knowledge about groundwater resources, including the monitoring of groundwater and integrated water resources planning. The National Centre for Groundwater and Well, created in 1926, contains well log data from more than 270,000 boreholes in Denmark. Monitoring activities involve both water levels and water quality, including pesticides. To integrate this knowledge about groundwater resources and use it to support management decisions, a National Water Resources Model is being developed to help in the evaluation of the impact on water resources of further withdrawals and climate change.

Australia provides one of the best examples of reporting and information sharing on water resources. This example is especially relevant for northern Ghana because Australia includes semi-arid and arid areas. To document the knowledge about water resources, the Australian Natural Resources Atlas (ANRA, 2011) contains the Australian Water Resources Assessment 2000, which documented knowledge about the quantity, quality, use, allocation and management of surface water and groundwater resources. This assessment is a very good example for Ghana of how relevant data and knowledge about water resources can be assembled and made available to support decision-informed management of water resources. This water resource assessment covers the following topics: context of water resources, water availability, water quality and water use, as well as a discussion of how to achieve sustainable management of water resources and the challenges facing such a management. An important practical component of the assessment is a summary of water availability within surface and groundwater management zones.

Based on the examples of other countries and the results of the HAP, WRC regular reports on the state of water resources could include the following sections: 1) an inventory of available data and reports respectively integrated in the WRC Hydrogeological Database and virtual electronic library, 2) an analysis of the acquired groundwater monitoring data and an interpretation of temporal trends in terms of groundwater availability and stresses, 3) an update of the estimation of groundwater use and of the proportion of the population having access to a reliable water source, including groundwater, 4) the identification of arising issues and concerns related to groundwater resources, and recommendation of the relevant key studies that could takle these issues. The report should also form a basis for the definition of priorities and actions of the WRC relative ot its water management activities: information archival, monitoring, knowledge development, data sharing and regulations. The report could also provide a perspective on the sustainable use of resources, including the allocation of water resources to community water supply and economic development, including irrigated agriculture.

6. CONCLUSIONS AND RECOMMENDATIONS

6.1 Main results and findings

The inventory, collection, validation and synthesis of existing hydrogeological information were carried out for northern Ghana with the purpose of improving groundwater resource management and development through enhanced knowledge and understanding of the hydrogeological setting.

During this study, publications and previous reports were collected and relevant documents were electronically preserved for future reference and dissemination among Ghanaian stakeholders of the water sector. Data from six electronic databases were validated and consolidated in one database to serve as a basis for future hydrogeological projects in northern Ghana. As the number of wells with reliable coordinates and minimum data requirements in the consolidated database was initially not sufficient, additional data collection from previous reports was carried out. While coverage of the study area in terms of spatial distribution of data is still far from complete, the amount of data collected was deemed sufficient to carry on with a hydrogeological analysis at the regional scale according to HAP's mandate.

In order to complete the available information and enhance the existing Water Resources Commission monitoring well network established in 2005, targeted field work notably involved drilling and construction of 27 new monitoring wells. Following well development, these wells were submitted to pumping tests and geophysical borehole logging. Groundwater level and groundwater quality monitoring of these wells, which was initiated in October 2007 for wells HAP01 to HAP12 and in November 2009 for wells HAP13 to HAP27, is still ongoing. Specific field work including rainfall, groundwater and soil sampling was also undertaken for the evaluation of groundwater recharge through the chloride mass balance method and for the characterization of groundwater geochemistry. While field data collected under the present study were useful in many ways (e.g. filling specific gaps, estimating recharge, validating qualitative descriptions), datasets that will result from the long term data collection programs initiated under HAP will be even more valuable for validating or revisiting previous estimates or hypotheses. The rainfall sampling program, geochemical sampling campaigns and the groundwater level and quality monitoring will notably provide precious information on groundwater recharge, chemistry and storage. Together with more accurate groundwater production data, the groundwater monitoring data could notably provide a reliable basis for a periodic inventory of groundwater resources in northern Ghana.

Collected data allowed a better definition of the two main hydrogeological contexts, the Precambrian basement (PCB) and the Voltaian sedimentary basin (VSB). General statistics on key hydrogeological parameters were summarized for each of these contexts and typical hydrostratigraphic units were defined on the basis of the consolidated database and literature. In PCB rocks, the saprolite is defined as a leaky aquifer but it mainly acts as a reservoir of groundwater feeding the underlying permeable fractures, which would provide most of the yield. The lower part of the saprolite can also provide significant amounts of water when weathering has enhanced hydraulic conductivity. In the VSB, the main aquifer is generally located in fractured rock as the regolith is often thinner and may not store significant amounts of water. This is supported by typical borehole characteristics (section 5.2.1.1) and regional hydrostratigraphic cross sections (section 5.1.2.2), which were derived from the consolidated database. The variations in surface topography and regolith thickness observed on the cross sections could also lead to localized and isolated aquifers, especially in the Precambrian basement setting.

Aquifer characteristics in the VSB are generally more variable than in the Precambrian basement, thus partly explaining the low drilling success rate computed from the consolidated database for some areas (e.g. Tamale, Tolon Kumbugu, West Mamprusi). Average borehole depth would be deeper in the VSB (54 m) than in the Precambrian basement (44 m) suggesting that the minimum required yield would generally be reached through shallower boreholes in the Precambrian basement than in the Voltaian sedimentary basin. This is consistent with regolith thickness statistics and interpolated regolith thickness that indicate a thinner weathered layer in the VSB (17.5 m compared to 25.2 m in the Precambrian basement) and thus a smaller volume for possible groundwater storage. This, together with other factors such as soil texture, climate and land use, can have implications on aquifer vulnerability and recharge. Thin or absent regolith could favour preferential recharge but would increase aquifer vulnerability. The regolith thickness map produced could thus be used as a crude indicator of aquifer vulnerability, which could actually be more representative than conventional vulnerability index methods whose suitability for arid and semi-arid contexts has been questioned (Robins *et al.*, 2007). Regolith thickness could also have implications on aquifer conditions; areas with thicker regolith are more likely to be characterized by confined conditions and by isolated aquifers where large variations in surface topography are observed.

Aquifers associated with the PCB would generally be characterized by lower yields and specific capacities than those associated to the Voltaian sedimentary basin (52 L/min and 9 L/min m compared to 69 L/min and 13 L/min m). However, both yield and specific capacity would be more variable in the VSB than in the Precambrian basement. Reliable transmissivity data were only available for some of the WRC monitoring wells. Values range from 0.1 to 40.9 m^2/d (avg. 12.1 m^2/d) for the VSB and from 0.6 to 29.8 m^2/d (avg. 7.8 m^2/d) for the Precambrian basement. An empirical relation linking specific capacity and transmissivity was developed to provide estimates of transmissivity values from the more commonly available specific capacity values (section 5.2.1.3). While such a relation can prove useful, transmissivity values derived from pumping test data should be preferred. Statistics on depth to groundwater revealed similar values for both hydrogeological contexts. As typical descriptions in literature often suggest a deeper groundwater table for contexts such as the VSB (i.e. with thinner regolith, unable to store significant amounts of water), additional data would be required in order to validate the values obtained in this study. Possible factors affecting the depth to groundwater statistics include the presence of confined or semi-confined conditions and the quality and quantity of the groundwater level data used. Concerning the latter, measurements available in the consolidated database were often taken at different times of the year and thus reflect different water table conditions, which could generate some uncertainty in the statistics. Aside from depth to groundwater statistics that present some differences for reasons stated above, statistics computed from the consolidated database are generally in agreement with the qualitative representation of typical hydrostratigraphic units presented in section 5.1.2.1. However, even though these statistics confirmed the difference in regolith thickness and the assumed location of typical productive aquifer zones for the two main contexts, uncertainty remains concerning characteristics of the fractured rock zones, notably the vertical and lateral distribution by geological context. Along with the calculation of statistics, potential drilling success rates were also estimated by hydrogeological context and region using data from HAP consolidated databases. Success rates are still regarded as key information for many water sector stakeholders in northern Ghana (e.g. NGOs, donor countries, consultants …). Representative drilling success rates obtained range from approximately 32 % (Tolon Kumbugu) to 82 % (Bawku East). On average, they are lower for the VSB than for the Precambrian basement. The low rates obtained for the VSB would mostly be caused by the variability of aquifer characteristics in this context and would thus not contradict the high yield and recharge values observed in some parts of the VSB. It should also be noted that there is a bias in favour of successful wells in collected databases, resulting from older projects which tended not to report negative (dry) boreholes. Therefore, practioners should, whenever possible, use success rates derived from more recent data at the seeming expense of a larger dataset.

Two representative hydrological basins were selected in each hydrogeological context for estimation of potentiometric surfaces. Three estimation methods were tested using 1) river water level data, 2) river water level and groundwater level data and 3) terrain morphology and hydrological characteristics of the basins. The third method yielded the best results with respect to topography and available groundwater levels from wells. Cross sections of the potentiometric surfaces derived with third method (section 5.1.4.3) notably show more realistic unsaturated zone thicknesses and potential discharge areas. While available information did not allow the representation of the regolith base on these cross sections, it can be assumed that areas with large variations in surface elevation and regolith thickness (e.g. depressions or valleys with thin regolith on interfluves and thick regolith at bottom) would be more likely characterized by localized and isolated aquifers. While computation of the potentiometric surface with the third estimation method proved longer than for the other two methods, it can provide a fairly realistic representation of the potentiometric surfaces by using readily available information such as surface elevation, slope and rivers. The resulting potentiometric surface can also be calibrated with available groundwater level data to provide more accurate results. While this method could serve as a template for basin or sub-basin level estimation of potentiometric surfaces, many assumptions however need verification before applying this method to other areas in northern Ghana. Notably, the existence of a hydraulic link between the main rivers and the integrated aquifer system intercepted by most wells and the assumed similarity between surface water basin boundaries and aquifer boundaries would need to be validated. Also, available groundwater levels were measured at different times of the year and often not in the same year so that groundwater level differences could sometime be misinterpreted. For most wells, casing height info was also lacking, thus introducing another source of error.

Geochemical data compiled in the consolidated database and analytical results obtained from the first groundwater sampling campaign of the HAP served as the basis for a geochemical characterization of groundwater. Hydrogeochemical characterization identified a generally high degree of chemical affinity between groundwaters of the Birimian Supergroup and Intrusive rocks, which indicates similar geochemical evolution along their respective flow paths. Groundwaters of the PCB display mixed-cations (Ca+Na+Mg) and HCO_3-dominated water types, which are associated with the weathering and dissolution of Na and Mg-bearing silicates as well as cations exchange reactions taking place at the rock matrix-groundwater interface. Their level of mineralization is generally moderate, suggesting a proportionally moderate residence time in the geological formations. In contrast, groundwaters of the VSB are generally sodic (Na-dominated) in nature. HCO_3 is also the most commonly found ion, although some groundwaters exhibit a rather Cl-dominated water type. Such water types are indicative of more advanced evolution stages and longer residence time for groundwater in the VSB formations. Isotopic groundwater age from ^{14}C supports the relation between longer residence times and the occurrence of more evolved geochemical water types found in the VSB. Heavier mineralization of groundwater occurs in phase with higher total dissolved solids contents. In addition to natural evaporative processes and interactions with the rock matrix, the concentration of Cl ions in some groundwaters could also be related to agricultural activities, more specifically, the infiltration of waters dedicated to animal watering and irrigation.

The assessment of groundwater quality in the project area also relied on both geochemical data from the consolidated database and newly obtained HAP groundwater geochemical data. The latter, obtained from the three groundwater sampling campaigns carried out between August 2010 and May 2011, showed that naturally-occurring elements and compound concentrations in groundwater were generally maximum for the third monitoring campaign, while they were minimum for the first one. However, the variability of concentrations could be related both to differences in sampling/analysis conditions and natural seasonal changes. Comparison of groundwater geochemical data with guidelines of the World Health Organization (WHO) for drinking water shows that groundwater in the northern regions of Ghana is generally of good quality. Certain quality problems were nevertheless highlighted. While most of these problems had been reported in previous work, the data collected under this project provides regional figures for the whole of northern Ghana as well as information on spatial distribution of values and concentrations. The parameters raising the most serious health concerns are lead and fluoride, as in both cases 11 % of the samples considered exceed the parameters WHO guideline values, which are respectively 0.01 mg/L and 1.5 mg/L. Elevated lead concentrations are essentially recorded in groundwaters of the Obosum Group, Oti-Pendjari Group and

Birimian Supergroup. Elevated fluoride concentrations can be observed in sedimentary formations of the Oti-Pendjari and Obosum groups as well as in Intrusive rocks and metamorphosed rocks of the Precambrian basement, notably in the Bongo-Bolgatanga area, where it is associated with the dissolution of fluorite (CaF_2) (Apambire, 1996). However, as high fluoride concentrations identified in the eastern part of the VSB were not documented in available previous studies, further investigation would be needed to identify the origin and processes related to the occurrence of such concentrations. From a global standpoint, groundwater in the Oti-Pendjari Group often display a relatively poor quality, where, in addition to lead and fluoride, high concentrations of arsenic, chloride and nitrates may be present. Groundwaters in the Obosum Group may display mediocre quality relative to iron, lead and chloride. Groundwater quality is primarily controlled by the geology and mineralogy of formations through which it flows, as well as the residence time that influences the level of groundwater geochemical evolution. Another groundwater quality issue, related to infrastructure sustainability and water aesthetic more than health, concerns low pH coupled to high iron and manganese concentrations. The latter come from local bedrock but also from corrosion of hand pump parts, notably in wells located in the Kwahu-Morago Group. In some areas with known aggressive groundwater, stainless steel riser pipes are now used instead of galvanized iron pipes to minimize corrosion effects (Harvey et al., 2002). Additionally, nitrates and nitrites contamination, which is strictly point-specific in the project area, is assumed to primarily originate from human and agricultural activities taking place at surface.

Groundwater recharge was initially evaluated with two methods, the soil moisture balance (SMB) based on existing climate data and the chloride mass balance (CMB) based on analyses of soil water extracted from soil samples obtained as part of HAP. Estimated recharge rates respectively range from 1.8 to 15.9 % (19-205 mm) of average annual rainfall for SMB and 1.1 to 7.8 % (12-80 mm) of average annual rainfall for the unsaturated zone CMB. If all assumptions were met, the unsaturated zone CMB would yield more representative long term values of recharge than the SMB. However, the SMB can be expected to be more representative regionally, as climate data used for this method vary less over short distances than do soil data used for unsaturated zone CMB. Since estimates from both of these methods only represent local diffuse recharge, and previous work suggests that localized recharge (e.g. through ponding or preferential pathways such as fractures) represents a major portion of the overall recharge, the saturated zone CMB was also implemented to better assess the overall recharge processes and magnitude. Resulting recharge estimates derived from shallow groundwater samples collected in hand-dug wells range from 0.5 to 36.5 % (5-389 mm) of average annual rainfall. However, even when supposing that all assumptions are met, results from this method are considered insufficient in term of quantity and coverage to constitute a statistically representative dataset to be used a reliable basis of comparison. Additional shallow groundwater samples with an improved spatial distribution would thus be required to support available data. Until results from such work are available, values obtained from this study with SMB and unsaturated CMB can serve as conservative estimates of groundwater recharge.

When compared with actual groundwater production estimated from literature and available data, these groundwater recharge values would suggest that the proportion of recharge actually used by groundwater exploitation is relatively low, ranging between 0.1 % and 1.3 % of average annual recharge from SMB estimates. Similar values could be derived from groundwater recharge estimates obtained from the chloride mass balance. As mentioned in previous studies, this suggests that renewable groundwater resources would not presently be overexploited at the regional scale, even though the number of wells drilled is rapidly increasing. Groundwater could thus provide a greater supply of potable water in northern Ghana, either for rural communities or small towns, and, according to local aquifer potential, could even be used to support agricultural production under careful sustainable management.

Even though actual groundwater production in Ghana is considered too small to affect the regional water balance, efforts should be put towards the sustainable management of groundwater resources as future increase in groundwater production is thought to be imminent.

Moreover, localized effects of mis-managed planning of larger pumping schemes may induce negative effects on local aquifers despite low impact on a regional scale. Implementation of systematic data collection in drilling programs (such as intended in the drilling license regulation mentioned in chapter 2) and of long term monitoring of wells would allow a more efficient utilization of funds invested by supporting decision-making and planning of groundwater resources development and exploitation. Efficient development, utilization and management of groundwater resources will also require the integration and efficient use of existing hydrogeological data. While this project has provided a basis for such activities by synthesizing available hydrogeological data and consolidating existing databases, additional work is still required to improve knowledge and understanding of northern Ghana hydrogeology as described in the next section. Dissemination of information together with capacity development of Ghanaian institutions and private sector would also be required to help achieve sustainability of groundwater resources management. In that perspective, the present report could be used as an initial version of regular reporting on the state of groundwater resources in northern Ghana (Section 5.7). Such regular (5 year) reporting would ensure the maintenance and exploitation of the WRC Water Resources Database and groundwater monitoring network. The report would also provide a view of the state of knowledge about groundwater resources as well as its exploitation, on the basis of which sustainable management decisions could be based.

6.2 Data gaps and future work

In retrospect, the collection and review of available data carried out during this project revealed information gaps that sometimes limited the interpretation of results. Gaps identified at regional scale mostly concern aquifer characteristics, notably transmissivity, vertical gradients and continuity of fractured zones. While such information is relatively costly and time-consuming to obtain at regional scale (e.g. packer tests, long term pumping tests, sampling and analysis of groundwater samples), it could greatly improve understanding of regional groundwater occurrence and flow dynamics, which is still poorly documented. Satellite imagery could also provide valuable information at the regional scale on geological structures that could have significant groundwater potential. Another aspect of regional hydrogeology that has not received much attention in previous studies in northern Ghana, and that could benefit from such data concerns the influence that geomorphology can exert on the geometry, extent and presence of aquifers. Taylor and Howard (2000) investigated this aspect in weathered crystalline rocks of Uganda and proposed a tectono-geomorphic model that can help estimate the thickness and extent of productive aquifer zones.

Other more specific data gaps concern available datasets for streamflow and groundwater level fluctuations, as available records were often found to be either too short or filled with gaps of variable time length. While this does not necessarily imply that these data cannot be useful, it introduces uncertainty in their interpretation (e.g. for estimation of recharge or baseflow) and can involve additional work in order to fill the gaps. Another data gap concerns typical soil properties such as texture, porosity, density and field capacity for which only few studies in northern Ghana provide information and only on a very local basis. Availability of reliable datasets for typical soil properties and streamflow would allow the estimation of groundwater recharge with different methods than those used in this study (e.g. hybrid techniques such as proposed by Maréchal *et al.*, 2006) or the improvement of estimates derived in this study. As mentioned before, several groundwater level datasets have significant data gaps as a result of transducer failures. However, fairly continuous datasets should be revisited, after a 5-year period, to provide recharge estimates with the water table fluctuation (WTF) method. Besides providing additional and independent estimates of recharge magnitude and spatial distribution, the combination of estimation methods would also help better understand recharge mechanisms. This information together with a firmer grip on aquifer hydraulics and groundwater geochemistry would likely lead to a better understanding of the overall aquifer dynamics in northern Ghana. Still, this study represents a necessary step towards such an understanding.

Numerical modeling of groundwater flow could also be applied to selected areas for which data is abundant. Modeling could contribute to the validation of an overall recharge rate that is consistent with observed groundwater levels.

6.3 Lessons learned

6.3.1 Data acquisition

Following the initial phase of data collection process, it was realized that the quantity and quality of available hydrogeological data had been overestimated during the project formulation. Consequently, much more efforts and time had to be dedicated to data gathering than initially anticipated. Hence, more resources have to be dedicated during the inception of projects such as the HAP to better assess data availability and the resources needed for data acquisition.

6.3.2 Groundwater geochemistry

During the geochemical characterization, it was recognized that a more detailed sampling and QA/QC (quality assurance and quality control) protocol for groundwater sampling and analyses would have been helpful in ensuring that the geochemical sampling program was implemented as planned. The section of the protocol regarding sampling could notably include a standard form for writing down field observations that could facilitate data interpretation (e.g. potential sources of contamination in the vicinity of the well sampled). In addition to this protocol, the use a "chain of custody" form for field and laboratory personnel would have been of assistance in tracking groundwater sample and analysis status more efficiently.

6.3.3 Standardization

As for data collection, more time than anticipated was dedicated to the validation of the data acquired under the HAP. This revealed the need for the standardization of hydrogeological data amongst the different water sector stakeholders and water supply projects. To ensure the acquisition of complete and uniform data in the future, templates for data acquisition could be provided to water supply projects and water sector stakeholders. Such templates were developed together with the WRC water database as a complementary tool for data entry. These templates could be adapted if required and distributed for voluntary use by larger water supply projects. Eventually, their use could be made mandatory through a change in regulations on water well drilling permitting.

The qualification of drilling contractors and the quality of their equipments is thought to have a potentially significant impact on the success rate of water well drilling. During the first drilling campaign of the HAP, a few monitoring wells were unsuccessful while the second campaign, carried out by a different drilling contractor, yielded successful wells only. Despite the fact that many factors other than the drilling contractor can contribute to an unsuccessful well, careful qualification of a drilling contractor could improve the success rate. Standardization or regulation concerning the qualification of the drilling contractors should therefore be considered in the future to help ensure quality drilling.

6.3.4 Groundwater level monitoring

Throughout the groundwater level monitoring carried out under the HAP, the pressure transducers (termed ‘divers’ from their commercial name) used for monitoring proved to have a very high failure rate. Ideally, regular retrieval of divers is required in order to minimize data gaps in the case of failures. It could also be envisioned to use telemetry to transfer data to a central site since the time and field cost of retrieving water level divers are quite high. Such an automatic data transfer would also reduce potential data gaps due to diver failures.

7. REFERENCES

Acheampong, P.K. (1986) Evaluation of Potential Evapotranspiration Methods for Ghana. GeoJournal 12 (4) : 409-415.

Acheampong, P.K. (1988) Water balance analysis for Ghana. Geography 73 (2) : 125-131.

Acheampong, S.Y. (1996) Geochemical evolution of the shallow groundwater system in the Southern Voltaian Sedimentary Basin of Ghana. Ph.D. dissertation, University of Nevada, Reno.

Acheampong, S.Y., Hess, J.W. (1998) Hydrogeologic and hydrochemical framework of the shallow groundwater system in the southern Voltaian Sedimentary Basin, Ghana. Hydrogeology Journal 6 (4) : 527-537.

Acworth, R.I. (1987) The development of crystalline basement aquifers in a tropical environment. Quarterly Journal of Engineering Geology & Hydrogeology 20 (4) : 265-272.

Adu, S.V. (1969) Soils of the Navrongo-Bawku area, Upper Region, Ghana. Soil Research Institute, Kumasi, Memoir No, 5, 95 p.

Affaton, P., Sougy, J., Trompette, R. (1980) The tectono-stratigraphic relationships between the Upper Precambrian and the Lower Paleozoic Volta Basin and the Pan-African Dahomeyide orogenic belt (West Africa). American Journal of Science 280 : 224-248.

African Development Bank (2004) Selected Statistics on African Countries. AFDB Statistics Division, Development Research Department, Vol. XXIII, 276 p.

Agyare, W.A. (2004) Soil characterization and modeling of spatial distribution of saturated hydraulic conductivity at two sites in the Volta Basin of Ghana. Glowa Volta project, Ecology and Development Series no 17.

Agyekum, W.A. (2004) Groundwater resources of Ghana with the focus on international shared aquifer boundaries. UNESCO-ISARM International Workshop – Managing shared aquifer resources in Africa. B. Appelgreen. Tripoli, Lybia, June 2002. United Nations Educational, Scientific and Cultural Organisation, IHP-VI Series on groundwater no.8, 600 p.

Ahialey, E.K., Serfoh-Armah, Y., Kortatsi, B.K. (2010) Hydrochemical analysis of groundwater in the Lower Pra Basin of Ghana. J. Water Resource and Protection, 2010, 2, 864-871.

Akudago, J.A., Kankam-Yeboah, K., Chegbeleh, L.P., Nishigaki, M. (2007) Assessment of well design and sustainability in hard-rock formations in northern Ghana. Hydrogeology Journal 15 (4) : 789-797.

Allen, R.G., Pereira, L.S., Raes, D. and Smith, M. (1998) Crop evapotranspiration - Guidelines for computing crop water requirements. FAO Irrigation and Drainage paper no. 56, 300 p.

Allison, G.B., Gee, G.W., Tyler, S.W. (1994) Vadose-zone techniques for estimating groundwater recharge in arid and semiarid regions. Soil Science Society of America Journal, 58: 6-14.

Andreini, M., van de Giesen, N., van Edig, A., Fosu, M., Andah, W. (2000) Volta basin water balance. ZEF-Discussion Papers on Development Policy No. 21, Center for Development Research (ZEF), Bonn, March 2000.

Anku, Y.S., Banoeng-Yakubo, B., Asiedu, D.K., Yidana, S.M. (2009) Water quality analysis of groundwater in crystalline basement rocks, Northern Ghana. Environmental Geology (2009) 58:989–997.

Apambire, W.B. (1996) Groundwater geochemistry and the genesis and distribution of groundwater fluoride in the Bolgatanga and Bongo districts, Ghana. M.Sc. Thesis. Carleton University, Ottawa, Ontario, Canada.

Apambire, W.B., Boyle, D.R., Michel, F.A. (1997) Geochemistry, genesis and health implications of fluoriferous groundwaters in the upper regions of Ghana. Environmental Geology 33 (1) : 13-24.

Apambire, W.B. (2000) Geochemical modeling and geomedical implications of fluoriferous groundwaters in the Upper East Region of Ghana. Ph.D. dissertation, University of Nevada, Reno, USA.

Appelo, C.A.J. and Postma, D. (1993) Geochemistry, groundwater and pollution. A.A. Balkema, Rotterdam, 536 p.

Asomaning, G. (1992) Groundwater resources of the Birim basin in Ghana. Journal of African Earth Sciences 15 (3-4) : 375-384.

Australian Natural Resources Atlas (ANRA) (2011) Australian Water Resources Assessment 2000. Department of Sustainabililty, Environment, Water, Population and Communities, http://www.anra.gov.au/topics/water/pubs/national/water_contents.html [accessed Nov. 2011].

Bannerman, R.R., Ayibotele, N.B. (1984) Some critical issues with monitoring crystalline rock aquifers for groundwater management in rural areas. IAHS Publication no. 144 : 47-57.

Bannerman, R.R. (1990) Appraisal of hydrogeological conditions and analysis of boreholes in the Nanumba and Western Gonja districts – Northern Region, Ghana. Unpublished report for Programme for Rural Action NORRIP/GTZ, Ghana, April 1990, 44 p.

Braimoh, A.K. (2004) Modeling land-use change in the Volta Basin of Ghana. GLOWA Volta project, Ecology and Development Series no 14.

Bromley, J., Edmunds, W.M., Fellman, E., Brouwer, J., Gaze, S.R. (1997) Estimation of rainfall inputs and direct recharge to the deep unsaturated zone of southern Niger using the chloride profile method. Journal of Hydrology 188-189: 139-154.

Buckley, D.K. (1986) Report on advisory visit to WaterAid projects in Ghana, Jan-Feb 86. British Geological Survey, Hydrogeology Research Group, March 1986, 67 p.

Canadian Council of Academies , 2009. Sustainable groundwater management in Canada.

Canadian International Development Agency (1999) Ghana - Building together for a better future. CIDA Africa and Middle Eat Branch, Ghana programming framework 1999/00 – 2004/05.

Centre for Policy Analysis (2002) An Overview of the Poverty Situation in Ghana. CEPA Research Working Papers, URL http://www.cepa.org.gh/research-working-papers.htm.

Chadha, D.K. (1999) A proposed new diagram for geochemical classification of natural waters and interpretation of chemical data. Hydrogeology Journal 7, 431–439.

Chilton, P.J., Foster, S.S.D. (1995) Hydrogeological characterisation and water-supply potential of basement aquifers in tropical Africa. Hydrogeology Journal 3 (1) : 36-49.

Clark, I.D., Fritz, P. (1997) Environmental Isotopes in Hydrogeology. Lewis Publishers, New York.

Cloutier, V., Lefebvre, R., Therrien, R., Savard, M. (2008) Multivariate statistical analysis of geochemical data as indicative of the hydrogeochemical evolution of groundwater in a sedimentary rock aquifer system. Journal of Hydrology, 353 : 294-313.

Cloutier, V., Lefebvre, R., Savard, M., Bourque, É., Therrien, R. (2006) Hydrogeochemistry and groundwater origin of the Basses-Laurentides sedimentary rock aquifer system, St. Lawrence Lowlands, Québec, Canada. Hydrogeology Journal, 14 (4) : 573-590.

Cook, P.G., Edmunds, W.M., Gaye, C.B. (1992) Estimating paleorecharge and paleoclimate from unsaturated zone profiles. Water Resources Research, 28 (10): 2721-2731.

Croteau, A., Nastev, M., Lefebvre, R., Lamontagne, L., Lamontagne, C., Lavigne, M.-A., Blanchette, D. (2005) Estimation of spatial and temporal distribution of recharge to Des Anglais river aquifer system, Quebec. 6th Joint IAH-CNC and CGS Conference, Saskatoon, Canada, 8 p.

Dakoure, D., 2003. Étude hydrogéologique et géochimique de la bordure sud-est du bassin sédimentaire de Taoudeni (Burkina Faso – Mali) – Essai de modélisation [In French]. Doctoral Thesis, Université Paris VI – Pierre et Marie Curie, École Doctorale : Géosciences et Ressources Naturelles, 214 p. and appendix.

Dapaah-Siakwan, S., Gyau-Boakye, P. (2000) Hydrogeologic framework and borehole yields in Ghana. Hydrogeology Journal 8 (4) : 405-416.

Darko, P.K., Krasny, J. (2000) Adequate depth of boreholes in hard rocks: A case study in Ghana. 30th IAH Congress - Groundwater: Past achievements and future challenges. O. Sililo. Cape Town, South Africa, Balkema : 121-125.

Darko, P.K., Krasny J. (2003) Quantitative limits for groundwater exploitation under natural conditions in southwest Ghana. Proceedings of the IAH International Conference on Groundwater in fractured rocks, Czech Republic, Sept. 2003, p. 141-142.

Geological Survey of Denmark and Greenland (GEUS) (2011) Programme Area 2 – Water Resources. Ministry of Climate, Energy and Building, Denmark. Internet site http://www.geus.dk/geuspage-uk.htm [accessed Nov. 2011].

Desconnets, J.C., Taupin, J.D., Lebel, T., Leduc, C. (1997) Hydrology of the HAPEX-Sahel Central Super-site : surface water drainage and aquifer recharge through the pool systems. Journal of hydrology 188-189 : 155-178.

Dethier, D.P., Lazarus, E.D. (2006) Geomorphic inferences from regolith thickness, chemical, denudation and CRN erosion rates near the glacial limit, Boulder Creek catchment and vicinity, Colorado. Geomorphology 75 : 384-399.

Devlin, J.F., Sophocleous, M. (2005) The persistence of the water budget myth and its relationship to sustainability. Hydrogeology Journal 13 (4) : 549-554.

Dewandel, B., Lachassagne, P., Wyns, R., Marechal, J.C., Krishnamurthy, N.S. (2006) A generalized 3-D geological and hydrogeological conceptual model of granite aquifers controlled by single or multiphase weathering. Journal of hydrology 330 (1-2) : 260-284.

Domenico, P.A., Schwartz, F.W. (1990) Physical and chemical hydrogeology. John Wiley & Sons, New York.

Edmunds, W.M., Fellman, E., Goni, I.B., Prudhomme, C. (2002) Spatial and temporal distribution of groundwater recharge in northern Nigeria. Hydrogeology Journal 10: 205-215.

Edmunds, W.M., Gaye, C.B. (1994) Estimating the spatial variability of groundwater recharge in the Sahel using chloride. J. of Hydrology 156: 47-59.

Eriksson, E., Khunakasem, V. (1969) Chloride concentration in groundwater recharge rate and rate of deposition of chloride in the Israel coastal plain. Journal of Hydrology, 7: 178-197.

Food and Agricultural Organisation (1995) Irrigation in Africa in figures. FAO Water Reports Series, URL http://www.fao.org/documents.

Freeze, R.A. and J.A. Cherry (1979) Groundwater, Prentice-hall inc. 379 p.

Friesen, J., Andreini, M., Andah, W., Amisigo, B., van de Giesen, N. (2005) Storage capacity and long-term water balance of the Volta Basin, West Africa. IAHS Publication no. 296 : 138-145.

Gaye, C.B., Edmunds, W.M. (1996) Groundwater recharge estimation using chloride, stable isotopes and tritium profiles in the sands of northwestern Senegal. Environmental Geology 27 (3) : 246-251.

Ghana Geological Survey Department (2007) Geology of Ghana - An overview. Interim geological map published in April 2007 and compiled by GEUS/GSD based on the maps of Watts, Griffis and McQuat Ltd (1994) and Affaton (1980; 1990)

Ghana Geological Survey Department (2009) Geological Map of Ghana – Scale 1:1 000 000. Published and edited the Ghana Geological Survey Department (Accra, Republic of Ghana) in cooperation with the Bundesanstalt für Geowissenschaften und Rohstoffe (Hannover, Federal Republic of Germany).

Gibbs, R.J. (1970) Mechanisms Controlling World Water Chemistry. Science, 170(3962), 088-1090.

Gill, H.E. 1969. A ground-water reconnaissance of the Republic of Ghana, with a description of geohydrologic provinces. US Geological Survey Water-Supply paper 1757-K.

Ginn, T.R., Murphy, E.M. (1997) A transient flux model for convective infiltration: Forward and inverse solutions for chloride mass balance studies. Water Resources Research 33 (9): 2065-2079.

Global Environment Facility – United Nations Environment Programme (2002) Volta River Basin preliminary transboundary diagnostic analysis. Final report, Project Development Facility, 125 p.

Gong, F. (2004) Analysis on different methods to fill in gaps in meteorological data. University of Waterloo, Ontario (for Natural Resources Canada, Canada Centre for Remote Sensing), 25 p.

Government of Ghana – Ministry of Water Resources, Works and Housing (2007) National water policy. Government of Ghana, June 2007.

Guiraud, R. (1988) L'hydrogéologie de l'Afrique. Journal of African Earth Sciences 7 (3) : 519-543.

Güler, C., Thyne, G.D., McCray, J.E., Turner, A.K. (2002) Evaluation of graphical and multivariate statistical methods for classification of water chemistry data. Hydrogeology Journal 10, 455-474.

Gyau-Boakye, P., Dapaah-Siakwan, S. (1999) Groundwater: Solution to Ghana's rural water supply industry. Journal of the Ghana Institution of Engineers, May 1999, 9 p.

Gyau-Boakye, P. (2001) Sources of rural water supply in Ghana. Water International 26 (1) : 96-104.

Harvey, P.A., Jawara, D., Reed, R.A. (2002) Sustainable handpump projects in Africa. Water, Engineering and Development Centre report, Loughborough University, UK, 33 p.

Hem, J.D. (1985) Study and interpretation of chemical characteristics of natural water, Third edition. U.S. Geological Survey, Water-supply paper 2254, 263 p.

Hounslow, A.W. (1995) Water quality data analysis and interpretation. CRC Lewis Publishers, Boca Raton, 397 p.

Huntley, D., Nommensen, R., Steffey, D. (1992) Use of specific capacity to assess transmissivity in fractured-rock aquifers. Ground Water 30 (3) : 396-402.

International Atomic Energy Agency (IAEA) (2006). Isotope Hydrology Information System. The ISOHIS Database. Accessible at http://www.iaea.org/water (September 2011).

International Centre for Tropical Agriculture (CIAT) (2004) Hole-filled seamless SRTM data v1. Consultative Group for International Agriculture Research - Consortium for Spatial Information (CGIAR-CSI), data from http://srtm.csi.cgiar.org.

International Monetary Fund (2000) Ghana: Statistical Appendix. IMF Staff Country Report No. 1, January 2000, 60 p.

International Monetary Fund (2005) Ghana: Statistical Appendix. IMF Country Report No. 05/286, August 2005, 73 p.

International Union of Soil Sciences - Working Group on World Reference Base (2006) World reference base for soil resources 2006 – A framework for international classification, correlation and communication. World Soil Resources Reports No.103, 2nd edition, Rome.

International Water Management Institute - Globalen Wasserkreislauf (2006) Agro-ecological zones of Ghana. GIS data obtained directly from GLOWA personnel in August 2006, publishing date unknown.

Jones, M.J. (1985) The weathered zone aquifers of the basement complex areas of Africa. Quarterly Journal of Engineering Geology & Hydrogeology 18 (1) : 35-46.

Kesse, G.O. (1985) The mineral and rock resources of Ghana. Balkema, Rotterdam, 610 p.

Key, R.M. (1992) An introduction to the crystalline basement of Africa. The hydrogeology of crystalline basement aquifers in Africa. Geological Society Special Publication (London) no. 66 : 29-57.

Kinzelbach, W., Aeschbach, W., Alberich, C., Goni, I.B., Beyerle, U., Brunner, P., Chiang, W.-H., Rueedi, J., and Zoellmann, K. (2002) A Survey of Methods for Groundwater Recharge in Arid and Semi-arid regions. Early Warning and Assessment Report Series, UNEP/DEWA/RS.02-2. United Nations Environment Programme, Nairobi, Kenya, 101 p.

Kortatsi, B.K. (2007) Hydrochemical framework of groundwater in the Ankobra Basin, Ghana. Aquatic Geochemistry (2007) 13:41–74.

Kortatsi, B.K., Tay, C.K., Anornu, G., Hayford, E., Dartey, G.A. (2008) Hydrogeochemical evaluation of groundwater in the lower Offin basin, Ghana. Environmental Geology (2008) 53:1651–1662.

Kuma, J.S., Younger, P.L. (2001) Pedological characteristics related to groundwater occurrence in the Tarkwa area, Ghana. Journal of African Earth Sciences 33 (2) : 363-376.

Kwei, C.A. (1997) Evaluation of groundwater potential in the Northern Region of Ghana. CIDA project, Comwasan Consult report, Ghana, March 1997, 66 p.

Langenegger, O. (1994) Groundwater quality and handpump corrosion. World Bank Water and sanitation report no. 8.

Larsson, I. (1984) Ground water in hard rocks. UNESCO, Project 8.6 of the Hydrological Programme, 228 p.

Leduc, C., Bromley, J., Schroeter, P. (1997) Water table fluctuation and recharge in semi-arid climate: some results of the HAPEX-Sahel hydrodynamic survey (Niger). Journal of hydrology 188-189 : 123-138.

Legchenko, A., Descloitres, M., Bost, A., Ruiz, L., Reddy, M., Girard, J.F., Sekhar, M., Kumar, M.S.M., Braun, J.J. (2006) Resolution of MRS applied to the characterization of hard-rock aquifers. Ground Water 44 (4) : 547-554.

LeGrand, H.E. (2004) A master conceptual model for hydrogeological site characterization in the Piedmont and Mountain Region of North Carolina. North Carolina Department of Environment and Natural Resources, Division of Water Quality, Groundwater Section, February 2004, 39 p.

Lerner, D.N., Issar, A.S., Simmers, I. (1990) Groundwater recharge: A guide to understanding and estimating natural recharge. IAH International Contributions to Hydrogeology 8 : 345.

Leube, A., Hirdes, W. (1990) The early Proterozoic Birimian Supergroup of Ghana and some aspects of its associated gold mineralization. Precambrian Research 46 (1-2) : 139-165.

Lubczynski, M., Roy, J. (2004) Magnetic Resonance Sounding: New Method for Ground Water Assessment. Ground Water 42 (2) : 291-303.

Lutz, A., Thomas, J.M., Pohll, G., McKay, W.A. (2007) Groundwater resource sustainability in the Nabogo Basin of Ghana. Journal of African Earth Sciences 47 (3) : 61-70.

MacDonald, A.M., Kemp, S.J., Davies, J. (2005) Transmissivity variations in mudstones. Ground Water 43 (2) : 259-269.

Marcotte, D. (1991) Cokriging with Matlab. Computers & Geosciences 17 (9) : 1265-1280.

Maréchal, J.C., Dewandel, B., Ahmed, S., Galeazzi, L., Zaidi, F.K. (2006) Combined estimation of specific yield and natural recharge in a semi-arid groundwater basin with irrigated agriculture. Journal of Hydrology 329 (1-4) : 281-293.

Martin, N., van de Giesen, N. (2005) Spatial distribution of groundwater production and development potential in the Volta River Basin of Ghana and Burkina Faso. Water International 30 (2) : 239-249.

Martin, N. 2006. Development of a water balance for the Atankwidi catchment, West Africa – A case study of groundwater recharge in a semi-arid climate. Cuvillier Verlag, Göttingen, Germany, 169 p.

McLin, S.G. (2005) Estimating aquifer transmissivity from specific capacity using MATLAB. Ground Water 43 (4) : 611-614.

Meteorological Services Department (2006) Monthly average rainfall dataset for the 1961-2005 period in northern Ghana. Data obtained directly from MSD personnel in August 2006.

Meteorological Services Department (2008) Annual average rainfall dataset for the 1971-2007 period in Ghana. Data obtained directly from MSD personnel in March 2008.

Milville F. (1991) Étude hydrodynamique et quantification de la recharge des aquifères en climat Soudano-Sahélien: Application à un bassin expérimental au Burkina Faso. IAHS Publication no. 199.

Murphy, E.M., Ginn, T.R., Phillips, J.L. (1996) Geochemical estimates of paleorecharge in the Pasco Basin: Evaluation of the chloride mass balance technique. Water Resources Research 32 (9): 2853-2868.

Nathan, R.R., Harris, F.R. (1970) The occurrence of groundwater. Prepared for the Ministry of Finance and Economic Planning, Nathan Consortium, Accra, February 1970, 33 p.

National Development Planning Commission (2003) Ghana Poverty Reduction Strategy 2003-2005: An Agenda for growth and prosperity – Volume 1: Analysis and policy statement. Government of Ghana, NDPC, volume 1 : 225 p.

National Development Planning Commission (2004) Ghana Poverty Reduction Strategy - 2003 Annual Progress Report. Government of Ghana, NDPC, published by IMF, IMF Country Report No. 04/207, July 2004, 159 p.

Obuobie, E. (2008) Estimation of groundwater recharge in the context of future climate change in the White Volta River Basin, West Africa. GLOWA Volta project, Ecology and Development Series no 62, 164 p.

Ofei, K.A. (2003) Terms and Access to Credit: Perceptions of SME /Entrepreneurs in Ghana. University of Ghana, School of Administration, Legon, Ghana. 43 p.

Ofosu, S. (2005) The Hydrogeology of the Voltaian Formation of the Northern Region of Ghana. M.Sc. Thesis. University of Reno, Nevada, U.S.A.

Ojo, O. (1969) Potential evapotranspiration and the water balance in West Africa. Archives for Meteorology, Geophysics and Bioclimatology, Series B, 17 : 239-260.

Omorinbola, E.O. (1984) Groundwater resources in tropical African regoliths. Proceedings of the Symposium on Challenges in African hydrology and water resources, Harare, Zimbabwe, IAHS Publication no. 144 : 15-23.

Osae, S., Asiedu, D.K., Banoeng-Yakubo, B., Koeberl, C., Dampare, S.B. (2006) Provenance and tectonic setting of Late Proterozoic Buem sandstones of southeastern Ghana: Evidence from geochemistry and detrital modes. Journal of African Earth Sciences 44 (1) : 85-96.

Pelig-Ba, K.B., Biney, C.A., Antawi, L.A. (1991) Trace metal concentrations in borehole waters from the Upper Regions and the accra plains of Ghana. Water, Air and Soil Pollution 59 (3-4) : 333-345.

Pelig-Ba, K.B. (1998) Trace elements in groundwater from some crystalline rocks in the Upper Regions of Ghana. Water, Air and Soil Pollution 103 (1-4) : 71-89.

Pelig-Ba, K.B. (1999) Hydrogeochemistry of groundwaters from the Voltaian and Birimian formations of Ghana. Unpublished Ph.D. Thesis, University Reading.

Pelig-Ba, K.B. (2004) Estimation of water balance in the Northern Region of Ghana. Ghana Journal of Development Studies 1 (2) : 118-141.

Pelig-Ba, K.B., Parker, A., Price, M. (2004) Trace element geochemistry from the Birrimian metasediments of the Northern Region of Ghana. Water, Air and Soil Pollution 153 (1-4) : 69-93.

Plant, J.A., Kinniburgh, D.G., Smedley, P.L., Fordyce, F.M. and Klinck, B.A. (2004) Arsenic and Selenium. In: Holland, H.D., Turekian, K.K., 2004, Treatise on Geochemistry, Volume 9, Environmental Geochemistry. Elsevier, Amsterdam: 17-66.

Piper, A.M. (1944) A graphic procedure in the geochemical interpretation of water-analyses. American Geophysical Union Papers, Hydrology, pp. 914–923

Razack, M., Huntley, D. (1991) Assessing transmissivity from specific capacity in a large and heterogeneous alluvial aquifer. Ground Water 29 (6) : 856-861.

Razack, M. Lasm, T. (2006) Geostatistical estimation of the transmissivity in a highly fractured metamorphic and crystalline aquifer (Man-Danane Region, Western Ivory Coast). Journal of Hydrology 325 (1-4) : 164-178.

Robins, N.S., Chilton, P.J., Cobbing, J.E. (2007) Adapting existing experience with aquifer vulnerability and groundwater protection for Africa. Journal of African Earth Sciences 47 (1) : 30-38.

Rushton, K.R., Eilers, V.H.M., Carter, R.C. (2006) Improved soil moisture balance methodology for recharge estimation. Journal of Hydrology 318 (1-4) : 379-399.

Salama, R.B., Ye, L., Broun, J. (1996) Comparative study of methods of preparing hydraulic-head surfaces and the introduction of automated hydrogeological-GIS techniques. Journal of hydrology 185 (1-4) : 115-136.

Sander, P., Chesley, M.M., Minor, T.B. (1996) Groundwater assessment using remote sensing and GIS in a rural groundwater project in Ghana: lessons learned. Hydrogeology Journal 4 (3) : 40-49.

Sandwidi, W.J.P. (2007) Groundwater potential to supply population demand within the Kompienga dam basin in Burkina Faso. Ph.D. dissertation, University of Bonn, Germany.

Scanlon, B.R. (2000) Uncertainties in estimating water fluxes and residence times using environmental tracers in an arid unsaturated zone. Water Resources Research, 36 (2): 395-409.

Scanlon, B.R., Healy, R.W., Cook, P.G. (2002) Choosing appropriate techniques for quantifying groundwater recharge. Hydrogeology Journal 10 (1) : 18-39.

Scanlon, B.R., Keese, K.E., Flint, A.L., Flint, L.E., Gaye, C.B., Edmunds, W.M., Simmers, I. (2006) Global synthesis of groundwater recharge in semiarid and arid regions. Hydrological Processes 20 (15) : 3335-3370.

Simmers, I. (1988) Estimation of natural groundwater recharge. NATO Advanced Research Workshop, Antalya, Turkey, Dordrecht Reidel. 510 p.

Smedley, P.L. (1996) Arsenic in rural groundwater in Ghana. Journal of African Earth Sciences 22 (4) : 459-470.

Smedley, P.L. and D.G Kinniburgh (2002) A review of the source, behaviour and distribution of arsenic in natural waters. Applied Geochemistry 17: 517-568.

Soil Research Institute (2006) Soil map of Ghana. Council for Scientific and Industrial Research, data obtained directly from SRI personnel in August 2006, publishing date unknown.

Solar and Wind Energy Resource Assessment (2005) Ghana Geospatial Toolkit Data. UNEP & Global Environment Facility Project, data from http://swera.unep.net.

Subyani, A., Sen, Z. (2006) Refined chloride mass-balance method and its application in Saudi Arabia. Hydrological processes 20 (20) : 4373-4380.

Sukhija, B.S., Reddy, D.V., Nagabhushanam, P., Hussain, S. (2003) Recharge processes: piston flow vs preferential flow in semi-arid aquifers of India. Hydrogeology Journal 11 (3) : 387-395.

Taylor, R.G., Howard, K.W.F. (2000) A tectono-geomorphic model of the hydrogeology of deeply weathered crystalline rock: Evidence from Uganda. Hydrogeology Journal 8 (3) : 279-294.

Thiery, D. (1988) Analysis of long-duration piezometric records from Burkina Faso used to determine aquifer recharge. NATO Advanced Research Workshop. I. Simmers. Antalya, Turkey, Dordrecht Reidel. Vol. 222 : 477-489.

United Nations Development Group (Sachs, J., McArthur, J., Schmidt-Traub, G., Bahadur, C., Faye, M., Kruk, M.) (2004) Millennium Development Goals Needs Assessments – Country Case Studies of Bangladesh, Cambodia, Ghana, Tanzania and Uganda. UN Millennium Project, Working Paper drafted in collaboration with BIDS, EPRC, ESRF, ISSER and University of Cambodia, January 2004, 225 p.

United States Geological Survey (USGS) (2011) The cooperative Water Program. Internet site http://water.usgs.gov/coop/ [accessed November 2011].

Water Resources Commission (2006) Drilling licence and groundwater development regulations. L.I. 1827, entry into force on March 15th 2007.

Welch, A.H. and Lico, M.S. (1998) Factors controling As and U in shallow ground water, southern Carson dessert, Nevada. Applied Geochemistry no.13: 521-539.

Wladis, D., Gustafson, G. (1999) Regional characterisation of hydraulic properties of rock using air-lift data. Hydrogeology Journal 7 (2) : 168-179.

Wood, W.W. (1999) Use and misuse of the chloride-mass balance method in estimating ground water recharge. Ground Water, 37 (1): 2-3.

World Health Organization and UNICEF (2000) Global water supply and sanitation assessment 2000 report. WHO-UNICEF Joint monitoring programme for water supply and sanitation, WHO publication, 80 p.

World Health Organization (2004) Guidelines for drinking-water quality - Volume 1: Recommandations. WHO publication, 3rd Edition, 515 p.

World Health Organization (2008) Guidelines for drinking-water quality: Incorporating 1st and 2nd addenda, Volume 1, Recommandations. WHO publication, 3rd Edition, 668 p.

World Health Organization and UNICEF (2004) Joint monitoring programme for water supply and sanitation – Coverage estimates of improved drinking water, Ghana. WHO publication, updated in July 2004, 5 p.

World Resources Institute (2003) Population, health and human well-being - Ghana. EarthTrends (Environmental Information Portal), from http://earthtrends.wri.org.

Wright, E.P. (1992) The hydrogeology of crystalline basement aquifers in Africa. Geological Society Special Publication (London) no. 66 : 1-27.

Wyns, R.J., Baltassat, M., Lachassagne, P., Legchenko, A., Vairon, J., Mathieu, F. (2004) Application of proton magnetic resonance soundings to groundwater reserve mapping in weathered basement rocks (Brittany, France). Bulletin de la Société Géologique de France 175 (1) : 21-34.

Yidana, S. M., Ophori, D., Banoeng-Yakubo, B. (2008) Hydrogeological and hydrochemical characterization of the Voltaian Basin: the Afram Plains area, Ghana. Environmental Geology 53 (6) : 1213-1223.

Yidana, S.M. (2008) Hydrogeological and hydrochemical characterization of the Voltaian Basin: the Afram Plains area, Ghana. Environmental Geology (2008) 53:1213–1223.

Yidana, S.M. (2010) Groundwater classification using multivariate statistical methods: Southern Ghana. Journal of African Earth Sciences 57: 455–469.

Yidana, S.M. (2011) A conceptual framework of groundwater flow in some crystalline aquifers in Southeastern Ghana. Journal of African Earth Sciences 59: 185–194.

Prepared by:

Marc-André Carrier
Hydrogeologist, GIS/Mapping Advisor
Date: July 2011

Christian Boyaud
Hydrogeologist, Geochemist
Date: September 2011

Reviewed by:

Rene Lefebvre
Technical Capacity Building Team Leader
Date: November 2011

Enoch Asare
WRC Chief Hydrogeologist
Date: December 2011

Appendix A

Penman-Monteith method

The calculation procedure described in Allen *et al.* (1998) to compute potential (or reference) evapotranspiration comprises four general steps :

1) Derivation of climatic parameters from maximum and minimum air temperatures ($T_{a\,max}$, $T_{a\,min}$), altitude (z) and wind speed (u_2);
2) Calculation of the vapour pressure deficit (e_s-e_a);
3) Determination of the net radiation (R_n) and soil heat flux (G);
4) Determination of *pET* using results from the previous steps.

The equations described hereafter are used to calculate potential (or reference) evapotranspiration for the recommended reference surface which consists of a grass reference crop with an assumed crop height of 0.12 m, a fixed surface resistance of 70 s/m and an albedo of 0.23. This reference surface was used for all meteorological stations considered in this study. Crop evapotranspiration, which accounts for the variability these crop characteristics (i.e. crop height, crop resistance, albedo …) was not computed here because of the unavailability of relevant data on crops in the northern regions.

1) Derivation of climatic parameters

- ATMOSPHERIC PRESSURE (P)

$$P = 101.3\left(\frac{293 - 0.065z}{293}\right)^{5.26}$$

in which P = atmospheric pressure (kPa), z = elevation above sea level of the measurement point/meteorological station (m).

- LATENT HEAT OF VAPORIZATION (λ)

$$\lambda = 2.501 - \left(2.361 \times 10^{-3} T_a\right)$$

in which λ = latent heat of vaporization (MJ/kg) and T_a = mean air temperature (°C). As λ only varies slightly over normal temperature ranges, the general equation recommended by the FAO uses a value of 2.45 MJ/kg. This value is already accounted for in the final equation, so does the unit conversion associated with it (i.e. MJ/m^{2}d to kg/m^{2}d).

- PSYCHOMETRIC CONSTANT (γ)

$$\gamma = \frac{c_p P}{\varepsilon\lambda} = 0.665 \times 10^{-3} P$$

in which γ = psychometric constant (kPa/°C), c_p = specific heat of air at constant pressure (1.013x10^{-3} MJ/kg°C), P = atmospheric pressure (kPa), ε = ratio of molecular weight of water vapour over dry air (0.622) and λ = latent heat of vaporization (MJ/kg).

- SATURATION VAPOUR PRESSURE (e_s)

$$e_s = 0.611 e^{\left(\frac{17.27 T_a}{T_a + 237.3}\right)}$$

in which e_s = saturation vapour pressure (kPa) and T_a = mean air temperature (°C). Due to the non-linearity of this relation, it is recommended to use the mean saturation vapour pressure as given by the following relation :

$$e_{smean} = 0.5\left(e_{s(T_{a\max})} + e_{s(T_{a\min})}\right)$$

in $e_{s\,mean}$ = mean saturation vapour pressure (kPa), $e_{s\,(Ta\,max)}$ = saturation vapour pressure at maximum air temperature (kPa) and $e_{s\,(Ta\,min)}$ = saturation vapour pressure at minimum air temperature (kPa). The use of the mean air temperature can lead to underestimation evapotranspiration.

- ACTUAL VAPOUR PRESSURE (e_a)

$$e_a = 0.5\left(e_{s(T_{a\max})}\frac{RH_{\min}}{100} + e_{s(T_{a\min})}\frac{RH_{\max}}{100}\right)$$

in which e_a = actual vapour pressure (kPa), $e_{s\,(Ta\,max)}$ = saturation vapour pressure at maximum air temperature (kPa), $e_{s\,(Ta\,min)}$ = saturation vapour pressure at minimum air temperature (kPa), RH_{min} = minimum relative humidity (%) and RH_{max} = maximum relative humidity (%).

- SLOPE OF VAPOUR PRESSURE CURVE (Δ)

$$\Delta = \frac{4098\left(e_s\right)\left(T_a\right)}{\left(T_a + 237.3\right)^2}$$

in which Δ = slope of vapour pressure curve (kPa/°C), T_a = mean air temperature (°C), e_s = mean saturation vapour pressure (kPa).

2) Calculation of the vapour pressure deficit (e_s-e_a)

- VAPOUR PRESSURE DEFICIT (e_s-e_a)

$$e_s - e_a = \left[0.5\left(e_{s(T_{a\max})} + e_{s(T_{a\min})}\right)\right] - \left[0.5\left(e_{s(T_{a\max})}\frac{RH_{\min}}{100} + e_{s(T_{a\min})}\frac{RH_{\max}}{100}\right)\right]$$

in e_s - e_a = vapour pressure deficit (kPa), $e_{s\,(Ta\,max)}$ = saturation vapour pressure at maximum air temperature (kPa), $e_{s\,(Ta\,min)}$ = saturation vapour pressure at minimum air temperature (kPa), RH_{min} = minimum relative humidity (%) and RH_{max} = maximum relative humidity (%).

3) Determination of the net radiation (R_n) and soil heat flux (G)

- EXTRATERRESTRIAL RADIATION (R_a)

$$R_a = \frac{(24)(60)}{\pi}G_{sc}d_r\left(\omega_s\sin(\varphi)\sin(\delta) + \cos(\varphi)\sin(\omega_s)\right)$$

$$\text{where}\quad d_r = 1 + 0.033\cos\left(\frac{2\pi J}{365}\right)$$

and $\delta = 0.409\sin\left(\frac{2\pi J}{365} - 1.39\right)$

and $\omega_s = \arccos(-\tan(\varphi)\tan(\delta))$

in which R_a = extraterrestrial radiation (MJ/m^{2}d), G_{sc} = solar constant (0.820 MJ/m^{2}min), d_r = inverse relative distance Earth-Sun (), ω_s = sunset hour angle (rad), φ = latitude (rad), δ = solar declination (rad) and J = number of the day in the year (from 1 to 365 or 366).

- SOLAR RADIATION (R_s)

As radiation data were not available at the moment of the present study, solar radiation was estimated with the following equation :

$$R_s = \left(a_s + b_s \frac{n}{N}\right) R_a$$

in which R_s = solar radiation (MJ/m^{2}d), n = actual duration of sunshine (hour), N = maximum possible duration of sunshine or daylight hours (hour), R_a = extraterrestrial radiation (MJ/m^{2}d), a_s = regression constant (fraction of extraterrestrial radiation reaching the earth when n = 0) (-) and b_s = slope (a_s + b_s represent fraction of extraterrestrial radiation reaching the earth when n = N) (-). When no solar radiation data are available or no calibration has been carried out for improved as and bs parameters, the recommended value for as and bs are respectively of 0.25 and 0.50.

- CLEAR-SKY SOLAR RADIATION (R_{so})

$$R_{so} = \left(0.75 + 2\times10^{-5} z\right) R_a$$

in which R_{so} = clear-sky solar radiation (MJ/m^{2}d), z = elevation above sea level of the measurement point/meteorological station (m) and R_a = extraterrestrial radiation (MJ/m^{2}d). Again, this relation is used as no radiation data were available.

- NET SOLAR RADIATION (R_{ns})

$$R_{ns} = (1-\alpha) R_s$$

in which R_{ns} = net solar radiation (MJ/m^{2}d), α = albedo (-) and R_s = solar radiation (MJ/m^{2}d). A value of 0.23 was used for albedo as potential evapotranspiration is computed for a grass reference crop.

- NET LONGWAVE RADIATION (R_{nl})

$$R_{nl} = \sigma\left(0.34 - 0.14\sqrt{e_a}\right)\left(\frac{T_{max}^{\ 4} + T_{min}^{\ 4}}{2}\right)\left(\frac{1.35 R_s}{R_{so}} - 0.35\right)$$

in which R_{nl} = net longwave radiation (MJ/m^{2}d), σ = Stefan-Boltzmann constant (4.309x10^{-9} MJ/K^{4}m^{2}d), e_a = actual vapour pressure (kPa), T_{max} = maximum absolute air temperature (°K), T_{min} = minimum absolute air temperature (°K), R_s = solar radiation (MJ/m^{2}d) and R_{so} = clear-sky solar radiation (MJ/m^{2}d).

- NET RADIATION (R_n)

$$R_n = R_{ns} - R_{nl}$$

in which R_n = net radiation (MJ/m^{2}d), R_{ns} = net solar radiation (MJ/m^{2}d) and R_{nl} = net longwave radiation (MJ/m^{2}d).

- SOIL HEAT FLUX (G)

$$G = c_s \frac{(T_i + T_{i-1})}{\Delta t} \Delta z$$

in which G = soil heat flux (MJ/m^{2}d), c_s = soil heat capacity (MJ/m^3°C), T_i = air temperature at time i (°C), T_{i-1} = air temperature at time $i-1$ (°C), Δt = length of time interval (day) and Δz = effective soil depth (m). For this study, as a monthly period is considered for a grass reference crop, the following relation can be derived:

$$G_{month\ i} = 0.07\left(T_{month\ i+1} - T_{month\ i-1}\right)$$

in which $G_{month\ i}$ = soil heat flux at month i (MJ/m^{2}d), $T_{month\ i+1}$ = air temperature at month $i+1$ (°C) and $T_{month\ i-1}$ = air temperature at month $i-1$ (°C). It is assumed here that $c_s \approx 2.1$ MJ/m^3°C and that $\Delta z \approx 2$ m.

4) Determination of *pET* using results from the previous steps

- POTENTIAL (OR REFERENCE) EVAPOTRANSPIRATION (pET)

$$pET = \frac{0.408\Delta\left(R_n - G\right) + \gamma\left(\frac{900}{T + 273}\right)u_2\left(e_s - e_a\right)}{\Delta + \gamma\left(1 + 0.34u_2\right)}$$

in which pET = mean daily potential (or reference) evapotranspiration (mm/d), Δ = slope of vapour pressure curve (kPa/°C), R_n = net radiation at crop surface (MJ/m^{2}d), G = soil heat flux density (MJ/m^{2}d), γ = psychometric constant (kPa/°C), T = mean air temperature (°C), u_2 = wind speed at 2 m height (m/s), e_s = saturation vapour pressure (kPa), e_a = actual vapour pressure (kPa). It was originally derived from the Penman equation:

$$\lambda pET = \frac{\Delta}{\Delta + \gamma} R_n + \frac{\gamma}{\Delta + \gamma} E_a$$

Finally, a unit conversion has to be carried out in order to convert MJ/m^{2}d into mm/d. As mentioned before, the latent heat term (in MJ/kg) is already accounted for in this equation so that the MJ/m^{2}d are automatically converted into kg/m^{2}d. The final conversion is usually not present in the general equation as it consists of multiplying the numerator by 1000 mm/m (unit conversion) and the denominator by 1000 kg/m^3 (water density) in order to convert kg/m^{2}d into mm/d.

Thornthwaite method

The potential evapotranspiration can be estimated with the Thornthwaite method in three steps as described by Xu and Singh (2001).

1) Annual heat index (*I*)

First the annual heat index (*I*) must be computed by summing monthly indices over a 12-month period. The monthly indices calculation is based on air temperature :

$$I = \sum_{j=1}^{12} i_j$$

$$\text{where } i = \left(\frac{T_a}{5}\right)^{1.51}$$

in which I = annual heat index (°C), i = monthly heat index for the month j (°C), T_a = mean air temperature (°C), j = number of months (1-12).

2) Unadjusted monthly values of potential evapotranspiration

The unadjusted monthly values of potential evapotranspiration are then calculated for a standard 30 day month with 12h of sunlight/day. The general Thornthwaite equation is :

$$pET' = 16\left(\frac{10T_a}{I}\right)^a$$

$$\text{where } a = 67.5x10^{-8} I^3 - 77.1x10^{-6} I^2 + 0.0179I + 0.492$$

in which pET' = unadjusted monthly potential evapotranspiration (mm/month), T_a = mean air temperature (°C), I = annual heat index (°C) and a = empirical exponent (-).

3) Adjusted monthly values of potential evapotranspiration

Finally, the values are adjusted depending on the number of days in a month and the duration of average daily daylight which is a function of season and latitude. The adjusted values are computed with the following equation :

$$pET = pET'\left(\frac{d}{12}\right)\left(\frac{N}{30}\right)$$

in which pET = adjusted monthly potential (or reference) evapotranspiration (mm/month), pET' = unadjusted monthly potential evapotranspiration (mm/month), d = mean duration of daily daylight (hours) and N = number of days in the month (days). The adjustment factor ((d/12)(N/30)), which corrects for day length variation according to latitude and month, has been calculated from sunrise and sunset tables available on the Internet for the following coordinates: latitude 8°0'0''N and longitude 2°0'0''W. The values obtained (table below) were used for all stations as they do not vary significantly.

	Jan	**Feb**	**Mar**	**Apr**	**May**	**June**	**July**	**Aug**	**Sept**	**Oct**	**Nov**	**Dec**
Adj. factor	1.009	0.923	1.040	1.025	1.075	1.048	1.079	1.065	1.013	1.028	0.980	1.005

Appendix B

Groundwater level-time plot from Murugu monitoring well (HAP 01)

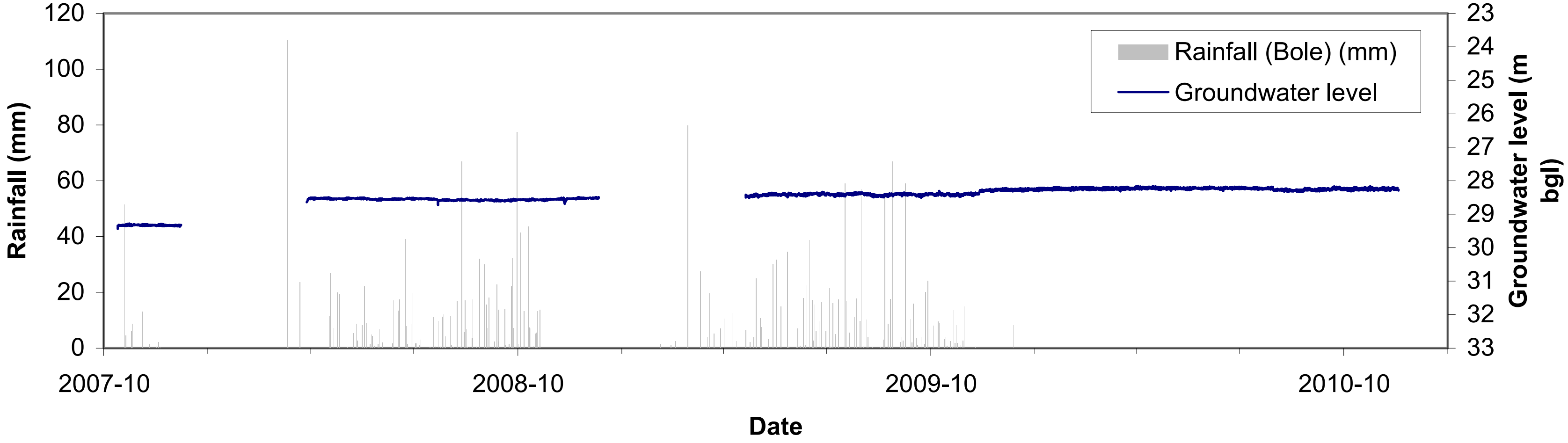

Groundwater level-time plot from Bauchipe monitoring well (HAP 02)

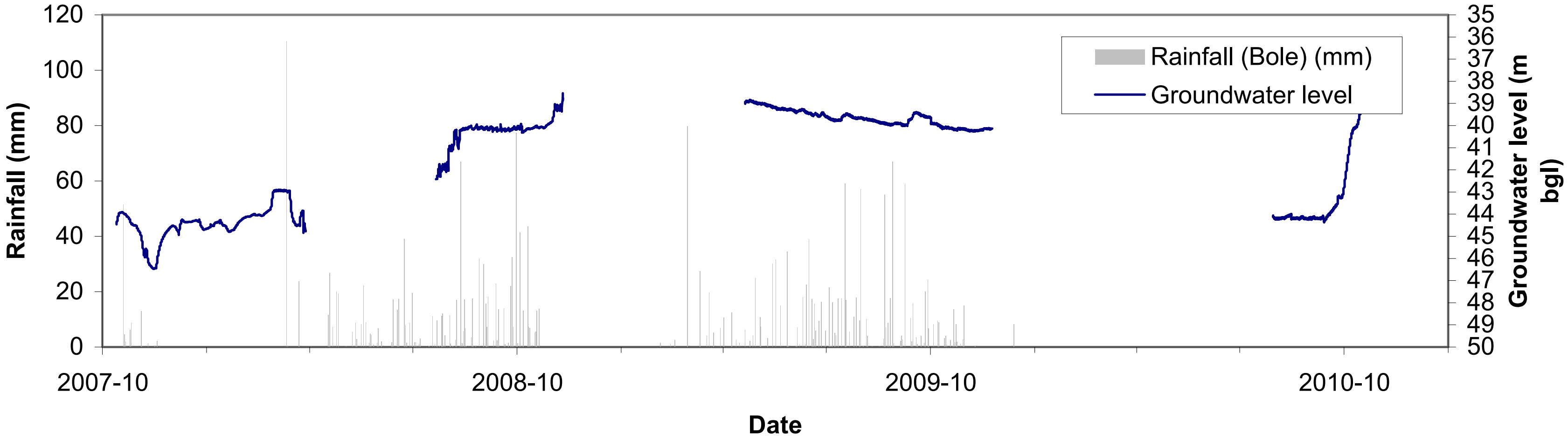

Groundwater level-time plot from Kanshegu monitoring well (HAP 04)

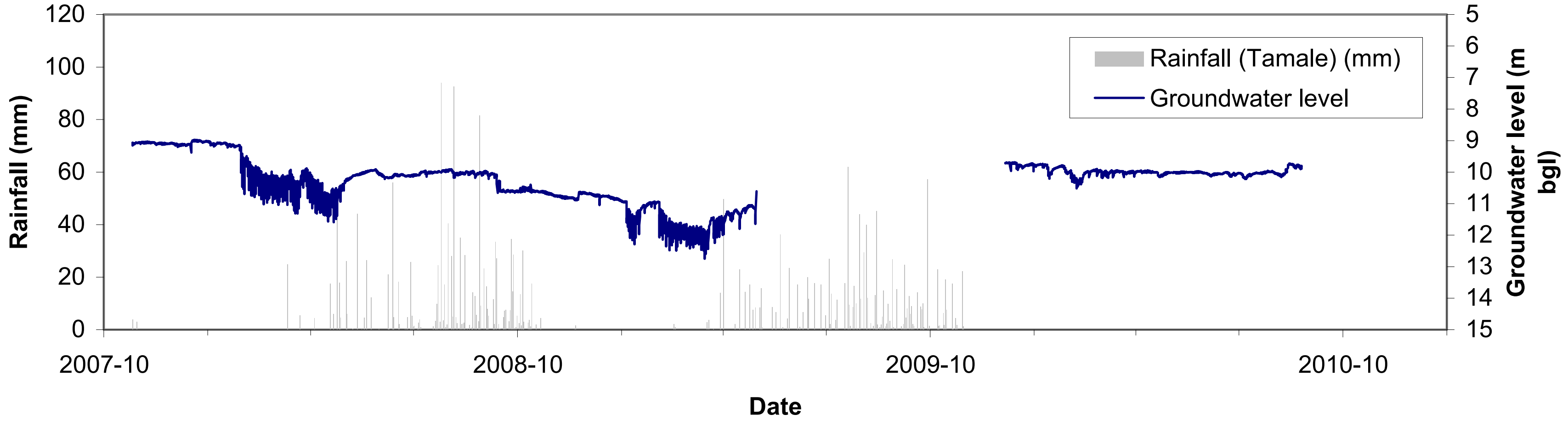

Groundwater level-time plot from Janga monitoring well (HAP 05)

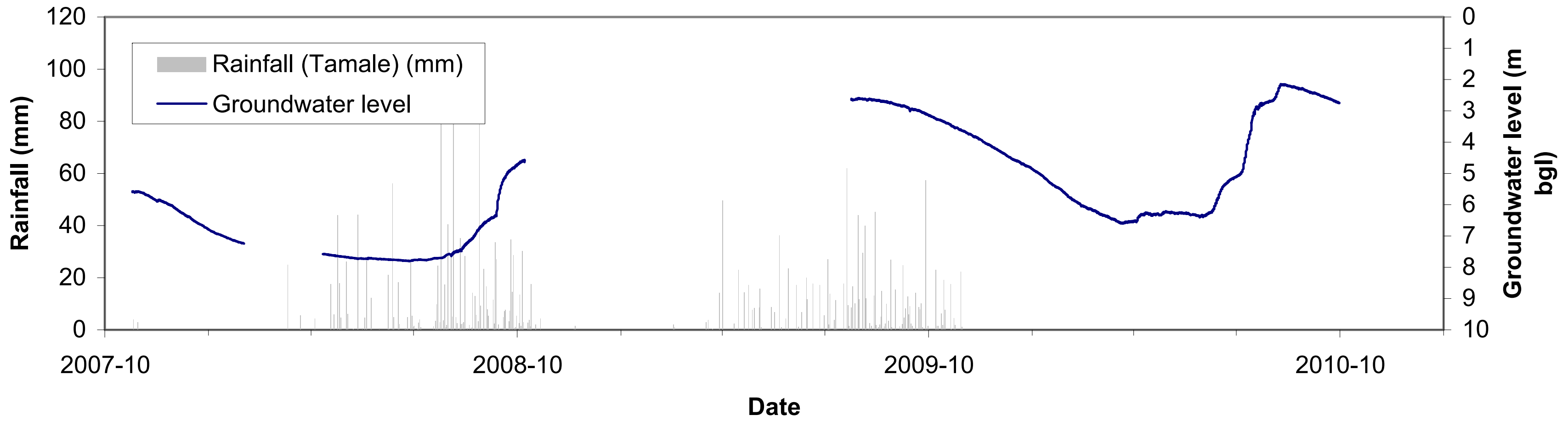

Groundwater level-time plot from Zabaraya monitoring well (HAP 07)

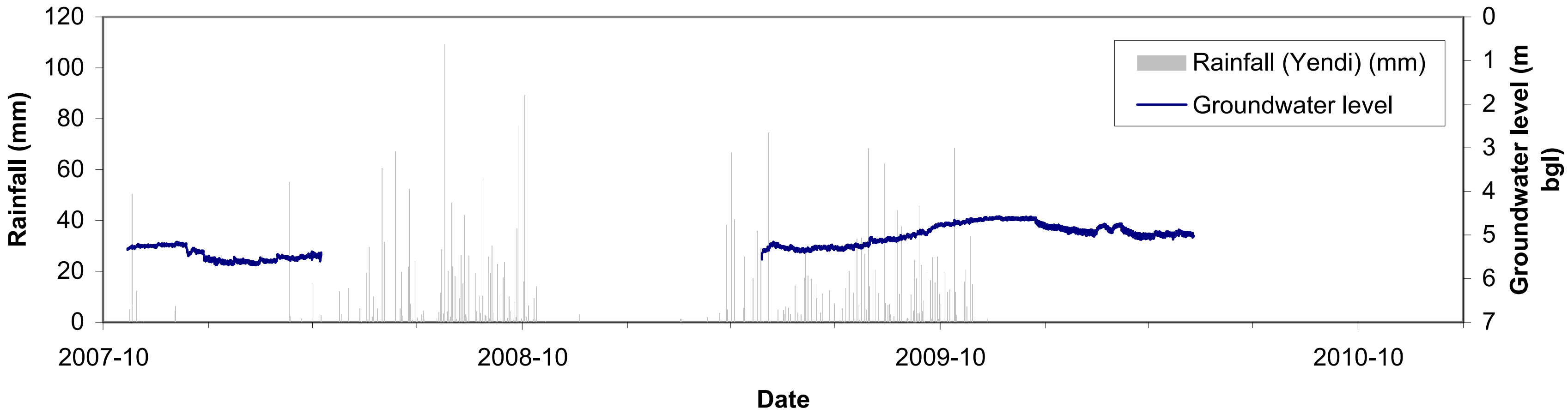

Groundwater level-time plot from Gnani monitoring well (HAP 08)

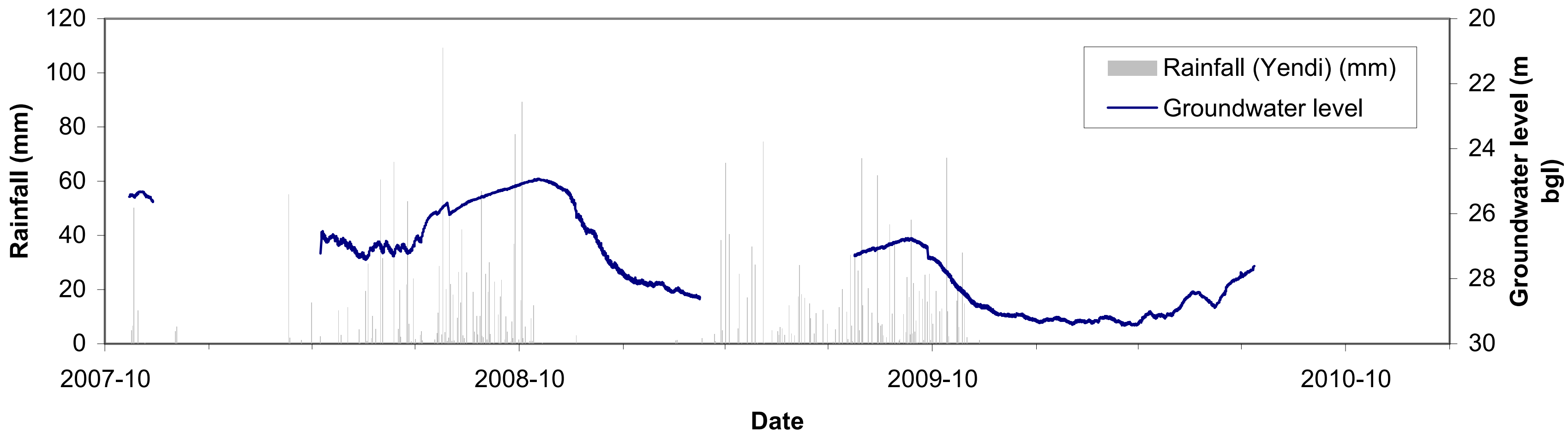

Groundwater level-time plot from Tachecku monitoring well (HAP 10)

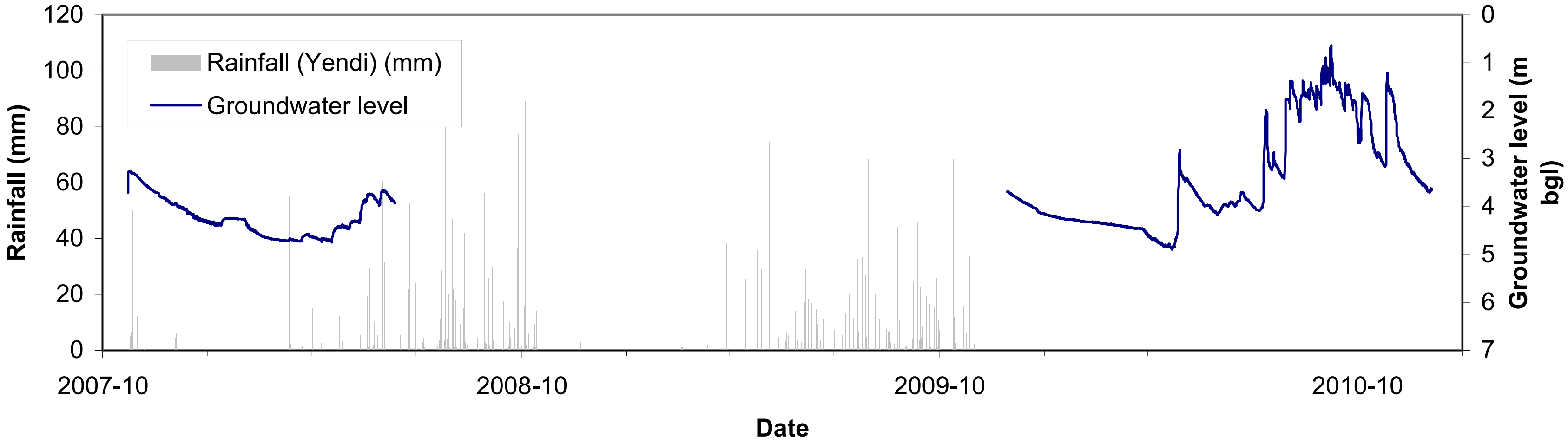

Groundwater level-time plot from Nalerigu monitoring well (HAP 11)

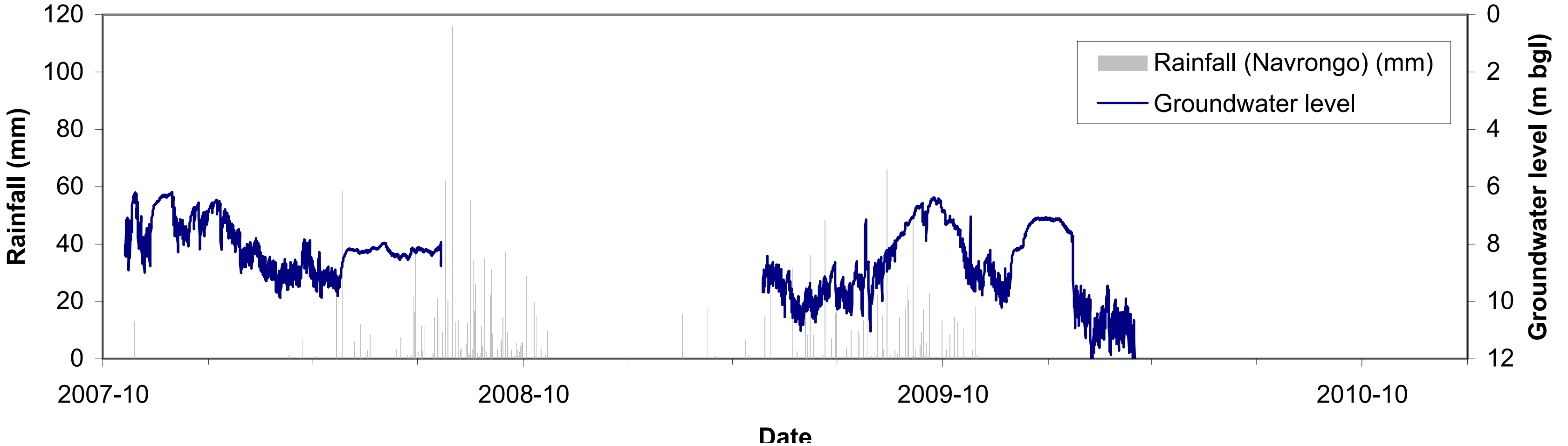

Groundwater level-time plot from Nakpeuk monitoring well (HAP 12)

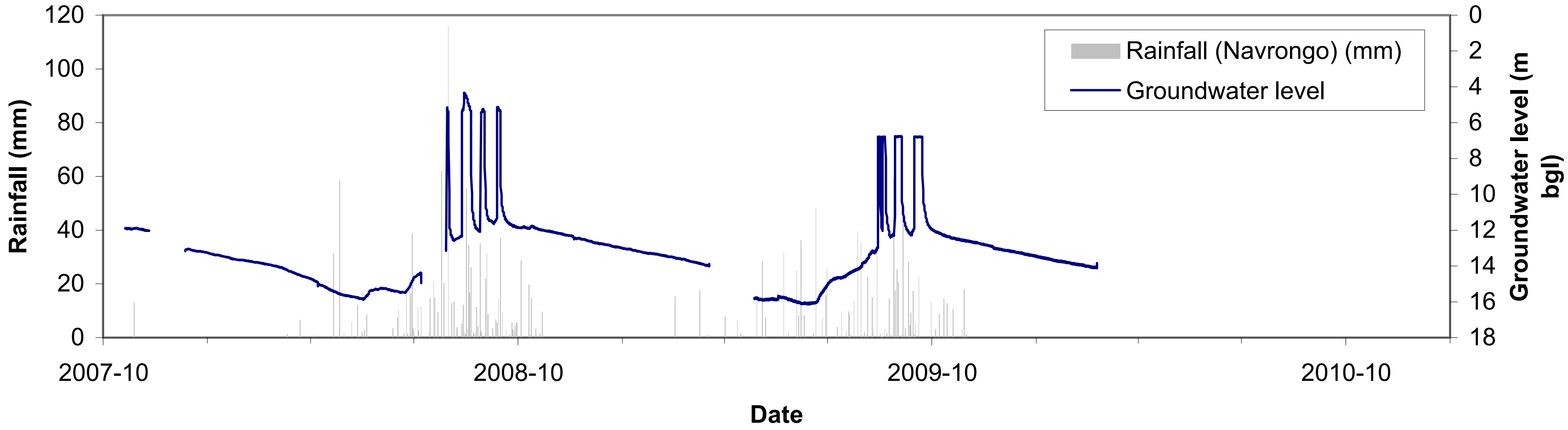

Groundwater level-time plot from Kabingo monitoring well (HAP 13)

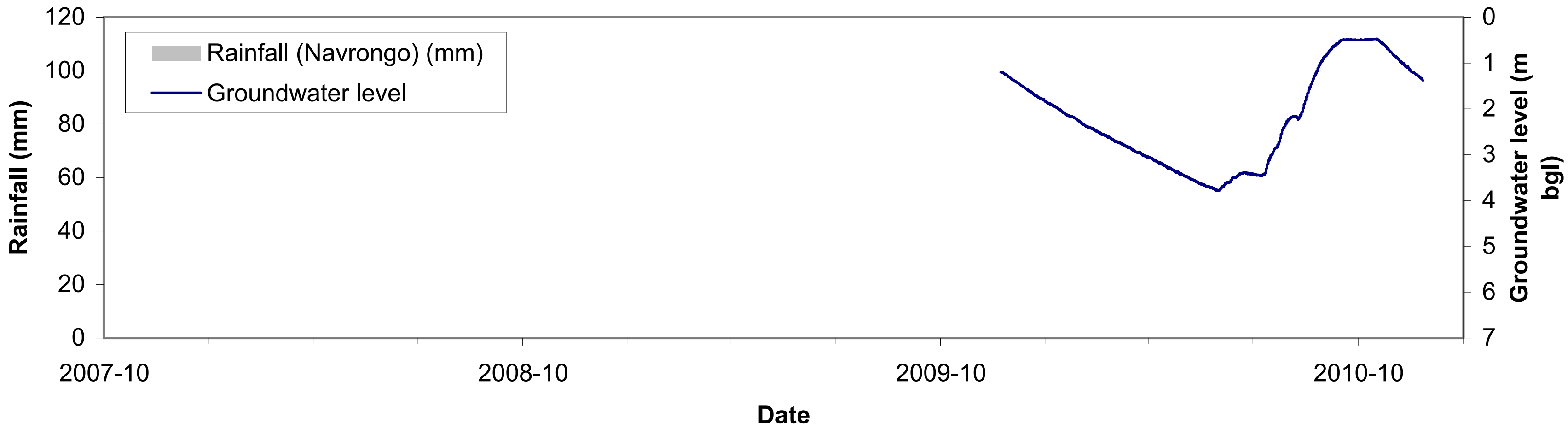

Groundwater level-time plot from Tuuni monitoring well (HAP 14)

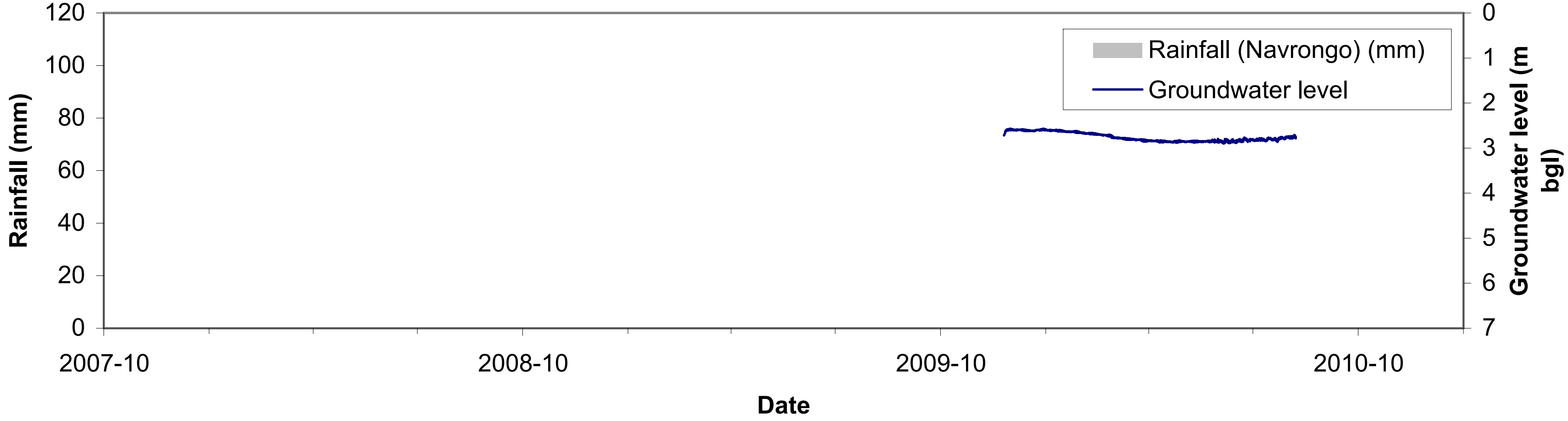

Groundwater level-time plot from Lentinkpa monitoring well (HAP 15)

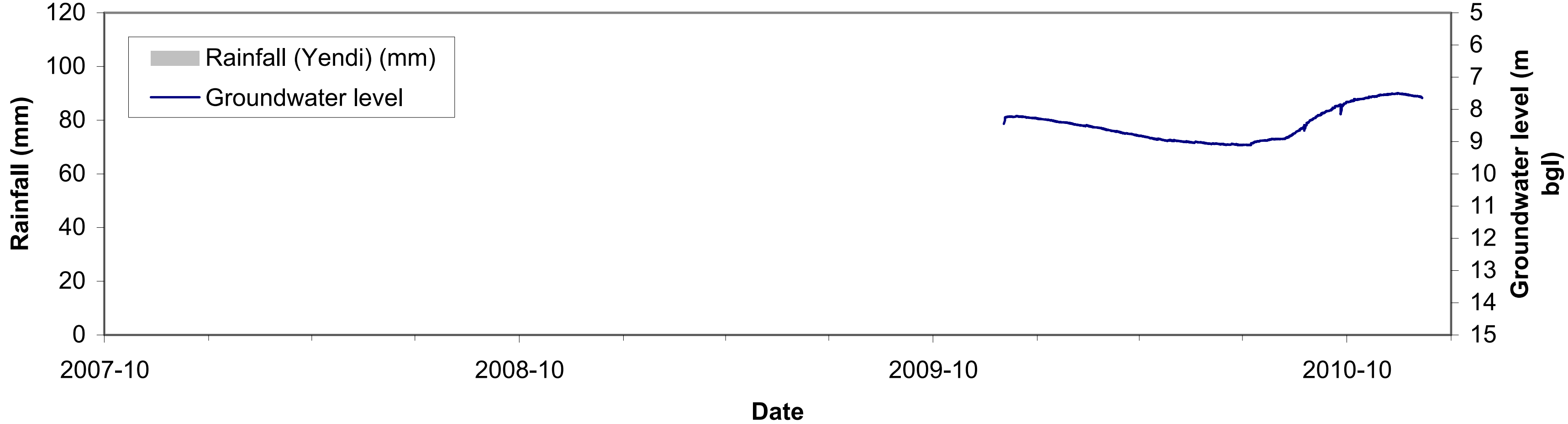

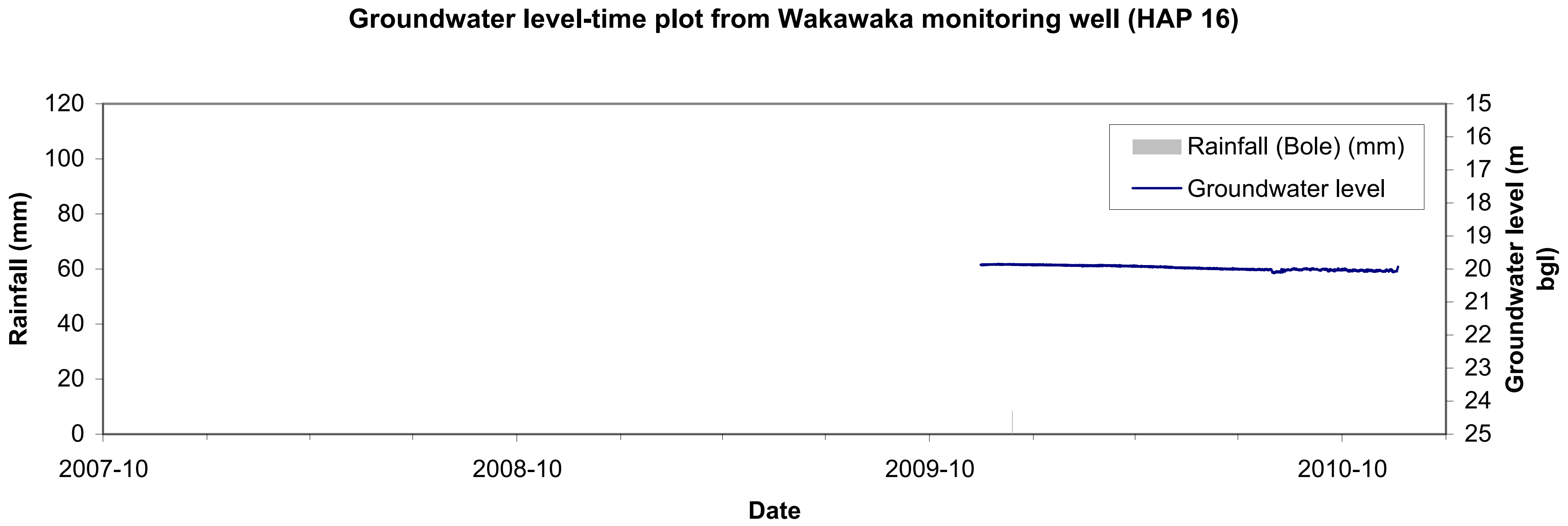

Groundwater level-time plot from Wakawaka monitoring well (HAP 16)
Rainfall (Bole) (mm)
Groundwater level
Rainfall (mm)
Groundwater level (m bgl)
Date
120
100
80
60
40
20
0
15
16
17
18
19
20
21
22
23
24
25
2007-10
2008-10
2009-10
2010-10

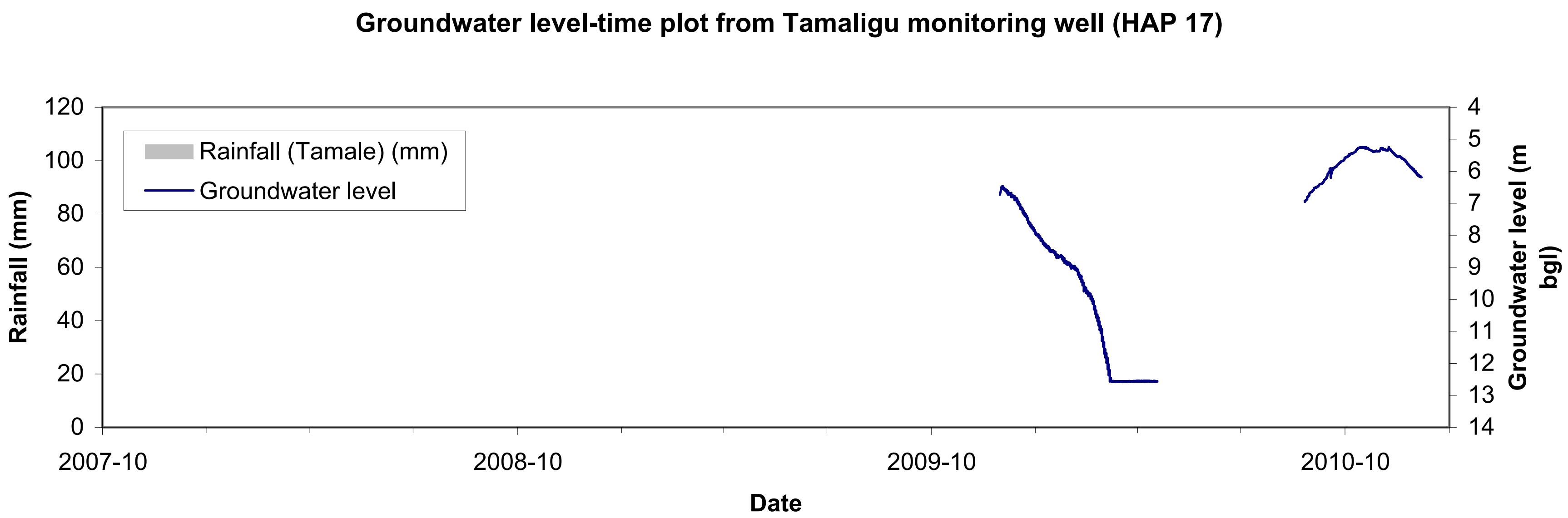

Groundwater level-time plot from Tamaligu monitoring well (HAP 17)
Rainfall (Tamale) (mm)
Groundwater level
Rainfall (mm)
Groundwater level (m bgl)
Date
120
100
80
60
40
20
0
4
5
6
7
8
9
10
11
12
13
14
2007-10
2008-10
2009-10
2010-10

Groundwater level-time plot from Sakpeigu monitoring well (HAP 18)

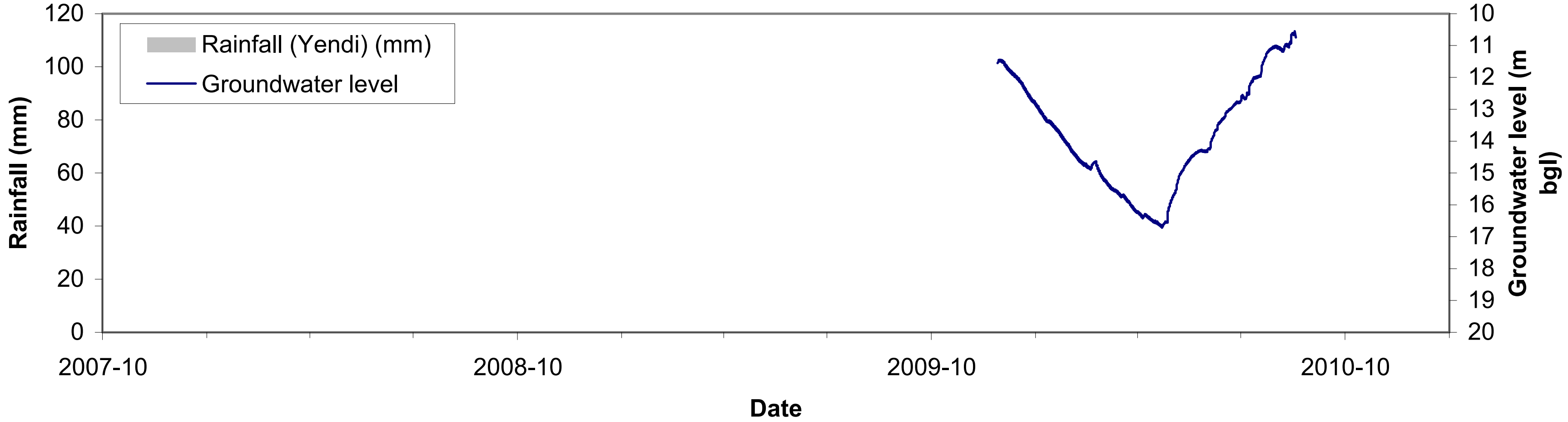

Groundwater level-time plot from Nawuni monitoring well (HAP 19)

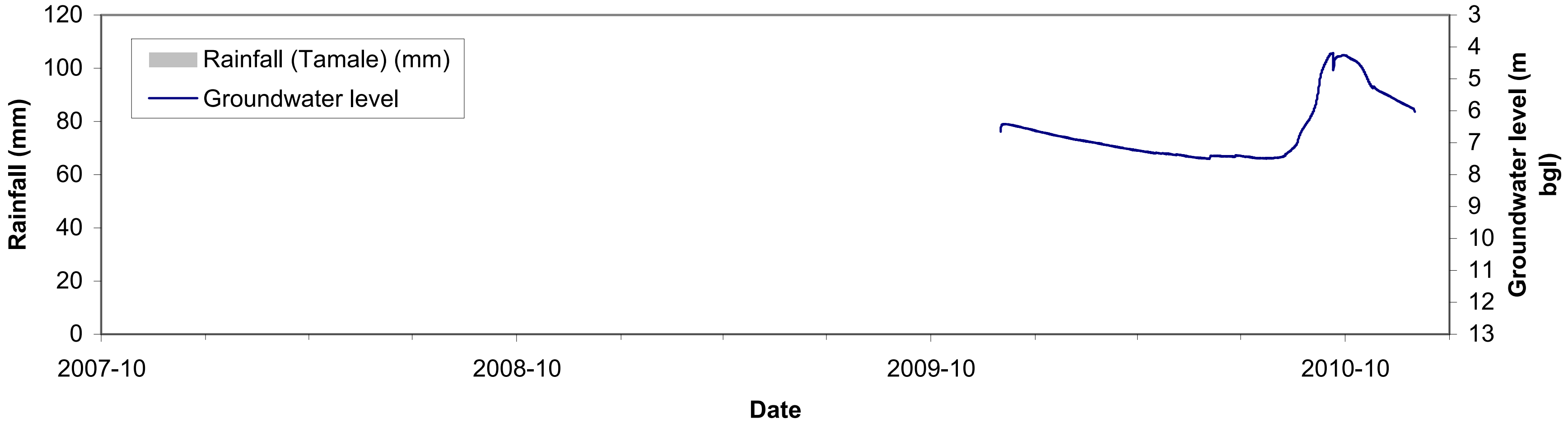

Groundwater level-time plot from Palari monitoring well (HAP 20)

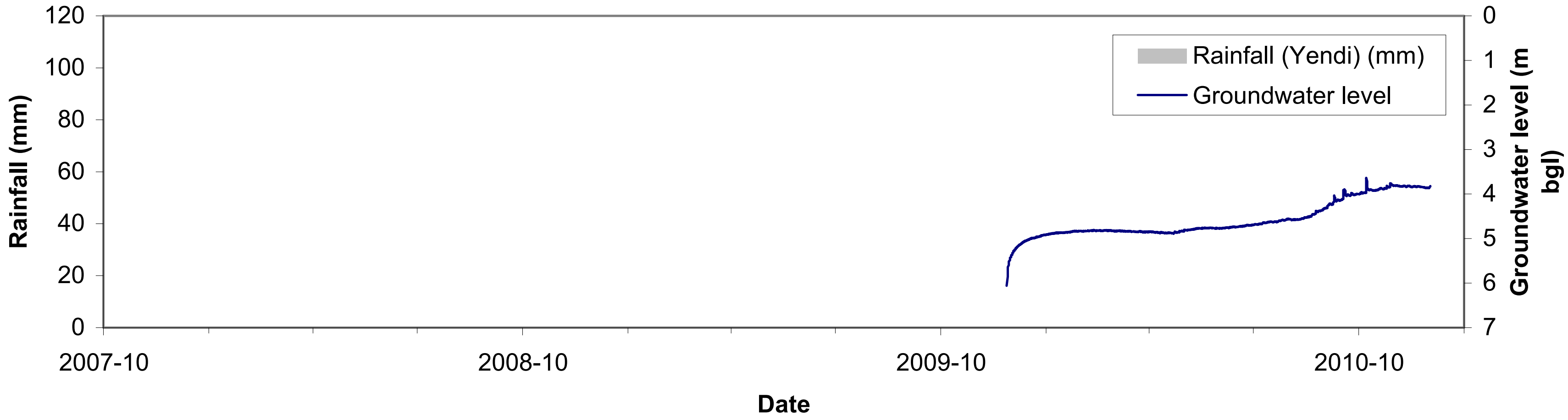

Groundwater level-time plot from Tantuya monitoring well (HAP 21)

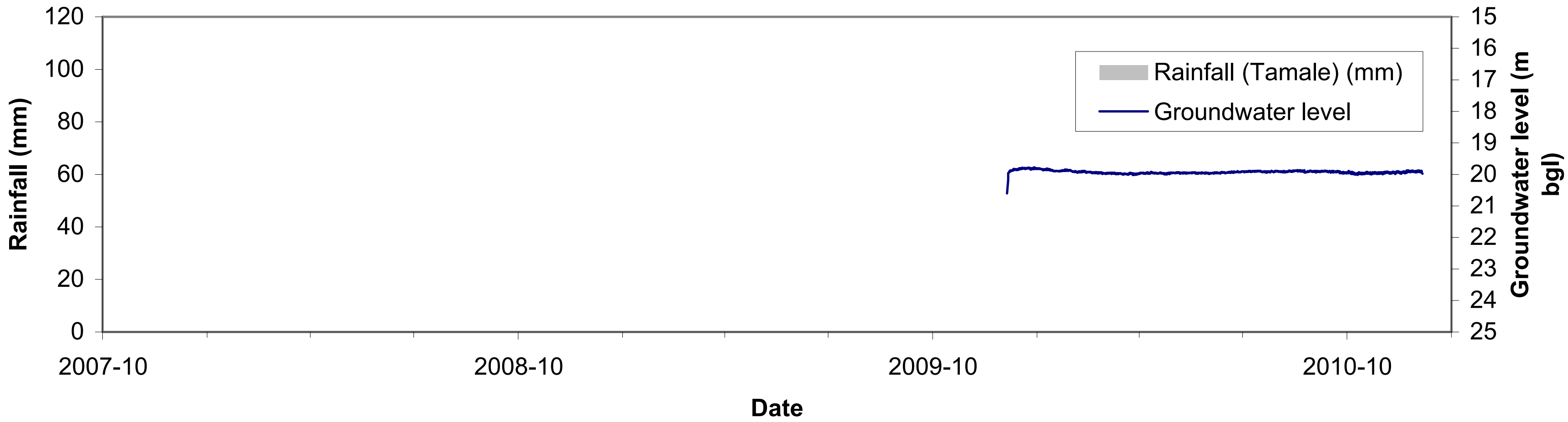

Groundwater level-time plot from Doninga monitoring well (HAP 22)

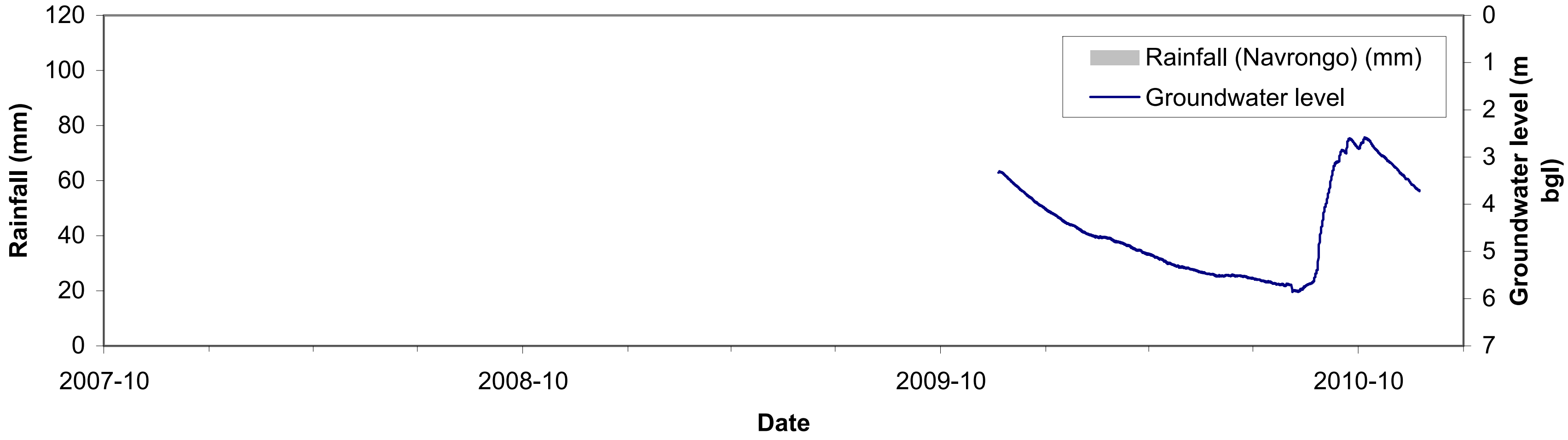

Groundwater level-time plot from Wahabu monitoring well (HAP 23)

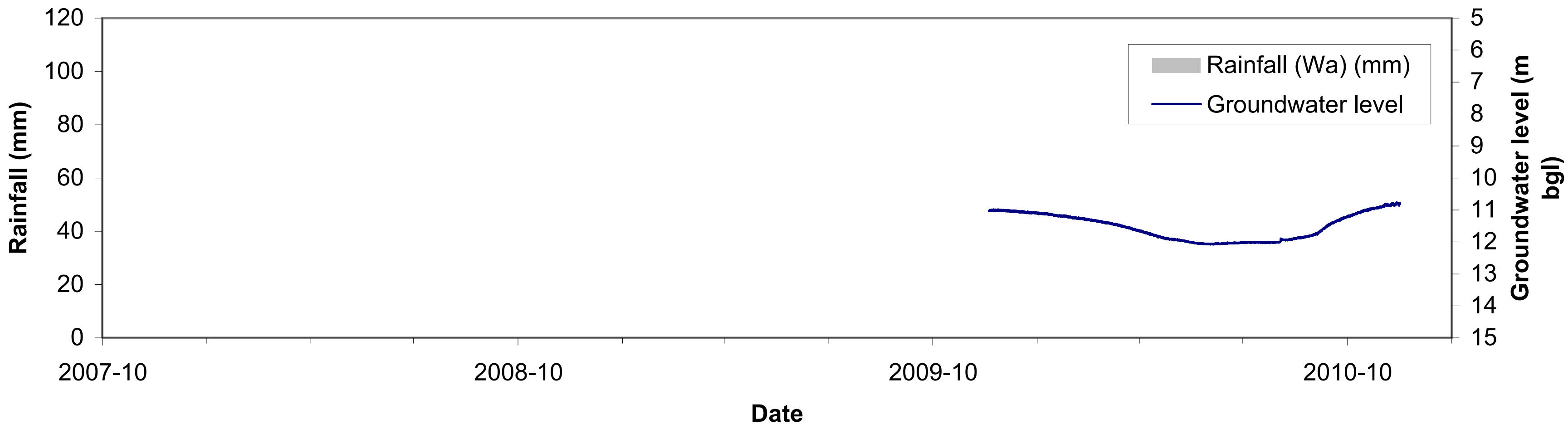

Groundwater level-time plot from Yanyounyiri monitoring well (HAP 24)

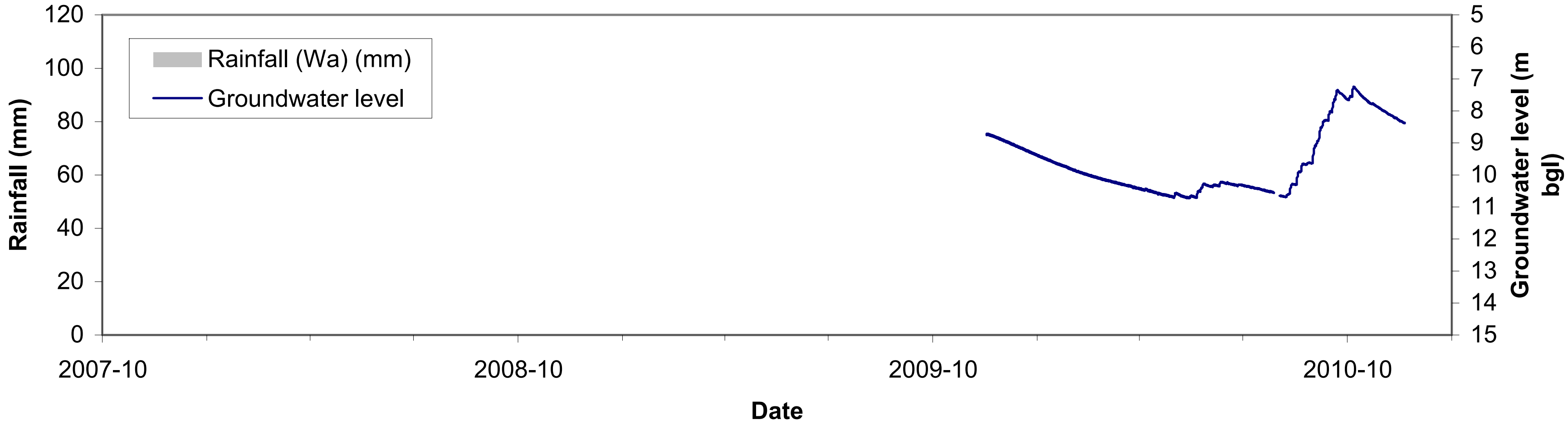

Groundwater level-time plot from Kabilpe monitoring well (HAP 25)

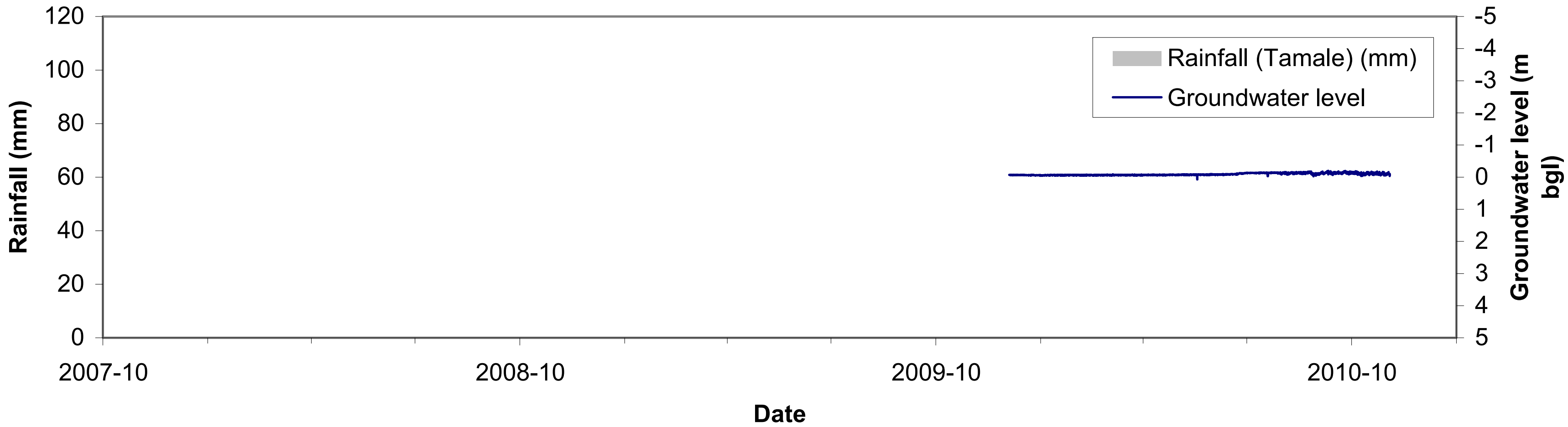

Groundwater level-time plot from Soma monitoring well (HAP 26)

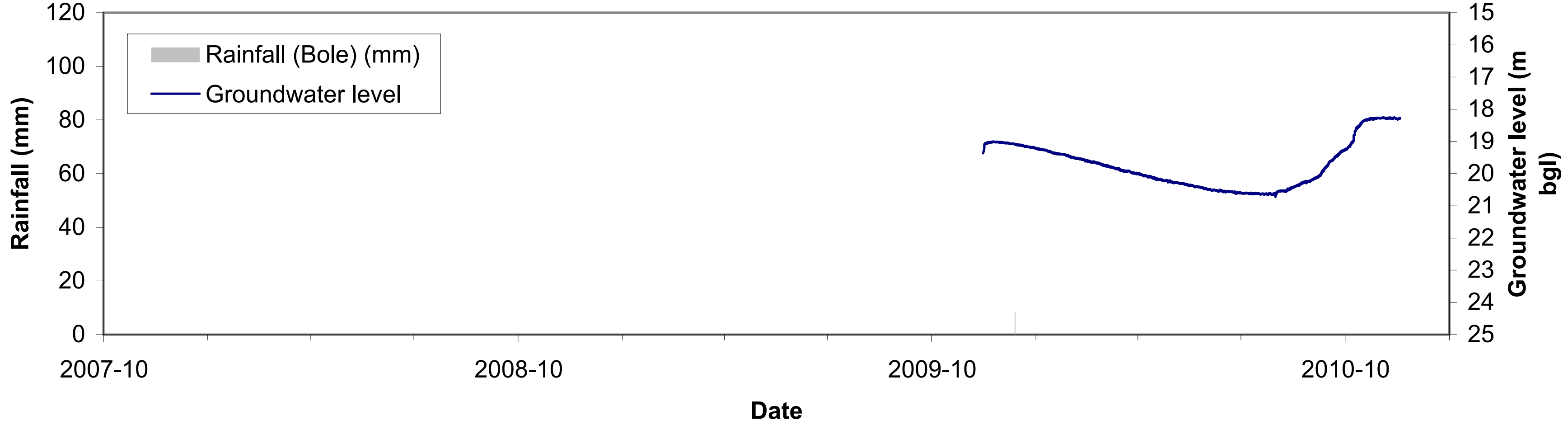

Groundwater level-time plot from Chepuri monitoring well (HAP 27)

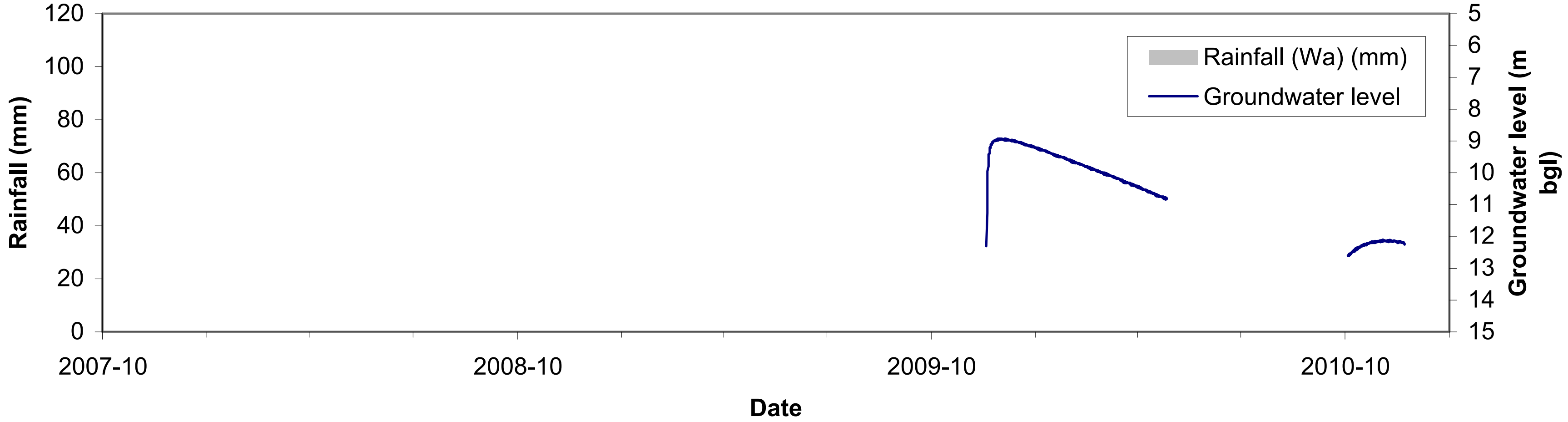

Groundwater level-time plot from Wa-Danko monitoring well (WVB 01)

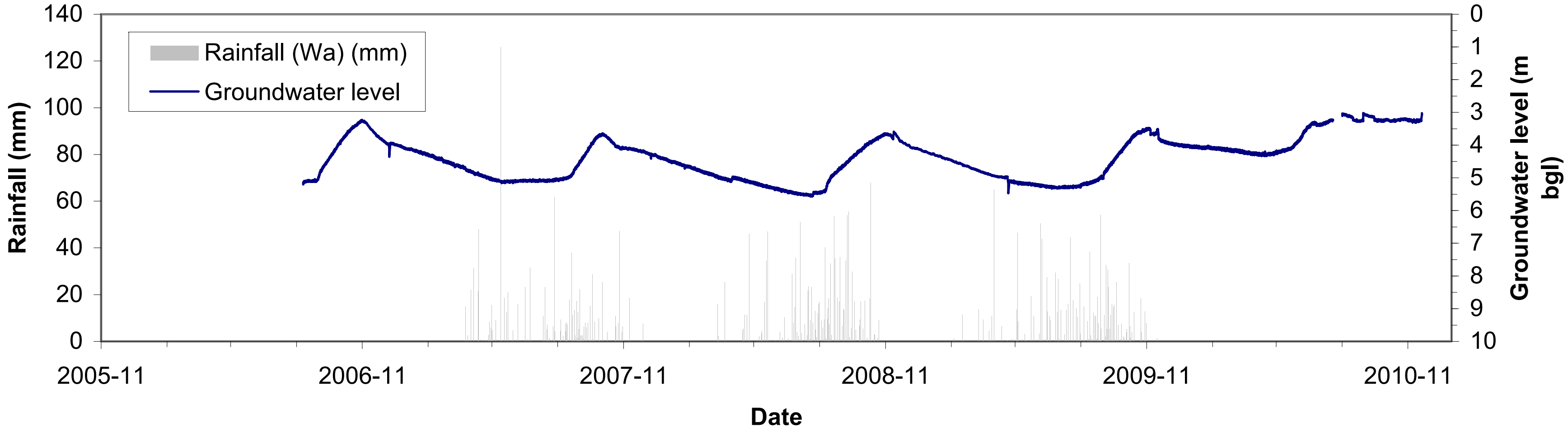

Groundwater level-time plot from Wa monitoring well (WVB 02)

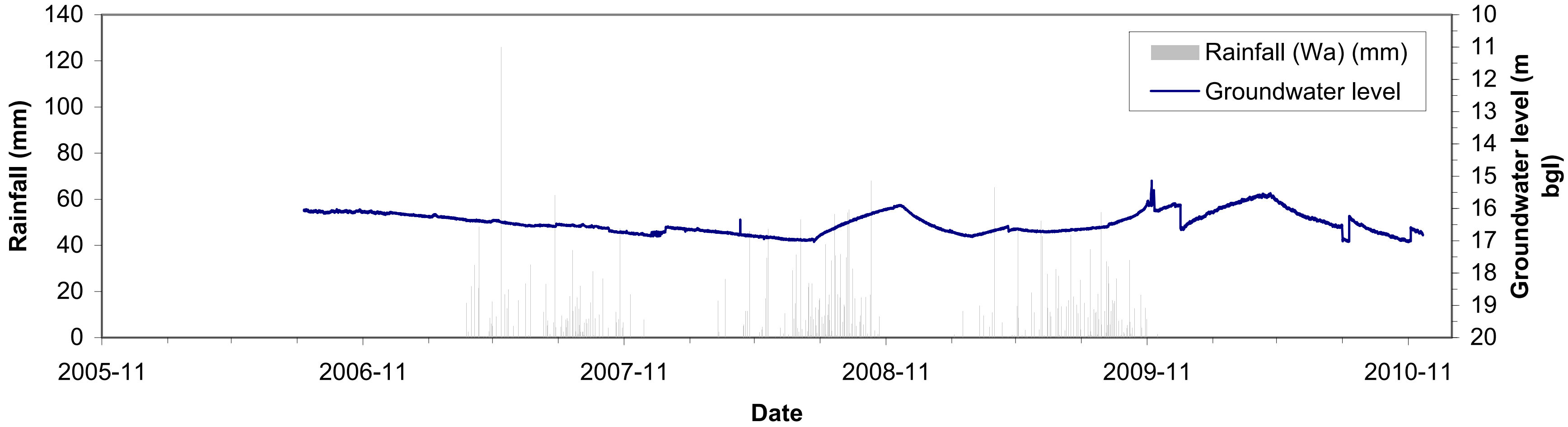

Groundwater level-time plot from Tumu monitoring well (WVB 03)

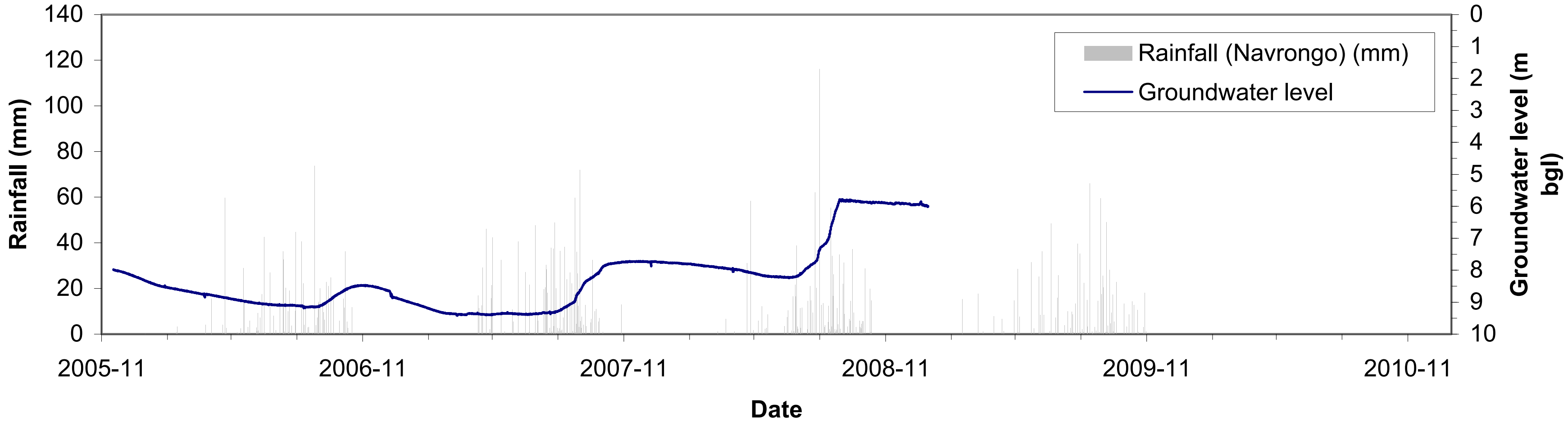

Groundwater level-time plot from Bonia monitoring well (WVB 04)

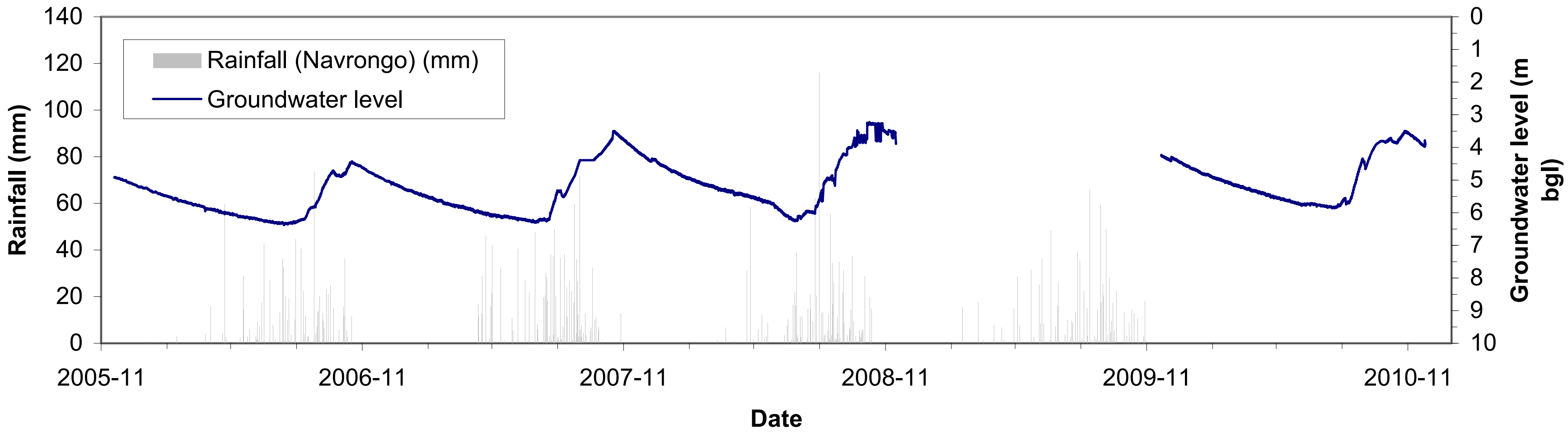

Groundwater level-time plot from Gowrie-Tingre monitoring well (WVB 05)

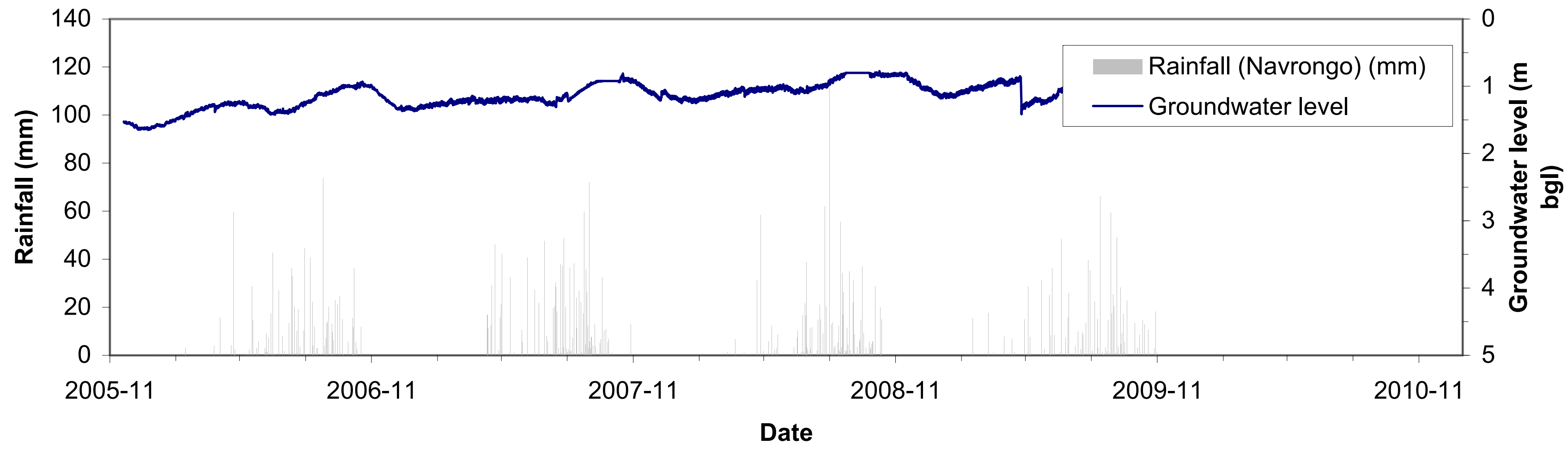

Groundwater level-time plot from Bongo-Nayire monitoring well (WVB 06)

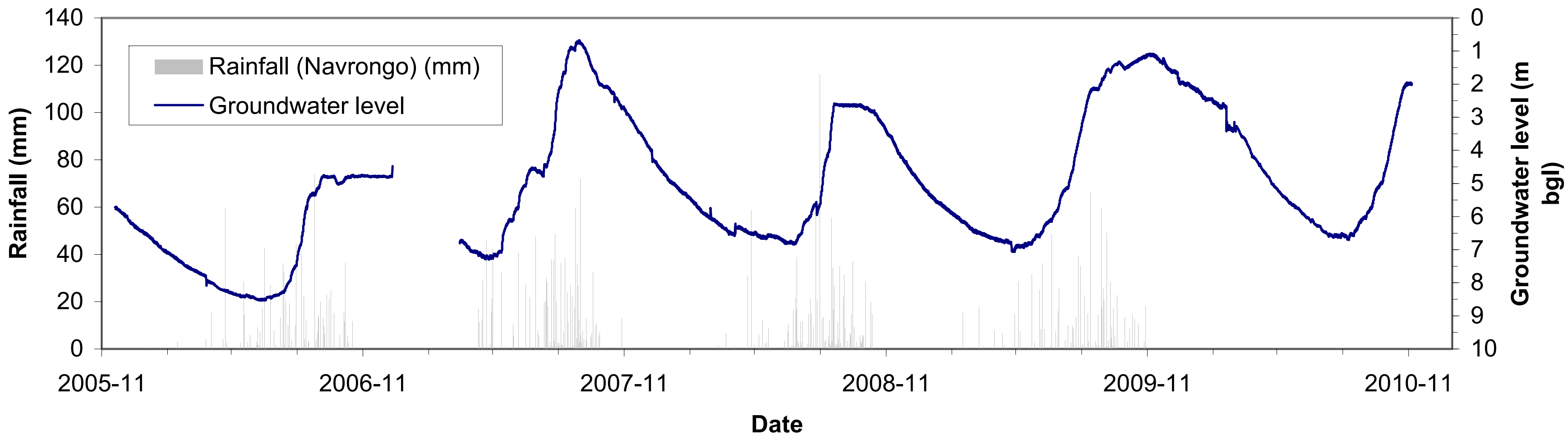

Groundwater level-time plot from Datuku monitoring well (WVB 07)

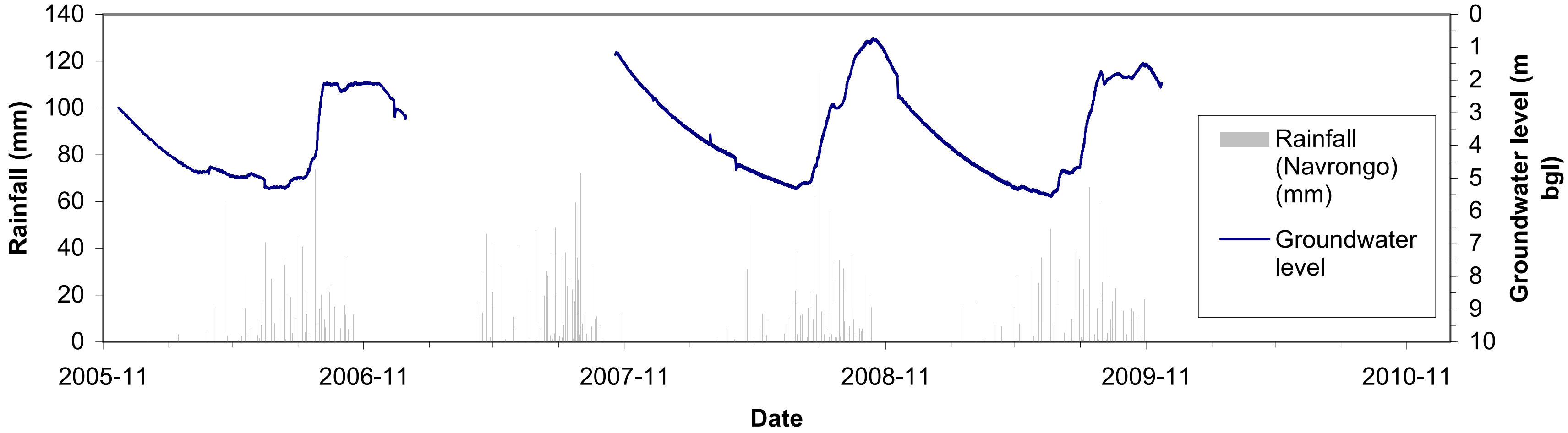

Groundwater level-time plot from Bawku monitoring well (WVB 08)

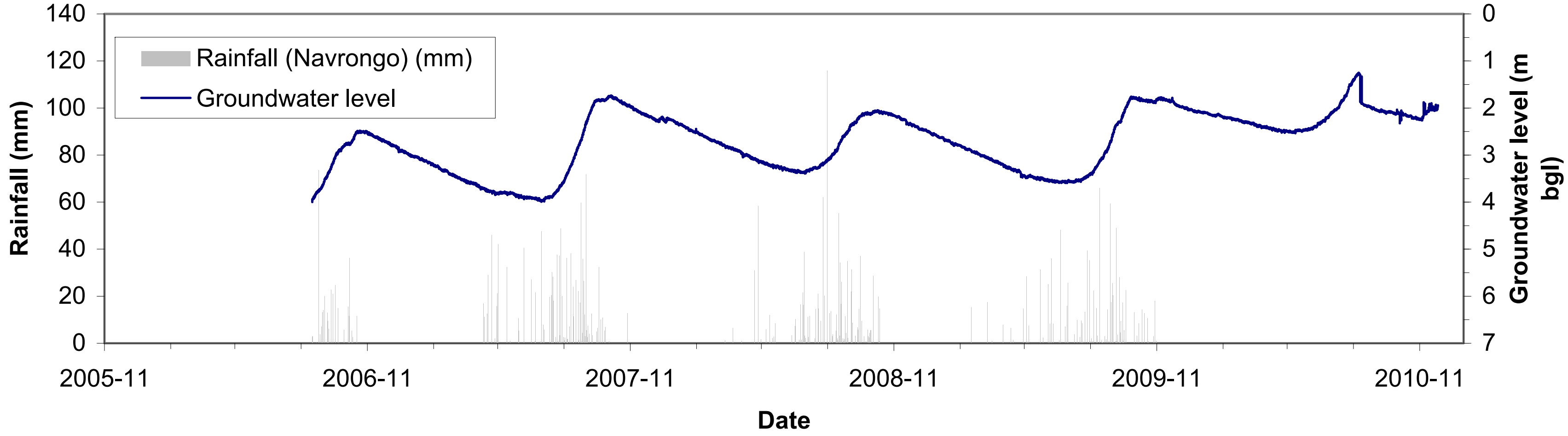

Groundwater level-time plot from Ducie monitoring well (WVB 09)

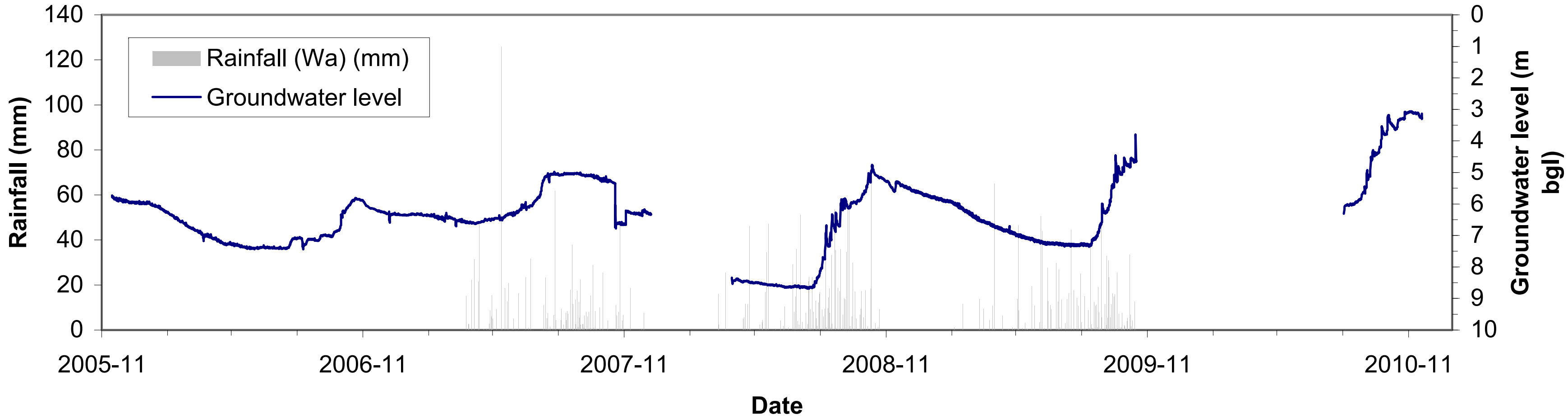

Groundwater level-time plot from Yagbum monitoring well (WVB 10)

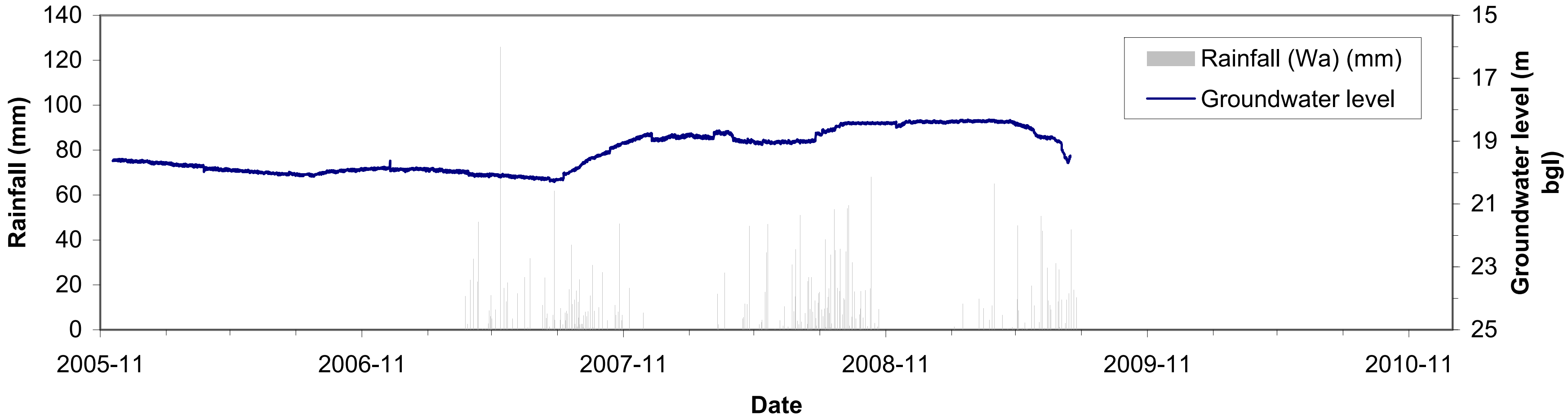

Groundwater level-time plot from Bugya-Pala monitoring well (WVB 11)

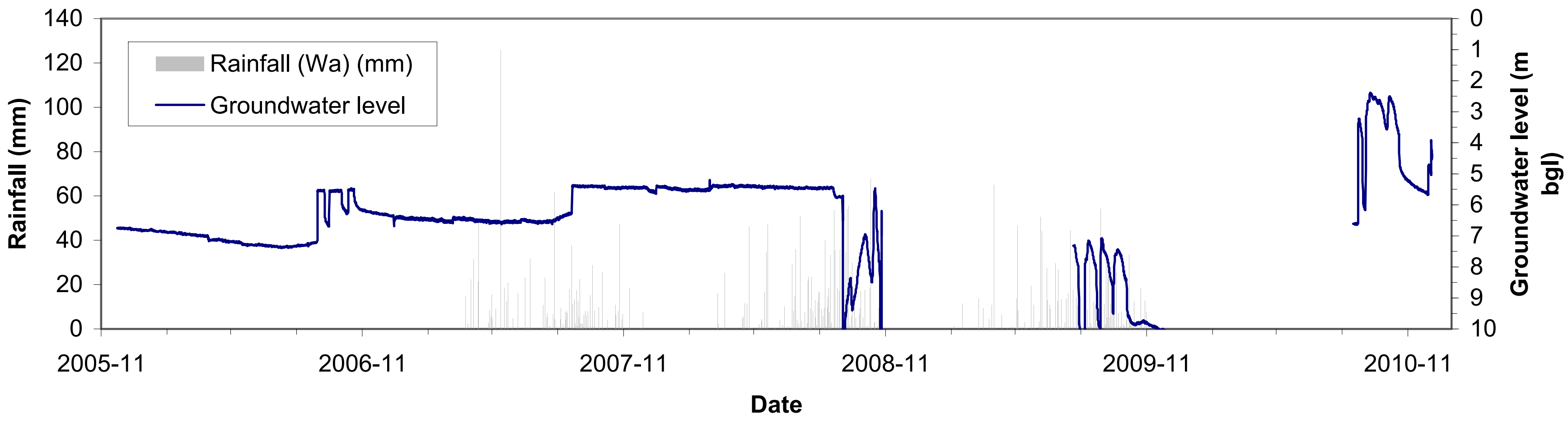

Groundwater level-time plot from Tinguri monitoring well (WVB 12)

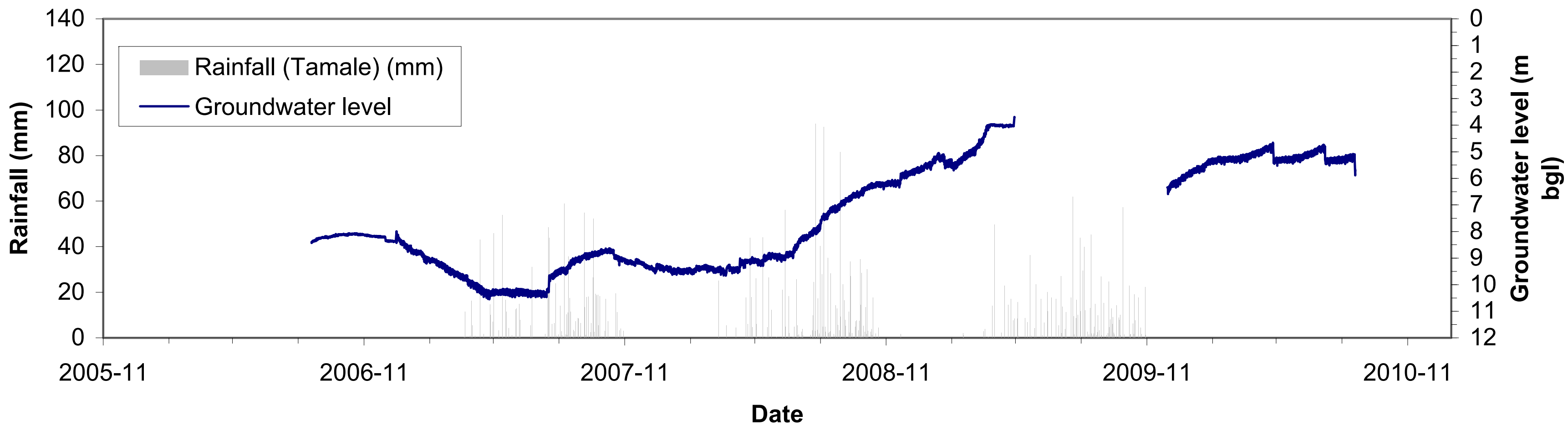

Groundwater level-time plot from Galiwei monitoring well (WVB 13)

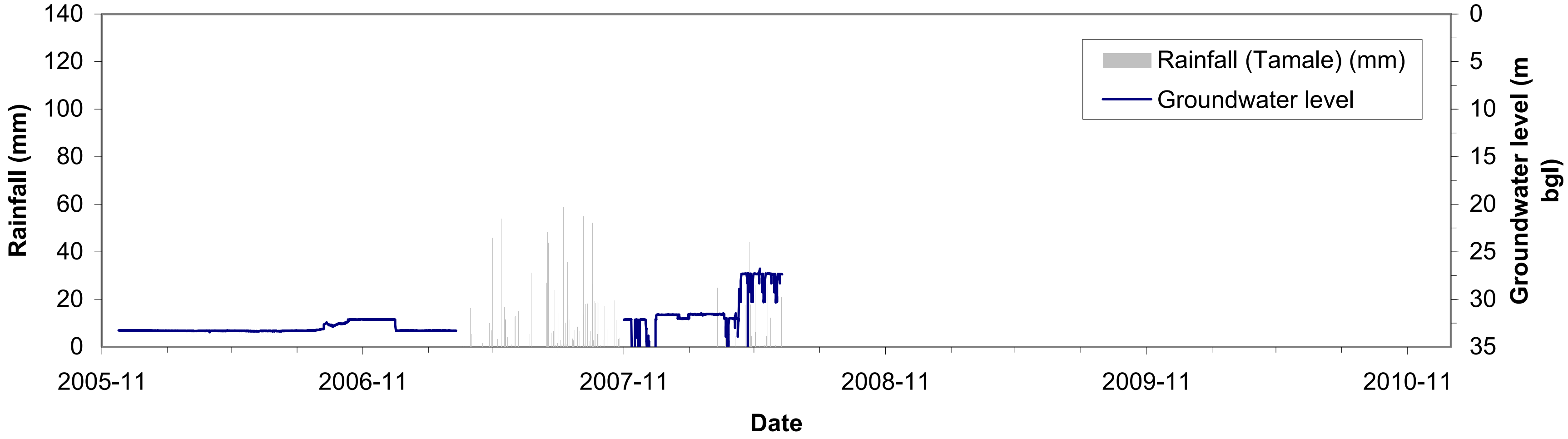

Appendix C

Soil moisture balance - Navrongo Station (1971-2001)

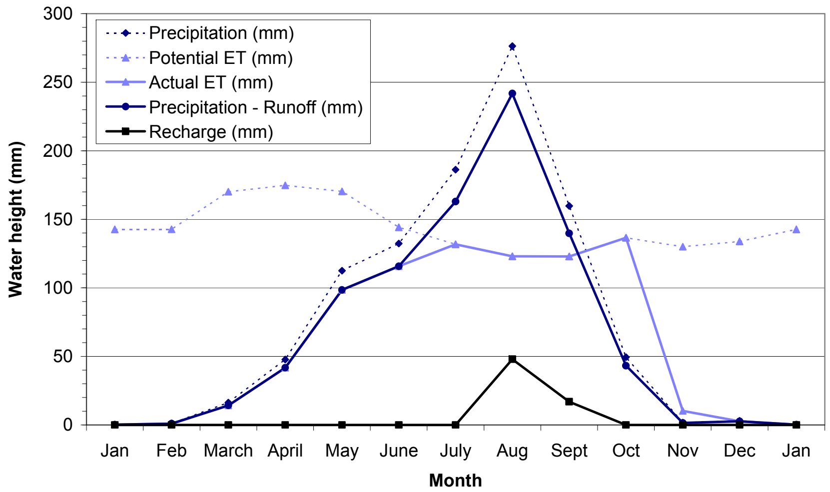

Soil moisture balance - Bole Station (1971-2001)

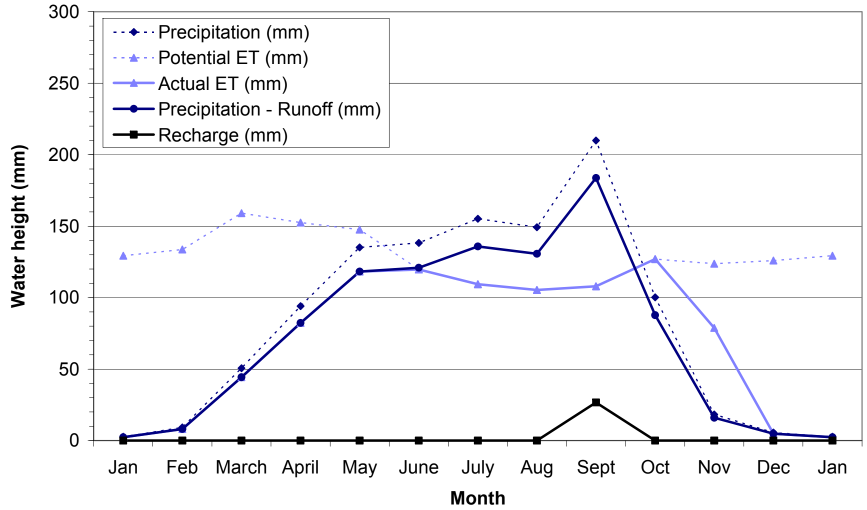

Soil moisture balance - Tamale Station (1971-2001)

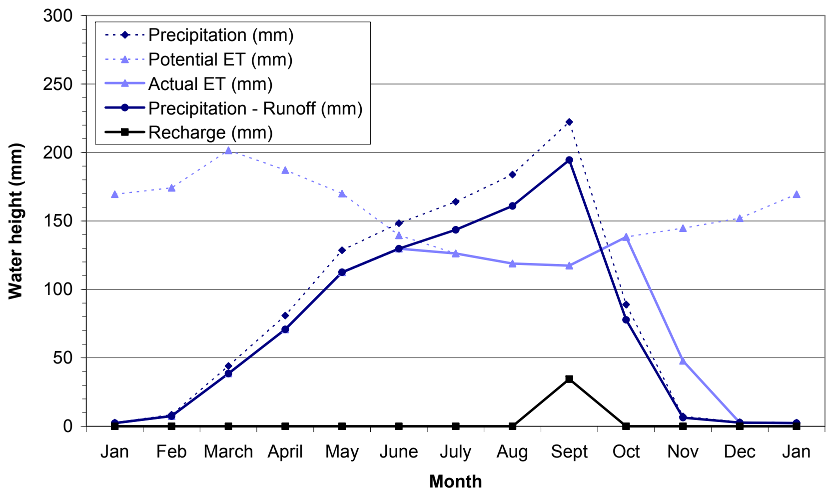

Soil moisture balance - Wa Station (1971-2001)

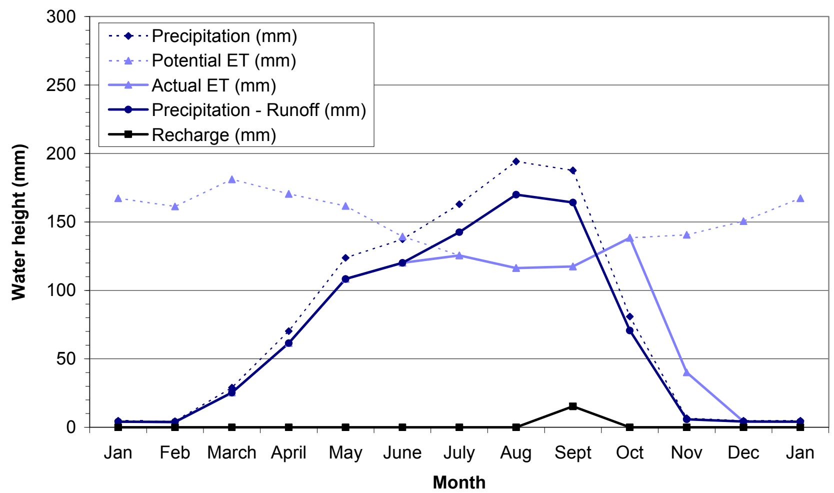

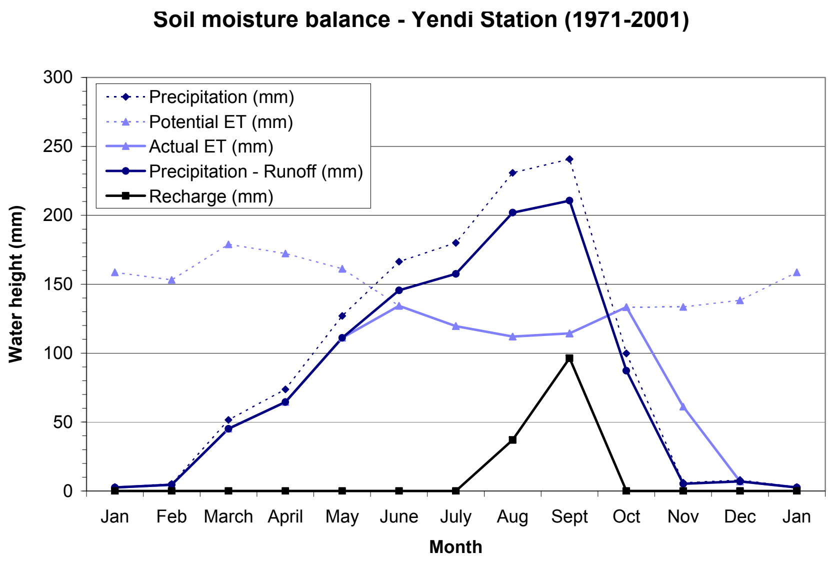

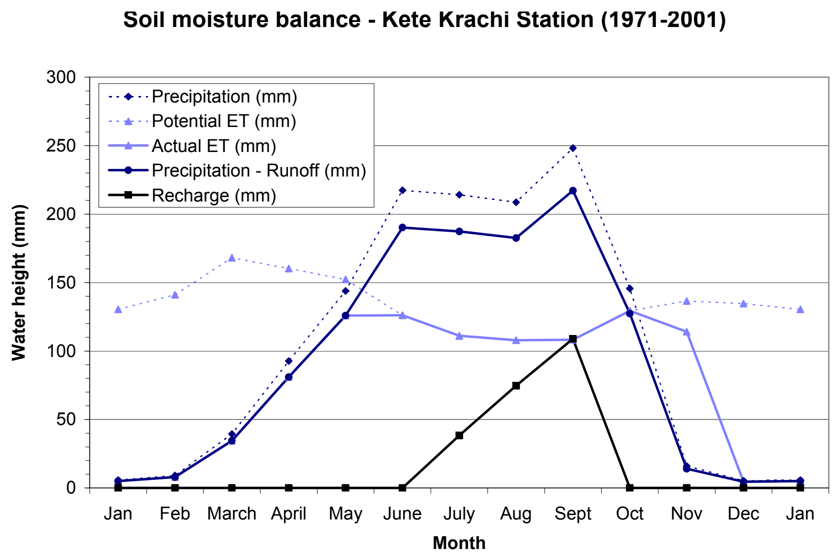

	Soil moisture balance - Annual values for 1971-2001 period											
Station	**Navrongo**		**Wa**		**Tamale**		**Yendi**		**Bole**		**Kete-Krachi**	
Region	Upper E.		Upper W.		Northern		Northern		Northern		Volta	
Units	(mm)	(%)	(mm)	(%)	(mm)	(%)	(mm)	(%)	(mm)	(%)	(mm)	(%)
Potential evapotr. (pET)	1723	-	1770	-	1839	-	1710	-	1541	-	1606	-
Precipitation (P)	987	100	1007	100	1083	100	1192	100	1069	100	1346	100
Runoff (Q) (1)	123	12.5	126	12.5	135	12.5	149	12.5	134	12.5	168	13
Actual evapotr. (aET)	798	80.9	866	86.0	913	84.3	910	76.3	908	85.0	956	71
Recharge (R)	65	6.6	15	1.5	34	3.2	133	11.2	27	2.5	222	16

<u>Notes</u>

(1) : Runoff values obtained with constant runoff coefficient of 12.5% of precipitation

Content of Appendix D (Electronic data - USB flash drive)

Appendix E

<u>Content of Appendix E (Electronic documents - USB flash drive)</u>

Appendix E-1: **Digital library of collected scientific publications and reports**

SNC·LAVALIN

www.snclavalin.com

SNC-Lavalin International inc.
455, René-Lévesque Blvd West
Montreal (Quebec)
H2Z 1Z3 Canada
Tel.: (514) 393-1000
Fax: (514) 861-1454